

The Pennsylvania State University

The Graduate School

Eberly College of Science

**USE OF HUMAN INDUCED-PLURIPOTENT STEM CELLS
TO UNDERSTAND MOLECULAR MECHANISMS OF
AUTISM**

A Dissertation in

Biology

by

Xin Tang

© 2014 Xin Tang

Submitted in Partial Fulfillment
of the Requirements
for the degree of

Doctor of Philosophy

May 2014

The dissertation of Xin Tang was reviewed and approved* by the following:

Gong Chen
Professor and Verne M. Willaman Chair in Life Sciences
Dissertation Advisor

Douglas Cavener
Professor of Biology
Head of Biology Department
Chair of the Dissertation Committee

Bernhard Luscher
Professor of Biology, Biochemistry and Molecular Biology, and Psychiatry

Melissa Rolls
Associate Professor of Biochemistry and Molecular Biology

Yingwei Mao
Assistant Professor of Biology

*Signatures are on file in the Graduate School

ABSTRACT

Despite having diverse capabilities, the human brain has limited ability in regenerating itself. This drawback hinders brain repair process in brain injury or neurodegenerative conditions, and imposes serious limitations to research efforts using human brain cells. In a major paradigm-shift, recent advances in stem cell biology have empowered scientists with the ability to generate a large quantity of human brain cells from stem cells. These technological breakthroughs not only offer great hope for regenerative medicine, but also make it possible to systematically study brain functions utilizing human brain cells.

In order to realize the full potential of stem cell technology in studying the human brain, it is critical to derive various human brain cell types in significant amount, at the maturation stages similar to the endogenous human brain cells. Different protocols have been used to differentiate human iPS cells (induced-Pluripotent Stem Cells) into neurons for disease modeling and transplantation, but their functional maturation process has varied greatly among different studies. In this dissertation, we demonstrate that laminin, a commonly used substrate for iPSC cultures, was inefficient in promoting full functional maturation of hiPSC-derived neurons. In contrast, astroglial substrate greatly accelerated the neurodevelopmental processes of hiPSC-derived neurons, which highlight a critical role of astrocytes in promoting neural differentiation and functional maturation of human neurons derived from hiPSCs. Moreover, our data provide a reliable protocol to generate functionally mature human neurons from stem cells, and present a thorough developmental timeline of normal human iPSC-derived neurons, as benchmarks to detect disease-relevant phenotypes and assess the efficiency of therapeutic agents.

We next employed our glia-NPC (Neuroprogenitor Cell) co-culture system to study the molecular mechanisms of Rett syndrome, a severe form of autism spectrum disorder mainly caused by dysfunction of a single gene MeCP2 (Methyl-CpG binding Protein 2) located on the X-chromosome (Chahrour and Zoghbi, 2007). Rett patients develop relatively normally within 6-18 months after birth but then display developmental regression with impaired motor function, cognitive deficit, and even premature death (Chahrour and Zoghbi, 2007). Previous studies have demonstrated that MeCP2 regulates global gene transcription, and have identified a variety of downstream signaling molecules in neurons (Zoghbi and Bear, 2012; Ebert et al., 2013a). However, why Rett patients show a delayed developmental regression after birth is still an unanswered question. In this dissertation, we demonstrated that KCC2 (Potassium Chloride Co-transporter 2), a K^+-Cl^- co-transporter that directly regulates both GABA and glutamatergic

functions, may mediate the functional output of MeCP2 in governing the course of brain development. We discovered that human neurons differentiated from induced pluripotent stem cells (iPSCs) originated from Rett patient showed a significant deficit in KCC2 expression and a delayed GABA functional switch, which were rescued by IGF-1 (Insulin-like Growth Factor-1) treatment. Moreover, introduction of KCC2 into Rett human neurons lead to a rescue of Rett-relevant deficits in excitatory synapse function to levels comparable as using MeCP2 restoration. We have confirmed our major findings from human neuron experiments in parallel studies carried out in cultured mouse neurons utilizing gene expression manipulation methods. We further demonstrated that MeCP2 interacts with REST (RE1-Silencing Transcription factor) to regulate KCC2 expression. Together, we propose that reduction in KCC2 expression in Rett neurons may contribute to the developmental regression due to deficits in GABA functional switch and glutamatergic synapses. Therefore, increasing KCC2 expression level may be a novel therapeutic approach for the treatment of Rett syndrome and other autism spectrum disorders at large.

In addition to our work on iPS cell-derived human neurons, we have developed a protocol to reproducibly generate human glial cells from iPS cells. Using the iPS cell-derived human glial cells and human astroglial cell lines, we have carefully analyzed the differences between human and mouse astrocytes in their gene expression and functional output. Interestingly, comparing to mouse glial cells, human glial cells strongly promote stem cell proliferation, but not their neuronal differentiation. When mouse neurons were cultured on human astrocytes, the formation of inhibitory synapses were greatly facilitated, while excitatory synapse formation was not changed. In addition, cultured human astrocytes secrete large amount of glutamate. Co-culture with neurons halted the secretion of glutamate from human astrocytes. Our functional experiments and parallel transcriptome-wide gene expression profiling highlight the inter-species difference between human and mouse astrocytes to aid future researches on understanding the unique functions of human brain, and will help develop effective therapies that target astrocytes to treat human brain diseases.

In summary, our work has established a streamlined procedure to reliably generate human neurons and glial cells from iPS cells, characterized the molecular and functional differences between human and mouse astrocytes, and discovered that deficiency in KCC2 is a core symptom of Rett syndrome. Our novel understandings on the biology of human neurons and glial cells in health and disease conditions will provide critical insight into the inner workings of human brain, and lead to rational development of novel therapeutic strategies to effectively rectify disturbances thereof.

TABLE OF CONTENTS

List of Figures	vii
List of Tables	x
List of Abbreviations	xi
Acknowledgements.....	xiv
Chapter 1 Introduction	1
1.1 Human iPS Cells and disease modeling.....	1
1.1.1 iPSC technology and the generation of patient-specific human iPS Cells	1
1.1.2 The neural development of iPS Cells mirrors human brain development.....	3
1.1.3 iPS Cells as tools to model human brain disorders	4
1.2 The role of KCC2 in neuronal development and function	6
1.2.1 KCC2 regulates GABA functional switch during development	7
1.2.2 Regulation of KCC2 and its function beyond ion transporter.....	8
1.2.3 KCC2 involves in the pathophysiology of brain disorders	10
1.3 Rett syndrome	12
1.3.1 Molecular basis of Rett syndrome	13
1.3.2 Neurobiology of Rett syndrome	15
1.3.3 Human iPS Cell models of Rett syndrome.....	19
1.4 Glial cells in health and disease	20
1.4.1 Glial cells modulate synapse function, regulate stem cell behaviors, and uptake neurotransmitter	21
1.4.2 Glial cells contribute to the pathogenesis of diseases	23
1.4.3 The molecular and functional differences between human and mouse glial cells.....	25
Chapter 2 Materials and Methods	27
2.1 Maintenance and differentiation of human iPSC-NPC cells	27
2.2 Primary astroglial and neuronal cell culture.....	27
2.3 Plasmid constructs and transfection	28
2.4 Virus production and infection.....	29
2.5 Immunostaining and imaging.....	29
2.6 Immunoblotting	30
2.7 Electrophysiology.....	30
2.8 Calcium imaging	32
2.9 Dendritic spine analysis.....	32
2.10 Sholl analysis on dendritic complexity.....	32
2.11 RNA extraction, qRT-PCR, and cDNA deep sequencing	33
2.12 Statistical analysis	33
Chapter 3 KCC2 Deficiency in Rett Syndrome Human Neurons Leads to Functional Deficits in both Excitatory and Inhibitory Neurotransmission	34

3.1 Results	35
3.1.1 Prolonged GABA functional switch in human neurons	35
3.1.2 Human neurons derived from iPSC have deficit in KCC2 expression	39
3.1.3 KCC2 is downstream of MeCP2, and is a key regulator of GABA functional switch and glutamatergic synapse formation	48
3.1.4 MeCP2 regulates KCC2 through the transcriptional repressor REST.	55
3.2 Discussion	59
3.2.1 The timecourse of KCC2 development in normal and Rett syndrome human iPSC-derived neurons	60
3.2.2 KCC2 is a key downstream gene of MeCP2 that directly regulates both inhibitory and excitatory neurotransmission	60
3.2.3 Targeting KCC2 to treat Rett syndrome.....	61
Chapter 4 Astroglial Cells Regulate the Developmental Timeline of Human Neurons Differentiated from induced Pluripotent Stem Cells.....	64
4.1 Results	65
4.1.1 Essential role of astroglial cells in neural differentiation	65
4.1.2 Neurons inhibit NPC survival and neural differentiation.....	70
4.1.3 Astrocytes promote dendritic development.....	72
4.1.4 Rapid expression of functional channels and receptors	73
4.1.5 Developmental Timeline of Synaptic Maturation	80
4.1.6 Generation of astrocytes from hiPSCs	87
4.2 Discussion	90
4.2.1 Essential role of astrocytes in promoting neural differentiation and rapid functional maturation of hiPSC-derived neurons	90
4.2.2 Astrocytes are critical for iPSC-derived neurons to form robust synaptic connections.....	91
4.1.3 Implication in neuron-glia interactions and disease modeling	91
Chapter 5 Comparison between Human and Mouse Astrocytes Reveals Key Molecular and Functional Differences	93
5.1 Results	94
5.1.1 Human astrocytes promote NPC proliferation but not neural differentiation	94
5.1.2 Human astrocytes express high levels of BDNF, and strongly promote the formation of inhibitory synapses	97
5.1.3 Human astrocytes accumulate and release large amount of glutamate	102
5.1.4 Compare the gene expression differences between human and mouse astrocytes	106
5.2 Discussion	109
5.2.1 Human astrocyte promote stem cell proliferation rather than differentiation	109
5.2.2 High BDNF in human astrocyte facilitate inhibitory synapse formation	113
5.2.3 Glutamate processing dysfunction in glial cells as a key contributor to pathological conditions of the human brain	113
Appendix Cofilin is a key regulator of neuronal calcium homeostasis.....	115
References	122

LIST OF FIGURES

Figure 3-1: GABA functional switch takes a long time in iPS cell-derived human neurons.	37
Figure 3-2: Human neurons derived from Rett iPS cells show deficits in GABA functional switch and glutamatergic transmission.	41
Figure 3-3: Rett patient-derived human neurons show reduced KCC2 but comparable NKCC1 expression.	43
Figure 3-4: Rett syndrome human neurons demonstrate deficits in excitatory synapse formation.	44
Figure 3-5: KCC2 regulates excitatory synaptic transmission in human neurons.	46
Figure 3-6: Rett human neurons show reduced spontaneous excitatory neurotransmission.	47
Figure 3-7: MeCP2 and KCC2 development timecourse in mouse neurons.	50
Figure 3-8: Cross validation of MeCP2 and KCC2 plasmids and antibodies.	51
Figure 3-9: KCC2 is a key downstream gene of MeCP2 that directly regulates dendritic spine and excitatory synapse.	54
Figure 3-10: MeCP2 regulates KCC2 through the transcriptional repressor REST.	57
Figure 3-11: MeCP2 Regulates KCC2 during neuronal maturation.	58
Figure 3-12: Working model	59
Figure 4-1: Confirmation of the neuroprogenitor properties derived from human iPSCs.	66
Figure 4-2: Astrocytes promote neuronal differentiation of human iPS cells.	67
Figure 4-3: Astrocytes promote neural differentiation when assessed with a different neuronal marker Tuj1 instead of doublecortin.	68
Figure 4-4: Astrocytes promote neural differentiation using hiPSC WT33 line-derived NPCs.	69
Figure 4-5: A variety of neuronal subtypes generated from human iPS cells.	69
Figure 4-6: Neurons suppress NPC proliferation and neuronal differentiation.	72
Figure 4-7: Astrocytes promote morphological development of hiPSC-derived neurons.	73
Figure 4-8: Astrocytes increase the expression of Na ⁺ and K ⁺ channels.	76

Figure 4-9: Astrocytes promote the development of action potential firing ability and passive membrane properties.	77
Figure 4-10: Astrocytes increase the expression of neurotransmitter receptors.	78
Figure 4-11: Rapid functional development of human iPS cell-derived neurons co-cultured with astrocytes.	79
Figure 4-12: Astrocytes are essential for synaptic maturation of human neurons.	82
Figure 4-13: Excitatory synaptic transmission precedes inhibitory synaptic transmission in human iPS cell-derived neurons.	84
Figure 4-14: Human neurons can incorporate into neural networks.	86
Figure 4-15: Generation of human glial cells from human iPS cell-derived NPCs.	88
Figure 4-16: Functional comparisons reveal cell-autonomous species difference between human and mouse neurons.	89
Figure 5-1: Human astrocytes promote stem cell proliferation but not neural differentiation.	96
Figure 5-2: Human astrocytes show stronger BDNF immunoreactivity comparing to mouse astrocytes.	99
Figure 5-3: Human astrocytes strongly promote the formation of inhibitory synapse in a BDNF-dependent manner.	100
Figure 5-4: Human and mouse astrocytes promote excitatory synapse formation to similar degrees.	101
Figure 5-5: The mouse neurons cultured on human astrocytes show reduced whole-cell glutamate current but similar GABA current.	102
Figure 5-6: Human astrocytes have enormous glutamate content and secrete glutamate.	105
Figure 5-7: The general structures of human and mouse astrocytes transcriptomes.	107
Figure 5-8: Gene expression profile obtained from qRT-PCR and deep sequencing methods are comparable.	108
Appendix-1: Cofilin regulates the percentage of neurons showing dendritic beading after excitotoxic challenge.	116
Appendix-2: LIMK and SSH are regulators of cofilin activity, which in turn regulates the beading percentage.	117
Appendix-3: Cofilin activity regulates whole-cell Calcium current amplitude in neurons.	118

Appendix-4: Cofilin activity regulates whole-cell NMDA current amplitude in neurons.....	120
Appendix-5: Downregulation of SSH activity reduce the mini EPSC frequency and amplitude.....	121

LIST OF TABLES

Table 1: Potential factors responsible for HA stimulation on stem cell proliferation.....	109
Table 2: Secreted proteins that are enriched in human astrocytes.	110
Table 3: Secreted proteins that are enriched in mouse astrocytes.....	111
Table 4: Comparison of the expression of glial genes contributing to synapse formation between human and mouse astrocytes	113
Table 5: Comparison of the expression of glial factors contributing to glutamate processing between human and mouse astrocytes	114

LIST OF ABBREVIATIONS

5-HT	5-hydroxytryptamine, also known as serotonin
a.u.	arbitrary unit
AIS	axon initial segment
ALS	amyotrophic lateral sclerosis
ASD	autism spectrum disorders
BBB	blood brain barrier
BDNF	brain-derived neurotrophic factor
BPA	bisphenol-A
CamK	Ca ²⁺ /calmodulin-dependent protein kinase
CCC	cation-chloride cotransporter
CDKL5	cyclin-dependent kinase-like 5
CHAT	choline acetyltransferase
CHIP	chromatin co-immunoprecipitation
CM	conditioned medium
CREB	cAMP response element-binding
DIV	days in vitro
Dlx5/6+	distal-less 5/6
DN	dominant negative
DNQX	6,7-dinitroquinoxaline-2,3-dione
EDTA	ethylenediaminetetraacetic acid
EGABA	GABA reversal/equilibrium potential
Egr4	early growth response 4
ESC	embryonic stem cells
F-actin/ G-actin	filamentous actin/globular actin
FBS	fetal bovine serum
FGF2	basic fibroblast growth factor 2
FL	full length
GABA	γ -aminobutyric acid
GAD	glutamate decarboxylase
GFAP	glial fibrillary acidic protein
GFP	green fluorescent protein

HA	human astrocyte
HEK	human embryonic kidney
HEPES	4-(2-hydroxyethyl)-1-piperazineethanesulfonic acid
IGF-1	insulin-like growth factor-1
iPSC	induced-pluripotent stem cells
KCC2	potassium chloride co-transporter 2
LEMPRA	lentivirus-mediated protein-replacement assay
Lysm	lysine motif
MA	mouse astrocyte
MBD	molecular binding domain
MeCP2	methyl-CpG binding protein 2
MEM	modified eagle's medium
mEPSCs	miniature excitatory postsynaptic currents
MGE	medial ganglionic eminence
mIPSCs	miniature inhibitory postsynaptic currents
mTOR	mammalian target of rapamycin
NCoR/SMRT	nuclear-receptor co-repressor/silencing mediator for retinoid or thyroid-hormone receptors
NG2	chondroitin sulfate proteoglycan 4
NGF	nerve growth factor
NKCC1	Na-K-Cl cotransporter
NLG-1	neuroligin-1
NMDA	N-methyl-D-aspartate
non TFed	non transfected
NPC	neuroprogenitor cell
PBS	phosphate buffered saline
PI3K/Akt	phosphatidylinositol-4,5-bisphosphate 3-kinase/ protein kinase B
PSD95	postsynaptic density protein 95 kDa
REST/NRSF	RE1-silencing transcription factor/neuron-restrictive silencer factor
ROCK	Rho-associated protein kinase
rpkm	reads per kilo base per million

RT-PCR	real-time polymerase chain reaction
shRNA	small hairpin RNA
Sim1	single-minded homolog 1
SOD	superoxide dismutase
SPARC	secreted protein acidic and rich in cysteine
SV2	synaptic vesicle glycoprotein 2
TF	transfection
TGF-beta	transforming growth factor beta
TH	tyrosine hydroxylase
TNF α	tumor necrosis factor alpha
TRD	transcriptional repression domains
TrkB	tropomyosin related kinase B
TSP	thrombospondin
TTX	tetrodotoxin
VGlut1	vesicular glutamate transporter 1
Viaat	vesicular inhibitory amino acid transporter
WNK1	lysine deficient protein kinase 1
WT	wild-type

ACKNOWLEDGEMENTS

When writing the Ph.D. dissertation, one could not help but to reflect upon the path he has ventured through to arrive at here and now. To me, graduate school has been an exhilarating and enriching journey full of joy, growth, and life lessons. I am cordially grateful and deeply indebted to those people who have generously lent me a helping hand when I was in need, and attentively guided me through my personal odyssey.

First and foremost, I would like to devote my deepest gratitude to Dr. Gong Chen. In 2009 he welcomed me into his lab with open arms, since then he treated me with a big heart. Dr. Chen's dedicated work ethic, rigorous scientific attitude, independent thinking style, and his determination and perseverance when facing difficulties, will have profound influence on my scientific career for many years to come. He has been, and will always be, my scientific role model and life coach.

I would also like to dedicate my sincere gratitude to my thesis committee members: Drs. Douglas Cavener, Bernhard Luscher, Melissa Rolls, and Yingwei Mao. You four were the dedicated review and advisory board for all my research projects, and have always been strong advocates for my career development. I would also want to take this opportunity to thank Dr. Gangyi Wu. Our late-night discussions on experiments, manuscripts, and science in general, have been very enriching to me. I have learned a great deal from my many professor friends, and I consider you amongst my most close mentor and advocates, with whom I will keep in contact with in the future, and make you proud with my achievements.

My special thanks go to Drs. Fred Gage and Maria Marchetto in the Salk Institute, and Drs. Alysson Muotri and Cassiano Carrromeu in the University of California San Diego. My human iPS cell work would not have been possible without your generous help with cell lines, reagents, and protocols. Moreover, thank you for inviting me to visit your groups in San Diego, I had a great time talking with you and your group members, and feel that I have learned a lot from my visit. We all share many common research interests, and I am sure our scientific paths will converge in a big way in the future. I would also want to thank Dr. Hong Ma and his student Chenlong Cao in the Fudan University for their help with the human versus mouse astrocyte transcriptome analysis project.

My family and friends have played a pivotal role in keeping me constantly strong and optimistic. I would like to thank my parents for always understanding me, always supporting me, and always nurturing me; thank my girlfriend Zaoli Zhang for her magic to make my bad days

bright and good days roll. My heartfelt ‘thank you’ also go to many friends and colleagues I was lucky to befriend with during my Penn State years, including but not limited to: Chicheng Sun, Xia Wu, Rosie Qin, Xinwei Han, Liye Zhang, Zhen Ren, Robert Holleran, Yan Wang, Li Zhou, Zhengguo Zhang, Alecia Wagner, Yuting Bai, Lei Zhang, Yong Tang, Zheng Wu, Xu Xu, Kai Du, Xuan Ye, Jingling Liu, Hongcheng Cai, Julie Kim, and Yuchen Chen. The good times I have spent with you guys are amongst the fondest memory of my Penn State years. I am looking forward to more fun and fruitful interactions with you in the days and years to come.

In conclusion, I would like to thank Dr. Chen again for offering me the opportunity to pursue the scientific questions that excite and inspire me, in his lab; and to thank every person who has assisted me in one way or another to make everything come together. When I later find myself reminiscing upon my Penn State graduate school years, the word, ‘rewarding’, will surely be the first to come to mind; for hard work is its own reward, and hard work is the solid bedrock I want to build my career on.

Chapter 1 Introduction

1.1 Human iPS Cells and disease modeling

The advent of iPSC (induced Pluripotent Stem Cells) technology has armed scientists with the ability to obtain stem cells that contain the patient's entire genetic information. Through this powerful technology, researchers can: 1) investigate the genetic and environmental programs that regulate the fate choice and developmental process of desired cell types. 2) Understand the molecular mechanism of human diseases through the study of patient-derived relevant cell types. 3) Obtain large amount of human cells to screening for compounds that have therapeutic potential, and apply these cells in transplantation-based therapy.

To realize the full potential of stem cell research, mastering the ability to derive various types of cells and tissues from stem cells is essential. In order to acquire this ability, it is crucial to understand the fate choice determinants and the detailed developmental process of these cells. Recent advances in the technologies to generate human stem cells (with the emphasis on iPS cells), the methods to derive functional brain cells from stem cells, and the applications of such cell types are reviewed in this section.

1.1.1 iPSC technology and the generation of patient-specific human iPS Cells

Human embryonic stem cells (ESC) have been a workhorse for stem cell research since the late 1990s (Thomson et al., 1998; Amit et al., 2000; Odorico et al., 2001; Zhang et al., 2001; Cowan et al., 2005). From studying human ES cells, scientists have obtained a broad understanding of the developmental programs and critical factors of various human organs and tissues including the brain (Di Giorgio et al., 2008; Marchetto et al., 2008). However, the sources of human ES cells are limited, and obtaining the ESC requires destroying the embryo, which is ethically challenging (Doerflinger, 1999; Childress, 2001; Daley et al., 2007).

In 2006, a seminal work from the Yamanaka group described a revolutionary method to generate stem cells from mouse fibroblasts, through retrovirus delivery of four transcriptional

factors including Oct4, Sox2, Klf4 and c-Myc (OSKM factors). The iPS cells have tremendous self-renewal capability, and can respond to external cues to differentiate into cell types from all three germ layers (Takahashi and Yamanaka, 2006). The generation of iPS cells from human somatic cells was achieved in 2007 (Takahashi et al., 2007; Yu et al., 2007). Since the original lentiviral infection of OSKM factors, various methods have been developed to generate human iPSC including: different combinations of pluripotent-induction factor sets (Yu et al., 2007), inducible expression of reprogramming factors with Doxycycline (Wernig et al., 2008), excise reprogramming factors from the genome after pluripotency-induction to create factor-free iPS Cells (Karow et al., 2011), delivery of OSKM factors through non-integrative sendai virus (Fusaki et al., 2009; Ban et al., 2011), transient plasmid transfection (Okita et al., 2008), microRNA circuit modulation (Anokye-Danso et al., 2011), and protein delivery (Zhou et al., 2009). Bioactive small molecules that activate or inhibit molecular pathways have been used in combination with OSKM factor methods to facilitate iPSC generation (Esteban et al., 2010), and to directly generate iPSC from fibroblasts (Hou et al., 2013a). In addition to fibroblast cells as the donor source, the iPSC can also be generated from peripheral blood cells (Staerk et al., 2010) and other terminally differentiated somatic cell types (Wernig et al., 2008).

iPS cells have been demonstrated to have the capacity to differentiate into various types of cells including heart (Itzhaki et al., 2011; Yazawa et al., 2011), blood (Hanna et al., 2007), and brain cells (Marchetto et al., 2010b). In comparison to embryonic stem cells, the iPSC followed similar developmental timecourse and responded to similar developmental cues (Shi et al., 2012). However, careful study revealed that the variability in differentiation potential across different clones are higher in iPSC, calling for improved methods to increase efficiency and reduce variability (Hu et al., 2010). Human iPS cell have been utilized to create disease models to recapitulate the pathological features of numerous diseases, including heart and vascular disease (Itzhaki et al., 2011; Liu et al., 2011), liver disease (Ghodsizadeh et al., 2010), and brain disease (Kim et al., 2011a; Israel et al., 2012). The disease-relevant phenotypes can be detected at the molecular expression level (Li et al., 2013), at the single cell level (Marchetto et al., 2010b), and at the multi-cell organization level (Itzhaki et al., 2011). Importantly, relevant types of human cells derived from iPS cells can be utilized to establish potential patient-specific therapies using the patient's own cells (Takahashi et al., 2007; Yu et al., 2007; Marchetto et al., 2010a; Mitne-Neto et al., 2011; Robinton and Daley, 2011).

With the iPS cell-based neuron model established, scientists have been testing the effect of bioactive compounds on the patient-derived neurons to achieve modeling of diseases, with

hopes of developing personalized medicine in the near future. The patients can be recruited to test the effect of drugs on their own cells before actually taking the drug, serving as their own guinea pigs to test the efficacy of proposed therapies (Marchetto et al., 2010a; Dajani et al., 2013). iPSC-based cell replacement therapy have also been attracting major attention. In two proof-of-principle experiments, the Jaenisch group has managed to transplant autologous iPSC-derived red blood cells into the sickle red blood cell anemia mouse model to treat the disease (Hanna et al., 2007), and transplanted dopaminergic neurons into the Parkinson's disease mouse model. The transplanted neurons survived for up to 16 weeks, and the motor symptoms of the mouse model was greatly recovered (Hargus et al., 2010).

1.1.2 The neural development of iPS Cells mirrors human brain development

The ontogeny of mouse brain development critical determinants has been well characterized thanks to advanced genetics, pharmacology, histology, and cell culture methods. Comparatively, the studies on human brain development were relatively lagging, mostly having been hindered by the limited access to human brain cells and tissues, especially at the early stage of development (Oberheim et al., 2009; Zhang and Barres, 2010). Research on human embryonic stem cell has shed light on the developmental process of human tissue and organs. Numerous studies on neurons derived from human ES cells have revealed that human neurons follow similar general developmental principles and respond to similar molecular cues as discovered from studies on the mouse brain development (Zhang et al., 2001; Perrier et al., 2004; Di Giorgio et al., 2008; Chambers et al., 2009).

Human iPSCs have been successfully differentiated into different subtypes of neurons, including glutamatergic cells (Lee et al., 2009; Hansen et al., 2011; Soldner et al., 2011; Bilican et al., 2012), GABAergic neurons (Maroof et al., 2013; Nicholas et al., 2013), cholinergic neurons (Hu et al., 2010), dopaminergic neurons (Hargus et al., 2010), and spinal motor neurons (Hu and Zhang, 2009). The neurons derived from iPS cells have been shown to be able to fire action potentials (Hu et al., 2010; Shi et al., 2012), form functional synapses (Bilican et al., 2012; Tang et al., 2013), and incorporate into the host brain after transplantation (Espuny-Camacho et al., 2013). Specific types of iPSC-derived neurons have been shown to ameliorate disease phenotype after transplantation into the brain (Hargus et al., 2010). However, different labs utilized different protocols to derive neurons from iPSC, making the results difficult to compare.

In the literature, iPSC-derived human neuron development took prolonged time, and the maturation stage these neurons could reach were not comparable to endogenous neurons of the brain (Shi et al., 2012; Espuny-Camacho et al., 2013; Nicholas et al., 2013). An optimized protocol to reliably generate human neurons from iPSC cells is greatly needed.

In addition to the ability to differentiate into neurons, the human iPSC cells also have the potential to differentiate into glial cells (Krencik et al., 2011; Krencik and Zhang, 2011; Juopperi et al., 2012). The differentiation process from iPSC to functional human glial cells take months, and the efficiency varies between different experiments. Microglial cells are originated from myeloid lineage. They migrate into the brain in abundant numbers, and contribute to important aspects of brain physiology (Derecki et al., 2012; Ferrini et al., 2013). Microglial cells can also be derived from stem cells (Almeida et al., 2012; Beutner et al., 2013), making it a useful model to study glial cell's participation in human brain development and pathological conditions.

The status quo of iPSC-based research is that different labs are using different protocols to differentiate human neurons from iPSCs, and so far there is no consensus as to when these human neurons are fully functional mature after differentiation. The fourth chapter of this dissertation provides a complete timecourse for the functional development of human neurons derived from iPSC cells.

1.1.3 iPSC Cells as tools to model human brain disorders

Human neurological disorders have been modeled by deriving disease-relevant cells from patient-specific iPSC Cells, and compared their disease-relevant molecular and functional properties with appropriate controls (Ebert et al., 2009; Lee et al., 2009; Marchetto et al., 2010b; Brennand et al., 2011; Grskovic et al., 2011; Itzhaki et al., 2011). The brain diseases that have been successfully modeled with stem cells include Rett syndrome (Marchetto et al., 2010b; Kim et al., 2011b; Ricciardi et al., 2012; Li et al., 2013), Fragile X syndrome (Liu et al., 2012), schizophrenia (Brennand et al., 2011), Alzheimer disease (Yagi et al., 2011; Israel et al., 2012; Koch et al., 2012), Amyotrophic Lateral Sclerosis (ALS) (Di Giorgio et al., 2007; Di Giorgio et al., 2008; Marchetto et al., 2008; Mitne-Neto et al., 2011), Timothy syndrome (Pasca et al., 2011; Yazawa et al., 2011; Krey et al., 2013), Down's syndrome (Mou et al., 2012), Parkinson's disease (Hargus et al., 2010; Soldner et al., 2011), Huntington's disease (An et al., 2012; Consortium, 2012; Juopperi et al., 2012), TDP-43 proteopathy (Bilican et al., 2012), myotonic dystrophy

(Marteyn et al., 2011), and familial dysautonomia (Lee et al., 2009). The phenotypes observed from iPSC model described in these literatures include deficits in cell size (Li et al., 2013), neurite complexity and plasticity (Krey et al., 2013), synapse formation (Marchetto et al., 2010b; Brennand et al., 2011), and protein synthesis/secretion (Mitne-Neto et al., 2011; Bilican et al., 2012; Israel et al., 2012; Koch et al., 2012).

Targeted genome editing technologies have also been employed to correct the disease-causing mutation, which hold the potential to be utilized in cell transplantation and replacement therapy. Importantly, by using genome editing methods such as Zinc Finger Nuclease (Sebastiano et al., 2011; Soldner et al., 2011), TALE Nuclease (Hockemeyer et al., 2011), and CRISPR/Cas system (Cong et al., 2013; Hou et al., 2013b), isogenic pairs of patient-driven stem cells and proper control cell lines can be generated. These powerful technologies allow scientists to compare between wild-type control iPS and disease iPS cells mutated specifically at the disease-causing site; or alternatively, between disease iPS cells and rescue cell line with the mutation site specifically corrected (Hockemeyer et al., 2011; Li et al., 2013).

Human iPSC-derived neurons have been used to test the efficacy of therapeutic compounds. Many drugs have been successfully demonstrated to rescue disease-related deficits in iPSC models including insulin-like growth factor -1 (IGF), brain-derived neurotrophin factor (BDNF) and gentamicin to treat Rett syndrome (Marchetto et al., 2010b; Li et al., 2013), loxapine to treat Schizophrenia (Brennand et al., 2011), and anacardic acid to treat ALS (Egawa et al., 2012). Much research efforts has been dedicated to establishing drug screening systems based on human brain cells derived from iPS cells. The trend of stem cell research is going toward generating more specific types of disease-relevant cells to reveal disease-related molecular mechanisms, and to use the iPSC-derived disease-relevant cells for drug screening and transplantation.

In order to obtain comparable functional neurons from different human iPS cell sources for disease modeling and drug screening, it is urgent to establish an optimized protocol that can be used by different labs to achieve reproducible results. In my thesis, we describe a method to reliably generate functionally mature human neurons from iPS cells for disease modeling. In addition to developmental maturation of multiple morphological and functional characteristics, with support from glial cells the human neurons could gradually upregulate their expression of KCC2 (Potassium-Chloride Co-transporter 2), which is a key molecule that regulates both glutamatergic and GABAergic neurotransmission. Our research efforts have not only established

the timeline of KCC2 expression and GABA functional switch in human neurons for the first time, but also revealed a novel link between KCC2 and Rett syndrome.

1.2 The role of KCC2 in neuronal development and function

KCC2 (Potassium Chloride Co-transporter 2, *Slc12a5*), a membrane K^+-Cl^- co-transporter, is the major Cl^- transporter in neurons (Blaesse et al., 2009). KCC2 is a member of the cation-chloride cotransporter family (CCC). There are nine known members of the CCC family, encoded by genes *Slc12a 1-9* (Gamba, 2005). KCC2 is one of the four K-Cl cotransporter isoforms. Another major type of CCC family is Na-K-2Cl cotransporter, including NKCC1 and NKCC2 (Payne et al., 2003). CCCs are large glycoproteins with 12 trans-membrane segments and two intracellular domains on both ends. The apparent weights of CCCs are between 120 to 200 kDa (Mercado et al., 2004).

The first appearance of KCCs in evolution was detected in the *Drosophila* nervous system, and the expression is restricted to neurons (Hekmat-Scafe, 2006). In both the rodent animal brain and human brain, the expression of KCC2 is restricted to neurons. KCC2 is a versatile protein, performing a variety of functions such as extruding Cl^- from the neuron (Rivera et al., 1999), binding and modulating cytoskeleton interaction protein (Li et al., 2007), and mediating stem cell differentiation and migration (Bortone and Polleux, 2009; Kim et al., 2012). Importantly, current research suggest that KCC2 can not only regulate inhibitory neurotransmission by controlling the polarity and efficacy of GABAergic inhibitory neurotransmission (Rivera et al., 1999), but also control dendritic spine formation and glutamatergic excitatory neurotransmission (Li et al., 2007).

In the light of the emerging consensus that numerous neurological disorders including Autism, Schizophrenia, and Alzheimer's disease have commonly rooted from disturbances in the excitation/inhibition ratio, KCC2 is a key molecule located strategically at the center of the delicate yin-yang balance between excitation and inhibition in the brain.

1.2.1 KCC2 regulates GABA functional switch during development

KCC2 expression levels are typically very low during early postnatal brain development in both human and rodents (Dzhala et al., 2005; Ben-Ari et al., 2012). In the developing mouse cortical and hippocampal regions, KCC2 expression is very low at birth, and the steepest KCC2 expression increase occurs between the first and second postnatal week (Rivera et al., 1999). This developmental timecourse of KCC2 expression is faithfully repeated in primary culture from mouse cortex (Fig. 4-16). In the human brain, the KCC2 mRNA is present at birth at relatively high level (Vanhatalo et al., 2005). However, the KCC2 protein content in neonatal human brain is low comparing to adult brain, and the steepest increase occurs between one-half to one year of age (Dzhala et al., 2005). The temporal and spatial pattern of KCC2 expression in the brain follow a rostral to caudal order during development, with the expression onset very early in the spinal cord and brain stem, and late in hippocampus and neocortex (Blaesse et al., 2009). In addition to the developmental changes, the expression of KCC2 and NKCC1 is not homogenous across different brain regions within the same brain, and even the microdomains within the same neuron. In certain brain regions such as the gonadotrophin-hormone-secreting neurons in the hypothalamus, the KCC2 expression is low well into adolescence age of the animal (Clarkson and Herbison, 2006). In the axon initial segment (AIS) of neurons from adult animal brains, high expression of NKCC1 can render GABA depolarizing. These findings highlight the heterogeneity of CCCs spatial distribution and their contribution to signal transmission and processing in the nervous system (Khirug et al., 2008).

GABA is the major inhibitory neurotransmitter in the brain. Since GABA_A receptors are ligand-gated Cl⁻ channels, proper maintenance of the transmembrane Cl⁻ gradient is critical for the polarity and efficacy of GABAergic function (Kahle et al., 2008). A series of work from the Kai Kaila group have revealed that a key function of KCC2, counteracting the activity of NKCC1 to extrude Cl⁻ from neurons, has significant functional implication in that it sets the Cl⁻ gradient and determines the polarity of GABA action (Rivera et al., 1999; Khirug et al., 2008; Blaesse et al., 2009). Importantly, since the KCC2 expression level is extremely low at the early stage of brain development, the reversal potential for GABA is so depolarized that when GABA is applied to the neuron, it depolarizes the neuron (GABA excitation), which is the polar opposite to the canonical inhibitory function of GABAergic neurotransmission in the adult brain (Rivera et al., 1999; Hubner et al., 2001).

Since the discovery of ‘GABA excitation’, this intriguing stage of brain development has been under intense investigation. Given that the development of GABAergic synapse temporally precedes glutamatergic synapses, one popular theory suggests that the main function for the excitatory action of GABA is to provide excitatory drive to the young nervous system prior to the maturation of the glutamatergic system. The excitatory action of GABA can lead to Ca^{2+} influx, and trigger downstream signaling cascade in neural stem cell (Ge et al., 2006; Kim et al., 2012) to promote stem cell survival and proper synaptic integration of new-born neurons into existing neural network. GABA excitation has also been found to be critical for the neurons in the developing nervous system for proper migration and normal morphology development (Cancedda et al., 2007; Bortone and Polleux, 2009).

Remarkably, premature termination of GABA excitation by forced expression of KCC2 leads to perturbations in brain development, instead of facilitating neuronal maturation. The neurons that has been genetically manipulated to skip GABA excitation stage demonstrate deficits in neuronal morphology (Horn et al., 2010) and disturbed excitation/inhibition balance (Akerman and Cline, 2006). Rodent neurons that prematurely express KCC2 before birth showed correct migration and cortical layering properties, but significantly reduced level of dendritic complexity even two weeks after birth (Cancedda et al., 2007). In the developing rodent Medial Ganglion Eminence (MGE), interneurons prematurely expressing KCC2 will stop migrating toward their destination in the cortex (Bortone and Polleux, 2009). These findings, together with the reports that GABA is excitatory in certain brain area and cell types well after the early brain development period (Clarkson and Herbison, 2006; Sun et al., 2012), highlight the importance of the strict temporal and spatial control of chloride transporter expression to ensure proper development and function of the brain.

1.2.2 Regulation of KCC2 and its function beyond ion transporter

Due to its critical function during brain development and function, the expression and activity of KCC2 are under stringent control in neurons. For instance, transcriptional factors REST (RE1-Silencing Transcription factor) can bind with the two RE-1 sites flanking the transcription start site of KCC2 promoter to suppress KCC2 expression (Yeo et al., 2009), while Egr4 (Early Growth Response 4) can activate the transcription of KCC2 gene (Uvarov et al.,

2006; Ludwig et al., 2011b). The expression of KCC2 is also regulated by numerous extracellular cues. BDNF (brain-derived neurotrophic factor) has been shown to both upregulate (Uvarov et al., 2006; Boulenguez et al., 2010; Ludwig et al., 2011a) and downregulate KCC2 expression (Rivera et al., 2004; Coull et al., 2005; Boulenguez et al., 2010). The apparent discrepancy in the literature regarding BDNF regulation of KCC2 may be due to the duration of BDNF application (short-term application decrease KCC2, whereas long-term application tend to increase), the specific types and developmental stages of the neurons analyzed, and the source of BDNF (i.e. BDNF secreted from microglia have been demonstrated to reduce KCC2 in spinal motor neurons). Another neurotrophic factor, IGF-1 (insulin-like growth factor-1), has been shown to regulate KCC2 activity in a tyrosine kinase-dependent manner (Kelsch et al., 2001). Taurine has been found to inhibit KCC2 function via WNK1 (lysine deficient protein kinase) pathway (Inoue et al., 2012), while activating 5-HT signaling can upregulate the function of KCC2 (Bos et al., 2013). Exposure of neurons to an environmental toxin, Bisphenol-A (BPA), leads to significant delay in KCC2 expression and is proposed to be the mechanism for BPA-caused mental retardation cases (Yeo et al., 2013). Interestingly, Zn^{2+} has been demonstrated to be a potent inhibitor of KCC2 function, for treatment of neurons with Zinc for only a few minutes is sufficient to inhibit KCC2 function in a reversible manner (Hershinkel et al., 2009). However, vesicular Zn^{2+} that co-released with glutamate potentiates KCC2 activity through activating GPR39, a G-protein coupled receptor that works as the metabotropic Zinc receptor in neurons (Chorin et al., 2011).

Early immunohistochemistry findings have pointed out that KCC2 is highly enriched in dendritic spines (Gulyas et al., 2001), suggesting the intriguing possibility that KCC2 may serve an important function in excitatory synapses. A discovery made in 2007 in the Kai Kaila lab have showed that in addition to KCC2's chloride transporter function, it also interacts with cytoskeleton proteins to regulate dendritic spine morphogenesis (Li et al., 2007). Neurons that lack KCC2 develop fewer dendritic spines. These spines usually lack clearly-defined spine heads, and exhibit long and thin filopodia-like morphology. Many of the abnormal spines on KCC2 are not functional due to the lack of pre- and post-synaptic protein clusters on the spine heads. Electrophysiological analyses revealed that the excitatory synaptic transmission is severely impaired in the neurons that have KCC2 deficit, corroborate the notion that KCC2 regulates excitatory neurotransmission in addition to its well-studied function in mediating inhibitory neurotransmission. Later molecular/cellular biology studies confirmed that the KCC2 regulation on spine morphology is independent of its ion transporter function (Fiumelli et al., 2012). The

KCC2 regulation of glutamatergic synapse function has added another layer of interest by discovering that the diffusion of AMPA receptors in the dendritic spine is also regulated by KCC2 (Gauvain et al., 2011).

This unexpected function of KCC2 in regulating cytoskeleton remodeling has been demonstrated to act through the direct interaction between KCC2 and the actin binding protein 4.1 N (Li et al., 2007). This reduction in spine density and atypical morphology has been confirmed in organotypical brain slices with electroporation-mediated expression of different KCC2 constructs (Fiumelli et al., 2012). Proper regulation of the density, size, morphology, and plasticity of dendritic spines has been demonstrated to be fundamental in the basic functioning of nervous system, especially for learning and memory (Gu et al., 2010; Bosch and Hayashi, 2011; Fortin et al., 2012; Fu et al., 2012; Lai et al., 2012). Disruption in dendritic spine structure and plasticity has been reported as a common pathological feature and contributing factor to various neurological disorders (Penzes et al., 2011; Landi et al., 2012; Yu and Lu, 2012; Yu et al., 2012). Restoration of KCC2 may prove to be a viable strategy to reverse the dendritic spine-related functional deficit in many neurological disorders.

1.2.3 KCC2 involves in the pathophysiology of brain disorders

KCC2 has proven to be a critical gene for proper brain function and for the survival of the organism. Global knockout of KCC2 gene in mouse model leads to the animal's death at birth (Hubner et al., 2001). Less severe types of KCC2 deficient animal model have been developed, in which massive brain development defect, behavior abnormalities (Tornberg et al., 2005), and impaired electrophysiology properties have been documented (Riekkari et al., 2008). Since the lack of KCC2 is incompatible with life, until now there is no report of a surviving human individual carrying mutations in the KCC2 gene (Blaesse et al., 2009). However, relatively mild disruptions in KCC2 expression and/or function have been documented in many neurological disorders.

One of the first diseases that have been linked to KCC2 deficit is temporal lobe epilepsy (Cohen et al., 2002). Many experimental evidence have pointed out that in epileptic brain, the constant high level of activity can lead to a significant downregulation of KCC2, which in turn exacerbates the system overexcitation by reducing GABAergic inhibition (Kobayashi and Buckmaster, 2003; Jin et al., 2005; Palma et al., 2006). Remarkably, in human neonatal infants before one year of age, potentiating GABAergic neurotransmission actually exacerbates the

epileptic condition (Dzhala et al., 2005). Treatment of neonatal seizure with bumetanide, a selective NKCC1 blocker, can reduce the intracellular Chloride level and ameliorate seizure severity (neonatal seizure). These findings highlight the contribution of GABA excitation to both normal human brain development and in neurological disorders.

In the brain injury and stroke condition, the KCC2 expression level is also found to be significantly reduced around the transient focal cerebral ischemia loci (Jaenisch et al., 2010). The underlying mechanism is likely to be through NMDA-mediated phosphorylation and internalization of KCC2 (Lee et al., 2011). Interestingly, during the stressful period of child-birth labor, the surge of oxytocin from maternal bloodstream can lead to a temporary increase in KCC2 expression in the fetus, effectively preventing excitotoxicity and cell death during delivery (Khazipov et al., 2008).

In neuropsychiatric disorders, a disruption in KCC2 mRNA level has been reported in schizophrenia patients (Arion and Lewis, 2011; Hyde et al., 2011). Differences in expression levels of specific KCC2 transcripts have also been linked to Schizophrenia and affective disorders (Tao et al., 2012). Mutation in the cell adhesion molecule critical for GABAergic synapse formation, neuroligin 2 (NL2), is found in schizophrenia patients (Sun et al., 2011). Unexpectedly, knockdown of NL2 can lead to a significant decrease in KCC2, suggesting KCC2's participation in the pathogenesis of some genetically-defined schizophrenia cases (Sun et al., 2013). Altered KCC2 expression has also been implied in mediating stress axis behaviors (Hewitt et al., 2009). In two recent clinical studies, children with general autism spectrum disorders and children with Fragile-X syndrome, a specific monogenic form of autism (Hagerman et al., 2010), can both be phenotypically treated with NKCC1 blocker bumetanide (Lemonnier et al., 2012; Lemonnier et al., 2013). Two recent research articles have described a delayed GABA functional switch in Fragile-X syndrome mouse model (He et al., 2014), valporate acid-induced autism model (Tyzio et al., 2014), and the alleviation of Fragile-X syndrome-related GABA functional switch deficit in the offspring by treating mutant mother with oxytocin or bumetanide (Tyzio et al., 2014). These findings suggest the intriguing possibility that KCC2 dysfunction may be the core symptom and molecular underpinning responsible for various neurodevelopmental and neuropsychiatric disorders.

In the spinal cord, where the expression onset of KCC2 was the earliest during development, disease-related downregulation of KCC2 can lead to various neurological conditions. After spinal cord injury, KCC2 downregulation in motor neurons leads to spasticity (Boulenguez et al., 2010). Similar spasticity can also be observed after intrathecal BDNF

injection since acute BDNF application is known to downregulate KCC2. Interestingly, later application of BDNF restores KCC2 and alleviates spasticity symptoms. Along the same vein, it has also been discovered that microglia secreted BDNF downregulates KCC2 in sensory neurons, leading to over-excitation and neuropathic pain (Coull et al., 2005).

Remarkably, animal models with KCC2 deficiency develop pathological features similar to those observed in MeCP2 knockout mouse including breathing irregularity (Hubner et al., 2001), smaller body weight (Tornberg et al., 2005), and impaired learning and memory (Tornberg et al., 2005). On the other hand, NKCC1 knockout mouse model suffers from heightened anxiety, imbalance, and severe deafness (Delpire et al., 1999; Flagella et al., 1999). These phenotypes are strikingly similar to mouse model of MeCP2 duplication syndrome (Na et al., 2012b; Samaco et al., 2012), and to the human MeCP2 duplication syndrome patient (Van Esch et al., 2005; del Gaudio et al., 2006). However, it is unknown whether KCC2 plays any functional role in Rett syndrome. In my thesis, we used iPS cell-derived human neurons to establish developmental timecourses of KCC2 expression and GABA functional switch in wild-type and Rett syndrome neurons. We found that human Rett neurons have severe reduction in KCC2 expression, and consequent deficits in both GABA functional switch and glutamatergic synapse development. Our findings revealed a link between KCC2 and Rett syndrome, and may provide a novel framework to understand the pathological causes of autism spectrum disorders at large.

1.3 Rett syndrome

Rett syndrome is a prototype neurodevelopmental disorder categorized as one of the autism spectrum disorders (ASD) (Levy et al., 2009). MeCP2 (Methyl-CpG binding Protein 2) *de novo* mutations in human contribute to more than 80% of Rett syndrome cases, and in more than 95% of classical Rett cases MeCP2 mutation(s) can be found (Chahrour and Zoghbi, 2007; Cohen and Greenberg, 2008). MeCP2 duplication also leads to phenotypes in human patients (del Gaudio et al., 2006; Na et al., 2012a). Human Rett patients suffer from seizure, progressive spasticity, and mental retardation (Weaving et al., 2005; Chahrour and Zoghbi, 2007). Abnormalities in dendritic spine structure in the Rett patient brain have been documented (Chapleau et al., 2009). In animal models of Rett syndrome, synaptic transmission (Dani and Nelson, 2009), disturbed excitation-inhibition balance (Dani et al., 2005), and abnormal spine structure and plasticity have been described (Landi et al., 2012; Zoghbi and Bear, 2012).

Human neurons derived from iPSCs originated from Rett syndrome patients displayed similar synaptic and spine deficits observed in human Rett patients and animal models (Marchetto et al., 2010b; Ricciardi et al., 2012; Li et al., 2013). Deficiencies in a number of signaling molecules, including BDNF (Chang et al., 2006; Zhou et al., 2006), mTOR (Ricciardi et al., 2011; Li et al., 2013), and insulin-like growth factor -1 (IGF-1) (Marchetto et al., 2010b; Li et al., 2013) have been shown to mediate Rett-related phenotypes in mouse models of Rett syndrome or in human iPSC-derived Rett neurons. However, the ultimate signaling molecule that is downstream of MeCP2 and directly regulates synaptic functions remains unknown.

1.3.1 Molecular basis of Rett syndrome

Rett syndrome is a neural developmental disorder defined by the Austrian neurologist Andreas Rett (Rett, 1966). Rett syndrome affects mostly girls; the patients develop normally for 6-18 months before falling into general developmental stagnation and regression (Chahrour and Zoghbi, 2007). Human Rett patients suffer from microcephaly, seizure, progressive spasticity, loss of intentional hand control, stereotypical movement, and mental deterioration (Weaving et al., 2003; Weaving et al., 2005; Jian et al., 2006). In addition to the nervous system defects, weight loss, cardiac abnormalities, breathing abnormalities and high mortality rate have also been reported in Rett patients (Erlandson and Hagberg, 2005; Weaving et al., 2005).

The molecular culprit for Rett syndrome is MeCP2 (Meehan et al., 1992; Amir et al., 1999). Over 95% of the classical Rett syndrome cases have mutation in the MeCP2 gene (Wan et al., 1999; Trappe et al., 2001). Pathogenic mutations include missense mutation, nonsense mutation and frameshift mutations (Christodoulou et al., 2003; Gill et al., 2003; Weaving et al., 2003). The most severe disease causing mutations are nonsense mutation that lead to truncated non-functional protein, and the mutation in the nuclear localization signal sequence of MeCP2. Disease-causing missense mutations found in Rett patients are mainly located in the molecular binding domain (MBD) and the C-terminus of transcriptional repression domains (TRD). For instance, mutation at the 306 amino acid site inside the MBD abolished MeCP2 interaction with the NCoR/SMRT (nuclear-receptor co-repressor/silencing mediator for retinoid or thyroid-hormone receptors) transcriptional repression complex and conferred Rett-like phenotype in animal model (Ebert et al., 2013a; Lyst et al., 2013). Interestingly, a small AT-hook domain in the MeCP2 gene has recently been found to determine the clinical course of Rett syndrome (Baker et

al., 2013). The analysis of different mutations in the MeCP2 gene and correlation to phenotype will provide much insight into the function of MeCP2, and its interaction mechanisms with other molecular machineries to regulate neuronal function.

The expression of MeCP2 is widespread across many brain structures (Shahbazian et al., 2002a; Kishi and Macklis, 2004). In the brain, MeCP2 protein level is relatively low during the embryo stage of development, gradually increasing in early postnatal periods, and then sharply increases right before the period of major synaptogenesis and neuronal maturation (Shahbazian et al., 2002a; Cohen et al., 2003; Kishi and Macklis, 2004). MeCP2 is enriched in neurons. It was estimated from CHIP (Chromatin Co-Immunoprecipitation) analysis that 89% of brain MeCP2 is located in the neuronal nuclei (Shahbazian et al., 2002a; Cohen et al., 2003; Kishi and Macklis, 2004; Zhou et al., 2006; Lyst et al., 2013). However, expressions of MeCP2 are also detected in glia (Ballas et al., 2009; Maezawa et al., 2009; Lioy et al., 2011) and microglia cells (Maezawa and Jin, 2010; Derecki et al., 2012).

MeCP2 binds extensively to the genome in near-hectomer level, and controls the expression of many genes (Skene et al., 2010a; Cohen et al., 2011). The transcriptome analyses between wild-type control and MeCP2 knockout mouse brain demonstrated a subtle but detectable change in gene expression profile, suggesting that although MeCP2 binds with the genome globally, it specifically regulates a subgroup of genes (Tudor et al., 2002). The classical view of MeCP2 function is that it regulates gene expression through binding to the methylated CpG sites within the promoter, and inhibits gene expression by preventing the recruitment of transcriptional machinery components (Jones et al., 1998; Jaenisch and Bird, 2003). This MeCP2 repression model has attracted much attention in the research field, and has been proven correct for the regulation of many genes such as BDNF. MeCP2 can undergo phosphorylation at different sites. The Michael Greenberg lab has nicely demonstrated that neuronal activity phosphorylates MeCP2 at S421 site, leading to its release from the BDNF promoter and an elevated BDNF expression level (Zhou et al., 2006).

However, Rett patients usually suffer from reduced body weight and microcephaly (Chahrour and Zoghbi, 2007; Scala et al., 2007). Similarly, loss of MeCP2 in animal model also leads to a marked decrease in body and brain size (Chen et al., 2001; Guy et al., 2001). Studies using human ES cells as model system also revealed that lack of MeCP2 leads to reduced transcription and translation (Li et al., 2013). Evidently MeCP2 also serves a transcriptional activator role. Recent discoveries pointed out that MeCP2 actually activates more genes that it represses, through binding with CREB (cAMP response element-binding) complex instead of the

HDAC/Sin3A (Histone deacetylases) repressor complex (Chahrour et al., 2008). MeCP2 can also bind with hydroxylated methylated CpG in the promoter regions and increase target gene expression (Mellen et al., 2012).

Another mechanism of MeCP2 regulation of gene expression is through modulating the expression of other transcriptional factors such as the master neuronal gene repressor REST/NRSF (RE1-Silencing Transcription factor/Neuron-Restrictive Silencer Factor) (Chen et al., 1998; Abuhatzira et al., 2007). Other studies have reported that MeCP2, CoREST (REST co-factor) and REST are recruited in one transcriptional repressor complex; synergize to repress neuronal genes at early stages of neural development (Ballas et al., 2005). The NCoR/SMRT transcriptional repressor complex interacts with MeCP2 at the R306 site. This interaction is also found to be critical for the proper modulation of neuronal gene expression (Lyst et al., 2013). Taken together, MeCP2 binding at the gene promoter seems to suppress the expression levels of a limited number of genes, while activating the expression of a large group of genes.

1.3.2 Neurobiology of Rett syndrome

Numerous knockout or knock-in animal models have been developed to study the neurobiology of Rett syndrome (Chen et al., 2001; Guy et al., 2001; Shahbazian et al., 2002b; Zhou et al., 2006; Goffin et al., 2011; Baker et al., 2013; Ebert et al., 2013b; Lyst et al., 2013). In general, animals that lack MeCP2 globally, or carrying severe hypomorphic copies of MeCP2 develop stereotypical Rett-like features including microcephaly, decreased mobility, breathing abnormality and premature death (Chen et al., 2001; Guy et al., 2001). More importantly, restoring the MeCP2 expression in the postnatal MeCP2 deficient animals with a genetic approach (Giacometti et al., 2007; Cobb et al., 2010), or using systemic delivery of Adeno-associated virus carrying the MeCP2 gene (Garg et al., 2013), rescued the Rett-like phenotypes. These loss-of-function and rescue experiments strengthen the causal relationship between MeCP2 and Rett-related phenotypes.

Careful morphology and functional analysis have revealed that in the animal models of Rett syndrome, reduction in synaptic transmission (Dani and Nelson, 2009), disturbed excitation-inhibition balance (Dani et al., 2005), and abnormal spine structure and plasticity were present (Landi et al., 2012). Similar abnormalities in dendritic spine structure (Chapleau et al., 2009), overactivation and seizure activity (Jian et al., 2006) have also been documented in the Rett

patient brain. Further mechanistic studies have demonstrated that MeCP2 regulates excitatory synaptic strength by regulating the number of glutamatergic synapses (Nelson et al., 2006; Chao et al., 2007) and synaptic scaling (Blackman et al., 2012). Deficits in GABAergic synapses have also been characterized in both pre- and post-synaptic compartments in the brainstem of Rett syndrome mouse model (Medrihan et al., 2008). In addition to the obvious important role MeCP2 plays in the early period of brain development, MeCP2 is also important for the maintenance and proper functioning of mature neurons in the adult brain (McGraw et al., 2011).

Studies from conditional knockout Rett syndrome animal models have provided important insights into MeCP2 function at specific times, in specific neural circuits. In the mouse brain, MeCP2 expression increases significantly during the first few weeks after birth (Cassel et al., 2004; Kishi and Macklis, 2004; Skene et al., 2010b). Postnatal MeCP2 inactivation experiments have revealed that MeCP2 is required for the survival of animals not only at early adulthood (8-14 weeks of mouse development, the typical timeframe for the premature death of MeCP2-null animals), but also at later age (30-45 weeks and beyond) (Cheval et al., 2012). These findings support the earlier study that adult deletion in MeCP2 leads to the development of Rett-like phenotypes and premature death (McGraw et al., 2011).

Tissue-specific knockout mouse model have revealed a multitude of MeCP2 functions in different cell types (Alvarez-Saavedra et al., 2007). Deletion of MeCP2 in CamK (Ca^{2+} /calmodulin-dependent protein kinase) positive postmitotic neurons distributed mostly in the forebrain region result in classical Rett-like behavior (Gemelli et al., 2006). Deletion of MeCP2 in *Viaat*⁺ (Vesicular inhibitory amino acid transporter) or *Dlx5/6*⁺ (Distal-less 5/6) GABAergic neurons both result in a reduction in the expression of GABA synthesizing enzyme GAD65 (Glutamate decarboxylase 65 kDa) and GAD67 in GABAergic neurons, a moderate reduction of GABA content in GABAergic neurons, and a mild but faithful recapitulation of Rett-like phenotypes (Chao et al., 2012). Selective deletion of MeCP2 in *Sim1*⁺ (Single-minded homolog 1) hypothalamic neurons result in increase in body weight, and deficits in motor coordination and learning and memory deficits (Fyffe et al., 2008), while selective deletion of MeCP2 in *TH*⁺ (Tyrosine hydroxylase) dopaminergic neurons and *PET1*⁺ serotonergic neurons decreased corresponding neurotransmitter synthesis in the neurons, thus leading to subtle but characteristic behavior phenotypes, such as hypoactivity and heightened aggression (Samaco et al., 2009). These cell-type specific knockout experiments have dissected the function of MeCP2 with precision at the neural circuit level, made detailed correlations between genetic-lesion in specific neural circuits and types of behavior abnormalities, and suggested that perturbation of MeCP2 in

a specific, albeit small, subset of neurons can contribute to corresponding phenotypes at the circuit and behavioral level.

In addition to neurons, MeCP2 deficits in glial cells also recapitulate many Rett-like phenotypes. Gene expression analysis in the glial cells cultured from Rett syndrome mouse models found disturbances including altered gene expression (Yasui et al., 2013) and impaired glutamate clearance (Okabe et al., 2012). In the year 2009, the Gail Mandel group made the surprising discovery that culturing WT neurons on MeCP2 KO glial cells result in a significant impairment in dendrite morphology development and neuronal maturation (Ballas et al., 2009). Later experiments in the animal model adapted the strategy to use tamoxifen-induced Cre transgene driven by GFAP (Glial fibrillary acidic protein) to achieve conditional knockout of MeCP2 specifically in glial cells after the stage of early brain development. Knocking out MeCP2 in glial cells in the adult brain triggered a number of Rett-like deficits including decreased body weight, hindlimb clasping, and irregular breath (Lioy et al., 2011). The neuronal morphology was not significantly altered in the glial knockout animals, probably due to the late timing of MeCP2 knockout induction. On the other hand, postnatal glial-specific activation of MeCP2 expression in a global MeCP2 knockout background lead to recovery of a multitude of disease-related deficits (Lioy et al., 2011).

Besides astrocytes, MeCP2's roles in other types of glial cells have also been explored using conditional knockout strategy. Knocking out MeCP2 specifically in oligodendrocyte lineage cells (NG2-Cre, Chondroitin sulfate proteoglycan 4) resulted in animals that were overall normal, but developed hindlimb clasping and hyperactive phenotypes. MeCP2 restoration specifically in NG2 cells within a global MeCP2 knockout background has lead to improvements in locomotor and hindlimb clasping phenotypes, but only mildly prolonged lifespan (Nguyen et al., 2013). MeCP2 deficient microglia have been demonstrated to have deficits in glutamate processing, and the excessive glutamate secreted by these microglial cells can lead to damage in neuronal dendrite and synapse in co-culture experiments (Maezawa and Jin, 2010). Surprisingly, transplant WT microglia cells into immune-ablated MeCP2 knockout mouse resulted in near-complete recoveries of most of the Rett-like phenotypes (Derecki et al., 2012). Similarly, Lysm-Cre (lysine motif) mediated reactivation of MeCP2 specifically in myeloid cells within a global knockout background lead to improvement in breathing pattern, body weight and lifespan (Derecki et al., 2012). In summary, MeCP2 mediates gene expression in glial cells, and confers non-cell autonomous effect onto neurons to mediate Rett-like pathology.

Remarkably, MeCP2 transgenic mouse lines that have higher MeCP2 protein expression than normal also develop autistic features including coordination deficits, heightened anxiety and synaptic plasticity impairments (Na et al., 2012b), reminiscent of human patients suffering from MeCP2 duplication syndrome (del Gaudio et al., 2006). The severity of the Rett-like phenotype corresponds with the deviation of MeCP2 expression from the normal level (Chao and Zoghbi, 2012). These findings highlight the importance of developing safe therapies to either restore MeCP2 levels comparable to normal neurons, or to find alternative strategies to rescue deficits in the molecular pathways downstream of MeCP2.

Therapeutic reagents have been tested on Rett syndrome mouse models to alleviate symptoms. One of the most well-studied molecule that hold the potential to treat Rett syndrome is BDNF. The expression of BDNF is regulated by MeCP2 (Chen et al., 2003; Zhou et al., 2006; Abuhatzira et al., 2007; Li and Pozzo-Miller, 2014), MeCP2 knockout mouse demonstrates decreased BDNF expression (Li and Pozzo-Miller, 2014), and postnatal restoration of BDNF expression rescues the Rett-like phenotypes in MeCP2 knockout animal models (Chang et al., 2006). Exogenous BDNF treatment of Rett syndrome has been tested on a mouse model and a rescue in synaptic functions has been reported (Kline et al., 2010). In addition, Ampakine has also been found to rescue pathological phenotypes in MeCP2-deficient mouse model by improving BDNF expression (Ogier et al., 2007). IGF-1 shares some common downstream signaling cascades with BDNF, including PI3K/Akt (Phosphatidylinositol-4,5-bisphosphate 3-kinase/Protein Kinase B) pathway, and is considered as a promising molecular pathway to target for the treatment of Rett syndrome. Treatment of MeCP2 mutant mice with a synthetic peptide that mimics the function of IGF-1 partially rescued the survival, behavioral and synaptic deficits (Tropea et al., 2009). This therapeutic potency of IGF-1 to Rett neurons was later confirmed in human iPSC and ES based Rett syndrome neuron model (Marchetto et al., 2010b; Li et al., 2013).

Human Rett patients develop relatively normally within 6-18 months after birth but then display developmental regression with impaired motor function and cognitive deficit (Chahrour and Zoghbi, 2007). Previous studies have demonstrated that MeCP2 regulates global gene transcription and identified a variety of downstream signaling molecules in neurons (Zoghbi and Bear, 2012; Ebert et al., 2013a). However, why Rett patients show a developmental regression with a delay in the onset after birth is still an unanswered question. In this thesis, we suggest that the deficits in KCC2, a gene that has a late-onset expression profile, may underlie the pathogenesis of Rett syndrome.

1.3.3 Human iPS Cell models of Rett syndrome

Rett syndrome is a monogenic neurodevelopmental disorder caused by the mutation of a single gene MeCP2, which makes it an ideal disease to model using iPSC technology. The first iPSC-based model of Rett syndrome was established in the Fred Gage lab (Marchetto et al., 2010b). Since then, a number of studies have been carried out using iPSC lines derived from Rett patients (Rastegar et al., 2009; Ananiev et al., 2011; Cheung et al., 2011; Kim et al., 2011b; Ricciardi et al., 2012; Li et al., 2013). The mutations covered in these studies are all from Rett patient-derived fibroblasts, with the exception of (Li et al., 2013), in which the authors used TALEN genomic editing technology to induce a mutation that lead to the deletion of the exon 3 of MeCP2 in human ES cells. The MeCP2 mutations in these studies including missense mutations (Marchetto et al., 2010b; Ananiev et al., 2011; Kim et al., 2011b), nonsense mutations (Marchetto et al., 2010b; Ananiev et al., 2011; Kim et al., 2011b), and deletion (Marchetto et al., 2010b; Cheung et al., 2011). Non-classical Rett syndrome with mutations in the CDKL5 (cyclin-dependent kinase-like 5) gene has also been successfully modeled using human iPS Cells (Ricciardi et al., 2012).

Human neurons derived from Rett syndrome patient stem cells displayed deficits in maturation including smaller neuronal soma size (Marchetto et al., 2010b; Ananiev et al., 2011; Cheung et al., 2011; Li et al., 2013) reduced dendrite arbor complexity (Li et al., 2013), reduced spine density and abnormal spine morphology (Marchetto et al., 2010b; Ricciardi et al., 2012), and impairment in electrophysiological activities (Marchetto et al., 2010b; Ricciardi et al., 2012; Li et al., 2013). From studying the iPSC model, scientists have discovered molecular pathways that are deficient in the Rett syndrome neurons, including Akt/mTOR (mammalian target of rapamycin) pathway (Li et al., 2013), the interaction between NLG-1 (Neuroigin-1) and PSD95 (Postsynaptic Density Protein 95 kDa) (Ricciardi et al., 2012), and IGF-1 signaling pathway (Marchetto et al., 2010b). Bioactive reagents including gentamycin (Marchetto et al., 2010b), BDNF (Marchetto et al., 2010b; Li et al., 2013), and IGF (Marchetto et al., 2010b; Li et al., 2013), have been applied to Rett human neuron models to test their therapeutic effect. Similar to results generated from Rett mouse model, gentamycin, IGF and BDNF all rescued the neuronal morphology and synaptic deficits observed in Rett human neuron model (Marchetto et al., 2010b; Li et al., 2013), providing compelling evidence to support the use of human neurons derived from Rett iPSC as a tool to model Rett syndrome, and screen for compounds with therapeutic potential.

In summary, despite the wealth of discoveries that have characterized the expression, function and regulation mechanisms of MeCP2, the ultimate signaling molecule(s) downstream of MeCP2 that directly regulates synaptic functions remains unknown. Novel contribution from research efforts utilizing both animal models and human iPSC models to gain deeper understanding of the molecular mechanism of Rett syndrome is in great need. In my thesis, we demonstrated that KCC2 is a key gene downstream of MeCP2 that directly regulates both excitatory and inhibitory neurotransmission. Our results provide a mechanistic explanation to the pathogenesis of Rett syndrome, and contribute to the formulation of a unified theory to understand other autism spectrum disorders.

1.4 Glial cells in health and disease

The star-shaped astrocytes in the brain never cease to amaze people, equally remarkable are the substantial transformations they undergo in disease conditions. It has become increasingly clear that glial cells are more than brain 'glues', as their name originally indicated. They actively participate in the development, maintenance, and function of the brain. Moreover, much insights have been gained from recent studies to reveal glial cell's involvement in various pathological conditions. What do astrocytes normally do? and how do these functions go awry under pathological conditions? These are significant questions that demand significant answers.

Looking at the molecular level, from studying the transcriptome of astroglial cells, one could easily appreciate that they express different sets of genes comparing to neurons and oligodendrocytes. What are the functions of these glial-enriched genes? Recent studies have revealed interesting differences between human and mouse astrocytes, and accumulating evidences suggest that human astrocytes are key determinants of our superior cognitive abilities. What are the fundamental differences between human and mouse astrocytes, and how do they influence brain function? In this section, I will review various literature on the topics mentioned above, with an emphasis on astroglial cells biology.

1.4.1 Glial cells modulate synapse function, regulate stem cell behaviors, and uptake neurotransmitter

Glial cells consist half the brain mass, provide fundamental support to the nervous system, and participate in many physiological processes (Barres, 2008). Three major types of glial cells are astrocytes, oligodendrocytes, and microglia. Astrocytes are star-shaped glial cells with many major processes, and send thousands of fine motile endfeet to contact neuron cell body and dendrites, synapses, blood vessels, and other astrocytes. It has been demonstrated that virtually all astrocytes have endfeet in contact with blood vessels, which can shuttle nutrients from the blood stream to the neurons (Nave, 2010a, b; Funfschilling et al., 2012). One of the most critical function of astrocytes is to buffer extracellular potassium, uptake neurotransmitters including glutamate and GABA to maintain environmental homeostasis (Schousboe et al., 2013). Astrocytes sense neurotransmitter release from neurons, form gap junctions between other astrocytes, generates and propagates calcium waves (Haydon, 2001; Nedergaard et al., 2003). This coupling between astrocytes contributes to the synchronization of neural network activities, setting tone for network activity, and participates in long-range information transmission (Haydon, 2001).

Importantly, bioactive molecules in the circulation must be taken up by astrocytes before they can reach the neurons. Ample evidence has also pointed out that astrocytes can respond to bioactive molecules, and send signals to neurons in response. Thus, astrocytes perform filtering, decoding and information processing function to mediate the communication between the blood and the brain (Begley and Brightman, 2003; Pardridge, 2003; Abbott et al., 2006). The selective gating and responsive decoding functions of astrocytes and the capillary endothelial cells they contact have been collectively termed the ‘Blood Brain Barrier’ (BBB). Astrocytes secrete many proteins with known or unknown functions (Keene et al., 2009; Hughes et al., 2010). Early studies in the cell culture system revealed that co-culturing neurons with astrocytes, even without physical contact between the two cell types, can significantly promote neuronal survival, proving that glial cells can secrete trophic factors to influence changes in neuron (Banker, 1980). Since then, a number of astrocyte-secreted neuroactive factors and cytokines have been identified including TNF α (Tumor necrosis factor alpha) (Lieberman et al., 1989), TGF-beta (Transforming growth factor beta) (Saad et al., 1991), NGF (Nerve growth factor) (Saad et al., 1991), Ephrin B (Ashton et al., 2012), IGF (Liu et al., 1994), BDNF (Coull et al., 2005).

A highly interesting aspect of astrocyte-neuron interaction suggests that glial cells are fundamentally important for neuronal synapse formation and plasticity (Banker, 1980; Haydon, 2001; Yang et al., 2003; Hama et al., 2004; Barres, 2008; Eroglu and Barres, 2010). In the year 2001, the Ben Barres group used highly purified retinal ganglion neurons as the model system to demonstrate that neurons virtually cannot develop functional synapse without the support from astrocyte. The nature of astrocytic support is through secreted proteins, for glial conditioned medium exerts similar beneficial effect on synapse formation. Careful studies later revealed the nature of the first key glial secreted protein that can promote synapse formation: Thrombospondin (TSP). TSP is a large extracellular matrix component that potently increases glutamatergic synapse number (Christopherson et al., 2005). Interestingly, these synapses induced by TSP are ultrastructurally normal but postsynaptically silent. Suggesting that additional factors may work with TSP synergistically to promote synapse formation. Later studies identified cholesterol as a critical factor for the maturation of presynaptic structure (Mauch et al., 2001), SPARC (secreted protein acidic and rich in cysteine) (Kucukdereli et al., 2011), and glypicans (Allen et al., 2012; de Wit et al., 2013) to be important for the maturation of the postsynaptic compartments of glutamatergic synapses. A recent study found that astrocytes facilitate the onset of excitatory synaptic events in neurons differentiated from human embryonic stem cells (Johnson et al., 2007). However, the precise role of glial cells in the differentiation and maturation of human neurons derived from iPSCs is still not well understood.

Interestingly, although it has been well demonstrated that astrocyte secreted factor(s) can potentiate inhibitory synaptic transmission (Kang et al., 1998) and secrete proteins to promote GABAergic synapse formation and the general development of GABAergic neurons (Hughes et al., 2010); so far no astrocytic factor that has the ability to increase GABAergic synapse formation has been identified. One candidate molecule is BDNF, which is a known molecule to increase the GABAergic synapse formation and GABAergic neurotransmission; loss of BDNF in neurons leads to local reduction in GABAergic synapses number (Kohara et al., 2007). The receptor of BDNF, TrkB (Tropomyosin related kinase B), has also been demonstrated to mediate astrocyte's ability to promote the formation of inhibitory synapses (Elmariah et al., 2005). However, the expression of BDNF in mouse astrocytes is low, and conditioned medium from BDNF deficient mouse astrocytes does not influence GABAergic synapse formation in treated neurons, suggesting the participation of astrocytic BDNF in GABAergic synapse formation is minimal in rodents (Elmariah et al., 2005).

Glial cells also influence stem cell behavior to shape brain composition and circuitry from embryonic development and beyond. During early stages of development, radial glial cells serve the function of stem cells, and pave the migratory path for the newly generated neurons to follow (Rakic, 1978; Hansen et al., 2010). Experimental evidence has also suggested that glial cells can regulate diverse stem cell functions such as proliferation (Lie et al., 2005; Chell and Brand, 2010), migration (Aarum et al., 2003), and differentiation (Song et al., 2002a; Ashton et al., 2012). How glial cells influence the fate choice of human iPS cells and how glial cells affect the functional development of the newborn human neurons derived from iPS cells remain poorly understood.

In my dissertation, we have demonstrated that astrocytes play a critical role in promoting both morphological and functional maturation of human neurons derived from iPSCs. Compared to commonly used substrate laminin, astrocytes significantly enhanced neuronal dendritic complexity, the expression of ionic channels and neurotransmitter receptors, and the frequency and amplitude of synaptic events. Human neurons were capable of firing action potentials and releasing neurotransmitters after plating hNPCs on astroglial substrate for only 1-2 weeks. We also demonstrated that the iPSC-derived human neurons can be incorporated into preexisting mouse neural network after one week of coculture. Our data suggest that astroglial cells are instrumental in promoting the functional development of human neurons derived from iPSCs. This study provides an important functional timeline of human neuronal development to guide future research using hiPSC-derived neurons for disease modeling and drug screening.

1.4.2 Glial cells contribute to the pathogenesis of diseases

The contributions of glial cells in various disease conditions have been well characterized. In brain and spinal cord injury, ischemia conditions, and in Alzheimer's disease, glial reactivity is greatly enhanced (Malhotra et al., 1990; Brenner, 2014). The cell bodies of reactive astrocytes migrate toward the center of injury, and the processes of reactive glial cells become more elaborate and motile (Pekny and Nilsson, 2005; Bardehle et al., 2013). The reactive astrocytes express different set of genes comparing to normal resting glial cells, including a marked upregulation of GFAP (Zamanian et al., 2012). Glial dysfunction can contribute to the exacerbation of diverse disease conditions (Hamby and Sofroniew, 2010).

Astrocytes can also influence neuronal function in non-cell autonomous manner. Recent research evidence pointed out that in the diseased brain; dysfunction on the astrocyte part can influence neurons and confer disease-related impairments. ALS (Amyotrophic lateral sclerosis) is a prime example of non-cell autonomous effect astrocytes can exert on neurons to confer a disease phenotype. The mutation in SOD (superoxide dismutase) gene in glial cells alone can cause pathological effect on neurons and lead to motor neuron death in a non-cell autonomous fashion. Conversely, plating SOD deficient neurons on WT astrocyte can halt neuronal death (Di Giorgio et al., 2007; Di Giorgio et al., 2008). Glial cells in the Rett syndrome animal model brain can also exert non-cell autonomous effect on neurons to hinder its maturation. When culturing WT neurons on the glial cells cultured from MeCP2 knockout mouse brain, the neurons develop fewer dendrites and smaller cell bodies, and exhibit deficits in functional maturation (Ballas et al., 2009). Conversely, in a MeCP2 knockout mouse brain, restoration of MeCP2 specifically in astrocytes in a global knockout background can lead to functional recovery at the behavioral level (Lioy et al., 2011). Unexpectedly, the transplantation of wild-type microglial cells into Rett syndrome mouse model with immune system ablated can also reverse many Rett-like disease phenotypes (Derecki et al., 2012), suggesting that microglial cells are also active participants of the complex biology of Rett syndrome pathogenesis.

Numerous studies have established that mouse glial cells can express glutamate transporters and uptake glutamate. However, in the case of brain cancer, the glutamate uptake property of astrocyte was actually reversed. Instead of clearing up glutamate from the extracellular space, glioma cells accumulated and secreted large amount of glutamate, leading to excitotoxicity, which further exacerbated the disease condition (Buckingham et al., 2011; Campbell et al., 2012). It has also been found that the Rett syndrome astrocytes have deficits in glutamate clearance (Okabe et al., 2012), and microglia from MeCP2 knockout mouse release elevated level of glutamate, causing damages in neuronal dendrite and synapses (Maezawa and Jin, 2010). These phenomena regarding altered astrocyte glutamate processing under disease conditions are intriguing as they are remarkable. It begs the question about the signaling cascade that triggered astrocyte to secrete, instead of uptake, glutamate; and spurs more experiments to elucidate how these impairments may contribute to various pathologies in the brain.

1.4.3 The molecular and functional differences between human and mouse glial cells

A human and a mouse brain share many basic biological principles, nonetheless they are fundamentally different in various aspects. The cognitive ability of a human brain is far more superior to all the other species in the animal kingdom, even to our very close evolutionary relative non-human primates. Rodent animal model and murine cell culture system have traditionally been central to biomedical research and drug testing. Understanding the difference between mouse and human brain is crucial for the successful translation of mouse model study results into disease-curing therapies to treat human neurological conditions.

The difference between human and mouse neurons have been well-documented. Generally, the neurons in the mouse brain reach maturation in one to two weeks, while neurons in the human brain generally develop very slowly. My own data suggest that human and mouse neurons exhibit fundamental differences in their development timelines of key morphological and functional characteristics (Fig. 4-16). Similarly, recent literature report that pluripotent stem cell-derived glutamatergic neurons (Espuny-Camacho et al., 2013) and interneurons (Nicholas et al., 2013) acquire mature neuronal properties very slowly. For example, stem cell-derived human interneurons undergo their development course according to an intrinsic timeline, as have been shown by comparative electrophysiology recordings on endogenous human interneuron subtypes at 22 gestation week (Nicholas et al., 2013).

Astrocytes consist of more than half the brain mass, yet the differences between human and mouse astrocytes have been poorly studied (Zhang and Barres, 2010). All therapeutic agents administered into the circulation must go through astrocytes to enter the brain, and astrocytes can be targeted by drug to treat brain conditions (Hertz et al., 2004). Elucidating the difference between human and mouse astrocytes is crucial. One key difference between human and mouse brain is that the human brain has a highly proliferative outer radial glial cell population. These stem cells self-renewal robustly, generating many neurons to populate our brain. As a result our brains have much thicker and more complex cortical architecture, especially in the prefrontal cortex (Hansen et al., 2010). It is safe to speculate that human glial cells may have a stronger ability to support stem cell division in order to generate enough cells to populate the brain.

Microarray experiments comparing the whole-brain transcriptome difference between human and mouse brain have been carried out (Miller et al., 2010). Cross-referencing the gene expression difference between human and mouse brain with the astrocyte transcriptome (Cahoy et al., 2008) revealed that a number of genes with highly different expression patterns were actually

astrocytic genes (Zhang and Barres, 2013), including GTF2I, ZFP36L2, HSPA2 and PRDX6. The function of these growth factors awaits further thorough studies.

Direct anatomical and functional study of human astrocytes from surgically dissected acute human tissue samples have revealed a few anatomically defined classes of astrocytes that are unique to humans, including regularly spaced varicosities astrocytes, and interlaminar localized astrocytes (Oberheim et al., 2009). The human astrocytes showed an extended morphology with approximately 10-fold increase in GFAP positive major processes, and propagate calcium wave four-folds faster than mouse astrocytes. These unique hominid features of human astrocytes may underlie the superior competence of our human brain.

An innovative approach to study the difference between human and mouse astrocytes was developed in the Nedergaard lab (Han et al., 2013). The researchers derived human glial progenitor cells from human pluripotent stem cells. These *in vitro*-purified human glial progenitor cells were then injected into mouse brain to study whether they can differentiate into functional human astrocytes *in vivo* and if so, whether the introduction of human astrocytes has any influence on mouse brain function. Surprisingly, not only did the human glial progenitor cells survive and differentiate into functional astrocytes that can form gap junctions and propagate calcium waves, the cognitive function of the recipient mouse were also significantly improved in comparison to sham injection controls. This groundbreaking study identifies astrocyte as a powerful factor in determining the cognitive function of nervous system, highlights the functional differences between human and mouse astrocytes, and emphasizes the importance to understand these differences for both basic research purpose and for therapeutic strategy development.

In my dissertation, we have demonstrated that human and mouse astrocytes are fundamentally different in their ability to process neurotransmitters, regulate stem cell function, and promote synapse formation. Selected datasets from a deep sequencing-based transcriptome analyses campaign, aim to systematically compare the gene expression profile between human and mouse astrocytes, will also be presented. These data will contribute significantly to the emerging research trend to elucidate the unique contribution of human astrocytes to our cognitive competence and disease conditions.

Chapter 2

Materials and Methods

2.1 Maintenance and differentiation of human iPSC-NPC cells

NPCs were derived from human iPS Cells (WT126 clone 8 and clone 6; N126I clone 6; WT33 clone 1; WT83 clone 7 and clone 6; Q83X clone 1 and clone 6) as described before (Marchetto et al., 2010b), and expanded in a proliferation medium that contained DMEM/F12 with Glutamax, B27-supplement (Invitrogen), N2 (Stem Cells), 500 ng/ml human Noggin (Fitzgerald), 10 μ M ROCK inhibitor (Rho-associated protein kinase inhibitor, Axxora), 20 ng/ml FGF2 (Basic Fibroblast Growth Factor 2, Invitrogen), and 1 μ g/ml laminin (Invitrogen). After cells reach ~ 80% confluence, they were gently dissociated with Triple (Invitrogen), resuspended in culture medium, and seeded onto coverslips in 24-well plates at a density of 40,000 to 80,000 cells per well. To start a neuronal differentiation process, hNPCs were exposed to a differentiation medium consisting of DMEM/F12 with Glutamax, N2, 0.5% FBS (Fetal Bovine Serum, Invitrogen), 1 μ M retinoic acid (Sigma), 200 nM ascorbic acid, 1 μ g/ml laminin, and 10 μ M ROCK inhibitor. In the case of using glial conditioned medium (GCM) for NPC differentiation, naive NPC differentiation medium was pre-incubated with mouse astrocytes for up to three days before use. The NPCs used in this study were about 10 – 15 passages after the original differentiation from hiPSCs.

2.2 Primary astroglial and neuronal cell culture

Astroglial cells were cultured from the cortical tissue of newborn mouse pups (postnatal day 3 to 5) similar to methods previously described (McCarthy and de Vellis, 1980; Yao et al., 2006; Deng et al., 2007; Jiang and Chen, 2009). Briefly, cortical tissue was dissected out and chopped into small cubes with dimensions around 1 mm, and incubated in 0.05% trypsin-EDTA solution (Invitrogen) for 30 min. After enzyme digestion, tissue blocks were triturated to dissociate the cells and centrifuged. The cell suspension was then plated onto 25 cm² flasks and maintained in 5% CO₂, 37 °C incubator for up to a week. The glial culture medium contained MEM, 5% FBS, 20 mM D-glucose, 2.5 mM L-glutamine, and 25 unit/ml penicillin/streptomycin.

To remove non-astrocytes, flasks were vigorously shaken to peel off loosely attached cells such as neurons and oligodendrocytes. Astrocytes were spreading as a thin layer and very difficult to be shaken off. After reaching confluence, the astroglial cells were trypsinized and resuspended before seeded on 12 mm coverslips as the substrate for neurons or NPCs.

Neurons were prepared from P1 mouse cortical tissue using similar protocol described above for glial culture (Yao et al., 2006; Deng et al., 2007), except that dissociated cells were directly plated on a monolayer of astrocytes. The neuronal seeding density was 4000 - 8000 cells/cm².

To prepare microisland culture, coverslip is coated with a non-permissive substrate of 10% agarose, microdots of permissive substrate (1% Poly-D-lysine + 1% collagen) were sprayed on top of the agarose coating to form small 'islands' for cells to attach and survive. The diameter of microislands were usually 200 to 500 μ m. A layer of astrocytes were first seeded as feeder. Low density of primary mouse neurons are subsequently seeded on the astrocyte-covered microislands. NPCs will then be seeded to the system one week after neuronal culture.

2.3 Plasmid constructs and transfection

Calcium-Phosphate transfection methods was performed using a protocol developed in our laboratory (Jiang and Chen, 2006). Reagents from Clontech CalPhos Mammalian Transfection Kit were used to prepare Calcium phosphate-DNA precipitates. Neuronal cultures were exposed to precipitates for 30 min and precipitates were washed off using transfection medium containing MEM (Modified Eagle's Medium) and 30 mM Glucose, pH adjusted to 7.2 with acetic acid.

The constructs used in my research are as follows: KCC2 and KCC2 shRNA constructs, gift from Dr. Yun Wang, Fudan University, Shanghai, China. promotor for KCC2 plasmid is CMV, the vector is pIRES2-EGFP. The MeCP2 and MeCP2 shRNA plasmids are generous gift from Dr. Michael Greenberg's lab, Harvard University, Boston, MA (Zhou et al., 2006). The construct is named LEMPRA (lentivirus-mediated protein-replacement assay). The promotor for MeCP2 shRNA is pU6, for MeCP2 is pUbiquitin. The REST full-length (FL) and REST dominant negative (DN) plasmids were gifts from Dr. David Anderson's lab, California Institute of Technology, Pasadena, CA (Chen et al., 1998). The backbone of the constructs are pBSKs, the

promoters are lac. The FUGW-GFP control constructs is gift from Dr. Roger Nicoll (Shipman et al., 2011). Human full-length cofilin constructs (peGFP-N1-cofilin-WT/S3E/S3A and pmRFP-N1-cofilin-WT/S3A), LIMK and SSH constructs were generously provided by Dr. James Bamburg (Colorado State University, Fort Collins, CO).

2.4 Virus production and infection

Lentiviral particles were prepared by transfecting HEK cells with GFP or KCC2 shRNA lentiviral construct, together with a VSVG vector to ensure proper packaging of virus particles. After transfection, the HEK supernatant were collected for three days, filtered, and subject to high speed spinning (30'000g) to pellet the virus particles. The pellets were dissolved in 50 µl PBS for 2 hours before aliquot for storage at -80 °C. Normally 10 µl virus preparation can give ~90% infection efficiency when applied to cultured neuronal or non-neuronal cells

2.5 Immunostaining and imaging

Cells used for immunofluorescence staining were washed with PBS, fixed in 4% paraformaldehyde for 40 min, and permeabilized with 0.1% Triton in PBS for 5 min. The Triton was then washed off and 5% donkey serum was applied to the cells for 30 min to block non-specific binding. The primary antibodies were added to the blocking solution and incubated overnight. The next day, excess primary antibodies were washed off and proper fluorophore-conjugated secondary antibodies were added to the coverslips and incubated for 45 min. After the secondary antibody incubation, coverslips were rinsed 6 times with PBS and then mounted with mounting solution (50% glycerol, 50% 0.1 M NaHCO₃ in water, pH 7.4). Epiluminescent images were acquired on a Nikon TE-2000-S microscope. Digital images were captured with Simple PCI imaging software. Confocal fluorescent images were collected using an Olympus FV1000 confocal microscope.

The human iPSC-lineage cells were distinguished from the feeder layer of mouse astrocytes by their immunoreactivity against human nuclei antigen (HuNu, Millipore). Neuronal differentiation of hiPSC-NPC was detected by antibodies specific for doublecortin (Abcam) and β -3 tubulin (Tuj1, Covance). To identify neuronal subtypes, we have used antibodies including

NeuN (Millipore), GABA (Abcam), Glutamate (Chemicon), Tyrosine Hydroxylase (TH, Millipore), Choline Acetyltransferase (CHAT, Millipore). To detect glial cells in our culture, we used antibodies against GFAP (Millipore), and S100 β (Abcam). The synaptic connections were identified with antibodies specific for SV2 (Synaptic vesicle glycoprotein 2, Developmental Studies Hybridoma Bank, University of Iowa, Iowa City, IA), synaptophysin (Chemicon), GAD67 (AnaSpec), VGlut (Synaptic Systems). MeCP2 expression was detected by antibodies against MeCP2 (Rabbit anti MeCP2, Diagenode; Mouse anti MeCP2, Abcam)

Brain Slice – Human hippocampal brain samples were acquired from NICHD brain tissue bank. The tissue blocks were dehydrated with 30 % sucrose. Sections of 20 μ m thickness were made using a cryostat (Leica). Sections were submerged in sodium citrate buffer (0.1M, pH 6.0) and heated to 95 °C for 20 min. Labeling of KCC2 was performed using a DAB peroxidase substrate kit (Vector labs).

2.6 Immunoblotting

The protein samples were collected from cultured cells and incubated in lysis buffer (in mM: 250 sucrose, 10 Tris, 10 HEPES, 1 mM EDTA, with protein kinase inhibitor and protease inhibitor, pH adjusted to 7.2), sonicated for 1 min to break down cellular organelles. The protein samples were separated on 12% SDS-PAGE gel and transferred to PVDF membrane. After a 30 min blocking with 5% milk in TBS, the PVDF membrane was incubated overnight at 4 °C with primary antibodies diluted in TBS-milk at the following concentrations: KCC2 (1:1000, Millipore), Actin (1:1000, BD Bioscience) NKCC1 (1:1000, Iowa Hybridoma bank) The membrane was rinsed with TBS, followed by TBS + 0.05% Tween 20 for 3 - 5 min, and then rinsed with water for three times before a chemiluminescence method (HRP substrate, Millipore) or Odyssey-Clx Western blot scanner (Li-Cor Biosciences) was used to detect the signal.

2.7 Electrophysiology

Whole-cell recordings were performed using the Multiclamp 700A patch-clamp amplifier (Molecular Devices, Palo Alto, CA) (Deng et al., 2007). The recording chamber was perfused continuously with a bath solution that consist of (in mM) 120 NaCl, 30 glucose, 25 HEPES, 5

KCl, 2 CaCl₂, 1 MgCl₂. pH was adjusted to 7.3 with NaOH. When recording glutamate currents, the 1 mM MgCl₂ was omitted from the bath solution to avoid Mg²⁺ blockade on NMDA receptors. Patch pipettes were pulled from borosilicate glass and fire-polished to a resistance of 4 - 6 MΩ when filled with pipette solution, consisting of (in mM) 147 KCl, 5 Na-phosphocreatine, 2 EGTA, 10 HEPES, 4 MgATP, and 0.5 Na₂GTP, pH 7.3 adjusted with KOH. The series resistance was typically 10 - 20 MΩ, and compensated by 20 - 40% when recording Na⁺/K⁺ currents. For voltage-clamp experiments, the membrane potential was typically held at -70 mV. Drugs were applied through a six-channel gravity-flow drug delivery system (VC-6, Warner Hamden, CT). Data were collected using pClamp 9 software (Molecular Devices, Palo Alto, CA), sampled at 10 kHz and filtered at 1 kHz.

To estimate GABA reversal potential (EGABA) in neurons, we performed gramicidin-perforated patch clamp recording to acquire GABA-mediated responses without altering intracellular Cl⁻ concentrations (Myers and Haydon, 1972; Chen et al., 1996). Gramicidin (Sigma) was first dissolved in DMSO to a concentration of 25 mg ml⁻¹, and then diluted in pipet solution to a final concentration of 50 μg ml⁻¹. The pipet solution contains (in mM) 147 KCl, 5 Na-phosphocreatine, 2 EGTA, 10 HEPES, 4 MgATP, and 0.5 Na₂GTP, pH 7.3 adjusted with KOH. The diluted gramicidin solution was usually effective for up to 2 h. To apply GABA locally, a fine pipet (2 - 3 μm opening) filled with 100 μM GABA solution was positioned close to the cell body (3 - 5 μm). A Picospritzer (Parker Instrumentation) was used to eject GABA solution with air pressure of 10 p.s.i. and duration of 100 ms. A constant perfusion of bath solution was applied during the experiment, which washed off GABA immediately.

Data were collected using pClamp 9 software (Molecular Devices, Palo Alto, CA), sampled at 10 kHz and filtered at 1 kHz. Off-line data analyses of GABA reversal potential was calculated using a linear regression equation of neuronal GABA responses recorded at different holding potentials. Synaptic events were analyzed using MiniAnalysis software (Synaptosoft, Decatur, GA). All experiments were performed at room temperature. All data were presented as mean ± SE. Student's *t* test and ANOVA test followed with Bonferroni correction were used for statistical analysis.

2.8 Calcium imaging

Calcium imaging of the neuronal responses to GABA (100 μ M) were performed as described previously (Jiang and Chen, 2009). Cells were incubated in bath solution containing 10 μ M fura-2 AM (Invitrogen) for 45 min at 37 °C. After dye loading, coverslips were washed in bath solution for 15 min to allow internalization of the dye. Coverslips were then transferred to a perfusion chamber mounted on microscope for continuous live cell imaging. Calcium signals were calculated as ratios of the fluorescent emission signals at 340 nm and 380 nm excitation wavelengths, and processed by Simple PCI imaging software (C-Imaging).

Human neurons with GABA-induced 340/380 emission ratio increase of greater than 0.1 were defined as responding to GABA, and the ratio of neurons responding to GABA from each coverslip was calculated from two to four imaging fields. After GABA stimulation, the human neurons were given 60 mM KCl stimulation. Cells that exhibit a 340/380 ratio increase less than 0.1 were excluded from the analysis.

2.9 Dendritic spine analysis

Dendritic spines were analyzed using ImageJ software and the NeuroJ plugin. The image acquisition and analysis were blind to the genes transfected. A total length of 100 μ m of dendrites per neuron were selected from the secondary branches of the dendritic tree. Both the number and the length/width of dendritic spines were quantified using ImageJ.

2.10 Sholl analysis on dendritic complexity

The Sholl analysis method (Wearne et al., 2005; Ristanovic et al., 2006) was used for the morphological assessment of individual cells based on fluorescent images of DCX immunostaining. A series of concentric circles with 20 μ m increments were radiated from the cell body. Each cell was traced and analyzed using NeuronStudio software (Mount Sinai School of Medicine, New York, NY). The number of intersections of dendrites made with these circles, as well as the number of branch points, were counted manually. The cell soma size was determined using ImageJ software on the phase contrast images of neurons.

2.11 RNA extraction, qRT-PCR, and cDNA deep sequencing

RNA samples from human or mouse astrocytes were collected using a RNA extraction kit (Nucleospin RNA extraction kit, Macherey Nagel). Reverse-transcription of RNA into cDNA was performed using first-strand reverse transcription kit (M-MLV RT first strand cDNA synthesis kit, Life Technologies). Quantitative RT-PCR experiments were performed using SYBR green dye (Invitrogen) and StepOne Real-Time PCR systems (Applied Biosystems), and repeated for 3-8 times. For deep sequencing experiments, RNA samples were collected and loaded into RNA storage cartridges (Gentegra) for stabilization and transportation. The reverse transcription and subsequent cDNA sequencing experiments, data collection, and rpkm (reads per kilo base per million) calculation were performed in Fudan University, China.

2.12 Statistical analysis

For the experiments comparing two groups of data, student's t-test were used to determine whether the difference was significant. For the experiments comparing multiple groups, one-way ANOVA with Bonferroni correction were used unless otherwise specified. Kolmogorov-Smirnov test were employed to detect the differences in cumulative distribution between two datasets.

Chapter 3

KCC2 Deficiency in Rett Syndrome Human Neurons Leads to Functional Deficits in both Excitatory and Inhibitory Neurotransmission

In this study, our lab collaborated with Dr. Maria Marchetto in the lab of Dr. Fred Gage at the Salk Institute, and Dr. Cassiano Carromeu in Dr. Alysson Muotri's lab at UCSD School of Medicine. They generously provided the WT126 and WT33 NPC cells for our research. Dr. Li Zhou did the western blot experiments. Julie Kim did the dendritic spine analysis. Lei Zhang did some cell culture work. Part of this work has been submitted to *Science* and is now under review.

3.1 Results

3.1.1 Prolonged GABA functional switch in human neurons

The excitation-inhibition balance is critical for brain functions. Many brain diseases including autism spectrum disorders are associated with an imbalance between glutamatergic excitation and GABAergic inhibition (Dani et al., 2005; Gogolla et al., 2009; Yizhar et al., 2011). We have previously demonstrated that human neurons derived from iPS cells originated from Rett syndrome patients (Rett neurons) showed significant glutamatergic deficits (Marchetto et al., 2010b). Recently, we demonstrated that astrocytes play a critical role in promoting the differentiation and functional maturation of human neurons derived from hiPSCs (Tang et al., 2013). During our continuous investigation of the molecular mechanisms of Rett syndrome using human iPS cells in culture, we found that the expression pattern of KCC2 (SLC12A5), a neuron-specific K^+ - Cl^- cotransporter, follows the prolonged timecourse of KCC2 expression during early human brain development (Dzhala et al., 2005). In the first month of culturing human neurons differentiated from hiPSC-derived neuroprogenitor cells (NPCs) on astrocytes (Tang et al., 2013), the KCC2 expression level was very low and almost undetectable (Fig. 3-1a). After two-month culture, we were able to detect KCC2 expression in 57.9 ± 6.5 % of neurons (Fig. 3-1b); and only after 3-month culture did most of the human neurons show high levels of KCC2 expression (Fig. 3-1c, 88.5 ± 3.7 %). On the other hand, if human neurons were cultured on laminin substrate instead of astrocytes, the KCC2 expression was absent even after 3-month in culture (Fig. 1d), which is consistent with our previous findings that human neurons develop more slowly without astroglial support (Tang et al., 2013).

KCC2 has been shown to play an important role during neural development (Represa and Ben-Ari, 2005; Ben-Ari et al., 2012). KCC2 functions in transporting Cl^- from intracellular to extracellular space to maintain low intracellular Cl^- concentration (Rivera et al., 1999). During brain development, immature neurons typically have high Cl^- concentration due to the absence of KCC2 and high level of NKCC1 (Dzhala et al., 2005), while mature neurons have low concentration of Cl^- due to increased expression level of KCC2 (Ben-Ari et al., 2012). Because GABA_A receptors (GABA_A-Rs) are coupled with internal Cl^- channels, the Cl^- reversal potential

for GABA_A-Rs (E_{GABA}) is typically depolarized in immature neurons but hyperpolarized in mature neurons (Chen et al., 1996). Therefore, GABA undergoes a functional switch from excitation to inhibition during brain development, largely governed by KCC2 expression level (Chen et al., 1996; Ben-Ari et al., 2012). The absence of KCC2 immunostaining in immature human iPSC-derived neurons prompted us to investigate whether GABA played an excitatory function in this early developing stage. We used ratiometric Ca^{2+} imaging to measure GABA-induced Ca^{2+} responses as previously reported (van den Pol et al., 1996). After one-month culture on astrocytes, the majority of neurons showed significant GABA-evoked elevation in Ca^{2+} levels (Fig. 3-1e), suggesting that GABA induced a membrane depolarization and consequently the activation of Ca^{2+} channels. After two-month culture on astrocytes, most neurons showed little response to GABA application (Fig. 3-1f). After 3-month culture, many neurons showed synchronous Ca^{2+} transient increase, an indication of synchronous network activity in this mature stage. GABA application significantly suppressed the spontaneous Ca^{2+} increase, suggesting an inhibitory GABA function in mature neurons (Fig. 3-1g). In contrast, after 3-month culture on laminin, 50% of neurons still showed Ca^{2+} responses upon GABA application (Fig. 3-1h), consistent with the notion that without astroglial support, human neurons remain immature after a longer time (Tang et al., 2013).

Next, we performed patch clamp recordings to directly measure membrane potential changes in response to GABA application. One-month old neurons cultured on astrocytes showed large membrane depolarization and sometimes overlaying action potentials upon GABA application (Fig. 3-1i). Two-month old neurons cultured on astrocytes showed small membrane hyperpolarization (Fig. 3-1j). Three-month old neurons cultured on astrocytes showed large membrane hyperpolarization, which significantly suppressed action potential firing (Fig. 3-1k). In contrast, 3-month old neurons cultured on laminin showed large GABA-evoked membrane depolarization with overlaying action potentials, confirming their immature status (Fig. 3-1l). We further measured GABA reversal potential (E_{GABA}) at different stages using gramicidin-perforated patch recording to keep intracellular Cl^- intact (Chen et al., 1996). We found that one-month old neurons cultured on astrocytes had E_{GABA} between -40 and -50 mV (Fig. 3-1m), whereas 3-month old neurons cultured on astrocytes showed E_{GABA} between -60 and -70 mV (Fig. 3-1n), a significant hyperpolarizing shift during neuronal maturation. In contrast, the E_{GABA} of 3-month old neurons cultured on laminin was similar to that of 1-month old neurons cultured on astrocytes (Fig. 3-1o, quantified in Fig. 3-1p). Together, these results suggest that GABA functional switch

takes a long time to complete during human neuronal development, and astroglial support is essential to promote KCC2 expression and GABA functional switch.

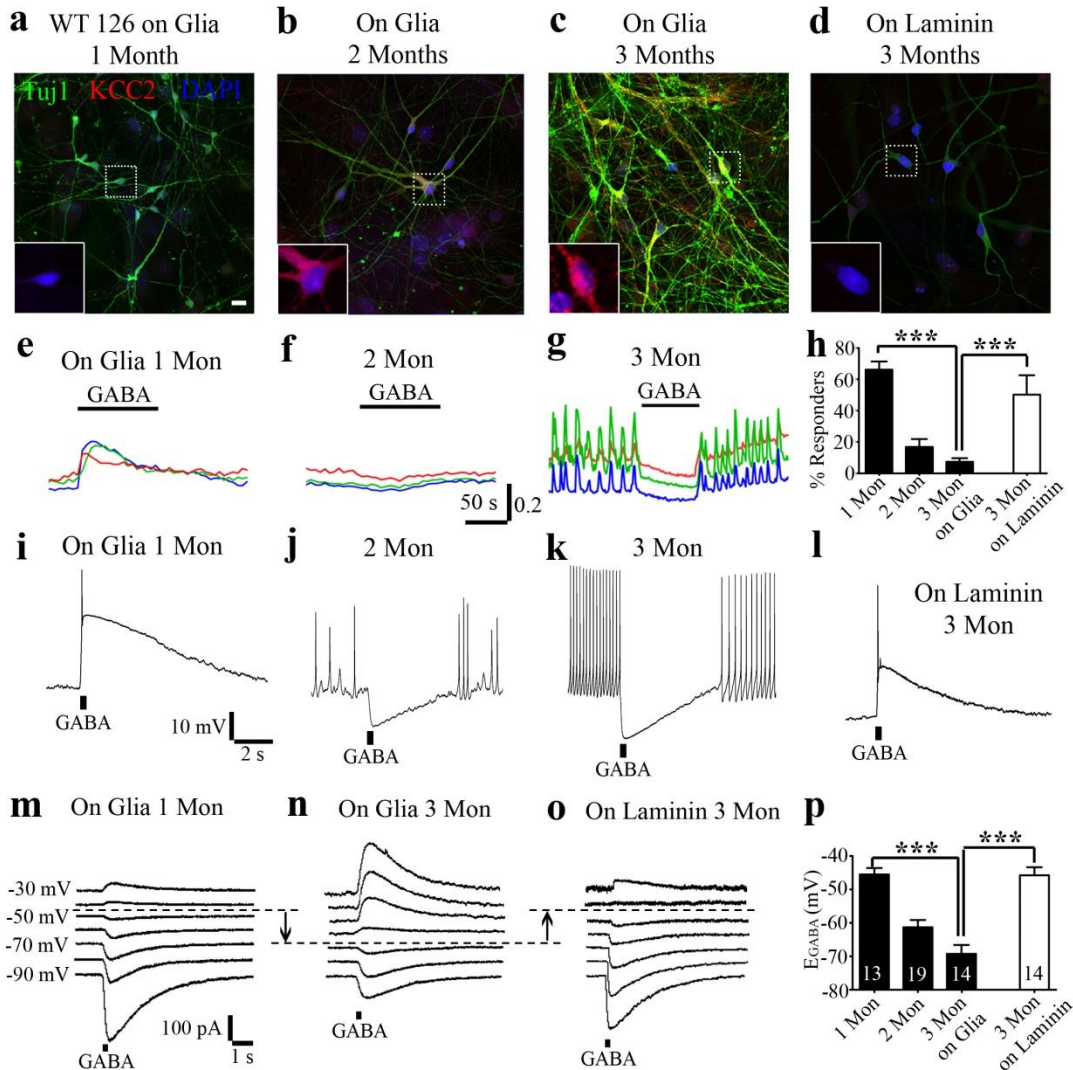


Figure 3-1: GABA functional switch takes a long time in iPS cell-derived human neurons.

a-d, Representative micrographs showing KCC2 immunostaining in human iPS-derived neurons (WT126) cultured on astrocytes for 1-month (**a**), 2-month (**b**), 3-month (**c**), or on laminin for 3-month (**d**). Note the gradual increase in KCC2 immunoreactivity (red, inserts) in Tuj1+ human neurons (green, scale bar = 10 μ m). In sharp contrast, when human neurons were

cultured on laminin substrate in the same differentiation medium, but with no glial cell support, KCC2 immunoreactivity was lacking even after three months in culture. The percentage of KCC2+ human neurons (defined as soma cytosolic KCC2 staining intensity $> 3\times$ of the background level) was low at one month after seeding on glial cells ($15.2 \pm 5.8 \%$, $n = 208$ cells from 6 independent repeats). The KCC2+ neuron percentage increased to more than half after two months in culture ($57.9 \pm 6.5 \%$, $n = 247$ cells from 8 independent repeats, *** $p < 0.001$ comparing to one-month human neurons, One-way ANOVA with Bonferroni correction). At three month, most of the neurons stained positive for KCC2 ($88.5 \pm 3.7 \%$, $n = 93$ cells from 5 independent repeats, *** $p < 0.001$ comparing to one-month human neurons, One-way ANOVA with Bonferroni correction). In sharp contrast, human neurons cultured on laminin showed very few neurons that stain positive for KCC2 even after three months in culture ($4.9 \pm 2.4 \%$, $n = 91$ cells from 5 independent repeats, *** $p < 0.001$ comparing to three-month human neuron on glia, One-way ANOVA with Bonferroni correction).

e-h, Representative GABA responses revealed by Fura-2 Calcium imaging showing that in human neurons one month after seeding on glial cells, the application of GABA ($100 \mu\text{M}$, 60 s) elicited an excitatory response, demonstrated by an increase in the intracellular Ca^{2+} level. On average, $66 \pm 5 \%$ of human neurons responded to GABA application at one month (**e**, $n = 241$ cells from 5 independent repeats. Error bars are mean \pm s.e.m.). The same GABA stimulation induces an inhibitory response in human neurons three months after culture (**g**, $6 \pm 2 \%$ of neurons responded to GABA, $n = 131$ cells from 5 independent repeats, *** $P < 0.001$ comparing to one-month human neuron). In contrast, most of the human neurons cultured on laminin responded to GABA with intracellular Ca^{2+} increase even after three months in culture (**h**, $50 \pm 13 \%$ respond to GABA, $n = 80$ cells from 4 independent repeats, *** $P < 0.001$ comparing to three-month human neuron). **i-l**, Representative GABA responses recorded from human neurons from one to three months in culture showing that, similar to Ca imaging results, GABA functional switch took place in human neurons from two months (**j**) to three months (**k**) after differentiation. The human neurons cultured on laminin for three months responded to GABA with membrane depolarization (**l**), similar to the neurons cultured on glial cells for only one month (**i**). These recordings were performed in current-clamp mode, using gramicidin-perforated patch configuration to maintain the intracellular Cl^- level.

m-p, Representative gramicidin-perforated patch recording traces in voltage-clamp mode (**m-o**) and quantified results (**p**) showing that GABA reversal potential (EGABA) became increasingly hyperpolarizing in human neurons during development. At one month after seeding on glial cells, the average EGABA was $-45.5 \pm 1.9 \text{ mV}$ (**m**, $n = 13$, pooled data from WT126 and WT33 NPC lines), and became more hyperpolarized to $-61.4 \pm 2.2 \text{ mV}$ at two-month time point ($n = 19$, *** $p < 0.001$ comparing to one month human neurons). The GABA reversal potential became even more hyperpolarized to $-69.3 \pm 2.9 \text{ mV}$ after three months of culture on glial cells (**n**, $n = 14$, *** $p < 0.001$ comparing to one-month human neurons). In contrast, human neurons cultured on laminin showed more depolarized EGABA even after three months in culture (**o**, $-45.8 \pm 2.5 \text{ mV}$, $n = 14$ cells, *** $p < 0.001$ comparing to three-month human neurons cultured on glia, n.s. comparing to one-month human neurons cultured on glia).

3.1.2 Human neurons derived from iPSC have deficit in KCC2 expression

Rett syndrome is a neurodevelopmental disorder. We next examined whether KCC2 is altered in Rett neurons. We used human neurons derived from iPSCs originated from a male Rett syndrome patient (Q83X) with a MeCP2 mutation at the amino acid residue 83 from glutamine to a stop codon, which resulted in the truncation and degradation of the MeCP2 protein. Immunostaining with MeCP2 confirmed the absence of MeCP2 signal in neurons derived from the Q83X Rett patient, but control neurons originated from the father (WT83, healthy control) of the Q83X Rett patient had strong MeCP2 staining in the nuclei (Fig. 3-2a-b). We then performed KCC2 immunostaining and found that similar to the WT126 neurons shown in Fig. 1, the WT83 neurons also showed gradual increase of KCC2 expression during 1-3 month culture on astrocytes (Fig. 3-2d-e). In contrast, Q83X Rett neurons showed little KCC2 staining even after 3-month culture on astrocytes (Fig. 3-2f-g). Our previous work demonstrated that IGF may rescue some functional deficits of Rett syndrome (Marchetto et al., 2010b). Therefore, we treated Q83X Rett neurons with IGF and found that MeCP2 was not increased in the nucleus (Fig. 3-2c), but KCC2 staining was significantly increased (Fig. 3-2h-i; quantified in Fig. 3-2j). Thus, IGF acts downstream of MeCP2 but upstream of KCC2 to regulate neuronal development. We also performed Western blot analysis to investigate the expression level of KCC2 and NKCC1 in the Rett syndrome neurons. A significant deficit in KCC2 expression was observed in two-month Q83X neurons comparing to parallel WT83 cultures. Treatment with IGF rescued the KCC2 expression deficit to levels comparable to those of the wild-type control (Fig. 3-3a-b). In contrast, the NKCC1 expression level was not significantly changed in the Q83X neurons, and IGF treatment did not alter NKCC1 expression (Fig. 3-3c-d).

The lack of KCC2 expression in Q83X Rett neurons led us to examine its consequence on E_{GABA} . Similar to WT126 neurons, the control WT83 neurons showed depolarized E_{GABA} after 1-month culture on astrocytes and a gradual hyperpolarized shift of E_{GABA} during neuronal maturation (Fig. 3-2n). In contrast, Q83X Rett neurons did not show a significant change of E_{GABA} even after 3-month culture on astrocytes (Fig. 3-2n). Interestingly, IGF treatment of Q83X Rett neurons significantly rescued the deficits of E_{GABA} shift (Fig. 3-2k-n), consistent with the rescue of KCC2 expression by IGF in Q83X Rett neurons. We have confirmed the finding that MeCP2-deficient neurons have a depolarized shift of E_{GABA} with human neurons differentiated from a different Q83X NPC clone (Q83X clone 6 at two-month time point: -47.0 ± 2.5 mV, $n = 10$; Q83X clone 6 + IGF: -58.8 ± 2.4 mV, $n = 6$, $p < 0.01$ comparing to Q83X; WT83 clone 7: -

$57.3 \pm 3.5\text{mV}$, $n = 6$, $p < 0.05$ comparing to Q83X), and in iPS cell-derived human neurons carrying a disease-related missense mutation N126I that disrupts the binding of MeCP2 to the DNA (N126I clone 6 at two-month time point: $-44.7 \pm 2.7\text{ mV}$, $n = 9$; N126I clone 6 + IGF: $-54.8 \pm 2.2\text{ mV}$, $n = 8$, $p < 0.05$ comparing to N126I; WT126 clone 6: $-55.4 \pm 2.3\text{ mV}$, $n = 8$, $p < 0.01$ comparing to N126I).

We further analyzed the functional deficits in Q83X Rett neurons, using patch-clamp recordings to detect miniature excitatory postsynaptic currents (mEPSCs). Compared to WT83 neurons, Q83X Rett neurons showed a significant decrease of mEPSC frequency (Fig. 3-4d, e). Quantitatively, the mEPSC frequency decreased from $0.74 \pm 0.11\text{ Hz}$ in WT83 neurons to $0.31 \pm 0.07\text{ Hz}$ in Q83X Rett neurons (Fig. 3-4g). Treatment of Q83X Rett neurons with IGF significantly rescued the mEPSC deficit (Fig. 3-4f, g; $0.90 \pm 0.16\text{ Hz}$). Interestingly, if knockdown KCC2 expression, IGF was not able to rescue the mEPSC deficit in Q83X Rett neurons (Fig. 3-4g), confirming that KCC2 is a key downstream effector of IGF in regulating neuronal development. Cumulative probability plot also showed a significant decrease of mEPSC frequency in Q83X Rett neurons (Fig. 3-4h). The average median amplitude of mEPSCs did not show significant change among different groups (Fig. 3-4i).

To confirm our findings in the Rett human neurons, we carried out a series of control experiments in human neurons. We first established that KCC2 indeed regulates excitatory synaptic formation in the human neuron through introducing KCC2 shRNA to neurons derived from another control line WT33. At the two-month time point, we detected a significant reduction in the frequency of miniature EPSC in the human neurons infected with KCC2 shRNA (Fig. 3-5-d), and IGF application cannot rescue the synaptic deficits in the presence of KCC2 shRNA (Fig. 3-5-e). The mEPSC amplitudes were comparable between the three conditions (Fig. 3-5-g), and the cell size are comparable (Fig. 3-5-h).

We also confirm in our iPSC system the earlier findings that Rett neurons demonstrate deficit in spontaneous excitatory neurotransmission (Marchetto et al., 2010b). Comparing to WT83 neurons (**d**), Q83X neurons showed significantly reduced spontaneous EPSC frequency (**e**, summarized in **g**) and amplitude (**h** and **i**). Treating the Q83X neurons with IGF rescued the sEPSC frequency deficit to a level comparable with WT83 control neurons.

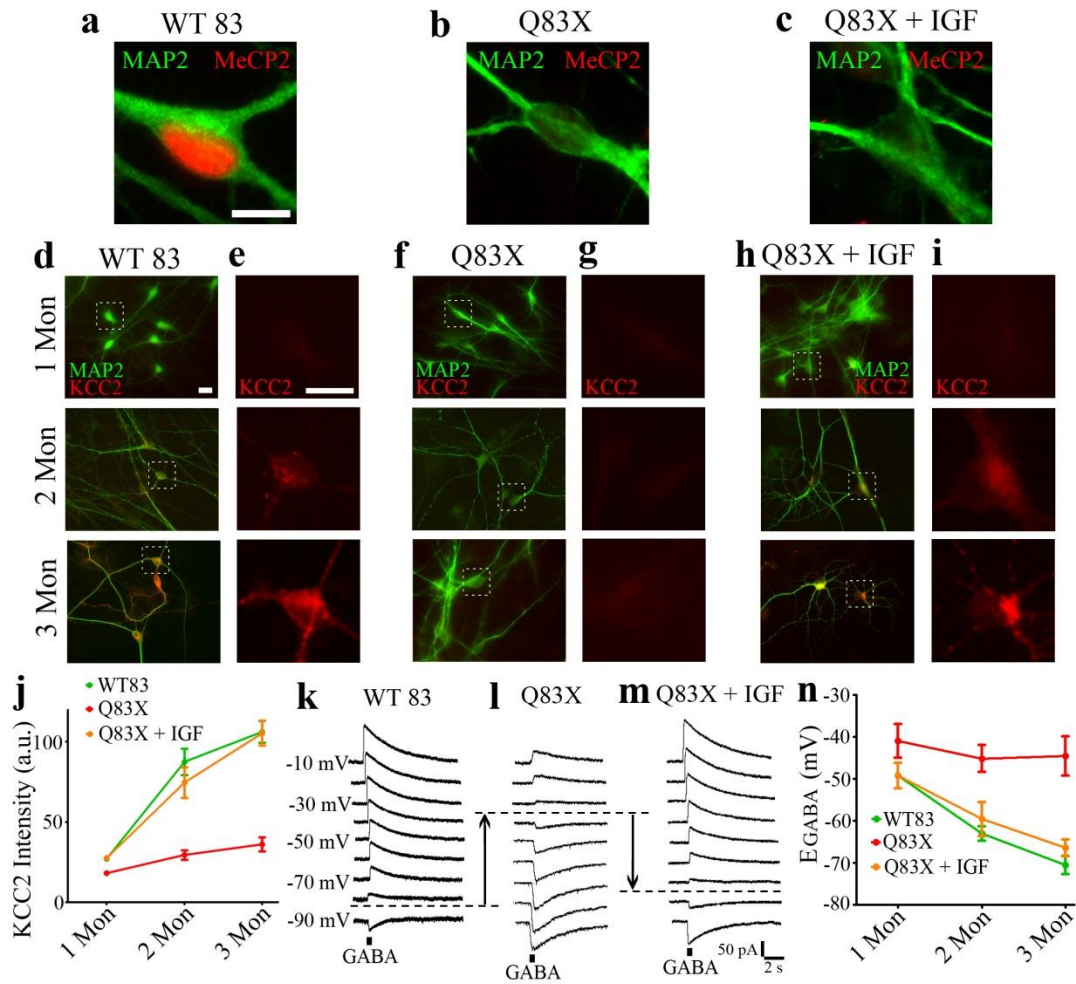


Figure 3-2: Human neurons derived from Rett iPSC cells show deficits in GABA functional switch and glutamatergic transmission.

a-c, Q83X mutant human neurons lack MeCP2 immunoreactivity (**b**) comparing to WT83 neurons (**a**). Treating Q83X culture with IGF did not restore MeCP2 expression (**c**). Scale bar = 10 μ m.

d-j, Representative micrographs showed that the KCC2 immunoreactivity showed a gradual increase from two to three months in culture in WT83 human neurons (**d-e**). The KCC2 signals were weak in Q83X neurons even after three months in culture (**f-g**). Treating the Q83X culture with IGF restored KCC2 expression (**h-i**). Panel (**j**) showed quantification of KCC2 staining intensity in neurons derived from the WT83 line, Q83X line, and Q83X line treated with IGF. The KCC2 immunoreactivity was significantly reduced in Q83X neurons comparing to WT83 at two-month (Q83X: 29 ± 3 a.u., $n = 86$ cells; WT83: 88 ± 8 a.u., $n = 48$ cells. *** $p < 0.001$, t-test), and three-month time point (Q83X: 36 ± 4 a.u., $n = 49$ cells; WT83: 106 ± 7 a.u., $n = 44$ cells. *** $p < 0.001$, t-test). Treatment with IGF-1 (10 ng/ml, first applied after 2 weeks in culture, then replenished every 2 - 3 weeks) significantly increased KCC2 immunoreactivity in the human neurons derived from Q83X iPSC lines (75 ± 10 a.u., $n = 41$ cells at two-month, *** p

< 0.001 comparing to two-month Q83X; 105 ± 8 a.u., $n = 41$ cells at three-month, *** $p < 0.001$ comparing to three-month Q83X, t-test).

k-n, Representative EGABA recording traces from human neurons derived from WT83 (**k**) or Q83X (**l**) lines, and from Q83X neurons treated with IGF treatment (**m**), followed by EGABA quantifications (**n**). At one-month, the EGABA was not significantly different between the three test groups (WT83: -49.2 ± 3.1 mV, $n = 11$; Q83X: -41.0 ± 4.0 mV, $n = 10$; Q83X + IGF: -49.3 ± 3.1 mV, $n = 11$. n.s. determined by t-test). After two months of differentiation, the EGABA for WT83 was significantly more hyperpolarized than Q83X neurons (WT 83: -63.0 ± 1.7 mV, $n = 11$; Q83X: -45.2 ± 3.2 mV, $n = 11$, *** $p < 0.001$ comparing to WT83 two-month; At three-month, the EGABA for WT83 was -70.5 ± 2.1 mV, $n = 10$; Q83X -44.6 ± 4.7 mV, $n = 11$, *** $p < 0.001$ comparing to WT83 three-month). The application of IGF from early in culture (around two weeks) rescued the GABA functional switch deficit in Q83X neurons at the two-month (-59.6 ± 4.1 mV, $n = 9$. * $p < 0.05$ comparing to Q83X two-month, t-test) and three-month time points (-66.5 ± 2.0 mV, $n = 10$. *** $p < 0.001$ comparing to Q83X three-month, t-test).

Interestingly, treating Q83X neurons with IGF for only one month (applied at two-month and recorded at three-month) can also rectify the EGABA deficit (-63.0 ± 2.8 mV, $n = 9$, *** $p < 0.001$ comparing to three-month Q83X), while adding IGF to WT83 does not affect EGABA (recordings were done at three month, EGABA = -66.5 ± 3.0 mV, $n = 6$, $p = 0.3$ comparing to three-month WT83, t-test). Oxytocin, a drug that is currently under clinical trials to treat autism, did not rescue EGABA deficit in the Q83X neurons (1 μ M oxytocin was applied 2 - 4 weeks before experiment, recordings were done at three months, EGABA = -43.0 ± 2.9 mV, $n = 6$, $p = 0.77$ comparing to three-month Q83X, *** $p < 0.001$ comparing to three-month WT83, t-test).

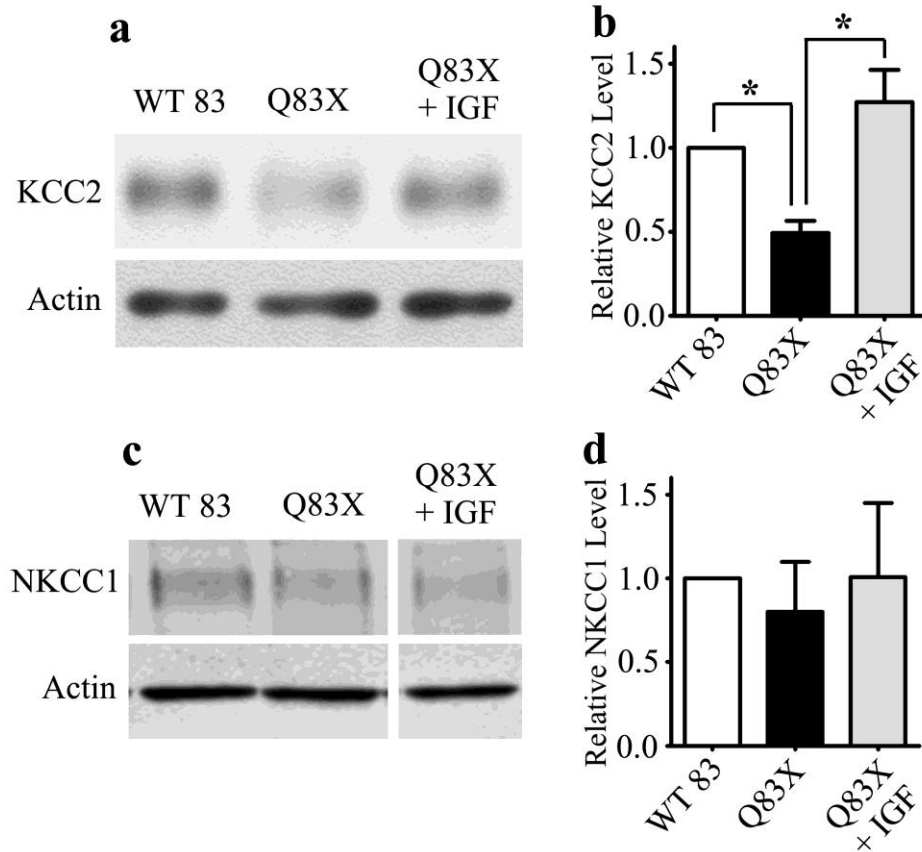


Figure 3-3: Rett patient-derived human neurons show reduced KCC2 but comparable NKCC1 expression.

Rett syndrome patient-derived Q83X neurons demonstrated a reduction in KCC2 but preserved NKCC1 expression comparing to wild-type control neurons. **(a-b)** Representative Western blot **(b)** probing KCC2 showed that comparing to WT83 neurons, Rett syndrome Q83X neurons had significant reduction in KCC2 expression (49 ± 7 % of WT 83 level, $n = 3$ independent repeats; $p = 0.019$ comparing to WT83, unpaired t-test). The KCC2 deficit in Q83X neurons can be rescued by IGF treatment (127 ± 19 % of WT83 level, $p = 0.022$ comparing to Q83X; $p = 0.26$ comparing to WT83). **(c-d)** NKCC1 expression level was not changed in Q83X neurons (Q83X: 80 ± 29 % of WT83 level, $p = 0.57$; Q83X + IGF: 101 ± 43 % of WT83 level, $p = 0.71$, determined by unpaired t-test).

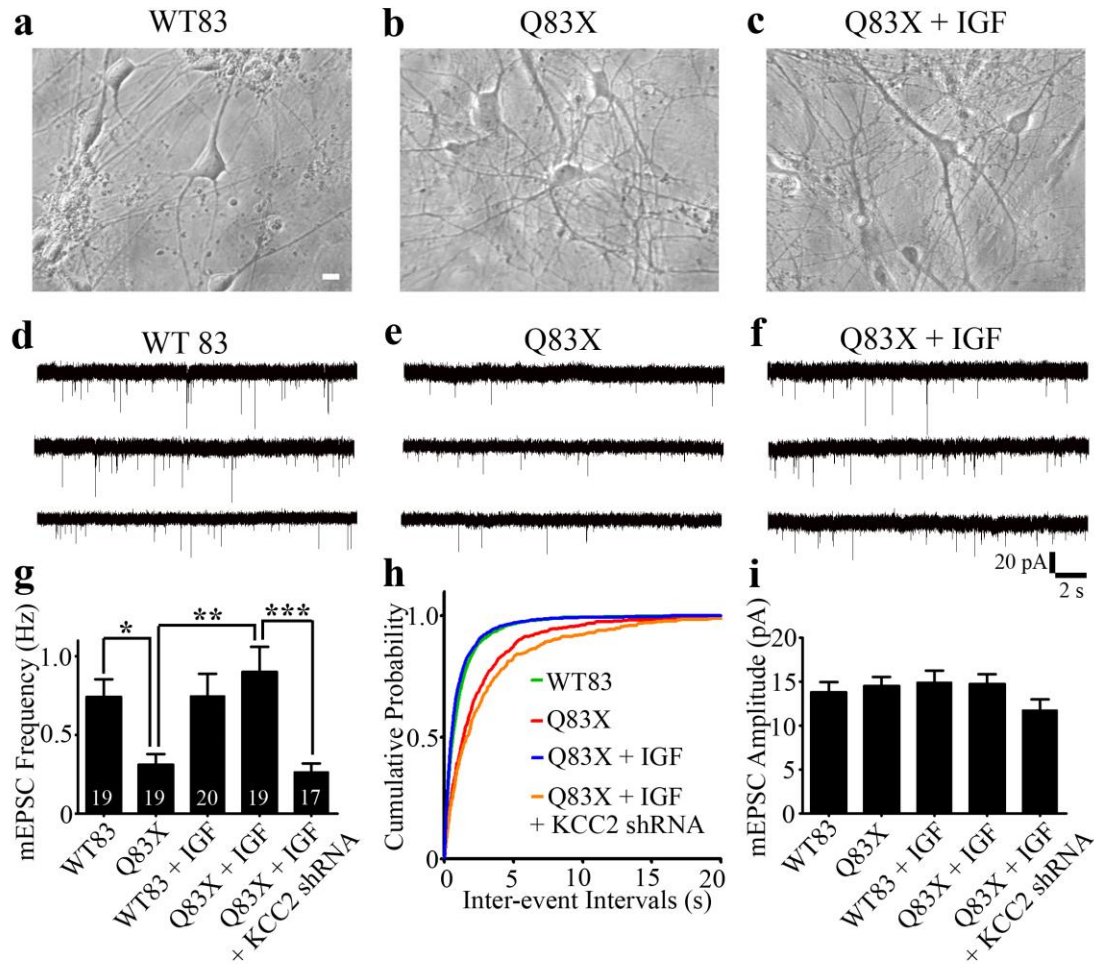


Figure 3-4: Rett syndrome human neurons demonstrate deficits in excitatory synapse formation.

a-c, Representative pictures showing human neurons derived from WT83, Q83X NPC lines, and from Q83X line with IGF treatment. **d-f** Comparing to WT83 neurons (**d**), Q83X iPSC-derived neurons demonstrated significantly reduced mini EPSC frequency (**e**, the mEPSC frequency in 2-3 month WT83 neurons was 0.74 ± 0.11 Hz, $n = 19$; Q83X: 0.31 ± 0.07 Hz, $n = 19$, $*p < 0.05$ comparing to WT83, One-way ANOVA with Bonferroni correction). IGF treatment completely rescued the mEPSC reduction in Q83X neurons (**f**, 0.90 ± 0.16 Hz, $n = 19$, $**p < 0.01$ comparing to Q83X), while having little effect on WT83 neurons. (**g**, 0.75 ± 0.14 Hz, $n = 20$). Interestingly, in the Q83X neurons with prior KCC2 shRNA lentivirus infection, IGF application can no longer rescue the mEPSC reduction (**g**, Q83X + IGF + KCC2 shRNA: 0.27 ± 0.05 Hz, $n = 17$, $***p < 0.001$ comparing to Q83X + IGF). (**h**) Cumulative distribution of the time intervals between synaptic events recorded from WT83 (green), Q83X (red), Q83X + IGF (blue) and Q83X + IGF + KCC2 shRNA (orange) neurons. Comparing to WT83 neurons, the interevent interval distribution of Q83X neurons showed a significant shift toward longer intervals. ($P < 0.001$, Kolmogorov-Smirnov test). Note that the interevent interval distribution curve of Q83X neuron with IGF treatment (blue) largely overlapped with WT83 (green). Such

potent rescue can not work if the neuronal KCC2 have been knocked down (orange, $P < 0.001$ comparing to Q83X + IGF, Kolmogorov-Smirnov test). The mini EPSC amplitude were comparable between all experiment groups (**i**, $p = 0.33$, One-way ANOVA with Bonferroni correction). Our data strongly suggests that Rett syndrome neurons exhibit reduced excitatory synaptic transmission due to lack of KCC2, and IGF rescues the synaptic deficit through upregulation of KCC2.

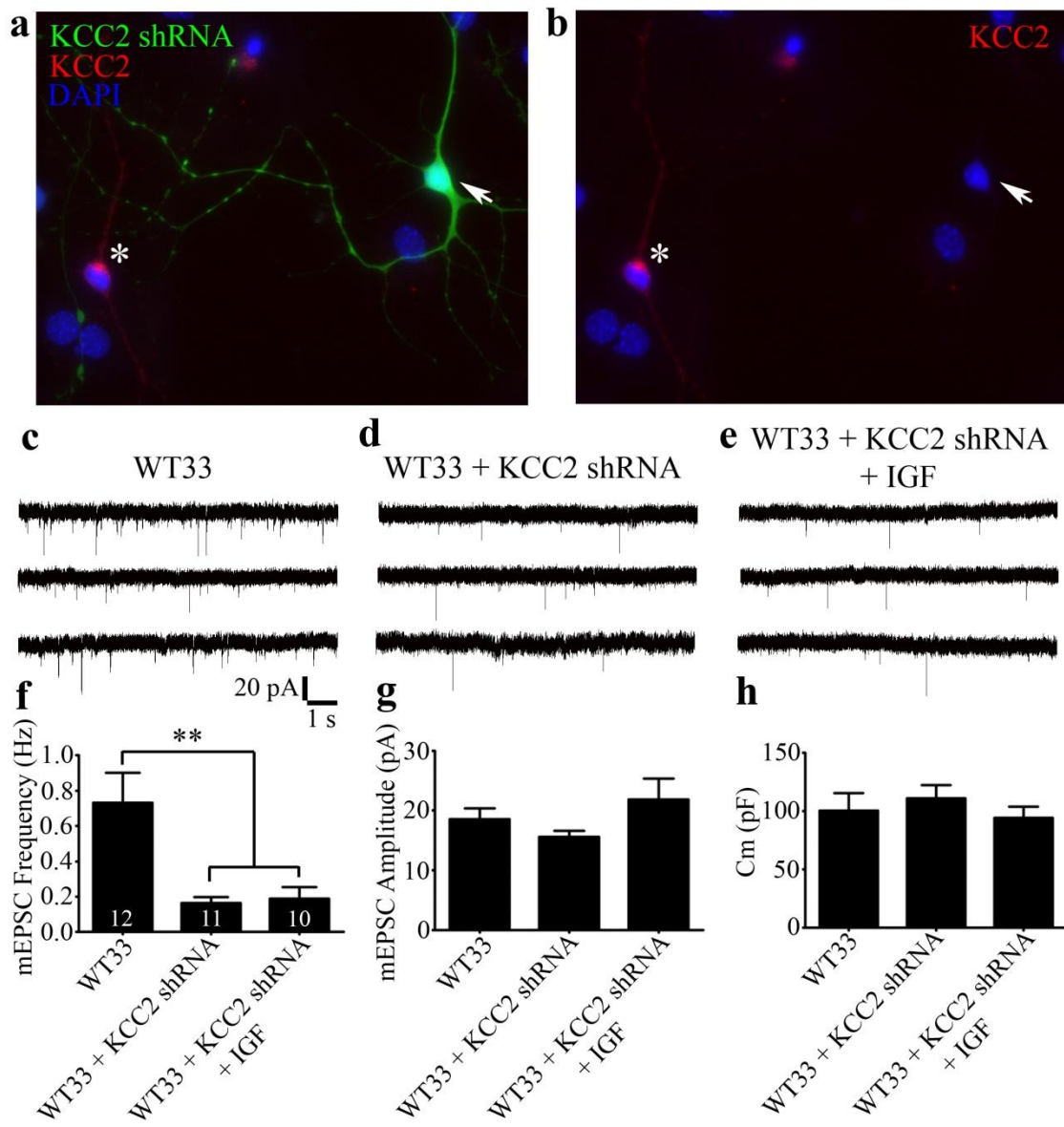


Figure 3-5: KCC2 regulates excitatory synaptic transmission in human neurons.

Knocking-down KCC2 expression in human neurons through lentivirus infection significantly impaired the formation of excitatory synapses, and IGF treatment can not rescue the KCC2 shRNA-induced synaptic deficit. Two-month human neurons derived from WT33 were utilized for this analysis, and the KCC2 lentivirus and IGF were added to the culture at one-month time point. A significant reduction in the mini EPSC frequencies were observed in KCC2 shRNA infected neurons both in the presence or absence of IGF **a-b**, Representative immunostaining against KCC2 showing that KCC2 expression is present in WT33 human neurons two months after culture (asterisk), but absent in human neurons infected with KCC2 shRNA virus (arrow). **c-e**, Representative traces showing the mini EPSC recorded from WT33 neurons (**c**), WT33 neurons infected with KCC2 shRNA (**d**), and KCC2 shRNA infected neuron treated with IGF (**e**). The mini EPSC frequency were 0.73 ± 0.17 Hz in WT33 neurons, 0.16 ± 0.03 Hz in WT33 + KCC2 shRNA condition, and 0.19 ± 0.06 Hz in WT33 + KCC2 shRNA + IGF condition. (**f**, ** $P < 0.01$, comparing to WT33). The mini EPSC amplitude (**g**) and cell capacitance (**h**, Cm) were not significantly different between all the conditions ($p = 0.17$ for amplitude, $p = 0.65$ for capacitance. One-way ANOVA with Bonferroni correction).

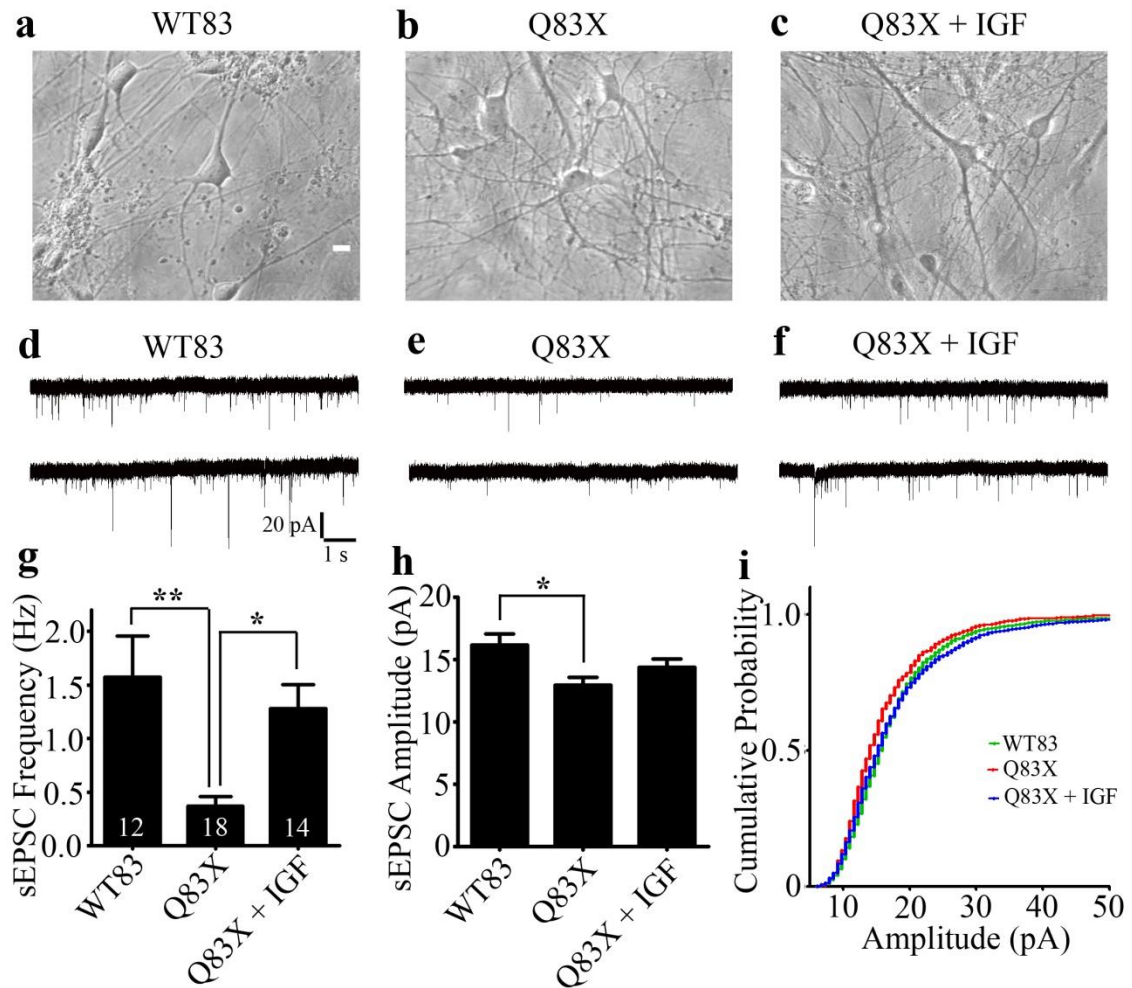


Figure 3-6: Rett human neurons show reduced spontaneous excitatory neurotransmission.

Rett syndrome patient-derived Q83X neurons demonstrated a reduction in spontaneous EPSC frequency and amplitude. Treatment with IGF1 can rescue the deficit in sEPSC. (**a** to **c**), representative phase contrast images showing that the neuronal morphology and density of WT83 (**a**), Q83X (**b**), and Q83X + IGF (**c**) cultures were comparable. (**d** to **f**) electrophysiology recording reveals that Q83X neurons (**e**) have reduced spontaneous excitatory neurotransmission comparing to WT83 (**d**), and treating Q83X neurons with IGF (**f**) can rescue the sEPSC frequency deficit. (**g** to **i**) The spontaneous EPSC frequency was 1.57 ± 0.38 Hz in WT83 neurons, amplitude was 16.02 ± 0.85 pA, $n = 12$; in Q83X neurons, frequency 0.37 ± 0.09 Hz, amplitude 12.95 ± 0.64 pA, $n = 18$, $**p < 0.01$ comparing frequency with WT83, $*p < 0.05$ comparing amplitude with WT83; in Q83X + IGF condition, frequency 1.28 ± 0.22 Hz, amplitude 14.39 ± 0.68 pA, $n = 14$. $*P < 0.05$, comparing frequency with Q83X. (**i**) Careful analysis of the distribution of sEPSC amplitude revealed that IGF treatment can restore sEPSC amplitude to wild-type level ($p < 0.001$ comparing WT83 and Q83X; $p < 0.001$ comparing Q83X and Q83X + IGF; $p = 0.017$ comparing WT83 and Q83X + IGF. Kolmogorov-Smirnov two sample test).

3.1.3 KCC2 is downstream of MeCP2, and is a key regulator of GABA functional switch and glutamatergic synapse formation

We further investigated MeCP2 regulation of KCC2 in cultured mouse cortical neurons through a series of molecular manipulations. In order to achieve these goals, we first established a molecular expression timeline of both MeCP2 and KCC2 in the mouse neuronal culture system (Fig. 3-7). We received MeCP2 shRNA and knockdown-resistant MeCP2* constructs from Dr. Michael Greenberg at Harvard Medical School, and KCC2 and KCC2 shRNA plasmids from Dr. Yun Wang at Fudan University, China. Cross validation results of KCC2 and MeCP2 plasmids and antibodies were presented in (Fig. 3-8). We found that knockdown MeCP2 in cortical neurons significantly reduced KCC2 expression level (Fig. 3-9-b, see also Fig. 3-10-c), consistent with the findings in human iPSC-derived Rett neurons (Fig. 3-2-d-e). Overexpression of MeCP2 in WT neurons increased KCC2 expression level, and coexpression of a mutant MeCP2 that was resistant to MeCP2 shRNA rescued the effect of MeCP2 shRNA (Fig. 3-9-c-d). Overexpression of knockdown-resistant KCC2 construct in the presence of MeCP2 shRNA rescued the KCC2 level (Fig. 3-9-d). Similarly to what we found in human Rett neurons (Fig. 3-2-h-i), treatment of MeCP2 shRNA-expressing neurons with IGF also rescued KCC2 level (Fig. 3-10-f, summarized in Fig. 3-9-d), confirming our observation in human iPSC-derived neurons. In contrast, IGF treatment did not rescue the KCC2 level in neurons expressing KCC2 shRNA (Fig. 3-8-f), which could only be rescued by mutant KCC2 that was resistant to KCC2 shRNA (Fig. 3-8-d).

In parallel with the KCC2 immunostaining analysis, we also investigated changes of E_{GABA} and found that knockdown MeCP2 resulted in a significant shift of E_{GABA} toward a depolarized potential (Fig. 3-9-f, MeCP2 shRNA, -52.6 ± 1.1 mV; Fig. 3-9-e, control, -70.1 ± 2.3 mV; summarized in Fig. 3-9-h). The MeCP2 shRNA-induced E_{GABA} change was rescued by shRNA-resistant MeCP2 mutant, and by KCC2 coexpression or IGF treatment (Fig. 3-9-h). As a control, knockdown KCC2 also resulted in a depolarizing shift of E_{GABA} , but it could not be rescued by IGF and was only rescued by mutant KCC2 that is shRNA-resistant (Fig. 3-9-h), again confirming that IGF acts upstream of KCC2.

We further investigated the functional effect of MeCP2 and KCC2 on dendritic spines and mEPSCs in cultured mouse cortical neurons. Knockdown MeCP2 or KCC2 both resulted in a significant reduction of dendritic spines, compared to GFP-expressing controls (Fig. 3-11-a-c). More importantly, coexpression of KCC2 together with MeCP2 shRNA rescued the spine deficit (Fig. 3-11-d), suggesting that KCC2 acts downstream of MeCP2 to regulate spine morphogenesis.

IGF treatment of neurons expressing MeCP2 shRNA also rescued spine deficit (Fig. 3-11-e), but further knockdown of KCC2 resulted into a reduction of spines that could not be rescued by IGF (Fig. 3-11-f). The quantitative analysis of spine density under various MeCP2 or KCC2 manipulations was summarized in Fig. 3-11-n. In addition, besides spine density changes, we also observed that dendritic spines became elongated after knockdown of MeCP2 or KCC2 (Fig. 3-11-a-c). Therefore, we quantified the ratio of spine length versus spine head width and found that the ratio was significantly increased after knocking down MeCP2 or KCC2 (Fig. 3-11-o).

In parallel with the dendritic spine studies, we also examined the effect of MeCP2 and KCC2 on mEPSCs in cultured mouse cortical neurons. Similar to the finding that knocking down MeCP2 resulted in reduced spines density, knockdown of MeCP2 or KCC2 both reduced the mEPSC frequency significantly (Fig. 3-11-h-j). Overexpression of KCC2 together with knockdown of MeCP2 rescued the reduction of mEPSCs (Fig. 3-11-k), again suggesting that KCC2 acts downstream of MeCP2. IGF treatment rescued the mEPSC deficit induced by MeCP2 shRNA but not when induced by KCC2 shRNA (Fig. 3-11-l-m), further indicating that IGF acts downstream of MeCP2 but upstream of KCC2. Quantified data in Fig. 3-11-p showed the changes of mEPSCs under various conditions of up- or down-regulation of MeCP2 or KCC2 levels. Together, our results in mouse cortical neurons confirmed our observation in human iPSC-derived neurons from Rett patients. We conclude that MeCP2 deficiency leads to the reduction in KCC2, which directly regulates synaptic functions. Our data also suggest that restoring KCC2 expression is a valid strategy to rescue synaptic deficits observed in Rett syndrome neurons.

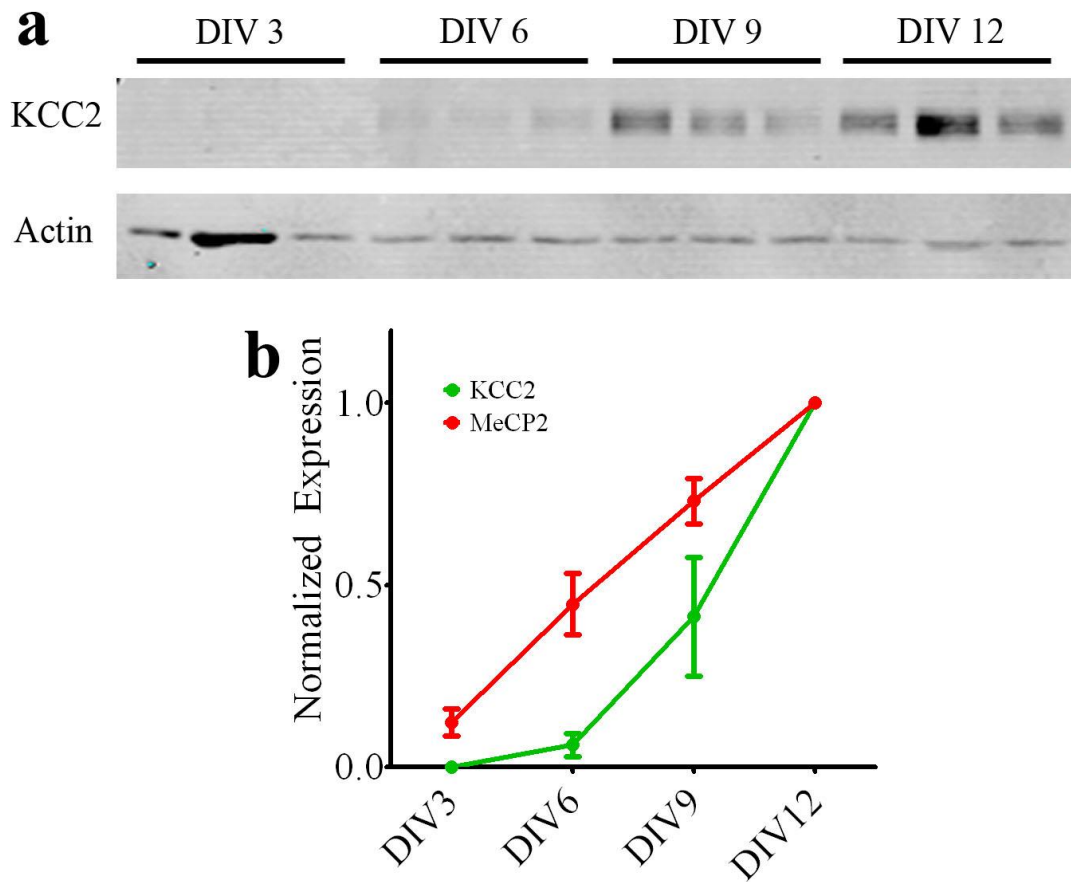


Figure 3-7: MeCP2 and KCC2 development timecourse in mouse neurons.

a, Western blot experiments revealed that the KCC2 expression level undergo dramatic increase in the first two postnatal weeks. Total protein samples were extracted from primary mouse cortex neuronal cultures. The data represent three biological replicates. **b**, quantified results showing the expression level of MeCP2 and KCC2 at different timepoints during development. Results were pooled from three replicates. MeCP2 immunofluorescence and KCC2 Western band signal were normalized to DIV12 level in this presentation.

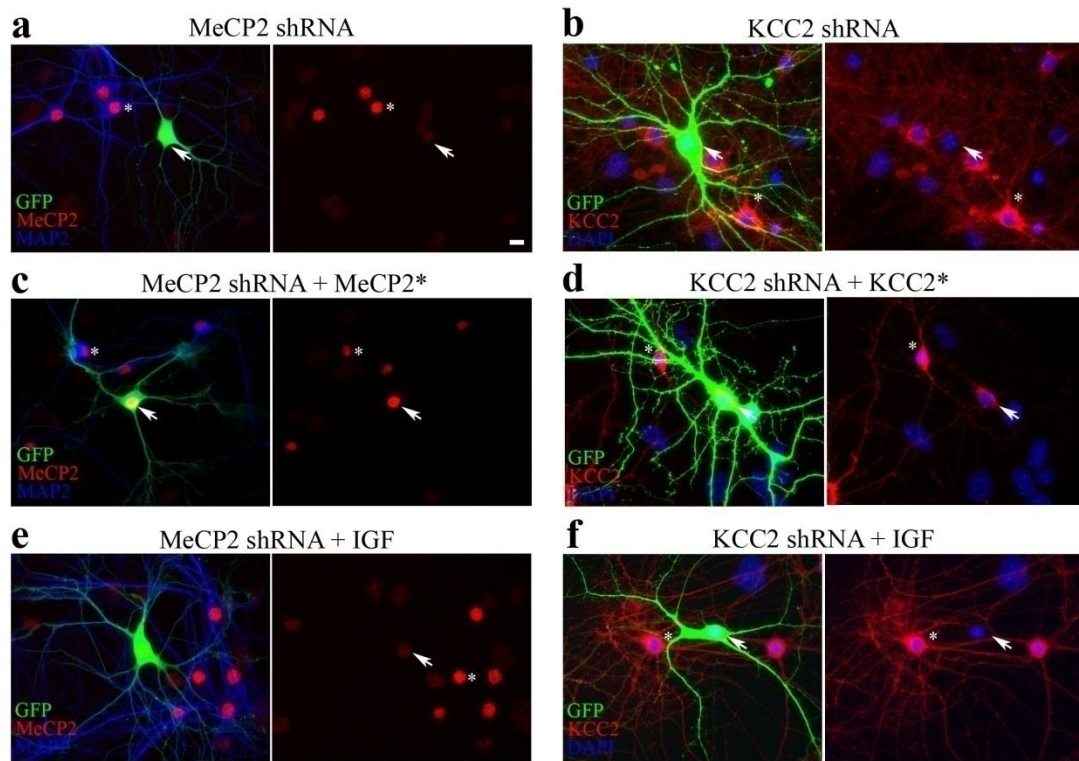


Figure 3-8: Cross validation of MeCP2 and KCC2 plasmids and antibodies.

The MeCP2 and KCC2 plasmids are specific and can be recognized by MeCP2 and KCC2 antibodies. Mouse cortical neurons were transfected with (a) MeCP2 shRNA, (c) MeCP2 shRNA plus knockdown-resistant version of MeCP2 (MeCP2*, generous gift from Dr. Michael Greenberg, Harvard University (Zhou et al., 2006)), or transfected with MeCP2 shRNA then treated with IGF (e). MeCP2 immunoreactivity was shown in red. Note a significant reduction in MeCP2 expression level in the MeCP2 shRNA transfected neurons (a, arrow). The knockdown-resistant version of MeCP2 can robustly express in the presence of MeCP2 shRNA (c). IGF treatment does not increase MeCP2 expression in MeCP2 shRNA knockdown neurons (e). KCC2 expression were also examined in neurons transfected with (b) KCC2 shRNA, (d) KCC2 shRNA and knockdown-resistant version of KCC2 (KCC2*, generous gift from Dr. Yun Wang, Fudan University, China), and (f) KCC2 shRNA transfected neurons treated with IGF. Similar conclusion can be draw that KCC2 shRNA can effectively reduce KCC2 expression, even in the presence of IGF. And KCC2* can restore KCC2 expression when co-transfected with KCC2 shRNA. Scale bar = 10 μ m. Arrows point to cells with denoted transfection, * indicates non-transfected control cells in the same microscopic view.

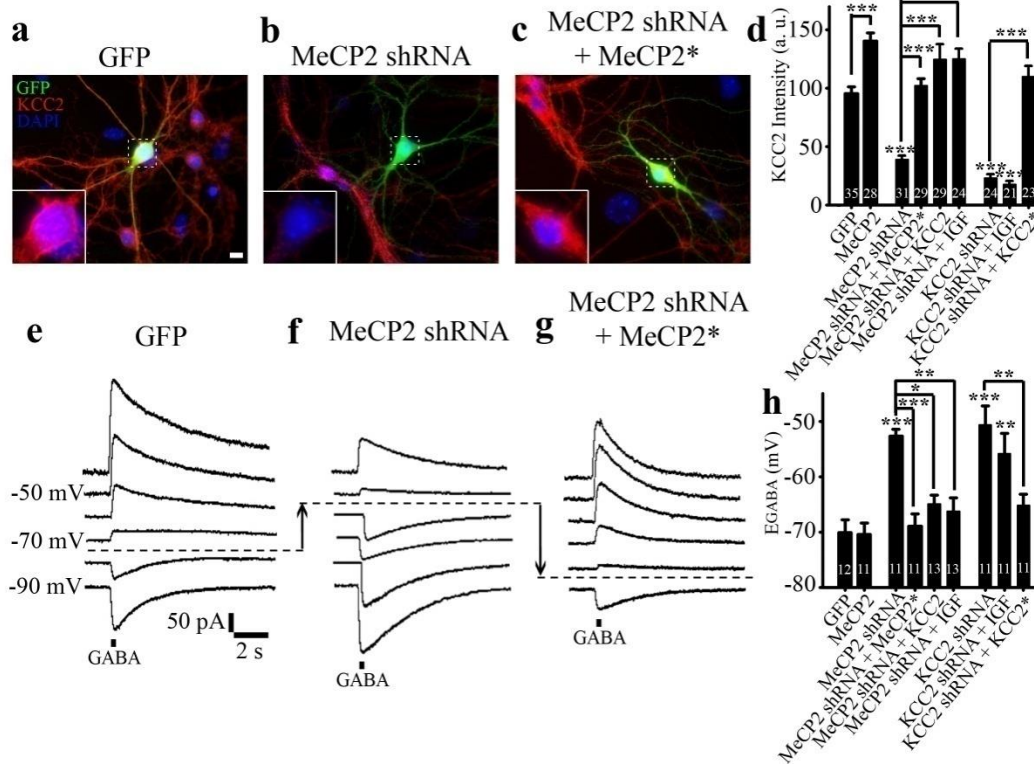


Figure 3-9: MeCP2 regulates KCC2 expression and GABA functional switch.

a-c, Representative micrograph showing that in mouse cortical neurons transfected with MeCP2 shRNA (**c**, MeCP2 KD), the KCC2 staining is diminished comparing to the neighboring non-transfected cells (**b**, Control). Scale bar = 10 μ m.

d, KCC2 staining intensity was significantly reduced when MeCP2 is knocked-down (GFP control, 95 ± 6 a.u., $n = 35$; MeCP2 shRNA: 39 ± 3 a.u., $n = 33$; *** $p < 0.001$, One-way ANOVA with Bonferroni correction). This reduction can be rescued by co-transfection of MeCP2* (human version of MeCP2 that cannot be knocked-down by the small-hairpin RNA that targets the mouse sequence (Zhou et al., 2006). 102 ± 6 a.u., $n = 29$, *** $p < 0.001$ comparing to MeCP2 shRNA), or IGF application (125 ± 8 a.u., $n = 24$, *** $p < 0.001$ comparing to MeCP2 shRNA).

e, Careful electrophysiological analysis of GABA reversal potential (EGABA) showing that neurons with reduced level of MeCP2 demonstrate significantly more depolarized GABA reversal potential (non-TFed: EGABA = -70.1 ± 2.3 mV, $n = 12$; MeCP2 shRNA: EGABA = -52.6 ± 1.1 mV, $n = 11$, *** $p < 0.001$, One-way ANOVA with Bonferroni correction). This deficiency in GABA functional switch in MeCP2 deficient neurons can be rescued by restoring MeCP2 expression (MeCP2 shRNA + MeCP2*: -68.9 ± 2.2 mV, $n = 13$, *** $p < 0.001$ comparing to MeCP2 shRNA group), overexpress KCC2 (MeCP2 + KCC2: -64.9 ± 1.6 mV, $n = 11$, * $p < 0.05$ comparing to MeCP2 shRNA group), or treat neurons with IGF (MeCP2 + IGF: -66.2 ± 2.4 mV, $n = 13$, ** $p < 0.01$ comparing to MeCP2 shRNA group). Similar to the KCC2 immunostaining results, applying IGF to KCC2 shRNA transfected neurons does not rescue the GABA functional switch deficit (KCC2 shRNA + IGF: -55.8 ± 3.6 mV, $n = 11$, ** $p < 0.01$

comparing to non-TFed group. n.s. comparing to KCC2 shRNA group, in which EGABA = -50.6 ± 3.4 mV, n = 11).

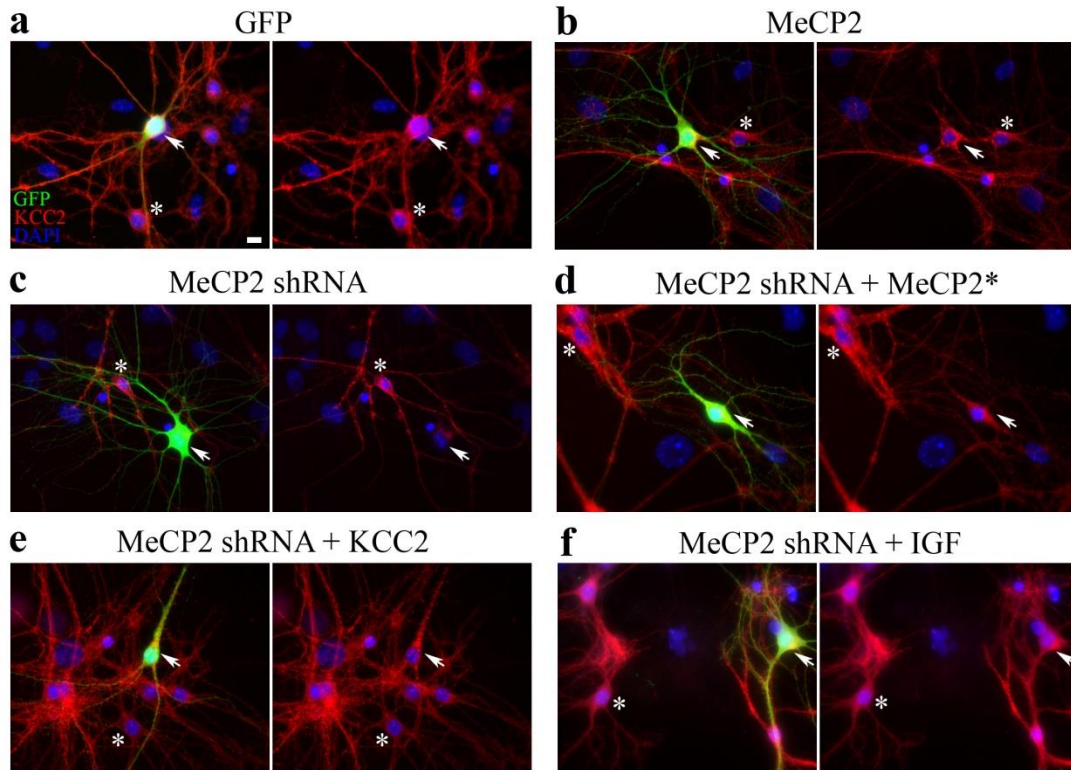


Figure 3-10: Representative micrographs showing that MeCP2 regulate KCC2 expression.

The neurons were transfected with various plasmids and stained for GFP (green), KCC2 (red), DAPI (blue). GFP expressing neurons (a) showed similar KCC2 staining intensity comparing to neighboring non-transfected neurons. Overexpress MeCP2 (b) does not significantly change KCC2 intensity, while knocking down MeCP2 with a shRNA construct lead to a significant reduction in KCC2 immunoreactivity (c). The reduction in KCC2 caused by MeCP2 deficiency can be rescued by restoring MeCP2 (d), overexpress KCC2 (e), or IGF treatment (f).

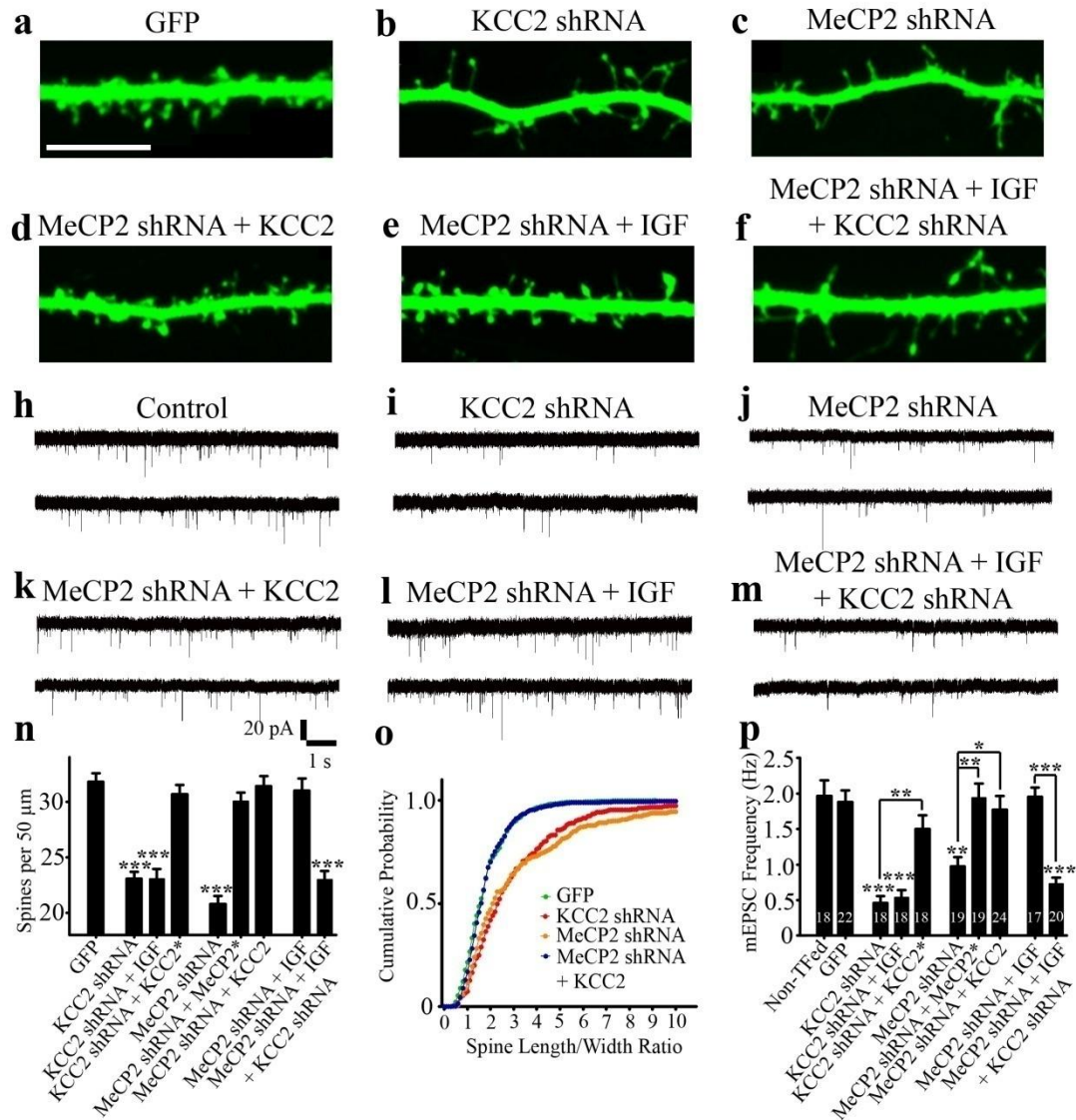


Figure 3-9: KCC2 is a key downstream gene of MeCP2 that directly regulates dendritic spine and excitatory synapse.

a-f, Representative confocal micrographs showing dendritic spine densities and morphologies in neurons that had different MeCP2 or KCC2 gene manipulations (scale bar = 10 μ m). Note the reduced number of spines and elongated spine morphology in both KCC2 shRNA and MeCP2 shRNA transfected neurons (**b-c**). Neurons with reduced level of MeCP2

demonstrate significantly fewer dendritic spines ($n = 15$ to 16 neurons were analyzed per condition. A total length of 50 to $100 \mu\text{m}$ of dendrite was analyzed per neuron. GFP: 31.8 ± 0.8 spines per $50 \mu\text{m}$; MeCP2 shRNA: 20.8 ± 0.7 , *** $p < 0.001$ summarized in panel **n**). This deficiency in spine density in MeCP2 deficient neurons can be rescued by restoring MeCP2 expression (30.1 ± 0.8 spines per $50 \mu\text{m}$, *** $p < 0.001$ comparing to MeCP2 shRNA group), overexpress KCC2 (**d**, 31.4 ± 0.9 spines per $50 \mu\text{m}$, *** $p < 0.001$ comparing to MeCP2 shRNA group), or treat neurons with IGF (**e**, 31.0 ± 1.1 spines per $50 \mu\text{m}$, *** $p < 0.001$ comparing to MeCP2 shRNA group). Interestingly, when knocking down both MeCP2 and KCC2 in the same neuron, IGF can no longer rescue the spine deficiency (**f**, 22.6 ± 0.7 spines per $50 \mu\text{m}$, *** $p < 0.001$ comparing to MeCP2 shRNA + IGF group). The cumulative distribution of spine width/length ratio in the GFP control, KCC2 shRNA, MeCP2 shRNA, and MeCP2 shRNA + KCC2 groups were summarized in panel (**s**). Similar to KCC2 shRNA transfected neurons, knocking-down MeCP2 in neurons result in elongated spine morphology (red and orange traces, *** $p < 0.001$ comparing to the green GFP control curve. Kolmogorov-Smirnov test). Overexpress KCC2 in MeCP2 knockdown neurons rescued the spine morphology deficiency to levels comparable to GFP control (blue trace, *** $p < 0.001$ comparing to orange MeCP2 shRNA curve; $p = 0.297$ comparing to green GFP curve).

h-m, Representative mini EPSC recording traces and quantified mEPSC frequency data (**p**) corroborate the spine data. Neurons that had reduced level of MeCP2 demonstrated significantly reduced mini EPSC frequency (**h**, Non-transfected control: 1.97 ± 0.22 Hz, $n = 18$; **j**, MeCP2 shRNA: 0.97 ± 0.13 Hz, $n = 19$; ** $p < 0.01$ comparing to Non-TFed, One-way ANOVA with Bonferroni correction). This deficiency in mEPSC frequency in MeCP2 knock-down neurons can be rescued by restoring MeCP2 expression (1.94 ± 0.20 Hz, $n = 19$, ** $p < 0.01$ comparing to MeCP2 shRNA group), overexpress KCC2 (**k**, 1.78 ± 0.19 Hz, $n = 24$, * $p < 0.05$ comparing to MeCP2 shRNA group), or treat neurons with IGF (**l**, 1.95 ± 0.13 Hz, $n = 17$, ** $p < 0.01$ comparing to MeCP2 shRNA group). Similar to the spine results shown earlier, when knocking down both MeCP2 and KCC2 in the same neuron, IGF can no longer rescue the mEPSC reduction (**m**, 0.73 ± 0.09 Hz, $n = 20$, *** $p < 0.001$ comparing to MeCP2 shRNA + IGF group; n.s. comparing to MeCP2 shRNA group).

3.1.4 MeCP2 regulates KCC2 through the transcriptional repressor REST.

We next investigated how MeCP2 regulates KCC2. MeCP2 may be a global transcription regulator and thus affects many downstream signaling pathways. A careful review of previous studies found that MeCP2 can regulate transcription repressor REST, a master regulator of neuronal gene expression (Ballas et al., 2005; Abuhatzira et al., 2007). The regulation of REST by MeCP2 is interesting because another study reported that KCC2 is regulated by REST (Yeo et al., 2009). Therefore, we hypothesized that MeCP2 may regulate KCC2 through REST. Indeed, overexpression of REST in cultured mouse cortical neurons significantly reduced KCC2 expression level, compared to non-transfected control neurons (Fig. 3-12-a-b). More importantly,

coexpression of MeCP2 together with REST rescued the KCC2 deficit induced by REST alone (Fig. 3-12-c), suggesting that MeCP2 regulates REST, which in turn regulates KCC2. Interestingly, the IGF treatment failed to rescue the KCC2 deficit induced by REST overexpression (Fig. 3-12-d), likely due to transcriptional repression of KCC2 by REST. To further test the interaction between MeCP2 and REST and their effects on KCC2, we expressed a dominant negative mutant of REST (REST DN) in mouse neurons and found that KCC2 expression level was not altered (Fig. 3-12-e). Knockdown of MeCP2 induced a significant decrease of KCC2 expression in mouse neurons as shown above (Fig. 3-12-f). Interestingly, coexpressing REST DN with MeCP2 shRNA significantly rescued the KCC2 deficit induced by MeCP2 shRNA alone (Fig. 3-12-g, quantified data shown in Fig. 3-12-h), suggesting that REST mediates the MeCP2 regulation of KCC2.

In parallel with the changes in KCC2, we examined the effect of REST and MeCP2 on E_{GABA} and found that overexpressing REST caused a depolarizing shift of E_{GABA} (Fig. 3-12-i, j), consistent with a decrease of KCC2 level. Coexpressing MeCP2 together with REST rescued the E_{GABA} changes induced by REST alone (Fig. 3-12-k, quantified in Fig. 3-12-l), confirming that REST is regulated by MeCP2. Thus, we conclude that MeCP2 regulates KCC2 through the mediation of REST to effect on neuronal maturation, including GABA functional switch and glutamatergic transmission.

Taken together, we propose a model diagram to depict the interaction between MeCP2 and REST in mediating KCC2 expression and neuronal function (Fig. 3-14). In normal neurons, MeCP2 interacts with REST to prevent the latter from binding with the KCC2 promoter, allowing sufficient KCC2 expression. Therefore, normal neurons respond to GABA with membrane hyperpolarization and form robust dendritic spines. In the case of Rett syndrome neurons, the lack of MeCP2 leads to aberrant binding of REST to KCC2 promoter and suppression of KCC2 expression. As a result of KCC2 deficiency, Rett neurons respond to GABA with membrane depolarization, and develop fewer and elongated dendritic spines. IGF treatment of Rett neurons can restore KCC2 expression and rescue the GABA functional switch and dendritic spine deficiencies.

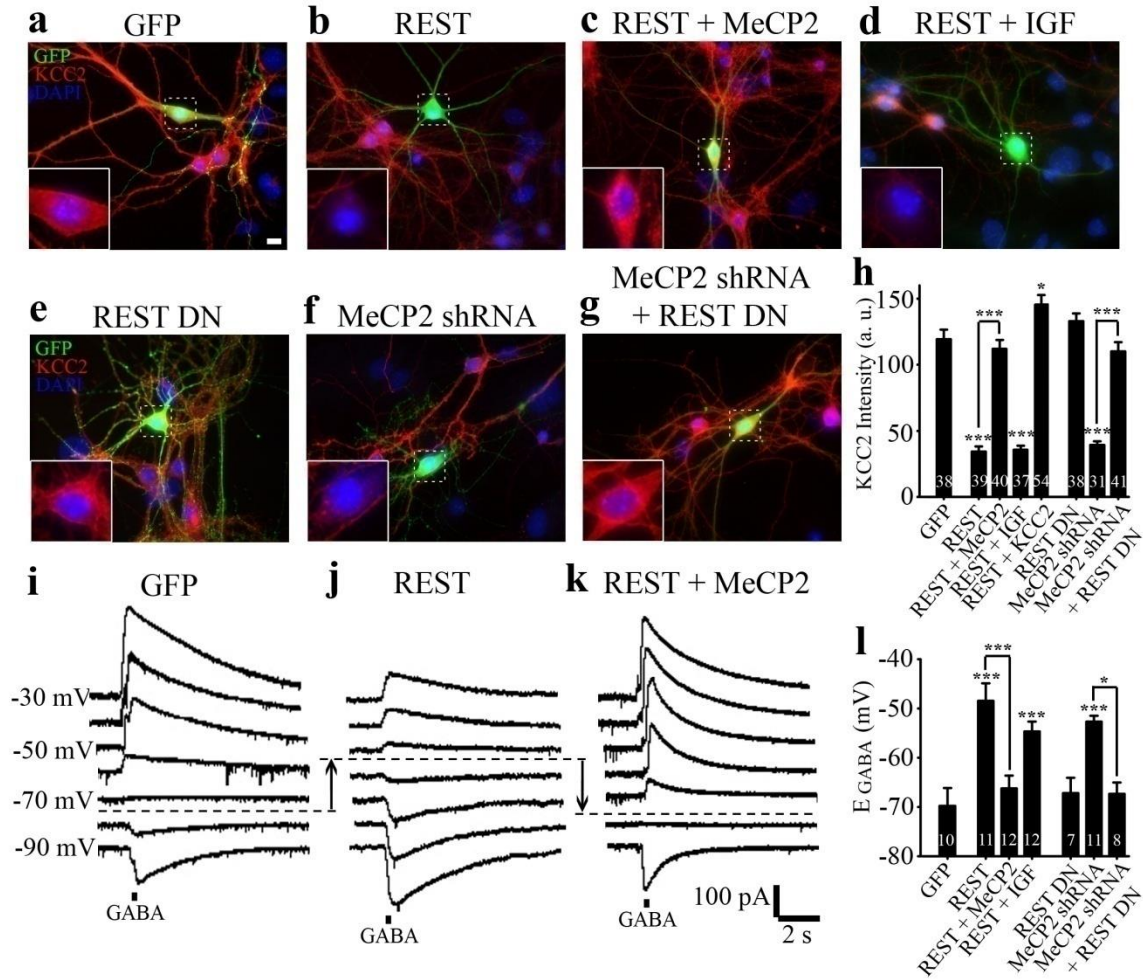


Figure 3-10: MeCP2 regulates KCC2 through the transcriptional repressor REST.

a-h, Representative micrographs and quantifications showed that in mouse cortical neurons transfected with REST, the KCC2 immunoreactivity (red) was significantly reduced comparing to the GFP transfected control cells (**a**, GFP: 119 ± 7 a.u., $n = 38$; **b**, REST: 35 ± 4 a.u., $n = 39$; $P < 0.001$ determined by one-way ANOVA with Bonferroni correction). When MeCP2 and REST were co-expressed in the same neuron, KCC2 expression was restored to normal level (**c**, REST + MeCP2: 112 ± 7 a.u., $n = 40$, $P < 0.001$ comparing to the REST group). Alternatively, the KCC2 reduction caused by knocking down MeCP2 with shRNA construct can be rescued by expressing a dominant negative version of REST (**f**, MeCP2 shRNA: 39 ± 3 a.u., $n = 33$; **e**, REST DN: 133 ± 6 a.u., $n = 38$; **g**, MeCP2 shRNA + REST DN: 110 ± 7 a.u., $n = 41$, $P < 0.001$ comparing MeCP2 shRNA and MeCP2 shRNA + REST DN). Adding IGF to neurons transfected with REST did not significantly increase KCC2 expression (**d**, REST + IGF: 36 ± 3 a.u., $n = 37$, n.s. comparing to the REST group). Scale bar = 10 μ m. **i** to **l**, Electrophysiological analysis of GABA reversal potential (EGABA) showed that neurons transfected with REST demonstrated significantly more depolarized GABA reversal potentials (**i**, GFP: EGABA = -69.8 ± 3.7 mV, $n = 10$; **j**, REST: -48.4 ± 3.5 mV, $n = 11$, *** $p < 0.001$, One-way ANOVA with Bonferroni correction). This deficiency in GABA functional switch in the REST transfected

neurons can be rescued by co-expression of MeCP2 (**k**, REST + MeCP2: -66.2 ± 2.6 mV, $n = 12$, *** $p < 0.001$ comparing to REST group). Alternatively, the GABA functional switch deficit caused by knocking down MeCP2 with shRNA construct can be rescued by expression of a dominant negative version of REST (MeCP2 shRNA: -52.6 ± 1.1 mV, $n = 11$; REST DN: -67.2 ± 3.1 mV, $n = 7$; MeCP2 shRNA + REST DN: -67.3 ± 2.2 mV, $n = 8$. $P < 0.001$ comparing MeCP2 shRNA and MeCP2 shRNA + REST DN). Adding IGF to REST transfected neurons caused a small hyperpolarizing shift of EGABA, possibly due to phosphorylation of KCC2 (REST + IGF: -54.6 ± 2.0 a.u., $n = 12$. n.s. comparing to the REST group).

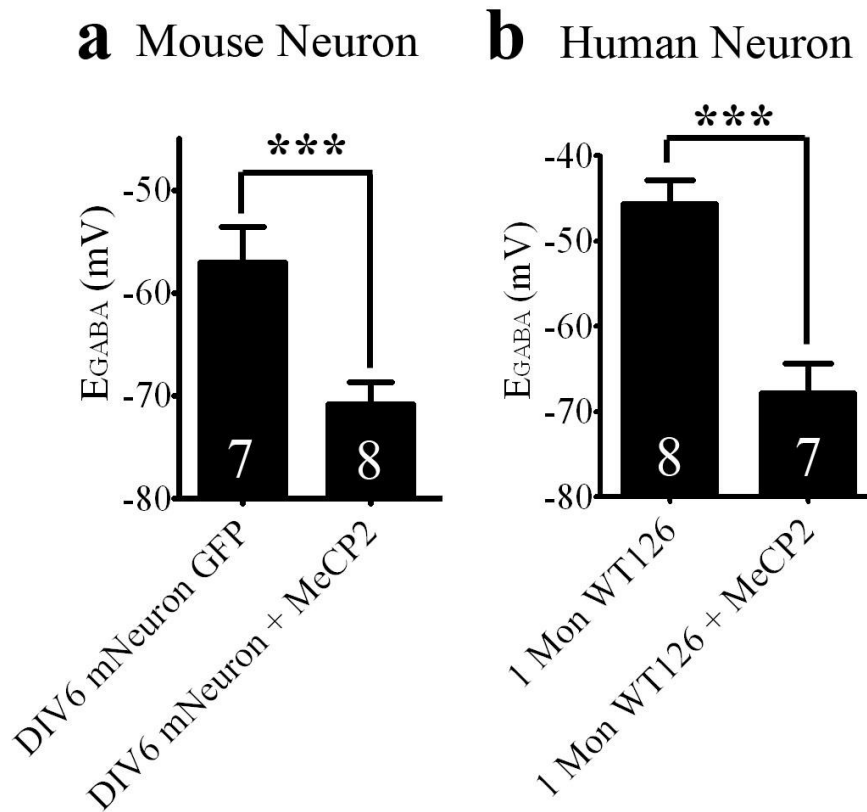


Figure 3-11: MeCP2 Regulates KCC2 during neuronal maturation.

When the expression level of MeCP2 is upregulated by plasmid transfection early in development (DIV6 for mouse neurons, one month for human neurons), EGABA became significantly more hyperpolarized, suggesting a corresponding increase in KCC2 expression.

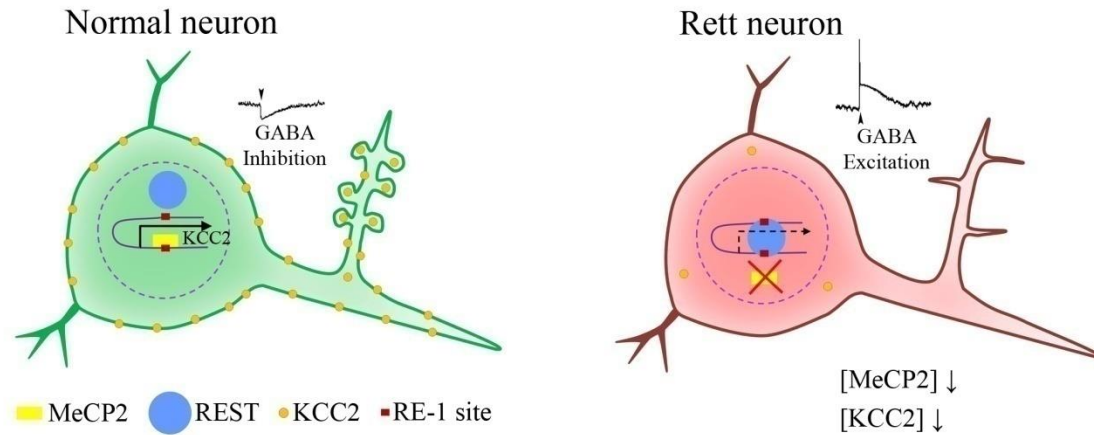


Figure 3-12: Working model

3.2 Discussion

In this study, we report a novel link between KCC2 and MeCP2. Using human neurons derived from iPSCs originated from Rett patient and healthy controls, we have found that the KCC2 expression level is very low in the Rett neurons, leading to impaired GABA functional switch from excitation to inhibition, which can be rescued by IGF treatment. We have confirmed these findings in parallel studies in mouse neurons. Specifically, knockdown MeCP2 in mouse neurons results in KCC2 reduction, which is accompanied with deficits in GABA functional switch and glutamatergic transmission. The MeCP2 shRNA-induced functional deficits can be rescued by KCC2 overexpression or IGF-1 treatment. Furthermore, we demonstrate that REST is a likely mediator linking MeCP2 to KCC2 function. Taken together, our data suggest that KCC2 may be an ultimate regulatory factor in mediating the converged functional outcome after global transcriptome regulation by MeCP2. We propose that upregulation of KCC2 expression level may rescue the impairment of both glutamatergic and GABAergic neurotransmission in Rett patients.

3.2.1 The timecourse of KCC2 development in normal and Rett syndrome human iPSC-derived neurons

During brain development, the expression of KCC2 has to be tightly regulated. Forced KCC2 expression prior to the normal developmental timecourse leads to deficits in neuronal maturation (Cancedda et al., 2007; Horn et al., 2010), whereas lack of KCC2 will cause massive brain development deficit and the death of the animal shortly after birth (Hubner et al., 2001). The developmental timecourse of KCC2 in the developing nervous system follows a general rule: KCC2 is late onset, gradually expressing in a caudal to rostral order (Rivera et al., 1999; Blaesse et al., 2009). In the neonatal mouse brain, the KCC2 expression level is very low in the cortical and hippocampal regions, and gradually increases to adult level in the first two postnatal weeks (Rivera et al., 1999). In the human brain development, KCC2 is a late onset molecule. The protein level of KCC2 at birth is only about 20% of adult level. A significant increase in KCC2 expression takes place in the first postnatal year, coincides with the timecourse of GABA functional switch in the neonatal brain (Dzhala et al., 2005; Ben-Ari et al., 2012).

In this study, we demonstrated that in wild-type human neurons derived from iPSC, KCC2 development follows a stereotypical order which is highly repeatable between different iPSC lines: the expression of KCC2 is low after one month culturing on astrocyte, gradually increasing to more than half the neurons expressing KCC2 at two month. At three month time point, the vast majority of neurons has substantial KCC2 expression and has completed the GABA functional switch. This prolonged timecourse of KCC2 development in human neurons mirrors the finding that GABA functional switch takes a long time in human postnatal development. Remarkably, in parallel NPC seeded on laminin instead of glial cells, the KCC2 expression is very low even after three months in culture, highlighting the participation of glial cells in regulating the developmental timecourse of KCC2.

3.2.2 KCC2 is a key downstream gene of MeCP2 that directly regulates both inhibitory and excitatory neurotransmission

The KCC2 expression level increases with early brain development in both humans and rodents (Dzhala et al., 2005). The expression of KCC2 can be regulated both by extrinsic factors (Kelsch et al., 2001; Rivera et al., 2004; Coull et al., 2005; Boulenguez et al., 2010; Bos et al., 2013; Yeo et al., 2013) and intrinsic transcriptional factors including REST (Uvarov et al., 2006;

Yeo et al., 2009; Ludwig et al., 2011b; Rinehart et al., 2011). MeCP2, the molecular culprit of Rett syndrome, is a master regulator enriched in neurons and regulates the expression of many neuronal genes (Zhou et al., 2006; Skene et al., 2010a; Cohen et al., 2011). In this study, we demonstrated that MeCP2 regulates the expression level of KCC2, and consequently controls GABA functional switch and determines glutamatergic neurotransmission efficacy. Our data identified KCC2 as the key downstream gene that mediates MeCP2's ability to control both excitatory and inhibitory neurotransmission.

Since KCC2 not only controls GABA functional switch from excitation to inhibition during brain development, but also localizes in dendritic spines to determine glutamatergic transmission. Therefore, KCC2 may be an important developmental marker for neuronal maturation. Since brain function requires a delicate balance between glutamatergic excitation and GABAergic inhibition, we propose that the completion of GABA functional switch from excitation to inhibition can be used as a milestone for neuronal maturation. Delayed GABA functional switch, such as demonstrated here in Rett neurons, may cause developmental retardation due to the continuous immature status of the neurons.

We also found that the MeCP2 regulation of KCC2 is mediated by REST. In normal neurons, MeCP2 can bind to the RE-1 site within the KCC2 promoter, thus preventing REST binding to KCC2 promoter to inhibit KCC2 gene expression (Yeo et al., 2009). In Rett neurons, where MeCP2 is deficient, REST can bind with an RE-1 site in the KCC2 promoter region as well as an additional RE-1 site in the intronic region of KCC2 gene to suppress KCC2 expression. MeCP2 can also directly modulate REST expression, adding an additional mechanism of regulation on REST-targeting genes (Abuhatzira et al., 2007). On the other hand, MeCP2 is also known to regulate BDNF (Chang et al., 2006; Zhou et al., 2006). Thus, we cannot exclude the possibility that MeCP2 regulates other factors such as BDNF, which in turn can regulate KCC2. While MeCP2 is known to regulate many downstream signaling molecules, our data suggest that the synaptic deficits triggered by the absence of MeCP2 in Rett neurons may be caused by the downregulation of KCC2.

3.2.3 Targeting KCC2 to treat Rett syndrome

Deficits in KCC2 expression have been linked to a number of neuropsychiatric disorders. A disruption in KCC2 mRNA level have been reported in schizophrenia patients (Arion and

Lewis, 2011; Hyde et al., 2011). Differences in expression levels of specific KCC2 transcripts have also been linked to Schizophrenia and affective disorders (Tao et al., 2012). Mutations in neuroligin 2 (NL2), the cell adhesion molecule critical for GABAergic synapse formation, are found in schizophrenia patients (Sun et al., 2011). Unexpectedly, reduction in NL2 can lead to a significant decrease in KCC2 expression, suggesting KCC2's participation in the pathogenesis of schizophrenia (Sun et al., 2013). Altered KCC2 expression has also been implied in mediating stress axis behaviors (Hewitt et al., 2009).

Recent clinical trial evidence pointed out that bumetanide, an inhibitor of NKCC1, can be used to reduce autistic behavior in patients (Lemonnier et al., 2012) and to treat Fragile-X syndrome (Lemonnier et al., 2013). Two recent research articles have also described a delayed GABA functional switch in mouse model of Fragile X syndrome (He et al., 2014), and the effect of maternal oxytocin on the offsprings' chloride homeostasis in the Fragile-X syndrome and VPA-induced autism model (Tyzio et al., 2014). Together with our own studies, we suggest that deficits in GABA functional switch may be an important contributor toward the pathogenesis of many autism spectrum disorders.

IGF treatment can partially rescue Rett-like symptoms in MeCP2 deficient mouse model (Tropea et al., 2009), and our previous work demonstrated that IGF can rescue some functional deficits in Rett syndrome human neurons (Marchetto et al., 2010b). In this study, our data suggest that IGF may relieve REST inhibition and rescue KCC2 expression in Rett neurons, which may serve as a mechanistic explanation for IGF treatment of Rett syndrome. Therapeutic strategies aim to restore MeCP2 expression level to treat Rett syndrome have yielded promising results in animal models (Giacometti et al., 2007; Garg et al., 2013). However, the recent discoveries indicate that maintaining proper expression level of MeCP2 is critical for neuronal function, which call for caution to the therapeutic approaches that manipulate MeCP2 level in human patients (del Gaudio et al., 2006; Na et al., 2012b). On the other hand, since disruption of KCC2 expression and function contributes to numerous neurological disorders, restoring KCC2 is emerging as a valuable therapeutic approach (De Koninck, 2007; Kahle et al., 2008). A number of compounds have been identified to promote the function of existing KCC2 or increase KCC2 expression level (Coull et al., 2005; Ferrini et al., 2013). Our study suggests that KCC2 may be a novel drug target for developing new therapy to treat Rett syndrome.

Additional experiments could be added to strengthen our conclusion. Human neurons derived from more NPC lines with different Rett syndrome-causing mutations should be analyzed to strengthen the robustness of our findings. *In vivo* confirmation in both MeCP2 knockout

animal and human Rett syndrome patient can provide insight into the applicability of our human neuron data in the whole brain setting. Detailed experiments to investigate the molecular mechanisms of how MeCP2 interacts with REST to regulate KCC2 should be carried out, and the mechanism of IGF rescue of KCC2 expression in the absence of MeCP2 should also be elucidated.

Since brain function requires a delicate balance between glutamatergic excitation and GABAergic inhibition, we propose that the completion of the GABA functional switch from excitation to inhibition can be used as a milestone for neuronal maturation. A delayed GABA functional switch, such as that demonstrated here in Rett neurons, may cause developmental retardation due to the continuous immature status of the neurons. Thus, deficits in the GABA functional switch, together with deficits in glutamatergic transmission, may be important contributing factors toward the pathogenesis of autism spectrum disorders. Correction of the GABA functional switch and glutamatergic deficits by targeting KCC2 function may be a novel therapeutic approach for autistic disorders.

Chapter 4

Astroglial Cells Regulate the Developmental Timeline of Human Neurons Differentiated from induced Pluripotent Stem Cells

In this study, our lab collaborated with Dr. Carol M. Marchetto in the lab of Dr. Fred Gage at the Salk Institute, and Dr. Cassiano Carromeu in Dr. Alysson Muotri's lab at UCSD School of Medicine. They provided the WT126 and WT33 NPC cells for our research. Dr. Li Zhou participated in the culturing of NPC cells and did the stem cell marker staining. Alecia Wagner did the Sholl Analysis. Dr. Chen and I designed the experiments, and I performed most of the experiments. Part of this work has been published on *Stem Cell Research* (Tang et al., 2013).

4.1 Results

4.1.1 Essential role of astroglial cells in neural differentiation

Human neural progenitor cells (hNPCs) were derived from hiPSCs reprogrammed from fibroblasts as described before (Marchetto et al., 2010b). The majority of the experiments were carried out using NPCs derived from hiPSC line WT126, unless otherwise stated (some experiments were confirmed using NPCs from hiPSC line WT33). These hNPCs were confirmed to express neural stem cell markers including Sox2, Nestin, and Musashi (Fig. 4-1). The neural differentiation process of hiPSCs appears to vary greatly in the published literature, ranging from weeks to months (Marchetto et al., 2010b; Zeng et al., 2010; Brennand et al., 2011; Hester et al., 2011). To establish a rapid neural differentiation protocol, we plated hNPCs on different substrates: laminin, laminin with glial-conditioned medium (GCM), or directly on a monolayer of astroglial cells prepared from neonatal mouse cortex. We found that neural differentiation was very slow when hNPCs were plated on laminin, but significantly faster when they were plated on astrocytes (Fig. 4-2). Notably, we detected a significant number of immature neurons labeled by doublecortin (DCX) at 7 days after plating (DAP) on astrocytes, but very few neurons on laminin (Fig. 4-2B; astrocyte, 12.6 ± 7.3 ; laminin, 0.6 ± 0.1 per imaging field; $p < 0.05$). Quantitative analysis also revealed that the total number of cells labeled by human nuclei (HuNu) was significantly higher when hNPCs were plated on astrocytes (7 DAP, 58.3 ± 19.5 per imaging field) than on laminin (12.5 ± 1.7 , $p < 0.05$), suggesting that astroglial cells promote not only neural differentiation but also cell proliferation and survival (Fig. 4-2C). Glial conditioned medium (GCM) showed beneficial effects in increasing the number of neurons and total cells when compared to laminin, but not as potent as the direct contact with astroglial cells (Fig. 4-2A-C), indicating that both diffusible and membrane-bound factors from astroglial cells are important for neural differentiation of hiPSCs. The neural differentiation efficiency, which is defined as the percentage of neurons (DCX+) among the total number of human cells, was 23% on astroglial substrate, but only 5% on laminin and 11% for GCM group. Immunostaining with a different neuronal marker Tuj1 also showed significantly enhanced neural differentiation on astroglial substrate compared to that on laminin (Fig. 4-3). Moreover, we performed similar experiments using a different hiPSC cell line WT33 and confirmed that both the number of DCX-positive neurons and total number of human cells were significantly higher on astroglial substrate than

that on laminin (Fig. 4-4). Among neurons differentiated from hNPCs when cultured on astrocytes, we not only detected glutamatergic and GABAergic neurons, but also found some dopaminergic and cholinergic neurons (Fig. 4-5). These results suggest that astroglial cells play a critical role in promoting neural differentiation and cell proliferation of hNPCs derived from hiPSCs.

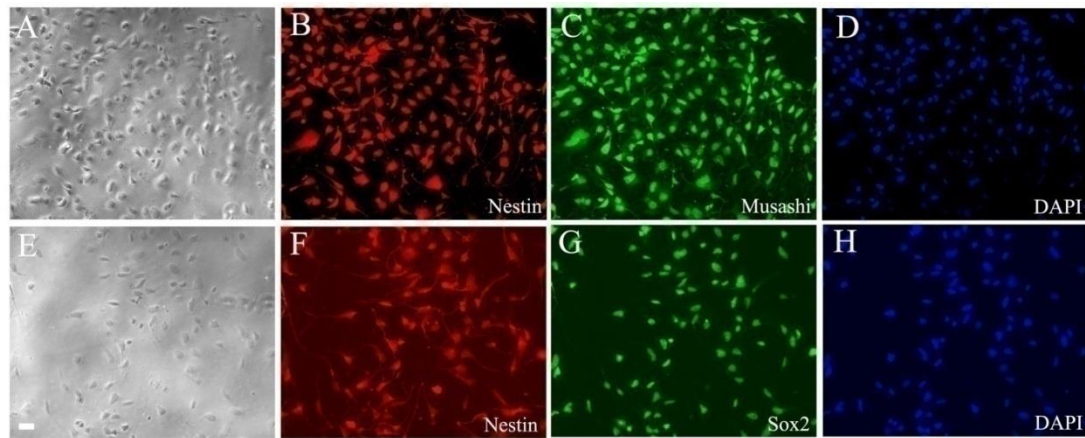


Figure 4-1: Confirmation of the neuroprogenitor properties derived from human iPSCs.

Cultured human NPCs express typical neural stem cell markers, including Nestin (B, F), Musashi (C), and Sox 2 (G). Scale bar = 10 μ m.

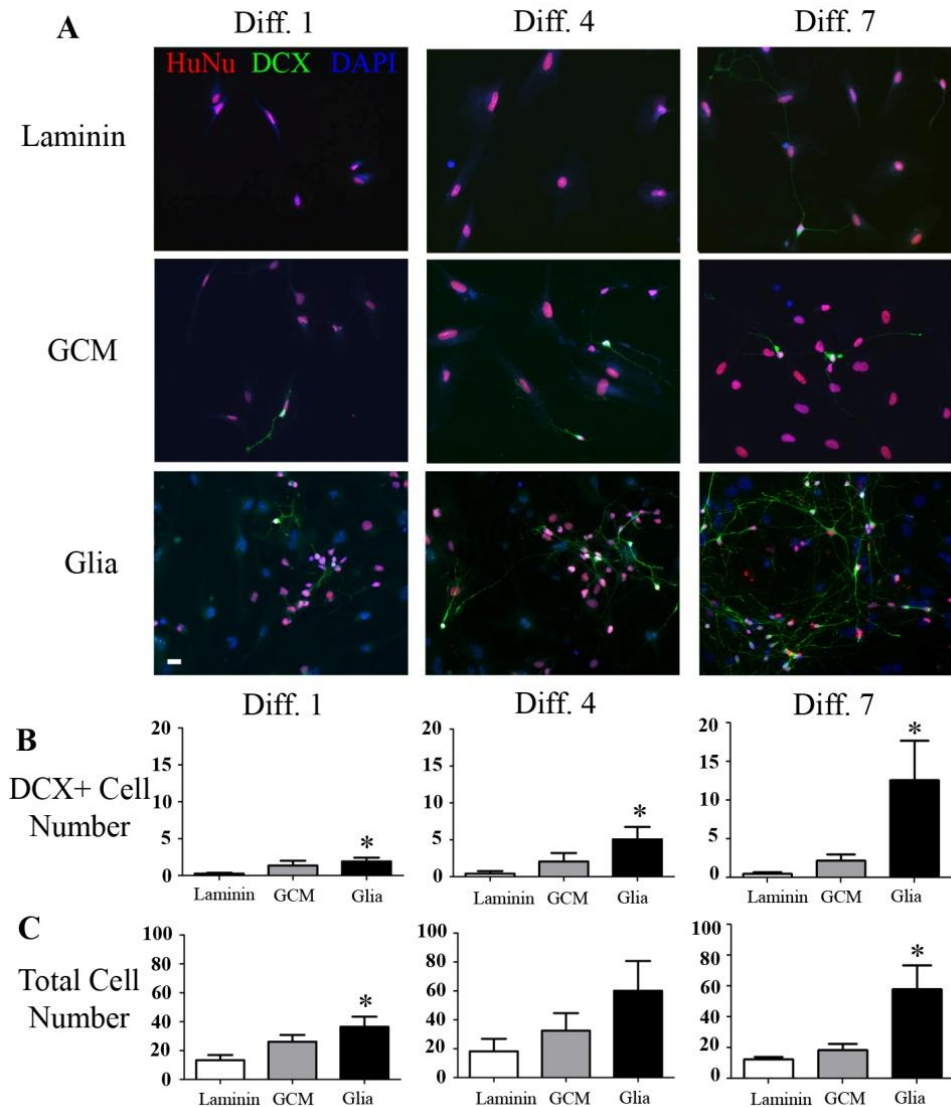


Figure 4-2: Astrocytes promote neuronal differentiation of human iPS cells.

(A) Representative images showing neuronal differentiation of human hNPCs within first week after plating under different conditions including laminin, laminin + GCM, and astroglial cells. Human nuclei (red) labels hiPSC-derived cells, and doublecortin (green) labels newly differentiated neurons. Scale bar = 10 μ m.

(B) Quantification of doublecortin positive (DCX+) cells (20x imaging field, 427 x 341 μ m) in different experiment groups. Data are presented as mean \pm SEM. $n > 7$ for each bar graph. * $p < 0.05$ (one-way ANOVA followed by Bonferroni correction).

(C) Quantification of total cell number (human nuclei labeled cells) under different conditions. $N = 7 - 10$ independent replicates. * $p < 0.05$, ** $p < 0.01$ (one-way ANOVA followed by Bonferroni correction).

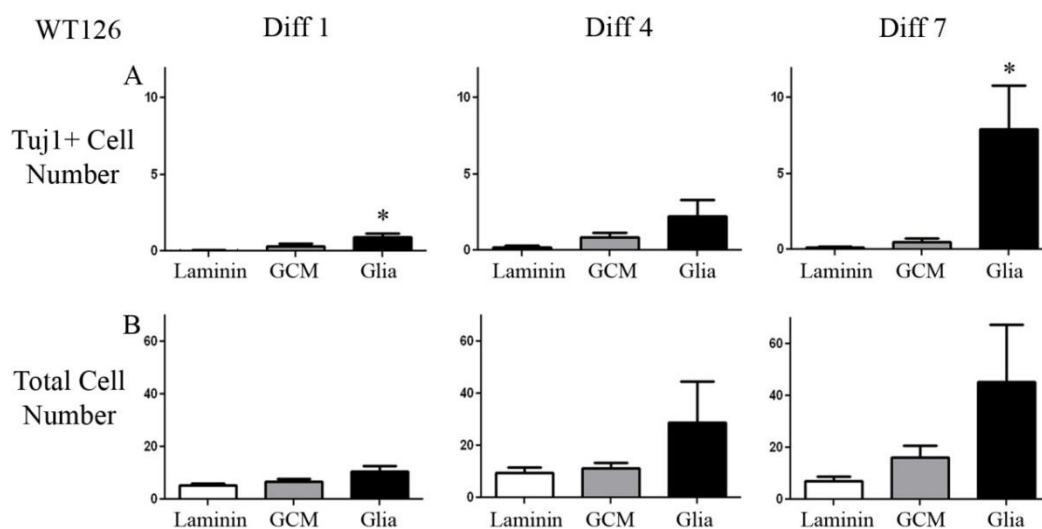


Figure 4-3: Astrocytes promote neural differentiation when assessed with a different neuronal marker Tuj1 instead of doublecortin.

(A) Quantification of Tuj1-positive neurons (20x imaging field, 427 x 341 μm) in different experimental groups. Data are presented as mean \pm SEM. N = 5 independent replicates. * $p < 0.05$, one-way ANOVA followed by Bonferroni correction.

(B) Quantification of total cell number (human nuclei-labeled cells) under different culture conditions.

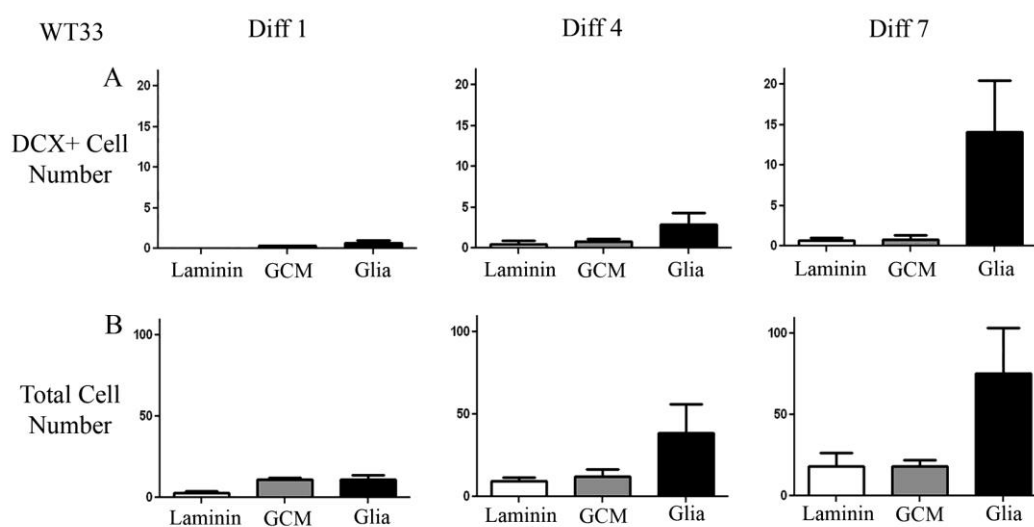


Figure 4-4: Astrocytes promote neural differentiation using hiPSC WT33 line-derived NPCs.

(A) Quantification of doublecortin positive (DCX+) cells (20x imaging field, 427 x 341 μm) in different experimental groups. Data are presented as mean \pm SEM. N = 4 independent replicates.
 (B) Quantification of total cell number (human nuclei-labeled cells) under different conditions. N = 4 independent replicates.

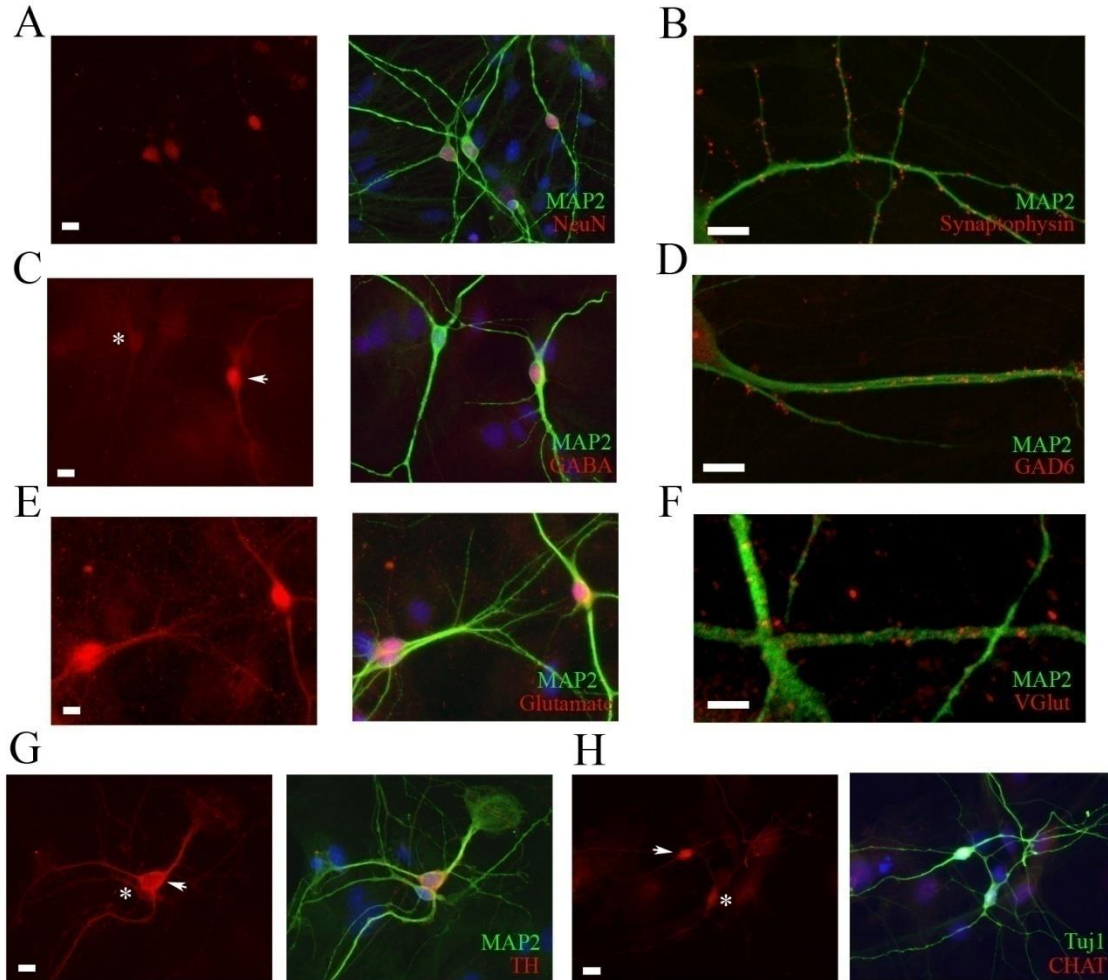


Figure 4-5: A variety of neuronal subtypes generated from human iPS cells.

Among mature human neuron populations (> 1 month in culture; NeuN, panel A), several different subtypes of neurons were detected, including GABA (C), glutamate (E), tyrosine hydroxylase (TH, panel G, labeling dopaminergic neurons), and choline acetyltransferase (CHAT, panel H, labeling cholinergic neurons). The human neurons also expressed a variety of synaptic markers, including synaptophysin (B), GAD6 (D), and VGlut (F). Arrows indicate

neurons positive for markers, whereas * indicates negatively stained neurons. Scale bar = 10 μm for panel A, C, E, G, and H; 5 μm for panel B, D, and F.

4.1.2 Neurons inhibit NPC survival and neural differentiation

In the nervous system, the stem cells are constantly under the influences from their cellular neighbors, mainly glial cells and neurons. Since my data showing clearly astrocytes can promote NPC neural differentiation, we next asked the question of how does neurons affect NPC's fate choice. We found that contrary to astrocyte's function to promote NPC survival, proliferation and neural differentiation; preexisting neurons suppress NPC proliferation and neuronal differentiation.

In order to study the interactions among a limited number of cells in a confined space, we utilized Microisland culture method to study preexisting neuron's effect on NPC fate (Jiang and Chen, 2006; Burgalossi et al., 2012). Glial cells were plated on microislands with the same density as in PDL coated coverslips, neurons were subsequently seeded in low density (1/10 to 1/20 of normal seeding density). One week after neuronal culture, NPC were seeded onto the microisland culture at the concentration of 40'000 to 80'000 NPCs per well in a 24-well plate. Analysis of NPC number and fate choice were performed one week after seeding from the microislands on the same coverslip, but with different numbers of neurons.

On the microisland without any preexisting neurons, NPC proliferate robustly as evidenced by the large number of HuNu+ cells on the island (Fig. 4-6-A, purple cells). Transversely, on the microisland with both neurons and glial cells, NPC proliferation was significantly halted (Fig. 4-6-B). A clear negative correlation can be observed between the number of neurons on the microisland and the number of NPC observed (Fig. 4-6-C, $n = 46, 24, 22, 13$ and 4 microislands were analyzed in each group, $p < 0.001$). This suppression on NPC number is not due to smaller size of microislands, for the microislands with more neurons were generally larger than the ones without neurons (Fig. 4-6-D).

Preliminary data that we generated demonstrate that when co-culturing h-iPSC-NPC with primary neurons, the survival and neuronal differentiation of h-iPSC-NPC will be significantly reduced. The strength of this suppression is positively correlated with the distance from primary neuron body, suggesting a contact/autocrine-mediated inhibition mechanism. For the surviving

NPC, the fate choices were biased toward non-neuronal fate when they were close to preexisting neurons (Fig. 4-6-E, mouse neuron in the center. Red arrow point to an NPC near a mouse neuron, which did not adapt neuronal fate. Green arrow point to an NPC underwent neuronal differentiation. Note its location was far away from the mouse neuron). When plotting the distance of all NPCs relative to the closest mouse neuron, against the NPC-derived neurons' distance against the closest mouse neuron, a clear shift toward longer distance was observed (Fig. 4-6-F), indicating that mouse neurons suppress the nearby NPC from adapting a neural fate.

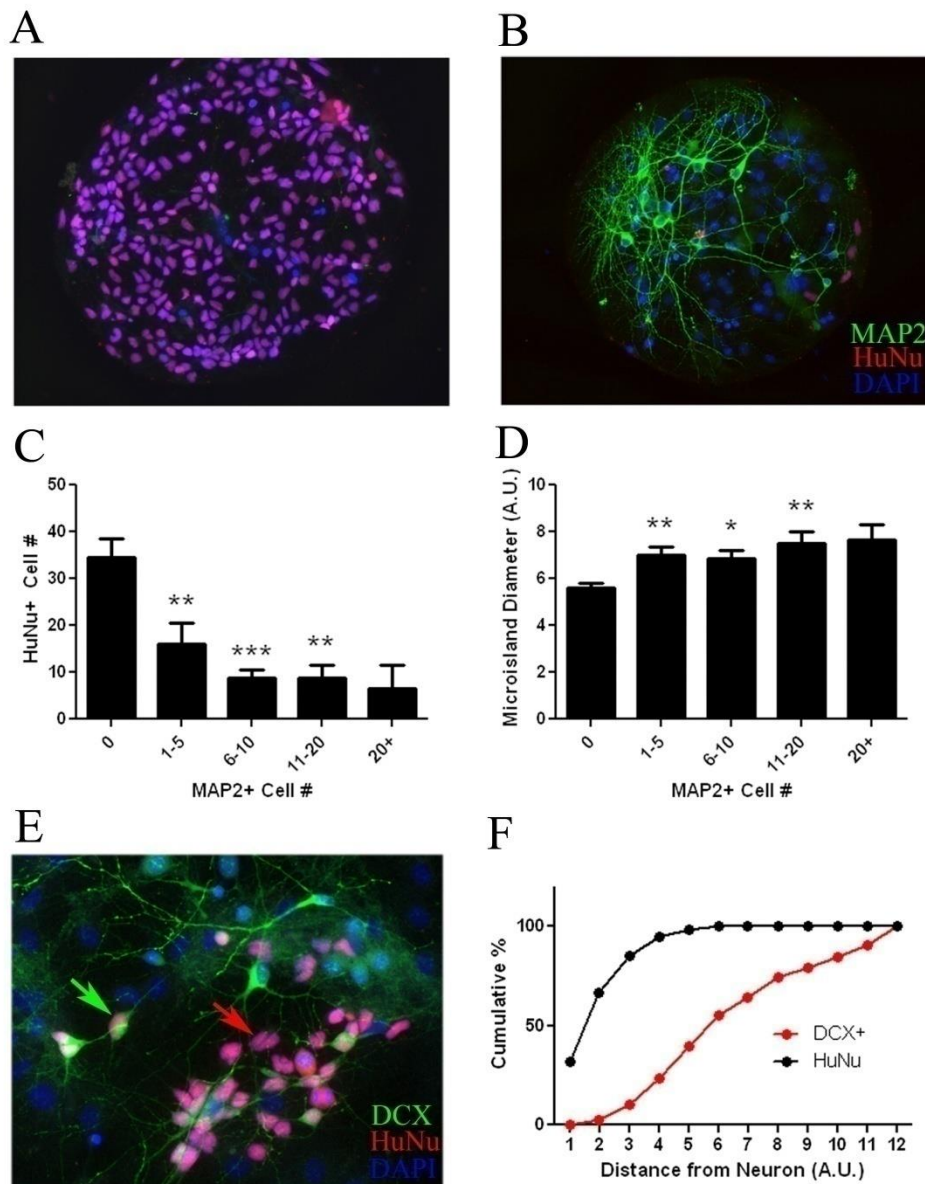


Figure 4-6: Neurons suppress NPC proliferation and neuronal differentiation.

Microisland culture method was used to study preexisting neuron's effect on NPC fate. On the microisland with glial cells (A, blue DAPI staining), NPC proliferate robustly one week after seeding (A, purple HuNu+ cells), whereas on the microisland with both neurons and glial cells (B), NPC proliferation was significantly halted. A clear negative correlation can be observed between the number of neurons on the microisland and the number of NPC observed one week after seeding (C, $n = 46, 24, 22, 13$ and 4 microislands were analyzed in each group). This suppression on NPC number is not due to smaller size of microislands, for the microislands with more neurons were generally larger than the ones without neurons (D). For the surviving NPC, the fate choices were biased toward non-neuronal fate when they were close to preexisting neurons (E, mouse neuron in the center. Red arrow point to an NPC near a mouse neuron, which did not adapt neuronal fate. Green arrow point to an NPC underwent neuronal differentiation. Note its location was far away from the mouse neuron). When plotting the distance of all NPC relative to the closest mouse neuron against the NPC-derived neurons' distance against the closest mouse neuron, a clear shift toward longer distance was observed, indicating that mouse neurons suppress the nearby NPC from adapting a neural fate.

4.1.3 Astrocytes promote dendritic development

The complexity of dendritic arborization is an important indicator of neuronal maturation. We found that plating hNPCs on astroglial cells resulted in neurons with increased dendritic complexity, whereas neurons on laminin showed fewer dendrites (Fig. 4-7-A). We utilized Sholl analysis (Fig. 4-7-B) (Wearne et al., 2005; Ristanovic et al., 2006) to quantitatively investigate the dendritic intersections (Fig. 4-7-C) and branch points (Fig. 4-7-D) in neurons cultured over a time course of two months. Specifically, after 7 DAP, doublecortin positive (DCX+) neurons differentiated on laminin only had 14.4 ± 2.2 intersections per cell ($n = 20$), but neurons differentiated on astrocytes had 34.2 ± 4.1 intersections per cell ($n = 20$, $p < 0.001$; Fig. 4-7-C). Similarly, the number of branch points of neurons differentiated on astrocytes (7 DAP; 5.0 ± 0.9 per cell; $n = 20$) was significantly greater than that on laminin (0.8 ± 0.2 per cell; $n = 20$; $p < 0.001$; Fig. 4-7-D). Furthermore, neurons on glial cells showed increased cell body size compared to those on laminin (Fig. 4-7-E, 7 DAP, 145 ± 12 a.u. for laminin group, 301 ± 32 a.u. for glial group, $p < 0.001$). Thus, astrocytes provide essential support to promote neuronal soma and dendritic development.

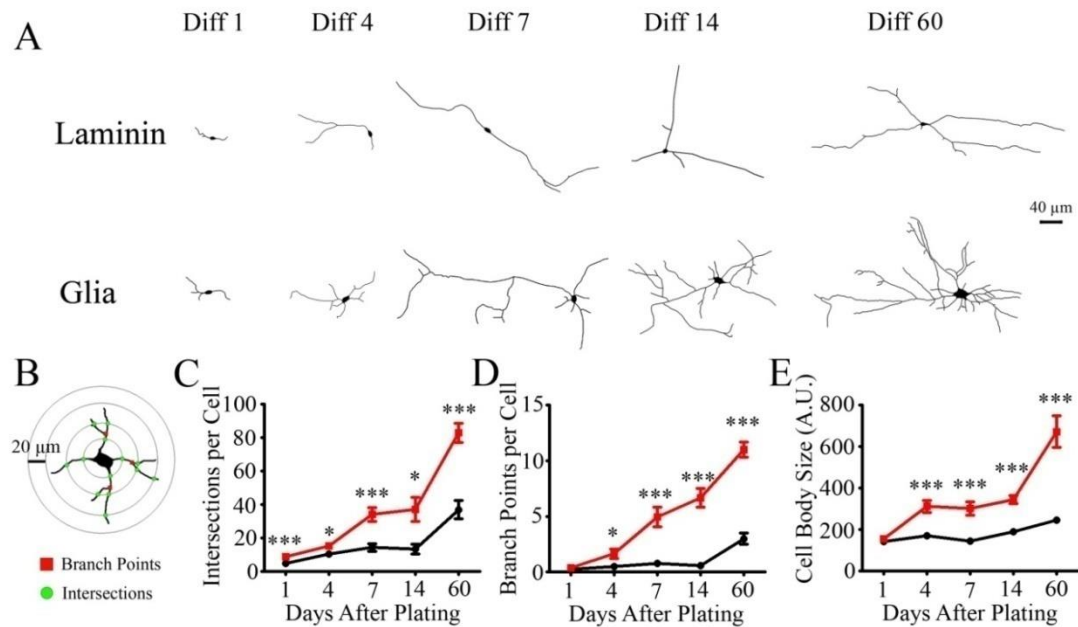


Figure 4-7: Astrocytes promote morphological development of hiPSC-derived neurons.

(A) Representative dendritic tree of hiPSC-derived neurons growing on laminin or glial cells at different time points.

(B) Schematic diagram showing the dendritic branch points (red dots) and intersections (green dots) used for Sholl analysis.

(C) Quantification of the average number of intersections that neurites cross on a series of concentric Sholl circles. For C-E: * $p < 0.05$, *** $p < 0.001$ (student's t test).

(D) Quantification of the average number of dendritic branch points.

(E) Quantification of the cell body size of hiPSC-derived neurons cultured on glial cells or laminin. $N = 20$ for each data point.

4.1.4 Rapid expression of functional channels and receptors

The ultimate function of neurons is their ability to fire action potentials and release neurotransmitters. We employed whole-cell patch-clamp recordings to investigate functional properties of neurons derived from hiPSCs. Remarkably, we were able to detect action potentials as early as four days after plating hNPCs on astroglial cells (Fig. 4-11-A-B, $n = 3$ out of 8). Moreover, spontaneous synaptic events were detected as early as six days after plating on astrocytes (Fig. 4-11-C - D, $n = 2$ out of 12). Such rapid functional differentiation has been verified by plating hNPCs from a different hiPSC line (WT33) on astrocytes (Fig. 4-11-E-F and

G-H). Our results suggest that hiPSC-derived neurons can fire action potentials and release neurotransmitters very early if provided adequate glial support.

We next systematically studied the action potential firing and passive membrane properties of hiPSC-derived neurons cultured on laminin versus on glial cells. Within two weeks of culture, neurons mainly fired single action potential upon membrane depolarization, regardless whether plated on laminin or glial cells. After three weeks in culture, 2/9 neurons on glial cells started to fire repetitive action potentials, but none of the neurons on laminin (0/6) could fire repetitive action potentials (Fig. 4-9-A). After 6 weeks of culture, 16/22 neurons cultured on glial cells fired repetitive action potential, in contrast to only 4/25 neurons cultured on laminin. After two months, the majority of neurons cultured on astrocytes all fired repetitive action potentials after membrane depolarization, but most of neurons cultured on laminin still fired single or a few action potentials (Fig. 4-9-B). Quantitatively, neurons cultured on glial cells showed decreased action potential threshold (Fig. 4-9-C), increased action potential height (Fig. 4D), and decreased action potential half-width (Fig. 4-9-E), compared to those cultured on laminin, suggesting that astrocytes promoted the maturation of action potential firing. Furthermore, we also quantified the passive membrane properties of neurons cultured on laminin or glial cells for up to two months (Fig. 4-9-F-H). Overall, neurons cultured on glial cells showed higher membrane capacitance (Fig. 4-9-F; 60 DAP: laminin, 27 ± 2 pF, $n = 22$; glia, 119 ± 10 pF, $n = 23$; $p < 0.001$), lower membrane resistance (Fig. 4-9-G; 60 DAP: laminin, 695 ± 87 M Ω , $n = 22$; glia, 302 ± 39 M Ω , $n = 23$; $p < 0.001$), and more hyperpolarized resting membrane potential (Fig. 4-9-H; 60 DAP: laminin, -44 ± 2 mV, $n = 22$; glia, -59 ± 3 mV, $n = 23$; $p < 0.001$). The increased membrane capacitance in neurons cultured on glial cells corresponded well with the increased cell body size shown in Fig. 4-7-E. Together, these results suggest that astrocytes promote the maturation of neuronal membrane properties and action potential firing capabilities of human iPSC-derived neurons.

We next investigated the developmental processes of sodium and potassium channel expression, as well as glutamate and GABA receptor expression in hiPSC-derived neurons. Both Na^+ and K^+ currents in neurons cultured on astrocytes were significantly larger than those cultured on laminin (Fig. 4-8-A-B). For example, at 7 DAP, whole-cell peak I_{K^+} at +50 mV was 2279 ± 171 pA ($n = 33$) in neurons cultured on astrocytes, but only 922 ± 144 pA on laminin (Fig. 4-8-C; $n = 15$, $p < 0.001$); and peak I_{Na^+} was 1094 ± 85 pA ($n = 33$) in neurons on astrocytes, and 388 ± 63 pA on laminin (Fig. 4-8-D; $n = 15$, $p < 0.001$). The expression of neurotransmitter receptors was also enhanced in neurons cultured on astrocytes (Fig. 4-10-A-B), similar to that

reported for mouse neurons (Chen et al., 1995). Quantitatively, at 7 DAP, the average whole-cell GABA receptor peak current was 1585 ± 256 pA ($n = 20$) in neurons cultured on astrocytes, and 498 ± 108 pA on laminin (Fig. 4-10-C; $n = 14$, $p < 0.001$); and the average glutamate receptor current was 229 ± 44 pA ($n = 20$) in neurons cultured on astrocytes, but only 40 ± 12 pA on laminin (Fig. 4-10-D; $n = 15$, $p < 0.001$). Notably, hiPSC-derived human neurons showed much larger GABA receptor currents than glutamate receptor currents, similar to our previous findings on mouse embryonic neurons (Deng et al., 2007), suggesting an evolutionarily conserved role of GABA during early neural development. We further investigated the expression of NMDA receptors in our hiPSC-derived neurons (Fig. 4-10-E-G). NMDA receptors are calcium permeable and have been demonstrated to play important roles in neural development and synaptic plasticity. We detected clear NMDA currents in 6 week old human neurons cultured on glial cells (Fig. 4-10-E; 168 ± 42 pA, $n = 6$) but not in neurons cultured on laminin. After two months of culture, NMDA currents in neurons cultured on glial cells showed a significant increase (Fig. 4-10-F; 1341 ± 232 pA, $n = 8$), whereas the same age of neurons cultured on laminin showed an order of magnitude smaller NMDA current (Fig. 4-10-G, 164 ± 50 pA, $n = 7$, $p < 0.001$). Therefore, astroglial cells play a pivotal role in promoting the expression of functional channels and receptors in neurons differentiated from hiPSCs.

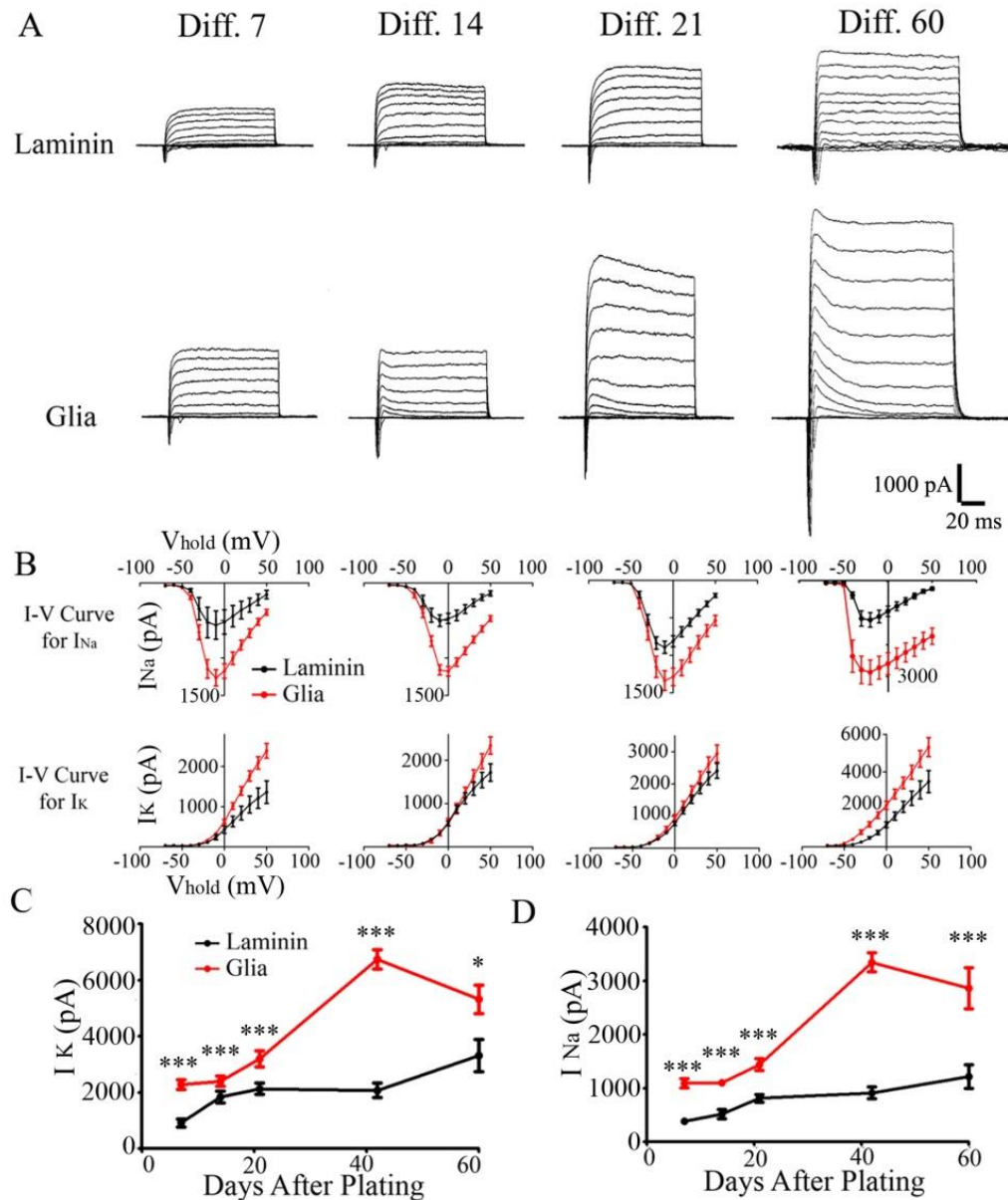


Figure 4-8: Astrocytes increase the expression of Na⁺ and K⁺ channels.

(A) Representative whole-cell Na⁺ and K⁺ currents recorded from hiPSC-derived neurons cultured up to two months on laminin versus astrocytes.

(B) The I-V curves for peak Na⁺ (I_{Na}) and K⁺ (I_K) currents recorded from hiPSC-derived neurons cultured with or without glial cells.

(C) The developmental curves for peak K⁺ currents in human neurons cultured for up to two months on laminin or astrocytes. * p < 0.05, ** p < 0.01, *** p < 0.001 (student's t-test).

(D) The developmental curves for peak Na⁺ currents in human neurons cultured for up to two months on laminin or astrocytes.

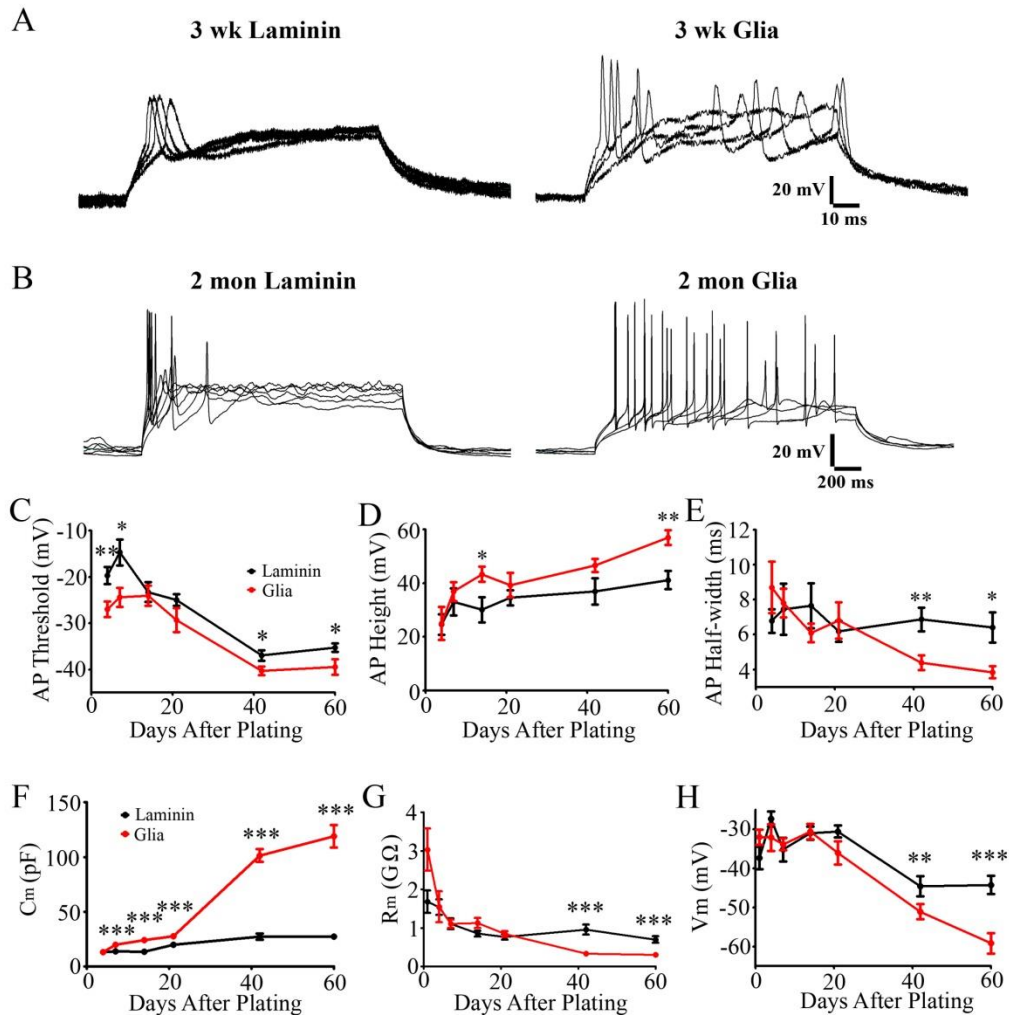


Figure 4-9: Astrocytes promote the development of action potential firing ability and passive membrane properties.

(A) Representative action potentials recorded from 2 weeks hiPSC-derived neurons growing on laminin versus glial cells.

(B) Representative action potentials recorded from 2 months hiPSC-derived neurons growing with or without glial support.

(C - E) The developmental curves for the threshold (C), amplitude (D), and half-width (E) of action potentials recorded from hiPSC-derived neurons growing with or without glial support. * $p < 0.05$, ** $p < 0.01$, *** $p < 0.001$ (student's t-test).

(F - H) The developmental curves for passive membrane properties including membrane capacitance (F), membrane resistance (G), and resting membrane potential (H) recorded from hiPSC-derived neurons growing on laminin versus astrocytes. * $p < 0.05$, ** $p < 0.01$, *** $p < 0.001$ (student's t-test).

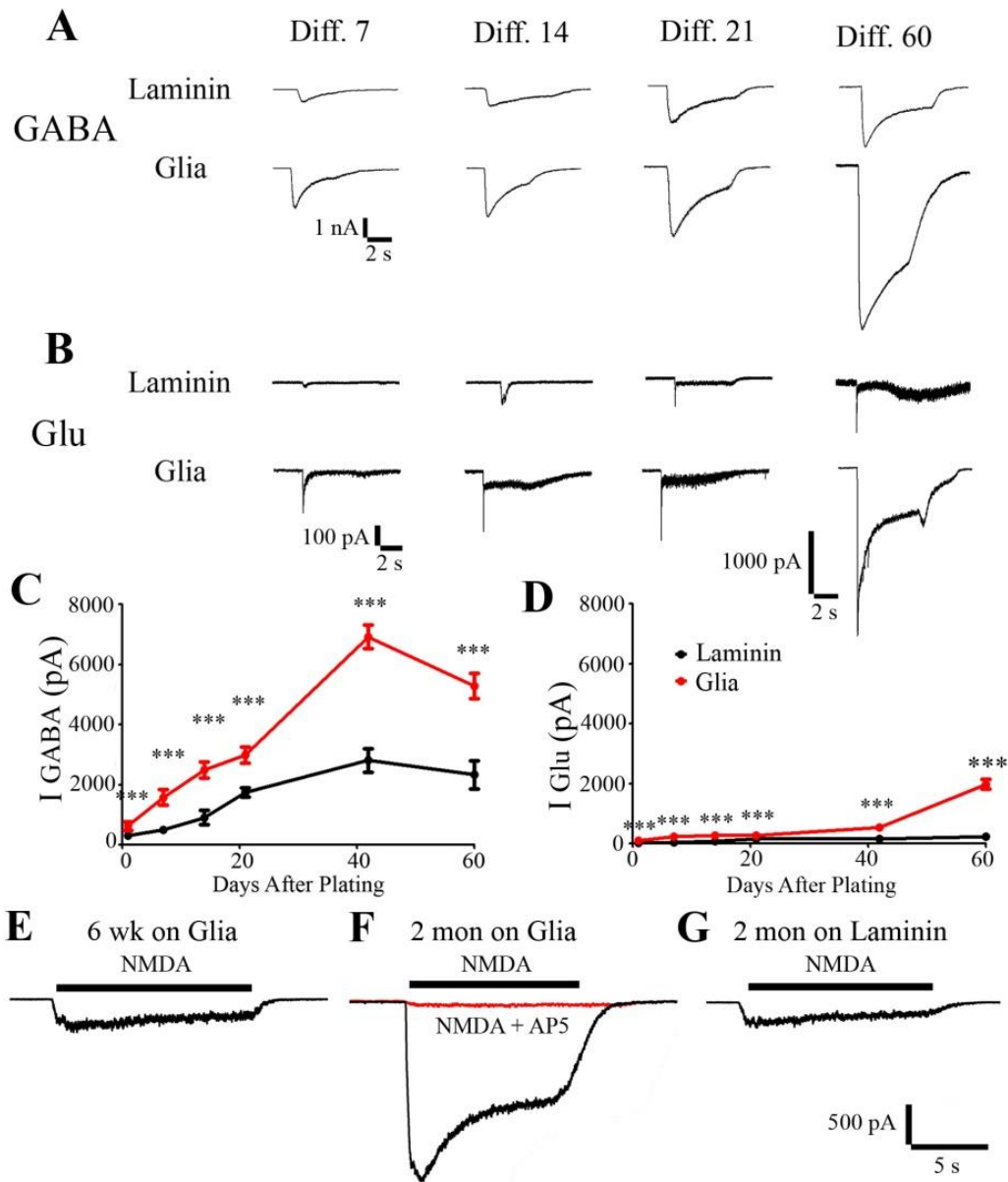


Figure 4-10: Astrocytes increase the expression of neurotransmitter receptors.

(A) Representative whole-cell GABA response traces recorded from hiPSC-derived neurons cultured up to two months on laminin versus astrocytes.

(B) Representative whole-cell glutamate (Glu) response traces recorded from hiPSC-derived neurons growing with or without glial support.

(C) The developmental curves for peak GABA currents in human neurons cultured for two months on laminin or astrocytes. * $p < 0.05$, ** $p < 0.01$, *** $p < 0.001$ (student's t-test).

(D) The developmental curves for peak glutamate currents in human neurons cultured for two months on laminin or astrocytes.

(E - G) Representative traces showing the development of whole-cell NMDA current in hiPSC-derived neurons cultured with or without glial cells. (E) NMDA current recorded from human neuron cultured on astrocyte for six weeks. (F) NMDA current recorded from human neuron cultured on astrocyte for two months. Note that the NMDA current can be largely blocked by AP5 (red trace). (G) NMDA current recorded from 2 month human neuron cultured on laminin.

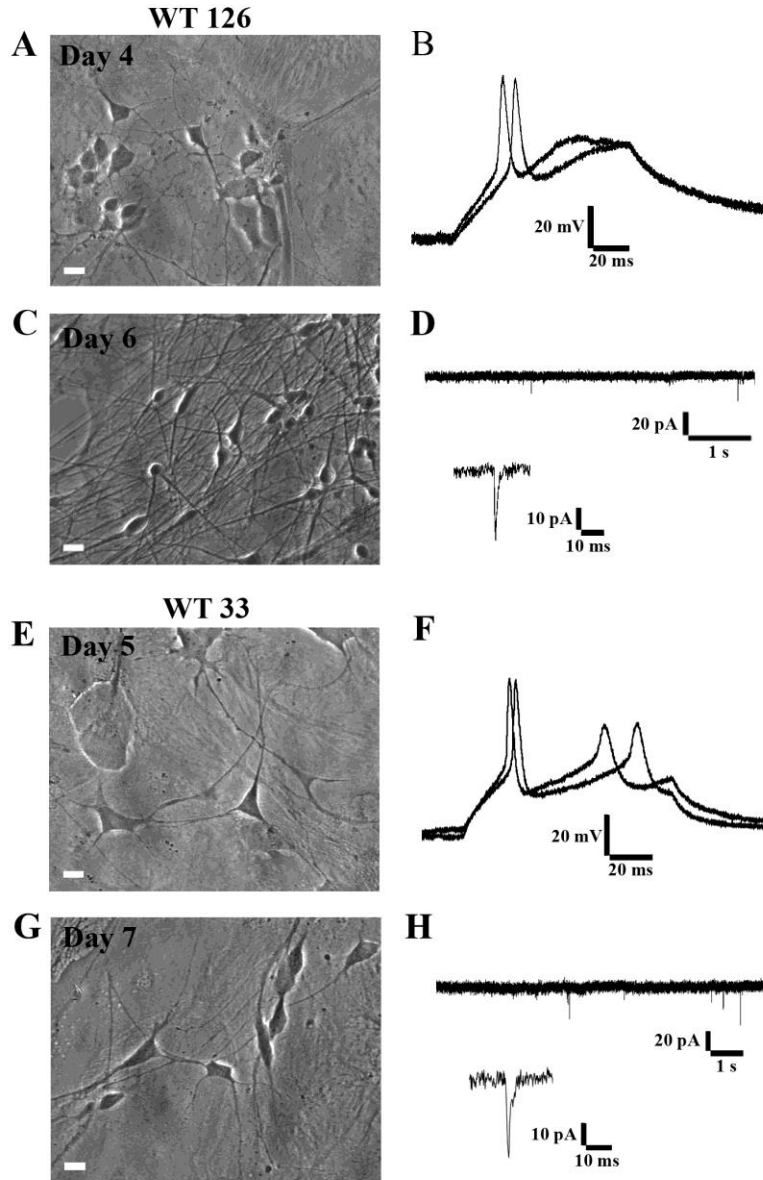


Figure 4-11: Rapid functional development of human iPS cell-derived neurons co-cultured with astrocytes.

(A) Phase image of cells (WT 126) cultured on astrocytes for four days.

(B) Representative action potentials detected 4 days after plating hNPCs on astrocytes.

(C & D) Phase image of cells (WT 126) after six days on astrocytes (C), and spontaneous synaptic events (D) detected from hiPSC-derived neurons.

(E - H) Cells from a different cell line (WT 33) also showed rapid action potential firing (E-F) and spontaneous synaptic events (G-H) after coculture with astrocytes. Scale bar = 10 μ m.

4.1.5 Developmental Timeline of Synaptic Maturation

Recent studies have reported the detection of synaptic events in neurons derived from hiPSCs (Lee et al., 2009; Hu et al., 2010; Marchetto et al., 2010b). However, it is still unclear when these neurons become functional, largely due to the variety of different protocols used. To establish a clear developmental timeline of synaptic maturation for hiPSC-derived neurons to guide future research, we took a systematic approach to record synaptic events in hiPSC-derived neurons from one week up to two months after culturing hNPCs on astrocytes. Immunostaining with synaptic marker SV2 revealed many synaptic puncta on neurons cultured on astrocytes but only a few on laminin (Fig. 4-12-A). This is confirmed by electrophysiological analysis that the majority of neurons plated on astrocytes showed a significant number of spontaneous synaptic events, but those cultured on laminin only showed a few events (Fig. 4-12-B). Quantitatively, neurons cultured on astrocytes for 21 days showed a high frequency of spontaneous synaptic events at 1.17 ± 0.34 Hz and amplitude of 23.3 ± 2.2 pA ($n = 12$), whereas neurons on laminin only showed a frequency of 0.04 ± 0.01 Hz (Fig. 4-12-C, $n = 11$, $p < 0.01$) and amplitude of 12.8 ± 0.5 pA (Fig. 4-12-D, $n = 9$, $p < 0.001$). Importantly, after 2 months of culture on astrocytes, human neurons showed spontaneous bursting activities (Fig. 4-12-B), suggesting that these neurons have formed extensive synaptic network and are highly synchronized through synaptic connections. Moreover, we used a different hiPSC line (WT33) to confirm that human neurons also showed robust synaptic events after 6 weeks of culture on astrocytes (Fig. 4-12-E). Thus, these data suggest that human neurons cultured on astrocytes will not show significant synaptic events till 3 weeks later, and neurons cultured on laminin are further delayed in terms of synaptic maturation.

We next investigated the relative proportion of glutamatergic versus GABAergic events recorded from hiPSC-derived neurons cultured on astrocytes from 2 weeks to 2 months. Interestingly, after 2 weeks of culture, the majority of events detected were rapidly decaying glutamatergic events (Fig. 4-13-A). Slow decaying GABAergic events increased significantly around 3 weeks in culture, and accounted for close to half of the total events by 2 months (Fig. 4-

13-B-C, quantified in Fig. 4-13-D-E). For example, GABAergic events consisted of $43 \pm 5.8\%$ of total synaptic events after two months of culture, suggesting that our hiPSC-derived neurons have relatively balanced glutamatergic and GABAergic events when cultured on glial cells.

We further explored whether hiPSC-derived neurons can be rapidly integrated into the pre-existing neural network. For this purpose, we seeded hNPCs (labeled with green fluorescent dye CFDA) onto mouse neurons that had been cultured for 1 week already (Deng et al., 2007). Dual whole-cell recordings revealed that newly differentiated human neurons could establish synaptic connections with mouse neurons as early as one week after coculture together (Fig. 4-14-A-B, $n = 5$). The synaptic events were only recorded when stimulating mouse neurons to evoke synaptic transmission (Fig. 4-14-B). Stimulating one-week old human neurons did not evoke any synaptic responses (data not shown). After one month of culture on astrocytes, dual whole-cell recordings between a pair of human neurons were able to record evoked synaptic responses (Fig. 4-14-C-D, WT 126), suggesting functional maturation of the presynaptic release machinery in these human neurons. We also performed similar experiments using a different hiPSC line (WT 33) and recorded evoked synaptic responses between a pair of human neurons (Fig. 4-14-E-F, $n = 9$). Therefore, after coculture with astrocytes, hiPSC-derived neurons are capable of forming fully functional synaptic networks both with preexisting neurons and among themselves.

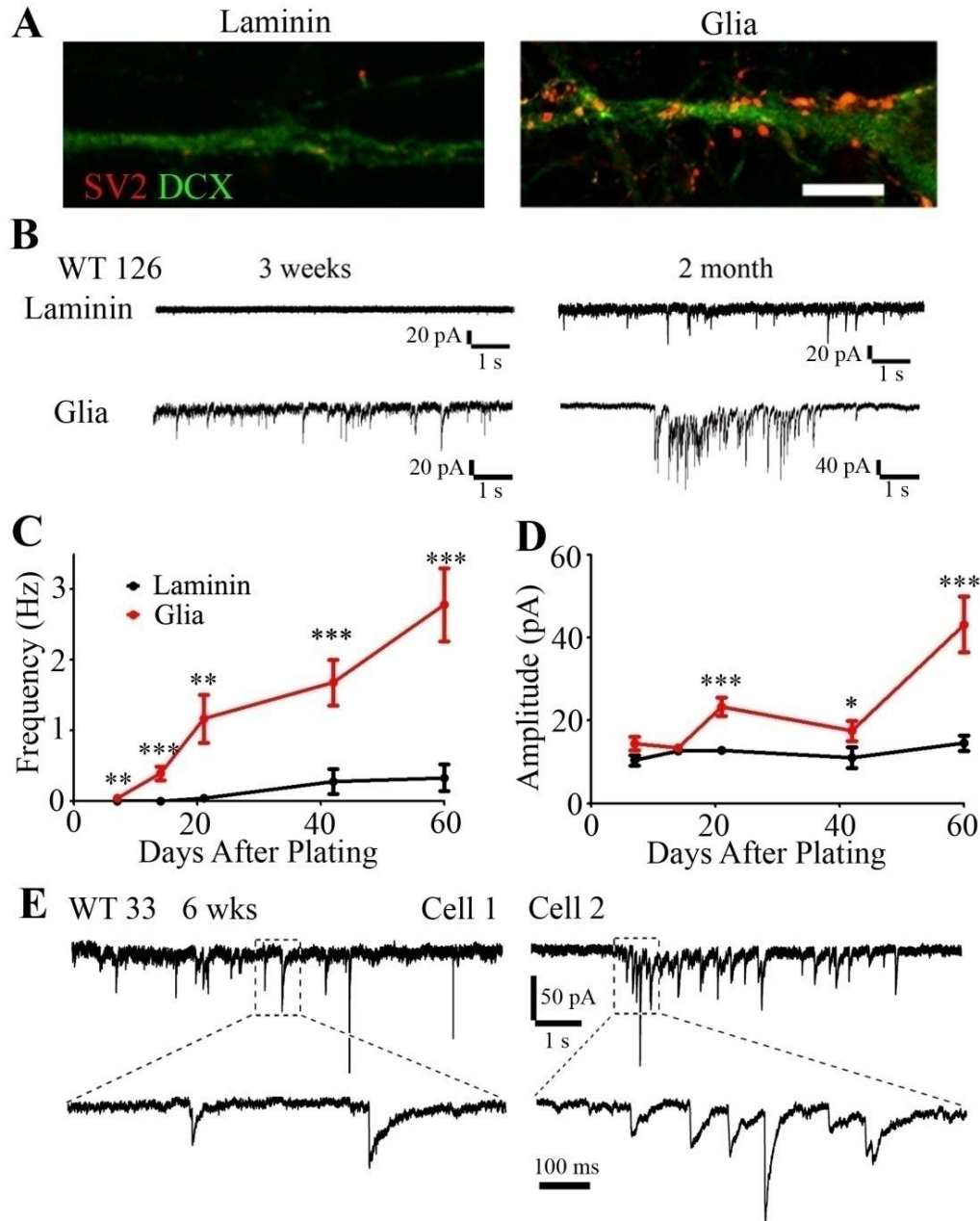


Figure 4-12: Astrocytes are essential for synaptic maturation of human neurons.

(A) Representative images showing SV2-labeled synaptic puncta along the DCX+ neurites of hiPSC-derived neurons developing for two months on laminin or astrocytes. Scale bar = 10 μ m.

(B) Representative traces showing spontaneous synaptic events recorded from hiPSC-derived neurons after plating hNPCs on laminin or astrocytes for three weeks and two months.

(C & D) Quantified results illustrating that hiPSC-derived neurons supported by glial cells consistently show higher frequency (C) and larger amplitude (D) of spontaneous synaptic events than those on laminin. * $p < 0.05$, ** $p < 0.01$, *** $p < 0.001$ (student's t-test).

(E) Representative traces showing spontaneous synaptic events recorded from human neurons derived from a different iPSC line (WT 33) after plating on astrocytes for six weeks.

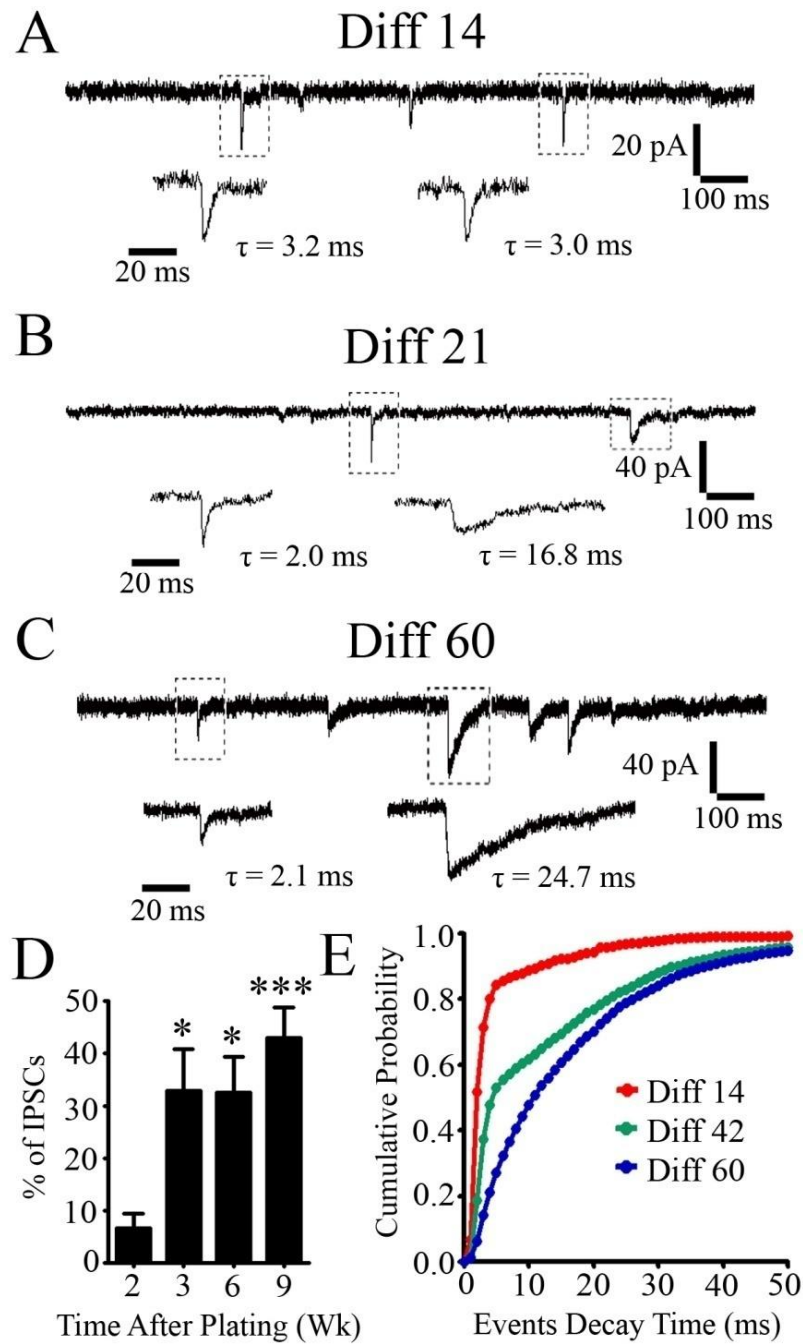


Figure 4-13: Excitatory synaptic transmission precedes inhibitory synaptic transmission in human iPS cell-derived neurons.

(A - C) Representative traces showing spontaneous synaptic events recorded from human neurons at 14 (A), 21 (B), and 60 (C) days after plating on astrocytes. Note that the initially appeared

synaptic responses were usually fast-decaying glutamatergic events (A), but slow-decaying GABAergic events appeared later.

(D) Quantified results showing that the percentage of spontaneous IPSCs among all events increased as the human neurons mature. * $p < 0.05$, *** $p < 0.001$ (one-way ANOVA followed by Bonferroni correction).

(E) Cumulative probability plot of decay time of spontaneous synaptic events recorded from hiPSC-derived neurons 14 (red), 42 (green) or 60 (blue) days in culture (1 ms bins, $p < 0.001$ by Kolmogorov-Smirnov test).

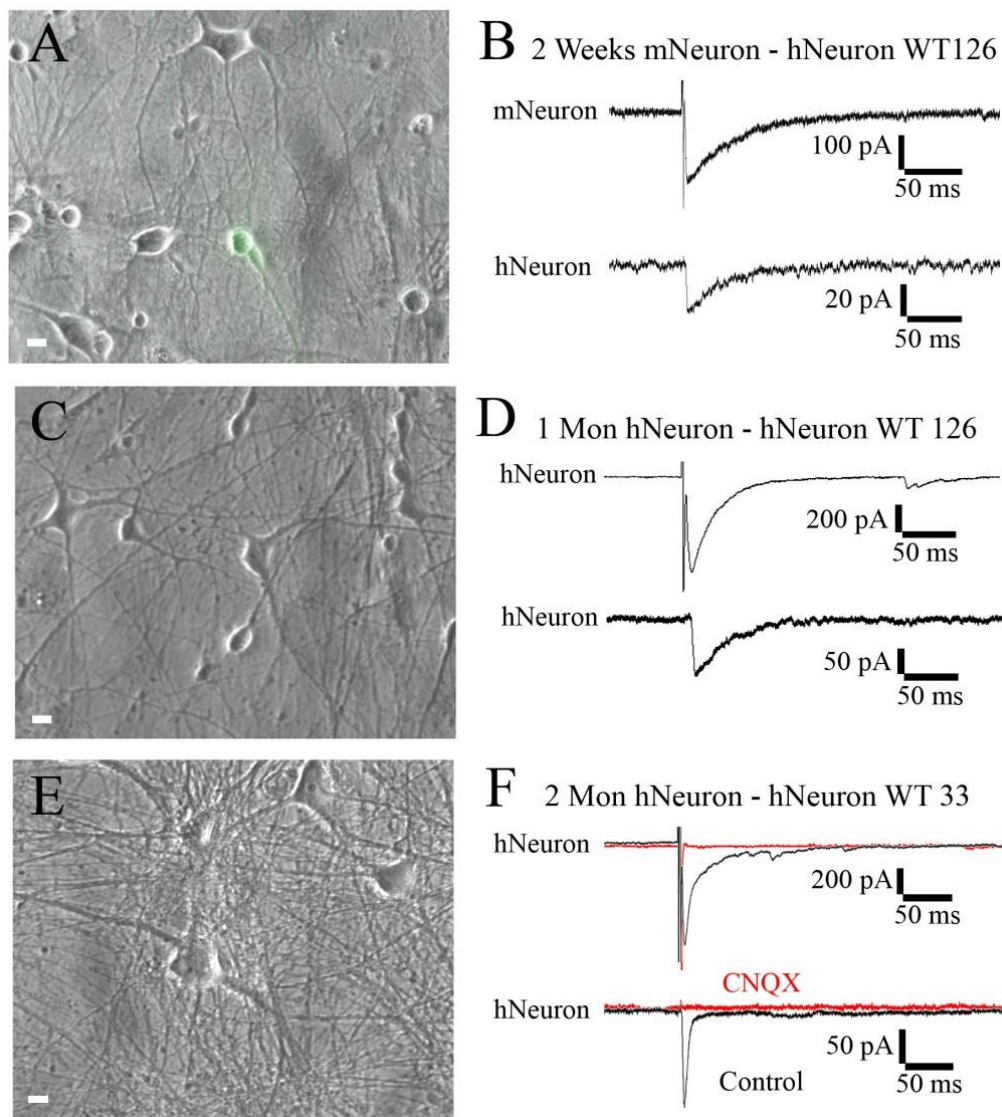


Figure 4-14: Human neurons can incorporate into neural networks.

(A - B) CFDA-labeled hiPSC-derived neurons (Green) received synaptic input as early as one week after co-cultured with primary mouse neurons.

(C - D) Dual whole-cell recordings on a pair of human neurons derived from hiPSCs (WT 126) revealed action potential-evoked synaptic responses after one month in coculture with astrocytes.

(E - F) Dual whole-cell recordings revealed functional synaptic connection between human neurons derived from a different hiPSC line (WT 33). Glutamate receptor antagonist CNQX blocked the evoked synaptic responses (red trace).

4.1.6 Generation of astrocytes from hiPSCs

Besides neural differentiation, we also observed glial differentiation from hiPSCs (Fig. 4-15). Similar to early neurogenesis and late gliogenesis in vivo, we found that after two months of plating hNPCs on laminin, a significant portion of HuNu+ cells began to express astroglial marker GFAP (Fig. 4-15-A). These glial cells could survive up to 3 - 4 months in culture, and developed into both GFAP+ and S100B+ astrocytes with elaborate processes (Fig. 4-15-B). As shown in Fig. 1, hNPCs cultured on glial cells mainly differentiated into MAP2+ neurons, but these hNPCs were typically derived from low-passage hiPSCs (Fig. 4-15-C). When we seeded high-passage (>20 passages) hNPCs onto glial cells, a significant portion of hNPCs also differentiated into GFAP+ astrocytes (Fig. 4-15-D). These data suggest that the fate determination of human iPSC-derived NPCs follow normal brain development principles, that neurons are generated by early progenitor cells whereas glial cells are generated by late progenitor cells.

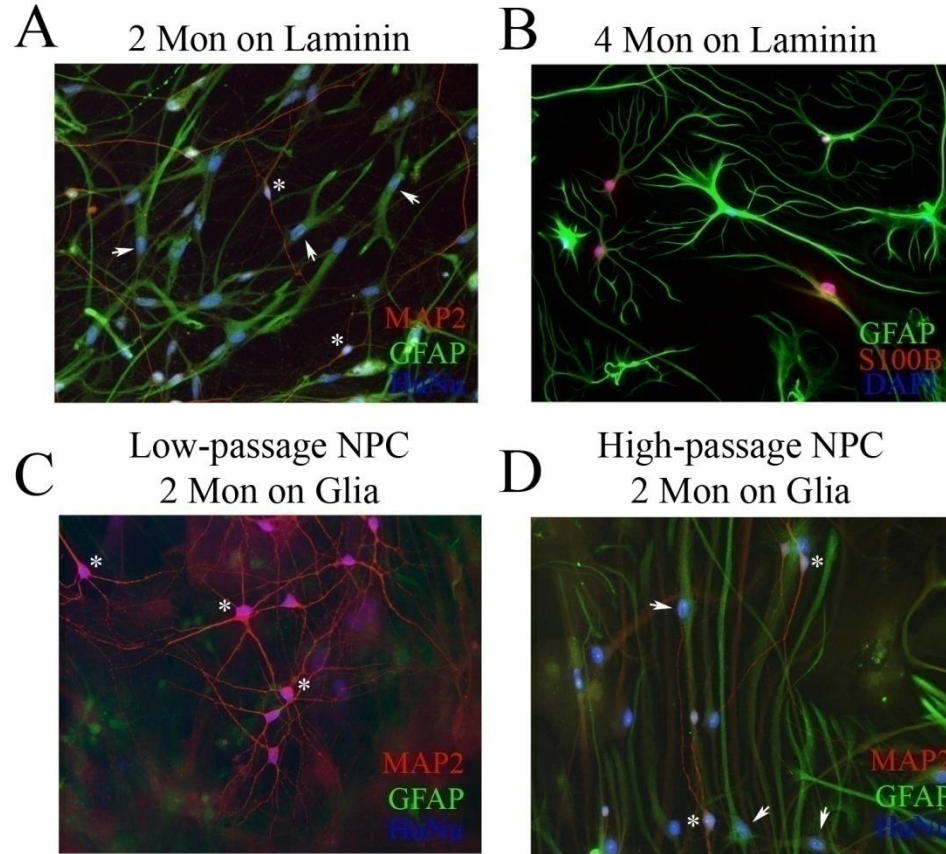


Figure 4-15: Generation of human glial cells from human iPS cell-derived NPCs.

(A) after two months culture on laminin, a significant portion of HuNu+ cells were immunopositive for astroglial marker GFAP (indicated by arrows). (B) These astroglial cells survived up to 3 - 4 months in culture, and were both GFAP+ and S100B+. (C) hNPCs derived from low passage of hiPSCs differentiated into MAP2+ neurons after cultured on glial cells (indicated by *). (D) A significant portion of high-passage (>20 passages) NPCs differentiated into GFAP+ glial cells (indicated by arrows).

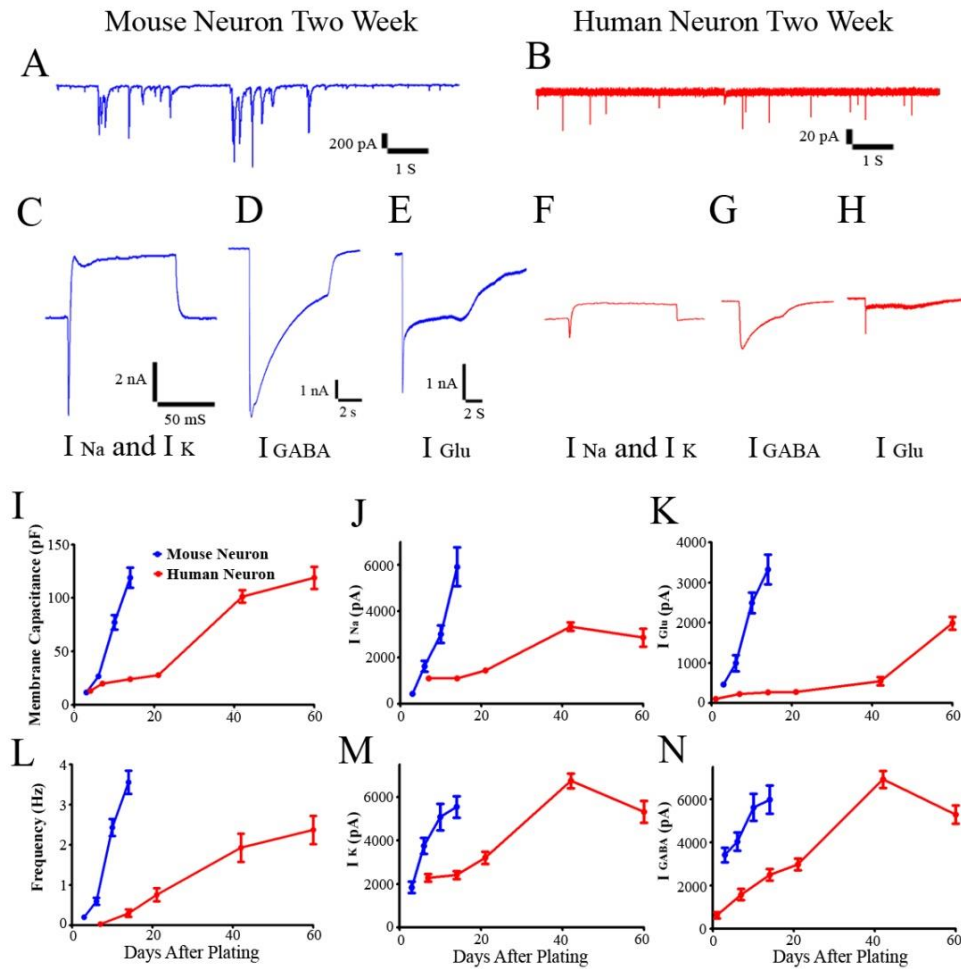


Figure 4-16: Functional comparisons reveal cell-autonomous species difference between human and mouse neurons.

(A-H) Representative electrophysiology recording traces from mouse and human neurons two weeks in culture. Comparing to mouse neurons seeded at the same time, human neurons showed fewer synaptic events (A-B, summarized in L), reduced Na and K currents (C and F, summarized in J and M), and lower whole-cell Glutamate (E and H, summarized in K) and GABA responses (D and G, summarized in N).

4.2 Discussion

In this chapter of my dissertation, we demonstrated that hiPSCs can be rapidly differentiated into functional neurons when cultured on a monolayer of astrocytes. In contrast, laminin is a poor substrate to promote neural differentiation, neuronal survival, and synaptic maturation of human neurons derived from hiPSCs. Astrocytes also significantly increased dendritic complexity and the surface expression of ionic channels and neurotransmitter receptors of human neurons. Our data depict a clear timeline of both morphological and functional development of human neurons derived from hiPSCs, which will be important to guide future research using hiPSC-derived neurons for disease modeling and drug screening.

4.2.1 Essential role of astrocytes in promoting neural differentiation and rapid functional maturation of hiPSC-derived neurons

Previous studies have reported that adult hippocampal astrocytes promote neural differentiation of adult neural stem cells (Song et al., 2002a). While some recent studies have cultured human embryonic stem cells (ESCs) or iPSCs with astrocytes to increase neural differentiation and synaptic function (Johnson et al., 2007; Marchetto et al., 2008; Hu et al., 2010; Brennand et al., 2011), the precise role of astrocytes in supporting human iPSC-derived neurons is not well understood. In this work, we have thoroughly investigated the role of astrocytes from the first day of plating human hNPCs until two months of growing on astrocytes. We found that astrocytes initially promote cell proliferation and survival of NPCs. After 24 hrs growing on astrocytes, the total number of cells more than doubled that on laminin. Astrocytes also promote neural differentiation as shown by significantly increased number and percentage of newborn neurons compared to laminin as the substrate. Importantly, we demonstrated that neurons differentiated from human hNPCs fired action potentials four days after plating on astrocytes, and within a week some sparse synaptic events could be detected. Such rapid differentiation of functional neurons from hiPSCs has not been reported before. Compared to the direct plating on astrocytes, glial-conditioned medium only partially increased neural differentiation, suggesting that astrocyte-secreted factors were not as potent as the direct contact with astrocytes, consistent with previous finding for adult rat NSCs (Song et al., 2002a).

4.2.2 Astrocytes are critical for iPSC-derived neurons to form robust synaptic connections

Astrocytes play an active role in regulating synapse formation among neurons (Barres, 2008; Eroglu and Barres, 2010). Previous studies have suggested that astrocytes also promote synapse formation in neurons derived from adult rat NSCs (Song et al., 2002b) and human ESCs (Johnson et al., 2007). In this study, we demonstrated that synapse development and function in the human neurons derived from hiPSCs were greatly enhanced by astrocytes. After three weeks in culture on astrocytes, human neurons showed robust synaptic events. Human neurons continue their developmental process after 2 months of culture on astrocytes by showing spontaneous bursting activities, an index of highly synchronized network activity (Opitz et al., 2002). Some published works showed that under the *in vitro* differentiation protocol with no astrocyte support, the synaptic events recorded in hiPSC- or ESC-derived neurons are mostly EPSCs (Kim et al., 2011a; Shi et al., 2012), while other work showing the detection of both EPSCs and IPSCs after long time in culture (Marchetto et al., 2010b). We carried out careful analysis on the synaptic events recorded from iPSC-derived human neurons cultured on astrocyte to separate spontaneous EPSCs versus IPSCs. Interestingly, within the first two weeks after plating hiPSC-derived hNPCs on astrocytes, the synaptic events were mainly EPSCs. After three weeks of culture on astrocytes, the spontaneous events developed into a mixture of both excitatory and inhibitory synaptic events, with the IPSCs accounting for 30-40% of the total events. Our data may suggest that glutamatergic neurons are generated earlier before GABAergic neurons when differentiated from hiPSCs. Alternatively, glutamatergic synapses are established faster than GABAergic synapses among iPSC-derived neurons. This finding of early EPSCs is important for future studies on human neuronal development using iPSC approach, because it is different from rodent neuronal cultures where GABAergic synapses typically precede glutamatergic synapses (Deng et al., 2007).

4.1.3 Implication in neuron-glia interactions and disease modeling

Besides promoting neuronal synapse formation, astrocytes regulate neuronal functions in various ways, including uptake of glutamate to reduce excitotoxicity, buffering extracellular K^+ , supplying nutrients to neurons, and taking part in brain-blood-barrier (Nedergaard et al., 2003; Molofsky et al., 2012). A series of recent studies showed that astrocytes expressing mutant

superoxide dismutase 1, which is linked to amyotrophic lateral sclerosis, are toxic to motor neurons derived from human or mouse ESCs (Di Giorgio et al., 2007; Nagai et al., 2007; Marchetto et al., 2008). Similarly, MeCP2-deficient astrocytes impose non-cell autonomous effects on neuronal dendrites and synaptic functions (Ballas et al., 2009; Maezawa et al., 2009). In global MeCP2 knockout mice, selective expression of MeCP2 only in astrocytes can partially rescue Rett syndrome deficits (Lioy et al., 2011). Thus, diseased astrocytes will negatively impact cocultured neurons, while healthy astrocytes will promote neuronal functions. This raises an important question regarding what kind of astrocytes to choose as the neuronal substrate when studying disease mechanisms using hiPSC-derived neurons. Because astrocytes have enormous influence on neuronal functions, it is possible that healthy astrocytes might mask certain phenotypes of cocultured neurons. In such case, it will be desirable to culture diseased neurons on diseased astrocytes to investigate potential effects of astrocytes. On the other hand, if diseased neurons still show significant phenotype in coculture with healthy astrocytes, the phenotype is likely cell autonomous within neurons. Together, our studies suggest that astrocytes play a critical role in promoting the functional maturation of hiPSC-derived neurons. Whether using astrocyte as the culture substrate, and which developmental stage of the neurons being used may have important implications in interpreting the results using hiPSCs for dismodeling and drug screening.

Chapter 5

Comparison between Human and Mouse Astrocytes Reveals Key Molecular and Functional Differences

In this study, our lab collaborated with Dr. Hong Ma's lab at Fudan University, China.

Chenlong Cao in Dr. Ma's lab performed deep sequencing results assembly and rpkm calculation for the human vs. mouse astrocyte transcriptome study.

5.1 Results

5.1.1 Human astrocytes promote NPC proliferation but not neural differentiation

Our data in Chapter four has demonstrated clearly that the support from mouse astrocyte is essential for the rapid neural differentiation and functional maturation of human neurons. This finding led us to question whether human astrocytes exert the same effect on human NPC. In order to accomplish this we employed human fetal glial cell lines purchased from SciCell (HA 1800 Remarkably, human astrocytes promote stem cell proliferation but not neural differentiation as mouse astrocytes do. When culturing the same batch of human NPC on human astrocytes (HA) or mouse astrocytes (MA) for a week, NPC proliferation was much more robust for NPC on HA, as evidenced by the large number of cells labeled positive for BrdU (Fig. 5-1-C, 130 ± 26 BrdU+ cells per imaging field for human astrocyte group, 35.2 ± 9 for mouse astrocyte group. $P < 0.001$, $N = 15$ imaging fields from three independent repeats. BrdU was added to the culture at day six after seeding NPC, and maintained for one day before fixation and subsequent immunostaining). Conversely, the number of DCX positive neurons among NPC cultured on HA was small compared to that of the MA (Fig. 5-1-D, 2.4 ± 1.0 neurons per imaging field for human astrocyte group; 9.9 ± 1.0 for mouse astrocyte group. $P < 0.01$). (Fig. 5-1-E-H) Not only was the number of neurons smaller from NPC cultured on HA, but the neurons also demonstrated smaller cell bodies and less elaborate dendrites. (Representative camera lucida reconstruction of the dendritic trees was presented as inserts in panel (Fig. 5-1-A) and (Fig. 5-1-B). The size of the cell body for the NPC-derived neurons on human astrocytes was significantly smaller compared to those on mouse astrocytes (Fig. 5-1-E, 302 ± 30 a.u. for human astrocyte group, 571 ± 59 for mouse astrocyte group. $N = 30$ cells each group; $P < 0.001$). Consistent with the smaller cell body size, the membrane capacitance for the neurons on human astrocyte was also significantly smaller (Fig. 5-1-H, 13.4 ± 1.0 pF for the human astrocyte group, $n = 16$; 20.4 ± 0.9 pF for the mouse astrocyte group, $n = 36$; $p < 0.001$). The complexity of dendritic trees was reduced in neurons cultured on human astrocytes, which have fewer Sholl circle intersections (Fig. 5-1-F, 10.4 ± 0.9 intersections for human astrocyte group; 31.1 ± 2.8 intersections for mouse astrocyte group; $n = 40$ cells per

condition; $p < 0.001$) and fewer branch points (Fig. 5-1-**G**, 0.68 ± 0.14 for human astrocyte group, 2.85 ± 0.28 for mouse astrocyte group; $n = 40$ cells per condition; $p < 0.001$).

Then, we investigated the functional properties of human neurons derived from culturing NPC on HA or MA. Two-weeks after plating, NPC-derived neurons on HA had comparable Na current amplitude with the neurons on MA (Fig. 5-1-**I**, 960 ± 216 pA for HA group, $n = 16$; 12640 ± 109 pA for MA group, $n = 36$. $P = 0.22$), but significantly decreased K current amplitude (Fig. 5-1-**J**, 1340 ± 258 pA for HA group, 2390 ± 199 pA for MA group; $p < 0.01$). (Fig. 5-1-**K-M**) The synaptic connections formed among neurons were also significantly reduced in the HA group, as evidenced by the reduced number of SV2 puncta along the dendrites in neurons cultured on HA (Fig. 5-1-**M**, 3.7 ± 0.6 puncta per 100 μm dendrite in HA group, $n = 17$; 12.2 ± 0.8 puncta in MA group, $n = 26$. $p < 0.001$). Taken together, my data suggest that human astrocytes robustly promote NPC proliferation, but generate fewer and less functionally mature neurons. The factors that may be involved in this process are discussed in the section four of chapter five.

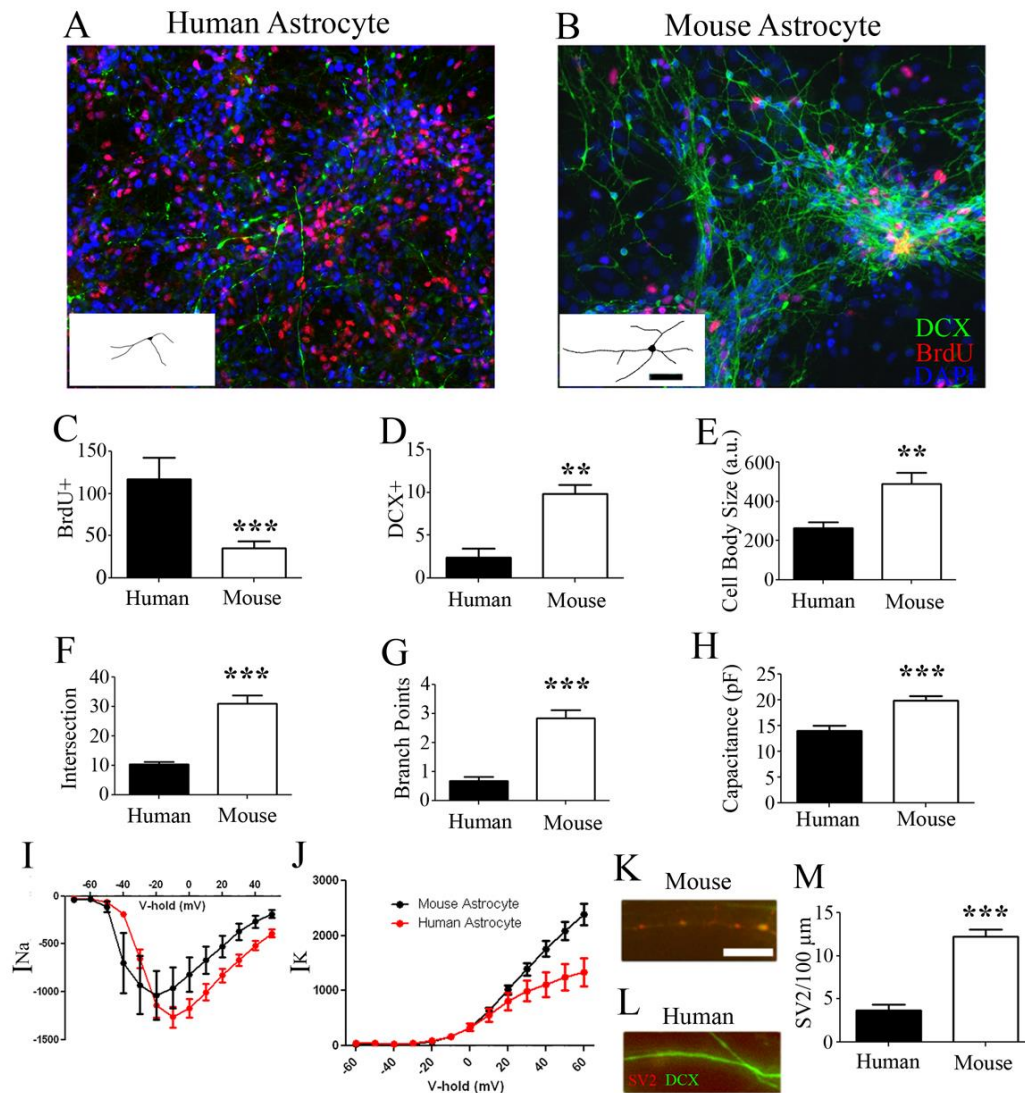


Figure 5-1: Human astrocytes promote stem cell proliferation but not neural differentiation.

(A-D) When culturing human NPC on human astrocyte, proliferation was robust as evidenced by the large number of cells labeled positive for BrdU (C, 130 ± 26 BrdU+ cells per imaging field for human astrocyte group, 35.2 ± 9 for mouse astrocyte group. $P < 0.001$, $N = 15$ imaging fields from three independent repeats. BrdU was added to the culture at day six after seeding NPC, and maintained for one day before fixation and subsequent immunostaining). Conversely, the number of DCX positive neurons among NPC cultured on human astrocyte were small comparing to the mouse astrocyte counterpart (D, 2.4 ± 1.0 neurons per imaging field for human astrocyte group; 9.9 ± 1.0 for mouse astrocyte group. $P < 0.01$). (E-H) The neurons developed on mouse astrocytes has bigger cell bodies and more elaborate dendrites. Representative camera lucida

reconstruction of the dendritic trees was presented as inserts in panel (A) and (B). The size of the cell body for the NPC-derived neurons on human astrocytes were significantly smaller comparing to those on mouse astrocytes (E, 302 ± 30 a.u. for human astrocyte group, 571 ± 59 for mouse astrocyte group. $N = 30$ cells each group; $P < 0.001$). Consistent with the smaller cell body size, the membrane capacitance for the neurons on human astrocyte were also significantly smaller (H, 13.4 ± 1.0 pF for the human astrocyte group, $n = 16$; 20.4 ± 0.9 pF for the mouse astrocyte group, $n = 36$; $p < 0.001$). The complexity of dendritic trees were reduced in neurons cultured on human astrocytes, which have fewer Sholl circle intersections (F, 10.4 ± 0.9 intersections for human astrocyte group; 31.1 ± 2.8 intersections for mouse astrocyte group; $n = 40$ cells per condition; $p < 0.001$) and fewer branch points (G, 0.68 ± 0.14 for human astrocyte group, 2.85 ± 0.28 for mouse astrocyte group; $n = 40$ cells per condition; $p < 0.001$). The electrophysiological properties for the NPC-derived neurons cultured on human astrocyte were also impaired comparing to mouse astrocyte counterpart. Two-weeks after plating, neurons has comparable Na current amplitude (I, 960 ± 216 pA for HA group, $n = 16$; 12640 ± 109 pA for MA group, $n = 36$. $P = 0.22$) but significantly decreased K current amplitude (J, 1340 ± 258 pA for HA group, 2390 ± 199 pA for MA group; $p < 0.01$). (K-M) The synaptic connections formed among neurons were also significantly reduced in the HA group, as evidenced by the reduced number of SV2 puncta along the dendrites in neurons cultured on HA (M, 3.7 ± 0.6 puncta per $100 \mu\text{m}$ dendrite in HA group, $n = 17$; 12.2 ± 0.8 puncta in MA group, $n = 26$. $p < 0.001$)

5.1.2 Human astrocytes express high levels of BDNF, and strongly promote the formation of inhibitory synapses

BDNF is a critical neuropeptide in the brain. Its expression can be detected in neurons, astrocytes and microglia. We compared the level of BDNF in both human and mouse astrocytes through immunostaining to probe BDNF expression level. In comparison to mouse astrocytes, human astrocytes have much stronger BDNF immunoreactivity. Quantified results in panel (Fig. 5-2-C) shows that the immunostaining intensity in HA was 91.6 ± 5.7 a.u., $n = 20$; while the intensity in MA was 40.2 ± 1.4 a.u., $n = 20$. $P < 0.001$. This difference is not due to higher background level in HA, for the experiments omitted primary BDNF antibody and instead used IgG, which showed comparable staining between the two conditions (22.1 ± 0.8 for HA IgG control, 19.9 ± 0.5 for MA IgG control. $n = 9$ cells per condition). Human iPSC-derived astrocytes also demonstrate strong BDNF immunoreactivity (Fig. 5-2-D-F)

BDNF is a key regulator of inhibitory synapse formation. Previous studies have highlighted the effect of neuronal BDNF on promoting inhibitory synapse formation, but the contribution of astrocytic BDNF to this process was deemed minimal from experiments conducted in the mouse model. Since we observed that HA have stronger BDNF staining, we

reasoned that HA may have a greater contribution to the formation of inhibitory synapses compared to MA. Indeed, we found that HA strongly promotes the formation of inhibitory synapse in a BDNF-dependent manner. When mouse neurons were cultured on human astrocytes, the density of GAD puncta along dendrites was significantly increased relative to the same batch of neurons cultured on mouse astrocytes (Fig. 5-3-A-C). Similarly, the mini IPSC frequency, an indicator of the number of functional GABAergic synapses, increased significantly compared to MA (Fig. 5-3-D-G). At one week time point, the mouse neurons cultured on HA have mini IPSC frequency of 0.62 ± 0.13 Hz, while neurons cultured on MA only have mIPSC frequency of 0.17 ± 0.02 Hz ($p < 0.001$). Recordings made with another human astrocyte line (HA Gibco) showed similar results (mIPSC frequency 0.63 ± 0.09 Hz, $p < 0.001$ comparing to MA). This inhibitory synapse-promoting effect can be blocked by adding TrkB antibody in the culture medium to block the BDNF signaling cascade (Fig. 5-3-C, G, When adding TrkB antibody to neurons cultured on HA Gibco, the increase in mIPSC frequency was diminished 0.29 ± 0.06 ; $p < 0.05$ comparing to HA Gibco group; n.s. comparing to MA group). In most of the experiment groups, the amplitude of mIPSC was similar. Only HA 1800 group showed an increase in mIPSC amplitude. The reason may be some gene expression difference between the human astrocyte sources.

On the other hand, culturing mouse neurons on HA does not significantly affect their excitatory synapse formation. Two-weeks after culture, the SV2 puncta density was comparable between mouse neurons cultured on HA (Fig. 5-4-A, 7.5 ± 0.5 puncta per $10 \mu\text{m}$ dendrite) and MA (Fig. 5-4-B, 7.9 ± 0.5 puncta per $10 \mu\text{m}$ dendrite, $p = 0.77$; quantified in C). (D-G) Mouse neurons cultured on human or mouse astrocytes have similar mini EPSC frequency, indicating that the number of excitatory synapses was not changed between the two conditions (2.3 ± 0.5 Hz for HA group, 2.2 ± 0.4 Hz for MA group, $p = 0.98$). These findings suggest that HA strongly and specifically promote inhibitory synapse formation in neurons.

To rule out the possibility that the changes in inhibitory synapse formation was due to a general increase in cell size or condition, we recorded whole-cell GABA current and glutamate current from neurons cultured on HA or MA. In the mouse neurons cultured on HA for two weeks, the whole-cell GABA current was slightly smaller than the neurons cultured on MA, and the difference was not significant (Fig. 5-5-B and D, -3763 ± 282 pA for HA group, $n = 19$, -4550 ± 392 pA for MA group, $n = 20$; $p = 0.08$). Interestingly, a significant reduction in whole-cell glutamate current comparing to neurons cultured on MA was observed from neurons cultured on

HA (1828 ± 159 pA for human astrocyte group, 3405 ± 235 pA for mouse astrocyte group, $p < 0.001$). (Fig. 5-5-A and C).

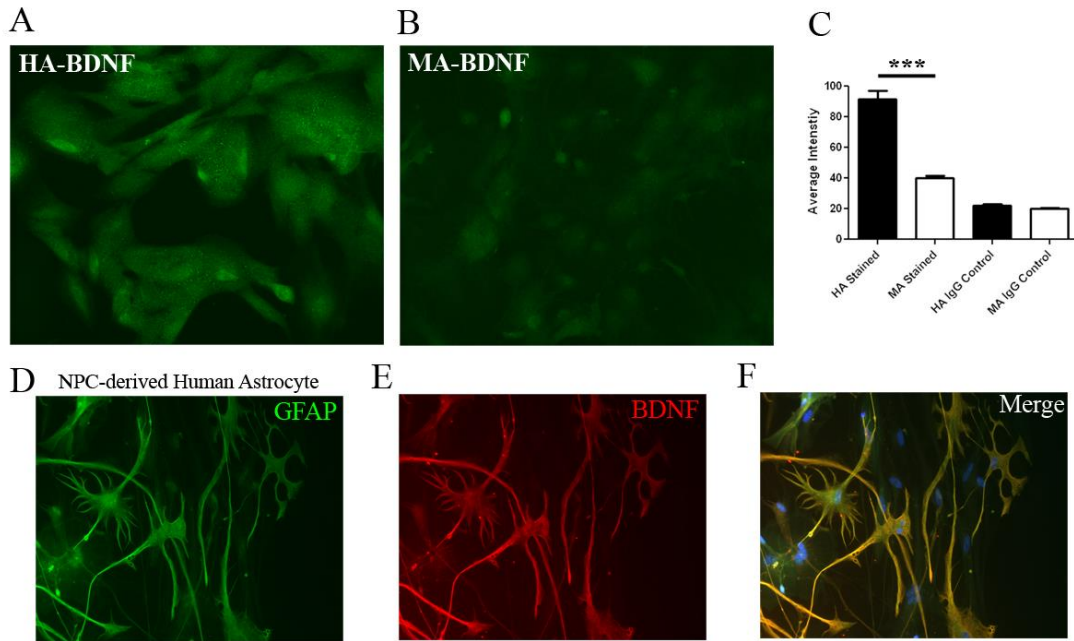


Figure 5-2: Human astrocytes show stronger BDNF immunoreactivity comparing to mouse astrocytes.

The BDNF level is significantly higher in the human astrocyte (A) comparing to mouse astrocyte (B). Quantified result in panel (C) showing that the immunostaining intensity in human astrocyte was 91.6 ± 5.7 a.u., $n = 20$; while the intensity in mouse astrocyte was 40.2 ± 1.4 a.u., $n = 20$. $P < 0.001$. The background level was comparable between two conditions (22.1 ± 0.8 for HA IgG control, 19.9 ± 0.5 for MA IgG control. $n = 9$ cells per condition). (D-F) Immunostaining of BDNF in GFAP+ NPC-derived human astrocytes showing strong BDNF immunoreactivity in human astrocytes.

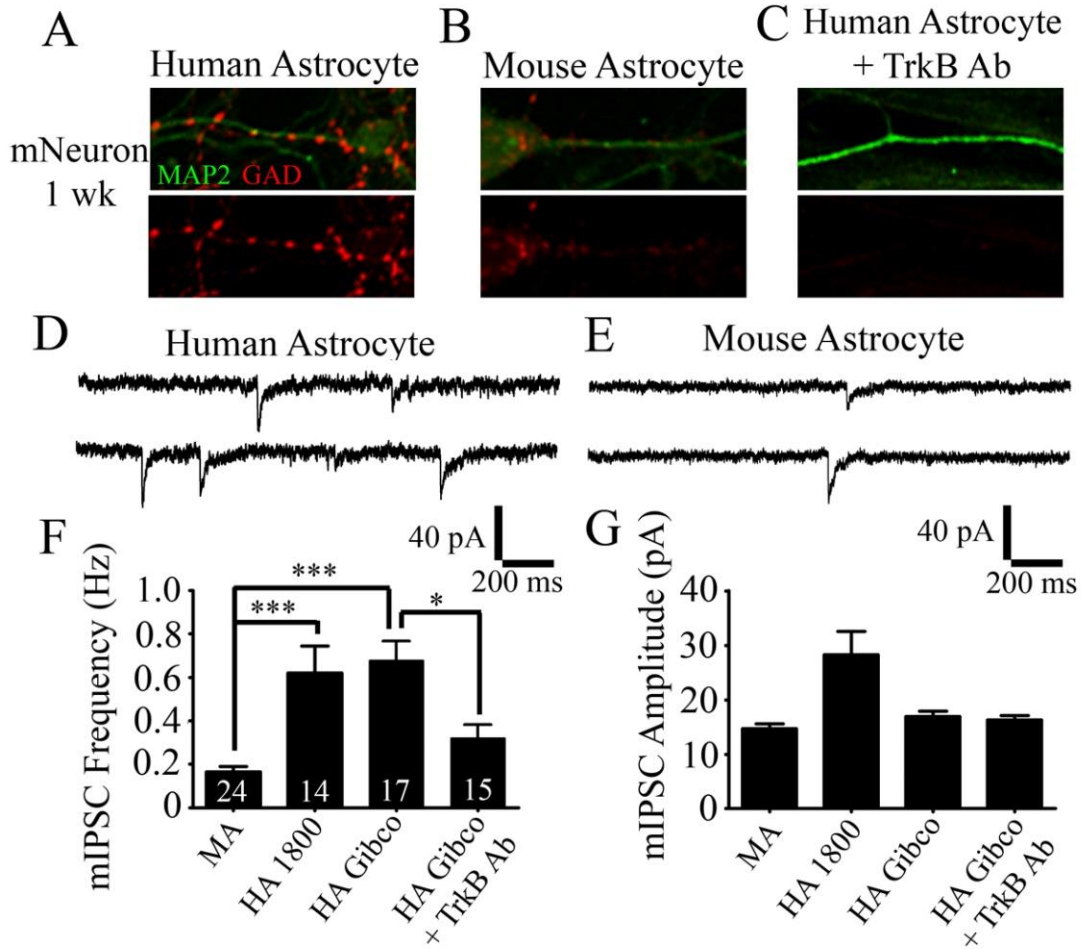


Figure 5-3: Human astrocytes strongly promote the formation of inhibitory synapse in a BDNF-dependent manner.

(A-C) When mouse neurons were cultured on human astrocyte (A), the density of GAD puncta along dendrites was significantly increased comparing to the same batch of neurons cultured on mouse astrocytes (B). This effect can be blocked by adding TrkB antibody in the culture medium to block the BDNF signaling cascade (C). (D-G) At one week time point, the mouse neurons cultured on human astrocytes have mini IPSC frequency of 0.62 ± 0.13 Hz, while neurons cultured on mouse astrocytes only have mIPSC frequency of 0.17 ± 0.02 Hz ($p < 0.001$). Another human astrocyte line (HA Gibco) showed the same effect (mIPSC frequency 0.63 ± 0.09 Hz, $p < 0.001$ comparing to MA). When adding TrkB antibody to neurons cultured on HA Gibco, the increase in mIPSC frequency was significantly decreased (0.29 ± 0.06 ; $p < 0.05$ comparing to HA Gibco group; n.s. comparing to MA group). HA 1800 group showed an significant increase in mIPSC amplitude, while the other groups stayed mostly the same.

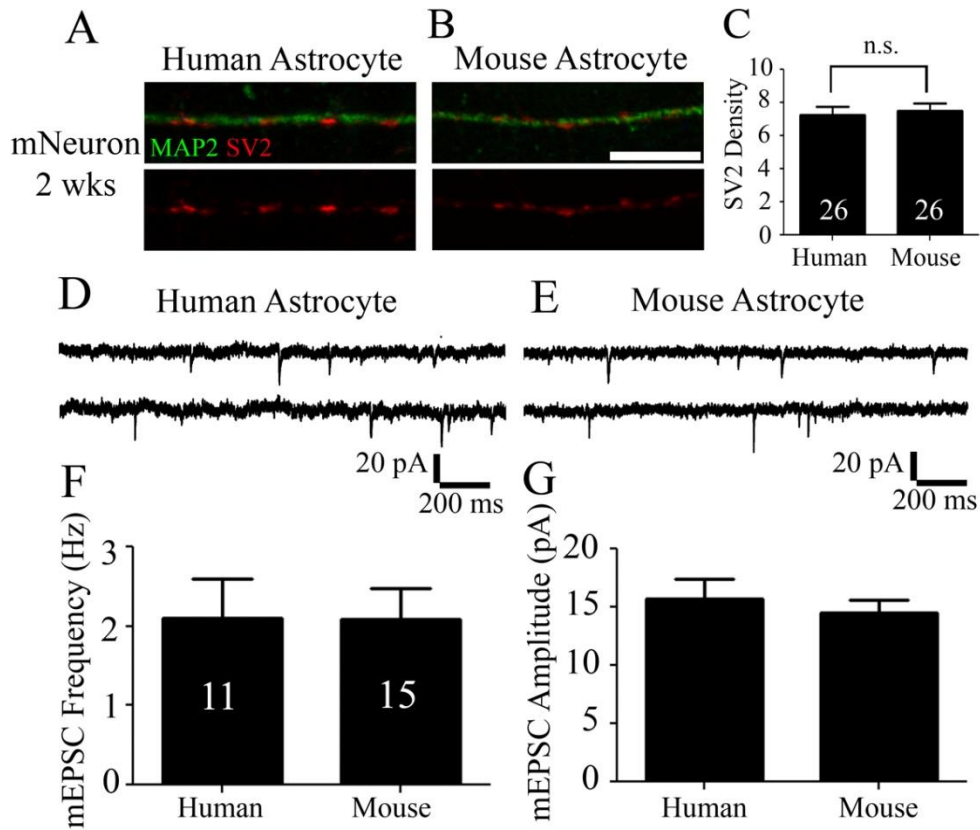


Figure 5-4: Human and mouse astrocytes promote excitatory synapse formation to similar degrees.

(A-C) At two-weeks time point, the SV2 puncta density was comparable between mouse neurons cultured on human astrocyte (A, 7.5 ± 0.5 puncta per $10 \mu\text{m}$ dendrite) and mouse astrocyte (B, 7.9 ± 0.5 puncta per $10 \mu\text{m}$ dendrite, $p = 0.77$; quantified in C). (D-G) Mouse neurons cultured on human or mouse astrocytes have similar excitatory neurotransmission (2.3 ± 0.5 Hz for human astrocyte group, 2.2 ± 0.4 Hz for mouse astrocyte group, $p = 0.98$).

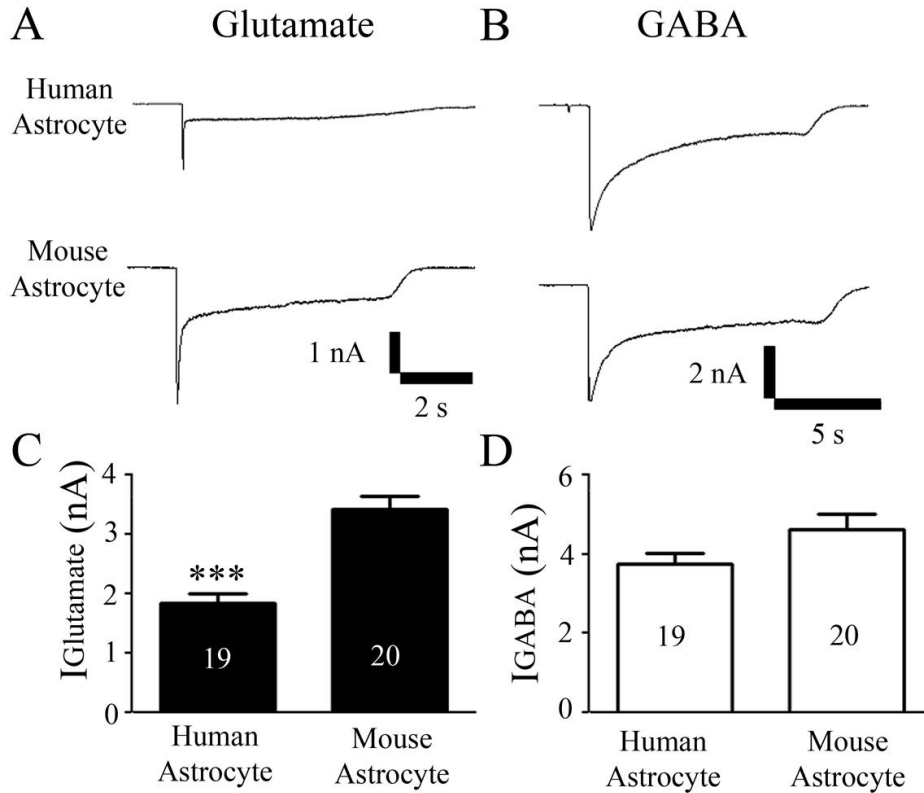


Figure 5-5: The mouse neurons cultured on human astrocytes show reduced whole-cell glutamate current but similar GABA current.

(A and C) Mouse neurons cultured on human astrocyte for two weeks showed reduced whole-cell glutamate current comparing to mouse astrocyte counterpart (1828 ± 159 pA for human astrocyte group, 3405 ± 235 pA for mouse astrocyte group, $p < 0.001$). (B and D) Whole-cell GABA current was not significantly different between mouse neurons cultured on human versus mouse astrocyte (-3763 ± 282 pA for human astrocyte group, $n = 19$, -4550 ± 392 pA for mouse astrocyte group, $n = 20$; $p = 0.08$).

5.1.3 Human astrocytes accumulate and release large amount of glutamate

The ability to process glutamate is a quintessential property of astrocytes. We examined the glutamate content of HA and MA using immunofluorescent staining. Surprisingly, human astrocytes showed enormous glutamate content (Fig. 5-6-A-C) in comparison to mouse astrocytes (137 ± 6 a.u. for HA, 32 ± 1 a.u. for MA, $n = 20$ cells per condition, $P < 0.001$. Control IgG staining: 24 ± 1 a.u. for HA, 22 ± 1 for MA, $n = 9$ cells per condition, $p = 0.23$). Then, we tested whether this high glutamate content was an artifact in the HA cell line. Human astrocytes were

generated from NPC through passaging and addition of CNTF. After two months in culture, immunostaining revealed that GFAP⁺ and S100 β ⁺ human astrocytes can be successfully derived from NPC (Fig. 5-6-D, one-month WT83 NPC cultured on laminin). The GFAP⁺ human astrocytes also stains positive for glutamate (Fig. 5-6-E, red, two-month WT83 NPC cultured on laminin). Surprisingly, human NPC cells did not stain positive for glutamate until after the glial differentiation process began. Large amount of glutamate can be observed to accumulate inside the cell when the HuNu⁺ human NPC begin to differentiate (Fig. 5-6-F, note NPC differentiated into both neuronal morphology and glial morphology begin to show high glutamate staining). (Fig. 5-6-G-I) As a negative control, human fibroblast lacked glutamate staining (data not shown).

To test whether the high level of glutamate was released from human astrocytes, we utilized neuronal cell death assay to demonstrate the presence of glutamate in the human astrocyte-conditioned medium (HA-CM). (Fig. 5-6-G) Standard curve showed that 10 μ M glutamate is sufficient to cause extensive excitotoxicity and massive cell death when added to two-weeks neuronal culture for one day (Control: 21.2 ± 3.5 MAP2⁺ neurons per 20X microscopic view, $n = 9$; 10 μ M glutamate: 0.9 ± 0.2 neurons, $n = 9$, $p < 0.001$). Adding human astrocyte conditioned medium to neuronal cultures essentially killed all neurons, even at the dilution of one-to-ten (Fig. 5-6-G, HA-CM 1:10: 0.8 ± 0.4 neurons per view, $p < 0.001$ comparing to control). The effect of HA-CM to cause neuronal death can be prevented by pre-treating the culture with NMDA receptor antagonist MK801, which suggests the involvement of NMDA-mediated glutamate excitotoxicity (Fig. 5-6-H, HA-CM: 0 neurons, $n = 9$; HA-CM + MK801: 24.1 ± 3.3 neurons per view, $p < 0.001$). Interestingly, when mouse neurons were cultured onto HA, not only did the neurons survive well, but the medium also no longer contained high level of glutamate, suggesting that signal from neurons can neutralize the glutamate secretion from human astrocytes.

To further test the hypothesis that human astrocytes release glutamate and mouse astrocytes can uptake glutamate, we designed a culture method where mouse astrocytes grown on a 24-well coverslip were added to a 6-well plate well full of human astrocyte (the rough area ratio between the coverslip and the well is 1:10). In this manner, the MA and HA were cultured in the same medium, but were not in physical contact as to not influence one other. Only one day of HA/MA 10:1 co-culture can significantly decrease glutamate content in the medium. Adding two coverslips to the HA culture (HA:MA = 5:1) can decrease the glutamate level in the medium to a low level where it does not cause detectable cell death when added to neuronal culture (Fig. 5-6-I,

HA:MA=10:1 group: 5.8 ± 0.9 neurons per view, $p < 0.001$ comparing to HA-CM (conditioned medium). HA:MA=5:1 group: 19.2 ± 4.7 neurons per view, $p < 0.001$ comparing to HA-CM; n.s. comparing to control group). After retracting the MA from the culture, the glutamate level of HA-CM returns to high levels after just one day. (Fig. 5-6-L-K) Additionally, we used electrophysiology to confirm the presence of high glutamate content by directly puffing HA-CM to primary cultured neurons and record cellular responses (Fig. 5-6-L). HA-CM elicited a large inward current (Fig. 5-6-M, black bar indicate the 100 ms medium puff), which can be reversibly blocked by DNQX (Fig. 5-6-N and O). Quantified results showed that HA-CM elicited significantly bigger current (4238 ± 316 pA, $n = 10$) when compared to naïve medium (140 ± 61 , $n = 6$, $p < 0.001$ comparing to HA-CM). The HA-CM triggered current can be largely blocked by DNQX (605 ± 193 pA, $p < 0.001$ comparing to HA-CM, quantified in Fig. 5-6-P). MA-CM triggered minimal current, indicating that the uptake of glutamate was complete.

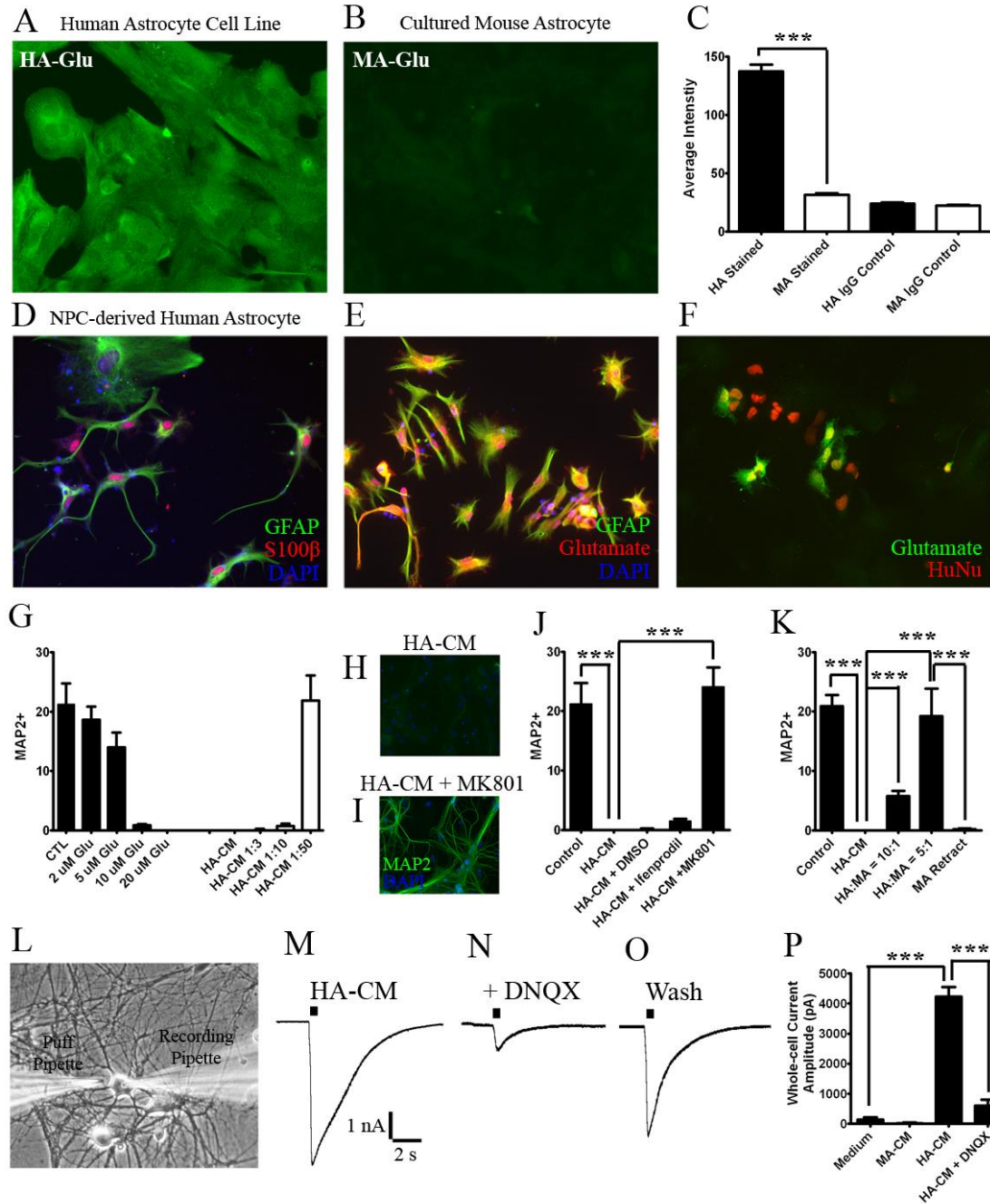


Figure 5-6: Human astrocytes have enormous glutamate content and secrete glutamate.

(A-C) Comparing to mouse astrocytes, human astrocyte has enormous glutamate content (137 ± 6 a.u. for HA, 32 ± 1 a.u. for MA, $n = 20$ cells per condition, $P < 0.001$. Control IgG staining: 24 ± 1 a.u. for HA, 22 ± 1 for MA, $n = 9$ cells per condition, $p = 0.23$). (D-F) Immunostaining showing that human GFAP+ and S100β+ astrocytes can be derived from NPC (D, one-month WT83 NPC cultured on laminin). The GFAP+ astrocytes also stains positive for glutamate (E, red, two-month WT83 NPC cultured on laminin). Human NPC did not stain

positive for glutamate before differentiation (Data not shown). However, once the differentiation starts, large amount of glutamate start to accumulate inside the cell (F). Human fibroblast also does not have glutamate staining (data not shown). (G-K) Utilizing neuronal cell death assay to demonstrate the presence of glutamate in the human astrocyte-conditioned medium (HA-CM). (G) Standard curve to show that 10 μ M glutamate is sufficient to cause excitotoxicity and major cell death (Control: 21.2 ± 3.5 MAP2+ neurons per 20X microscopic view, $n = 9$; 10 μ M glutamate: 0.9 ± 0.2 neurons, $n = 9$, $p < 0.001$). Adding human astrocyte conditioned medium to neuronal cultures essentially killed all neurons, even diluted one-to-ten (G, HA-CM 1:10: 0.8 ± 0.4 neurons per view, $p < 0.001$ comparing to control). The effect of HA-CM to cause neuronal death can be prevented by adding NMDA receptor antagonist MK801 to the medium (H, HA-CM: 0 neurons, $n = 9$; I, HA-CM + MK801: 24.1 ± 3.3 neurons per view, $p < 0.001$). Adding one 24-well coverslip with mouse astrocyte to 6-well full of human astrocyte for one day can significantly decrease glutamate content in the medium and increase cell survival when applied to neuronal culture (K, HA:MA=10:1: 5.8 ± 0.9 neurons per view, $p < 0.001$ comparing to HA-CM. HA:MA=5:1: 19.2 ± 4.7 neurons per view, $p < 0.001$ comparing to HA-CM). After retracting the MA for one day, the glutamate level of HA-CM returns to normal level. (L-K) Confirmation of glutamate content were also achieved by puffing HA-CM to primary cultured neurons and record cellular responses (L). HA-CM elicited a large inward current (M, black bar indicate 100 ms medium puff), which can be reversibly blocked by DNQX (N and O). Quantified results showing that HA-CM elicited significantly bigger current (4238 ± 316 pA, $n = 10$) comparing to naïve medium (140 ± 61 , $n = 6$, $p < 0.001$ comparing to HA-CM). The HA-CM triggered current can be largely blocked by DNQX (605 ± 193 pA, $p < 0.001$ comparing to HA-CM). MA-CM triggered minimal current, indicating that the uptake of glutamate was complete.

5.1.4 Compare the gene expression differences between human and mouse astrocytes

In order to elucidate the molecular mechanism underlying the many functional differences between HA and MA, we collaborated with Dr. Hong Ma's lab in Fudan University to conduct a large-scale sequencing to obtain the global gene expression profile. A total of 16810 genes were analyzed between human astrocyte (HA 1800 human astrocyte cell line, three replicates) and mouse astrocytes (P3-5, two replicates). Out of the 14362 genes that showed detectable expression in human or mouse astrocytes, 3145 genes were significantly different in their expression level between the two species (unpaired t-test, use $p < 0.01$ as criteria). Out of the 3145 differentially expressed genes, 669 genes were higher in human astrocytes (333 genes > 5 fold enrichment) and 2476 genes were higher in mouse astrocytes (649 genes > 5 fold enrichment). The general structure of the human and mouse astrocyte transcriptoms were presented in a Venn diagram (Fig. 5-7-A) and cumulative distribution plot of rpkm (Fig. 5-7-B). The sequencing results were highly comparable between the experimental repeats in both HA and MA groups (Fig. 5-7-C-D).

In parallel RT-PCR experiments were also performed to provide additional measurements for gene expression level. Sample gene expression profiles were plotted in Figure 5-8.

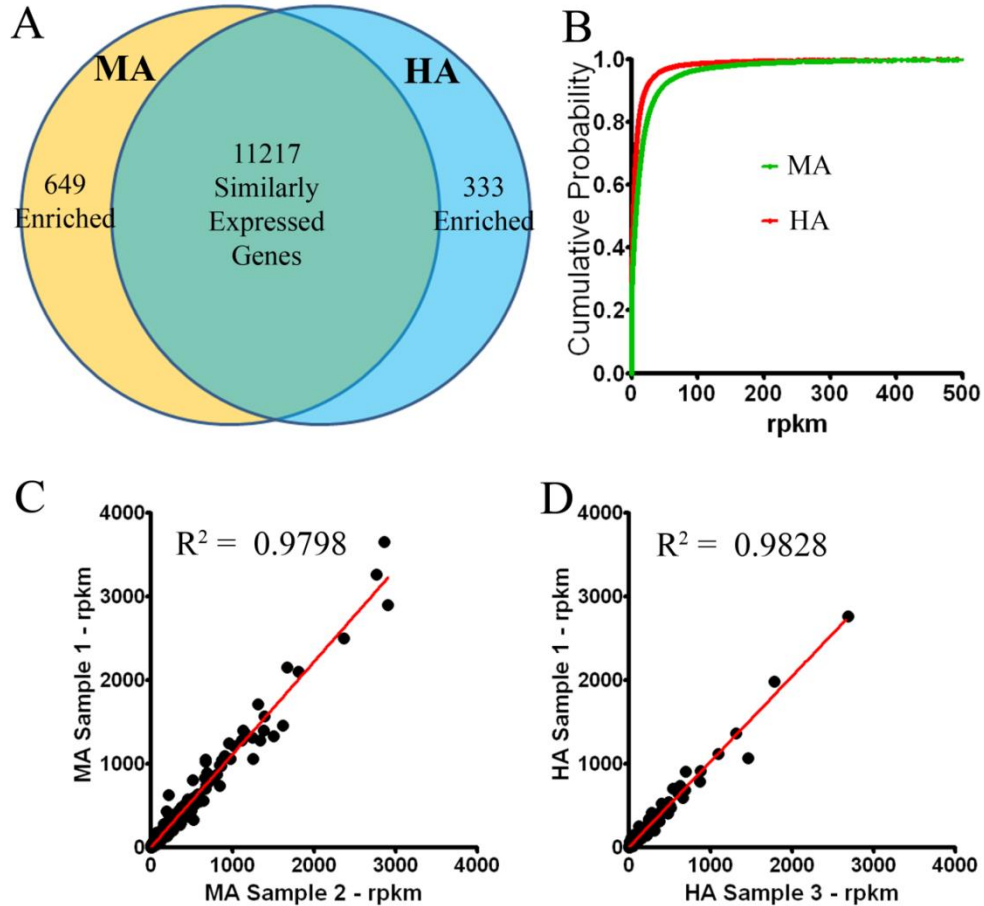


Figure 5-7: The general structures of human and mouse astrocytes transcriptomes.

(A) Venn diagram showing that the gene expression level between human astrocytes (HA) and mouse astrocytes (MA) are similar for most of the genes, only a small fraction of genes were enriched in HA or MA (982 out of 16810 genes analyzed). (B) The overall distribution of gene expression level (rpkms) in HA or MA. Overall MA has more robust gene expression than HA ($p < 0.001$, Kolmogorov-Smirnov test). (C-D) Correlation plot of two MA sequencing repeats, and two HA sequencing repeats. Note the near-perfect correlation of gene expression profile between two biological repeats.

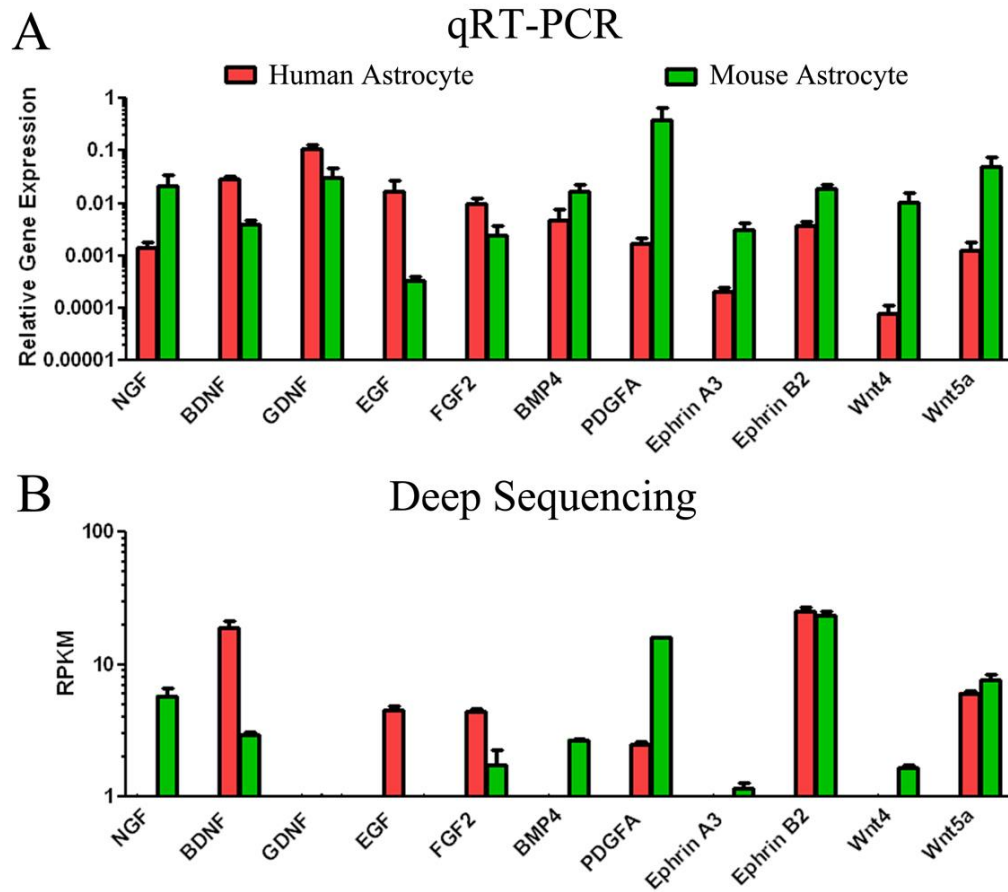


Figure 5-8: Gene expression profile obtained from qRT-PCR and deep sequencing methods are comparable.

Example gene expression profile of a selected list of genes in HA (Red) or MA (Green). Results from both qRT-PCR (A) and deep sequencing (B) experiments were shown for comparison of gene expression profile. The relative abundance of various genes was faithfully cross-validated by both deep sequencing and quantitative RT-PCR experiments. See detailed discussion in section 5.2.

5.2 Discussion

Glial cells consist of more than half the brain mass, yet studies on the roles glial cells play in health and disease was largely overlooked until recently. The differences between human and mouse astrocytes have been characterized, but their functional and molecular differences were poorly described. Understanding the species difference between human and mouse, particularly the difference in astrocytes, can provide a framework to help researchers interpret data generated from mouse model system, and lead to rational translation of this knowledge into therapies that can effectively treat human disease condition.

5.2.1 Human astrocyte promote stem cell proliferation rather than differentiation

The species difference between the human and mouse astrocytes is evident, given the vast differences between the brain structure and function. The conditioned medium from HA can exert similar proliferation-promoting effect as the human astrocytes. Therefore the responsible protein is very likely to be a secreted protein. We have compiled glial secretomes from a number of publications (Dowell et al., 2009; Keene et al., 2009; Greco et al., 2010; Jeon et al., 2010). Cross-referencing the compiled astrocyte secretome with our deep sequencing data revealed a number of secreted genes selectively enriched in either human or mouse astrocytes. Two full lists of genes are provided below to include the identified genes that are higher in human astrocyte or mouse astrocytes. These data can serve as valuable resources for future research on the differences between human and mouse astrocytes, and aid investigations on astrocyte functions in general.

Table 1: Potential factors responsible for HA stimulation on stem cell proliferation.

RPKM	FGF2	EGF	WNT3	GDNF	NGF	TGFB1	PDGFA	PDGFB	PDGFC	PDGFD	WNT5A
HA	6.42 ±	6.02 ±	1.61 ±	0.43 ±	0.77 ±	52.49 ±	2.51 ±	4.87 ±	14.47 ±	39.61 ±	7.82 ±
	0.39	0.38	0.21	0.08	0.10	4.27	0.12	0.21	0.42	1.99	0.41
MA	1.79 ±	0.33 ±	0.08 ±	0.13 ±	5.31 ±	2.84 ±	7.95 ±	19.2 ±	3.91 ±	5.64 ±	4.80 ±
	0.45	0.01	0.01	0.08	0.63	0.38	0.14	0.05	0.38	0.54	0.45

Table 2: Secreted proteins that are enriched in human astrocytes.

GENE NAME	GENE DESCRIPTION	H/M RATIO
TAGLN	transgelin	2.028552
TMSB10	thymosin, beta 10	3.852017
UCHL1	ubiquitin carboxy-terminal hydrolase L1	2.907161
SERPINE1	serpin peptidase inhibitor, clade E (nexin, plasminogen activator inhibitor type 1), member 1	11.92901
DKK3	dickkopf 3 homolog (Xenopus laevis)	9.011177
COL4A2	collagen, type IV, alpha 2	5.441627
SH3BGR13	SH3 domain binding glutamic acid-rich protein like 3	2.944449
SPP1	secreted phosphoprotein 1	9.133948
CD44	CD44 molecule (Indian blood group)	6.561701
ELN	elastin	2.771161
COL6A1	collagen, type VI, alpha 1	16.40761
SHISA5	shisa homolog 5 (Xenopus laevis)	3.076541
PLOD1	procollagen-lysine, 2-oxoglutarate 5-dioxygenase 1	3.57327
TGFB1I1	transforming growth factor beta 1 induced transcript 1	2.363761
COL5A1	collagen, type V, alpha 1	4.936088
TIMP1	TIMP metalloproteinase inhibitor 1	10.01547
TGFB1	transforming growth factor, beta 1	9.775938
STMN3	stathmin-like 3	3.355934
FBLN1	fibulin 1	6.561079
MMP2	matrix metalloproteinase 2 (gelatinase A, 72kDa gelatinase, 72kDa type IV collagenase)	3.12918
EFEMP1	EGF containing fibulin-like extracellular matrix protein 1	2.445332
LAMA4	laminin, alpha 4	9.4532
AEBP1	AE binding protein 1	2.334377
VCAN	versican	3.901002
LPCAT2	lysophosphatidylcholine acyltransferase 2	3.300706
DPP4	dipeptidyl-peptidase 4	159.4503
TNXB	tenascin XB	11.41183

Table 3: Secreted proteins that are enriched in mouse astrocytes.

GENE NAME	H/M RATIO
NPFF	0.194796
NDST1	0.192564
NDST1	0.192564
CHI3L1	0.186342
COL1A2	0.182879
LAMP2	0.174752
BTD	0.173284
TBL1X	0.167481
DAG1	0.163581
SCRN1	0.162097
HBEGF	0.160339
DLL1	0.159547
TCN2	0.145892
IGSF8	0.135487
ACYP2	0.134358
CCDC80	0.118436
GM2A	0.110371
PTGDS	0.10948
CHRD1	0.107488
IGFBP5	0.106779
CADM4	0.101072
GALC	0.089129
CTSL	0.089009
TXNDC16	0.088723
SOD3	0.086059
ECM1	0.075247
CSF1	0.066185
CD109	0.058766
MFAP4	0.054773
C4B	0.051499
LFNG	0.047199
GPC4	0.045202
SERPINE2	0.044259
CX3CL1	0.044245
CX3CL1	0.044245
CST3	0.041658

CTSZ	0.041255
CTSZ	0.041255
CD14	0.041104
SCG5	0.03813
IGFBP2	0.035415
SMPDL3A	0.030446
APOE	0.029604
RARRES2	0.027665
SERPINF1	0.024037
SORL1	0.023532
CP	0.023516
MT2	0.022312
CPE	0.016493
CPE	0.016493
IGFBP3	0.016248
PLXDC2	0.015439
VCAM1	0.015141
TPPP3	0.013795
BCAN	0.009799
COL2A1	0.009441
BGN	0.008929
FBLN5	0.008567
SPON1	0.007688
NID2	0.004866
IGF1	0.00411
CTSS	0.003445
ITIH3	0.002559
ITIH3	0.002559
CASQ1	0.002481
SPARCL1	0.002462
PTPRZ1	0.002392
A2M	0.001835
NCAN	0.000841
STMN2	0.000639
OGN	0.000582
SCG3	0.000476
PRELP	0.000464
FMOD	0.000122

5.2.2 High BDNF in human astrocyte facilitate inhibitory synapse formation

The high level of BDNF in human astrocytes is a surprising finding with significant implications in our understanding of human brain development. In the mouse brain, BDNF release is mostly from neurons (glial cells are thought to be not a significant contributor to inhibitory synapse formation). BDNF in the human brain can be released in significant amounts from astrocytes. This finding suggests that the principle of brain development may be fundamentally different between the human and mouse brain.

Different from previous studies on mouse neuron development (Deng et al., 2007), in the human neurons derived from NPC, glutamatergic synapse develop earlier than GABAergic synapse (Fig. 4-13). Whether this obvious discrepancy in the order of development is due to differences in intrinsic properties between human and mouse neurons, or whether the mouse glial cells provided an insufficient amount of BDNF to the human neuron to support early GABAergic synapse formation, are interesting questions that beget further investigations.

Table 4: Comparison of the expression of glial genes contributing to synapse formation between human and mouse astrocytes

RPKM	BDNF	THBS1	THBS2	SPARC	SPARCL1
HA	15.44 ± 2.27	116.82 ± 19.89	4.64 ± 1.47	543.23 ± 9.45	0.41 ± 0.14
MA	2.44 ± 0.21	379.4 ± 93	3.44 ± 0.04	1297.37 ± 132.11	120.39 ± 5.88

5.2.3 Glutamate processing dysfunction in glial cells as a key contributor to pathological conditions of the human brain

The finding that human astrocytes are capable of accumulating and releasing enormous amount of glutamate is surprising as it is thought-provoking. In the mouse model, astroglial cells uptake and convert glutamate into glutamine, which explains the low level of intracellular glutamate (Fig. 5-6-B). Only under brain cancer conditions can a high level of glutamate be detected in glial cells (Buckingham et al., 2011; Campbell et al., 2012). The finding that both

NPC-derived human astrocyte and human astrocyte cell lines accumulate large amount of glutamate suggests the interesting possibility that in normal human brain, the glutamate-secreting ability of astrocytes is under tight suppression for the proper functioning of the nervous system. The source of this suppression is likely to be the neurons, for co-culturing neuron with human astrocytes abolished the glutamate release. Extrapolating from this idea, one may even further question whether the suppression on human astrocyte glutamate secretion is compromised under certain stressful conditions, and whether this excessive glutamate release from astroglial cells contribute to the pathogenesis of human brain disease.

From the HA and MA transcriptome data, one could appreciate that the genes that are directly responsible for the synthesis of glutamate, GLS1 and GLS2, are not very different between HA and HA. The molecular mechanism behind the glutamate accumulation is likely due to the lack of the genes that are responsible for the uptake and degradation of glutamate (GLUL, SLC1A3, SLC1A2, GluD1, ABAT, GPT).

Table 5: Comparison of the expression of glial factors contributing to glutamate processing between human and mouse astrocytes

RPK M	GLU L	ABA T	GP T	GLUD 1	GRM 1	GRM 5	SLC1A 3	SLC1A 2	SLC6A 9	SOD1	GLS	GLS 2
HA	27.67 ± 2.51	2.80 ± 0.18	0.28 ± 0.03	23.13 ± 1.38	0.02 ± 0.01	0.02 ± 0.01	0.02 ± 0.01	9.96 ± 0.13	9.25 ± 0.39	188.9 9 ± 19.88	28.1 0 ± 2.05	0.32 ± 0.02
MA	189.10 ± 2.22	18.36 ± 0.32	3.78 ± 0.23	111.69 ±7.20	0.04 ± 0.01	1.48 ± 0.16	289.66 ± 8.96	8.12 ± 0.57	8.19 ± 0.38	433.7 2 ± 32.84	14.8 9 ± 0.04	0.29 ± 0.01

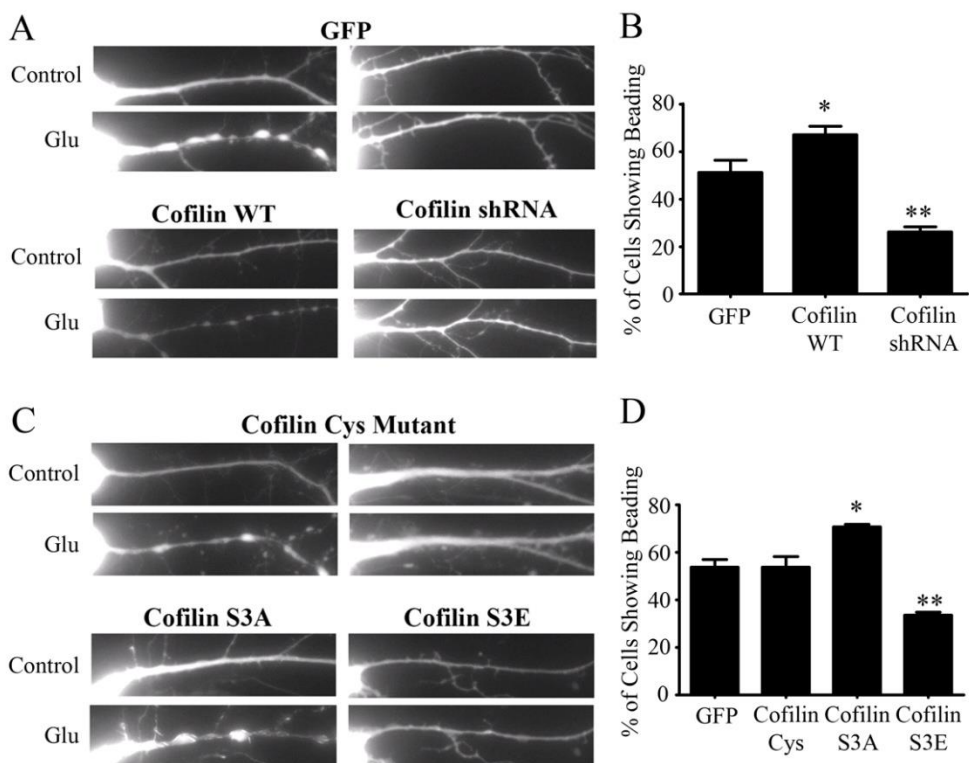
Appendix

Cofilin is a key regulator of neuronal calcium homeostasis

Cofilin is a key regulator of actin dynamics through its ability to depolymerize filamentous actin (F-actin) into globular actin (G-actin). Maintaining a proper calcium level is critical for neuronal functions, and disruptions in calcium homeostasis are documented in various neurological conditions. We investigated whether cofilin activity regulates neuronal calcium homeostasis. Mouse cortical neurons were used for experiments at DIV 10. Live imaging experiments were performed with constant perfusion of bath solution consisting of (in mM) 120 NaCl, 30 glucose, 25 HEPES, 5 KCl, 2 CaCl₂, 1 MgCl₂. pH was adjusted to 7.3 with NaOH. In each experiment, around 30 pictures of transfected neurons were taken before any treatment (Control). Glutamate was then applied at 100 μ M concentration for 10 minutes. The same neurons were found after the glutamate treatment to take after-stimulation pictures (Glu). The before- and after- stimulation pictures of the same neurons were paired for analysis.

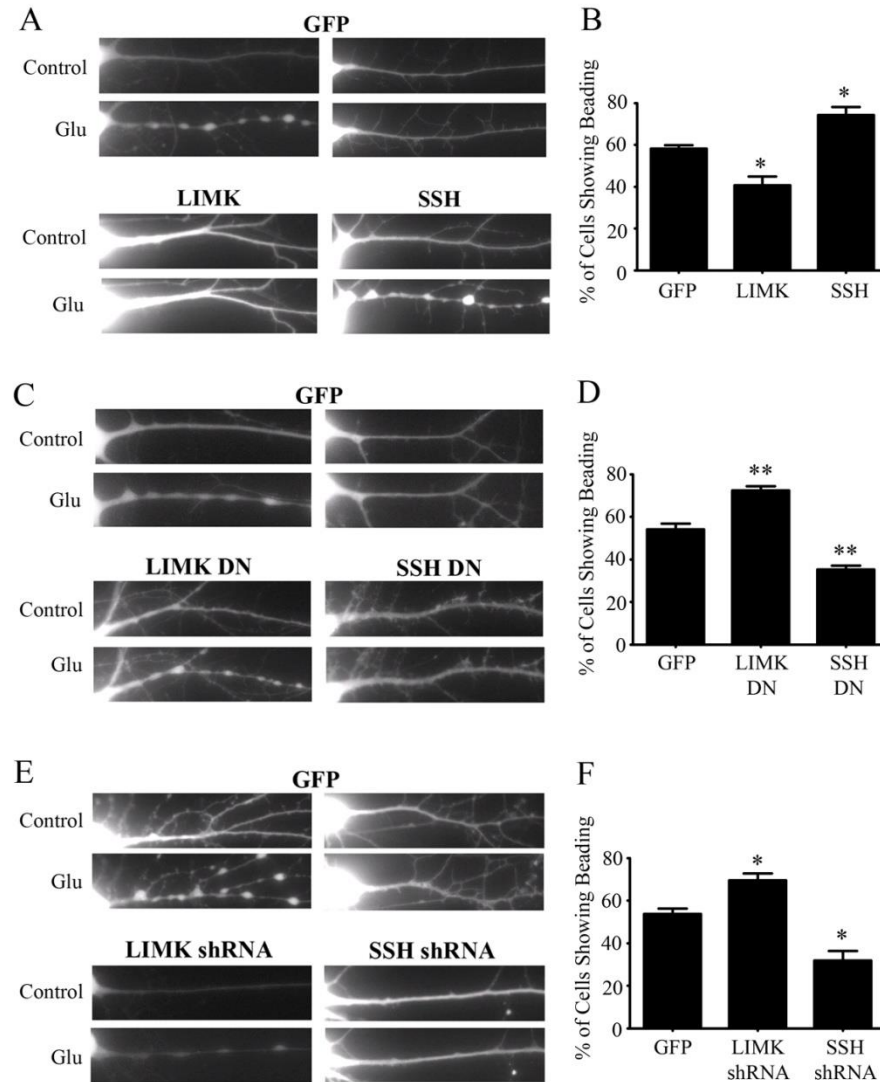
Neuron showing typical dendritic bubbling of $> 2x$ the width of the original dendrite was defined as a cell showing dendritic beading. From each repeat, ~ 30 neurons were analyzed, and the percentage of cells showing beading was calculated. Data presented in the bar graphs are results pooled from three to five independent repeats for each group.

Cofilin S3A is the constitutively-active cofilin mutant that cannot be phosphorylated, whereas cofilin S3E is the dominant-negative mutant. Cofilin Cys mutant is the oxidation-dead mutant, which should have no influence on its phosphorylation capability. Statistics were performed by one-way ANOVA with Bonferroni correction.



Appendix-1: Cofilin regulates the percentage of neurons showing dendritic beading after excitotoxic challenge.

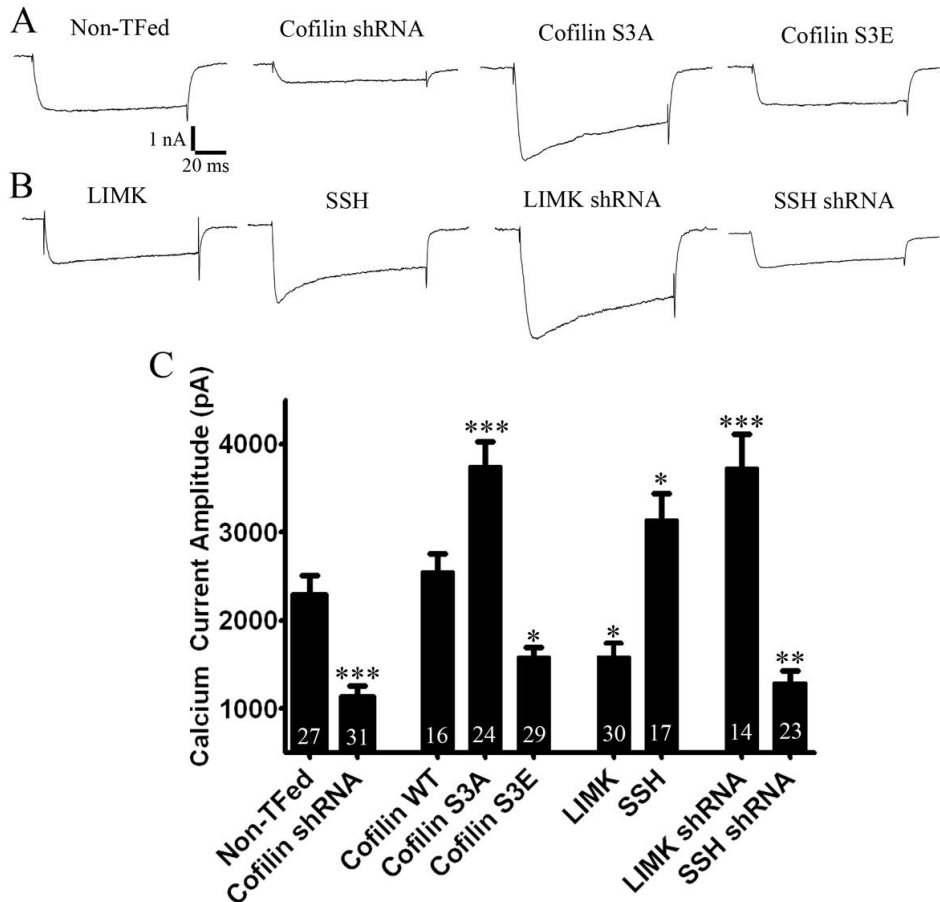
Plasmids were transfected into neurons between DIV 5-7, and experiments were performed at DIV 10. In GFP control neurons, close to half of the cells showed dendritic beading after 100 μ M glutamate treatment for 10 min. Overexpression of wild-type cofilin lead to an significant increase in the percentage of neurons showing beading, while decreased cofilin expression using shRNA construct against cofilin showed a decreased percentage (B, GFP: 51.2 ± 5.2 %, $n = 124$ neurons from 4 repeats; Cofilin WT: 64.4 ± 2.2 %, $n = 154$ neurons from 4 repeats, $p < 0.05$ comparing to GFP; Cofilin shRNA: 26.1 ± 2.2 %, $n = 207$ neurons from 5 repeats, $p < 0.01$ comparing to GFP). Expressing phosphorylation mutants of cofilin can mediate similar effects on dendritic beading. A constitutively-active mutant of cofilin (S3A) can significantly increase beading %, while a dominant negative mutant (S3E) can decrease the beading % (D, GFP: 53.8 ± 3.1 %, $n = 83$ neurons from 3 repeats; Cofilin S3A: 70.7 ± 1.1 %, $n = 181$ neurons from 4 repeats, $p < 0.05$ comparing to GFP; Cofilin S3E: 33.5 ± 1.2 %, $n = 148$ neurons from 4 repeats, $p < 0.01$ comparing to GFP). A Cys mutation of cofilin, which affects its oxidation but not phosphorylation, does not affect the beading percentage (53.7 ± 4.5 %, $n = 109$ neurons from 3 repeats, $p = 0.99$ comparing to GFP).



Appendix-2: LIMK and SSH are regulators of cofilin activity, which in turn regulates the beading percentage.

LIMK can decrease the percentage of neurons showing beading, while SSH increase it (B, GFP: 58.3 ± 1.7 %, $n = 165$ neurons from 4 repeats; LIMK: 40.8 ± 4.2 %, $n = 259$ neurons from 5 repeats, $p < 0.05$ comparing to GFP; SSH: 74.4 ± 3.8 %, $n = 178$ neurons from 5 repeats, $p < 0.01$). Conversely, the dominant negative versions of LIMK lead to an increase in beading percentage, while SSH-DN lead to a significant reduction (D, GFP: 54 ± 2.7 %, $n = 74$ neurons from two repeats; LIMK DN: 72.4 ± 2.1 %, $n = 173$ neurons from 4 repeats, $p < 0.01$ comparing to GFP; SSH DN: 35.4 ± 1.7 %, $n = 189$ neurons from 4 repeats, $p < 0.01$ comparing to GFP). Knocking down LIMK and SSH using respective shRNA constructs also influences the percentage of neurons showing beading (GFP: 53.8 ± 2.5 %, $n = 98$ neurons from 3 repeats;

LIMK shRNA: $69.5 \pm 3.4 \%$, $n = 173$ neurons from 5 repeats, $p < 0.01$ comparing to GFP; SSH shRNA: $31.8 \pm 4.6 \%$, $n = 219$ neurons from 5 repeats, $p < 0.01$ comparing to GFP).



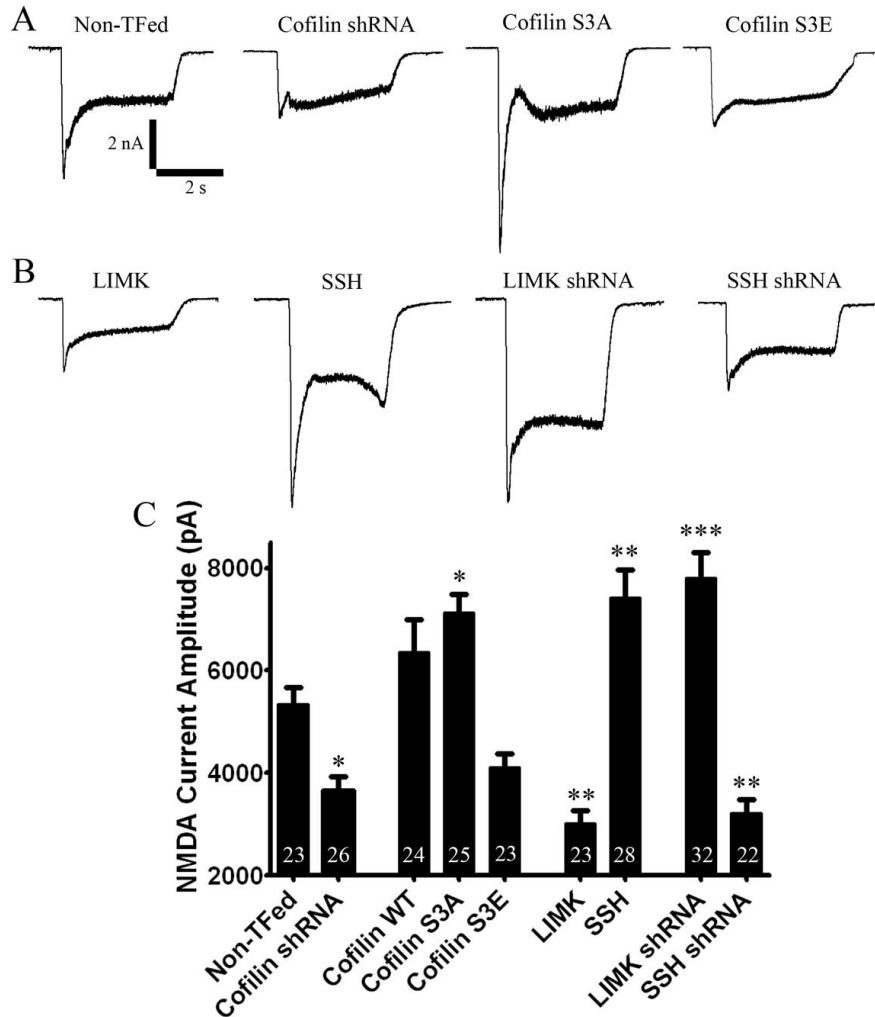
Appendix-3: Cofilin activity regulates whole-cell Calcium current amplitude in neurons.

When cofilin level was knocked-down by shRNA construct, the whole-cell calcium current decreased significantly (Non-TFed: 2296 ± 213 pA, $n = 27$ neurons; Cofilin shRNA: 1135 ± 122 pA, $n = 31$ neurons, $p < 0.001$ comparing to Non-TFed). Wild-type cofilin does not significantly influence Ca current amplitude, while the S3A mutant increases calcium current amplitude and S3E mutant decreases it (Cofilin WT: 2561 ± 202 pA, $n = 16$ neurons; Cofilin S3A: 3755 ± 277 pA, $n = 24$ neurons, $p < 0.001$; Cofilin S3E: 1593 ± 102 pA, $n = 29$ neurons, $p < 0.05$). The deactivator of cofilin activity, LIMK, can decrease Ca current amplitude; while the activator SSH increases it (LIMK: 1595 ± 152 pA, $n = 30$ neurons, $p < 0.05$; SSH: 3151 ± 290 pA, $n = 17$ neurons, $p < 0.05$). Knocking down LIMK level increases Ca current, whereas

knocking down SSH decreases it (LIMK shRNA: 3733 ± 383 pA, $n = 14$, $p < 0.001$; SSH shRNA: 1298 ± 133 pA, $n = 23$, $p < 0.05$).

Whole-cell patch-clamp recordings were performed using the Multiclamp 700A patch-clamp amplifier (Molecular Devices, Palo Alto, CA). Tetrodotoxin (TTX; 1 μ M) and tetraethylammounium (TEA; 15 mM) were added during recording to block voltage-dependent sodium channels and potassium channels. The series resistance was compensated to lower than 8 M Ω for all cells recorded. To record Ca current, the membrane potential was held at -70 mV baseline. A series of depolarizing voltage steps with 10 mV increament were delivered at 5 seconds intervals to elicit voltage-dependent Ca²⁺ Responses. Data were collected using pClamp 9 software (Molecular Devices, Palo Alto, CA), sampled at 10 kHz and filtered at 1 kHz. Off-line data analyses of Ca²⁺ currents amplitude were performed using pClamp 9 software. All experiments were performed at room temperature.

Statistics was performed by one-way ANOVA with Bonferroni correction. All comparisons were made with the Non-Transfected control group. Membrane capacitance of recorded cells was noted and subjected to the same statistical analysis. No statistically significant difference was detected between any of the experiment groups.



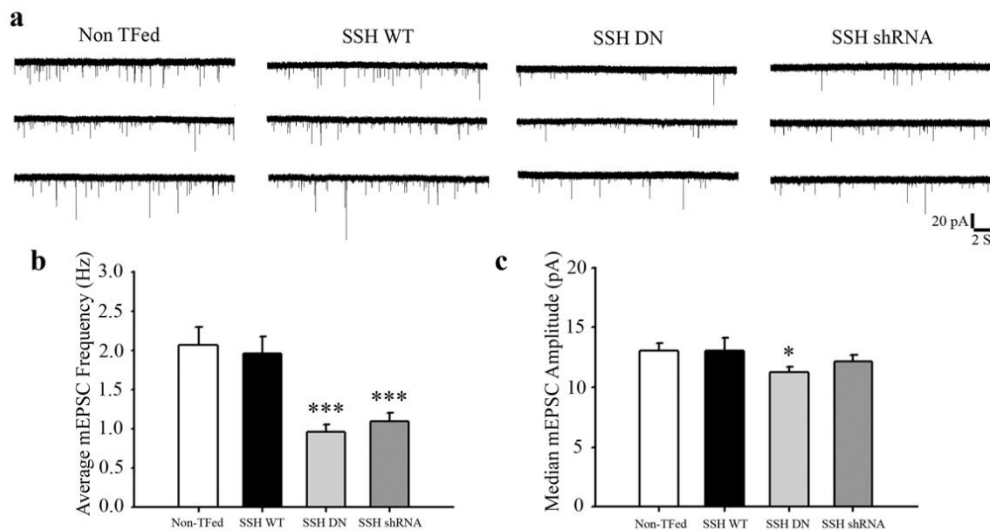
Appendix-4: Cofilin activity regulates whole-cell NMDA current amplitude in neurons.

When cofilin level was knocked-down by shRNA construct, the whole-cell NMDA current decreased significantly (Non-TFed: 5457 ± 323 pA, $n = 22$ neurons; Cofilin shRNA: 3629 ± 296 pA, $n = 25$ neurons, $p < 0.05$ comparing to Non-TFed). Wild-type cofilin does not significantly influence NMDA current amplitude, while the S3A mutant increases calcium current amplitude and S3E mutant decreases it (Cofilin WT: 6537 ± 633 pA, $n = 23$ neurons; Cofilin S3A: 7108 ± 366 pA, $n = 24$ neurons, $p < 0.05$; Cofilin S3E: 3985 ± 242 pA, $n = 22$ neurons, $p < 0.05$). The deactivator of cofilin activity, LIMK, can decrease NMDA current amplitude; while the activator SSH can increase it (LIMK: 3099 ± 242 pA, $n = 22$ neurons, $p < 0.01$; SSH: 7481 ± 554 pA, $n = 27$ neurons, $p < 0.01$). Knocking down LIMK level increases Ca current, whereas knocking down SSH decreases it (LIMK shRNA: 7771 ± 504 pA, $n = 31$, $p < 0.001$; SSH shRNA: 3178 ± 274 pA, $n = 21$, $p < 0.01$).

Magnesium was omitted from the bath solution to avoid voltage-dependent blockage of NMDA receptors. The pipette solution for NMDA current recording was (in mM) 147 KCl, 5 Na-phosphocreatine, 2 EGTA, 10 HEPES, 4 MgATP, and 0.5 Na₂GTP, pH 7.3 adjusted with KOH.

After breaking into whole-cell mode, the series resistance was compensated to lower than 10 M Ω for all the recordings.

Before NMDA application, the neurons were perfused with a NMDA current recording solution that contains 1 μ M TTX, 100 μ M Picrotoxin and 10 μ M glycine in Mg²⁺ free bath solution, to block Na channel, GABA_A receptor, and to maximize NMDA response. A five-second pulse of 100 μ M NMDA dissolved in the NMDA current recording solution was applied, and the peak NMDA responses were analyzed off-line using pClamp9 software.



Appendix-5: Downregulation of SSH activity reduce the mini EPSC frequency and amplitude.

The mini EPSC is reduced when SSH activity is downregulated through expression of a dominant negative version of SSH (Non-TFed: 2.1 ± 0.2 Hz, 13.1 ± 0.7 pA, $n = 26$; SSH DN: 0.96 ± 0.1 Hz, 11.2 ± 0.5 pA, $n = 27$ neurons, $p < 0.001$ comparing frequency to Non-TFed, $p < 0.05$ comparing amplitude), or by using shRNA construct to knockdown SSH (SSH shRNA: 1.1 ± 0.1 Hz, 12.2 ± 0.6 pA, $n = 19$, $p < 0.001$ comparing frequency to Non-TFed). Overexpress wild-type SSH does not affect mini EPSC frequency or amplitude (SSH WT: 2.0 ± 0.2 Hz, 13.1 ± 1.1 pA; n.s. comparing to Non-TFed).

References

- Aarum J, Sandberg K, Haeberlein SL, Persson MA (2003) Migration and differentiation of neural precursor cells can be directed by microglia. *Proc Natl Acad Sci U S A* 100:15983-15988.
- Abbott NJ, Ronnback L, Hansson E (2006) Astrocyte-endothelial interactions at the blood-brain barrier. *Nat Rev Neurosci* 7:41-53.
- Abuhatzira L, Makedonski K, Kaufman Y, Razin A, Shemer R (2007) MeCP2 deficiency in the brain decreases BDNF levels by REST/CoREST-mediated repression and increases TRKB production. *Epigenetics* 2:214-222.
- Akerman CJ, Cline HT (2006) Depolarizing GABAergic conductances regulate the balance of excitation to inhibition in the developing retinotectal circuit in vivo. *J Neurosci* 26:5117-5130.
- Allen NJ, Bennett ML, Foo LC, Wang GX, Chakraborty C, Smith SJ, Barres BA (2012) Astrocyte glypicans 4 and 6 promote formation of excitatory synapses via GluA1 AMPA receptors. *Nature* 486:410-414.
- Almeida S, Zhang Z, Coppola G, Mao W, Futai K, Karydas A, Geschwind MD, Tartaglia MC, Gao F, Gianni D, Sena-Esteves M, Geschwind DH, Miller BL, Farese RV, Jr., Gao FB (2012) Induced pluripotent stem cell models of progranulin-deficient frontotemporal dementia uncover specific reversible neuronal defects. *Cell Rep* 2:789-798.
- Alvarez-Saavedra M, Saez MA, Kang D, Zoghbi HY, Young JI (2007) Cell-specific expression of wild-type MeCP2 in mouse models of Rett syndrome yields insight about pathogenesis. *Hum Mol Genet* 16:2315-2325.
- Amir RE, Van den Veyver IB, Wan M, Tran CQ, Francke U, Zoghbi HY (1999) Rett syndrome is caused by mutations in X-linked MECP2, encoding methyl-CpG-binding protein 2. *Nature Genetics* 23:185-188.
- An MC, Zhang N, Scott G, Montoro D, Wittkop T, Mooney S, Melov S, Ellerby LM (2012) Genetic correction of Huntington's disease phenotypes in induced pluripotent stem cells. *Cell Stem Cell* 11:253-263.
- Ananiev G, Williams EC, Li H, Chang Q (2011) Isogenic pairs of wild type and mutant induced pluripotent stem cell (iPSC) lines from Rett syndrome patients as in vitro disease model. *PLoS One* 6:e25255.
- Anokye-Danso F, Trivedi CM, Jühr D, Gupta M, Cui Z, Tian Y, Zhang Y, Yang W, Gruber PJ, Epstein JA, Morrissey EE (2011) Highly efficient miRNA-mediated reprogramming of mouse and human somatic cells to pluripotency. *Cell Stem Cell* 8:376-388.
- Arion D, Lewis DA (2011) Altered expression of regulators of the cortical chloride transporters NKCC1 and KCC2 in schizophrenia. *Arch Gen Psychiatry* 68:21-31.
- Ashton RS, Conway A, Pangarkar C, Bergen J, Lim KI, Shah P, Bissell M, Schaffer DV (2012) Astrocytes regulate adult hippocampal neurogenesis through ephrin-B signaling. *Nat Neurosci* 15:1399-1406.
- Baker SA, Chen L, Wilkins AD, Yu P, Lichtarge O, Zoghbi HY (2013) An AT-hook domain in MeCP2 determines the clinical course of Rett syndrome and related disorders. *Cell* 152:984-996.

- Ballas N, Lioy DT, Grunseich C, Mandel G (2009) Non-cell autonomous influence of MeCP2-deficient glia on neuronal dendritic morphology. *Nat Neurosci* 12:311-317.
- Ballas N, Grunseich C, Lu DD, Speh JC, Mandel G (2005) REST and its corepressors mediate plasticity of neuronal gene chromatin throughout neurogenesis. *Cell* 121:645-657.
- Ban H, Nishishita N, Fusaki N, Tabata T, Saeki K, Shikamura M, Takada N, Inoue M, Hasegawa M, Kawamata S, Nishikawa S (2011) Efficient generation of transgene-free human induced pluripotent stem cells (iPSCs) by temperature-sensitive Sendai virus vectors. *Proc Natl Acad Sci U S A* 108:14234-14239.
- Banker GA (1980) Trophic interactions between astroglial cells and hippocampal neurons in culture. *Science* 209:809-810.
- Bardehle S, Kruger M, Buggenthin F, Schwausch J, Ninkovic J, Clevers H, Snippert HJ, Theis FJ, Meyer-Luehmann M, Bechmann I, Dimou L, Gotz M (2013) Live imaging of astrocyte responses to acute injury reveals selective juxtavascular proliferation. *Nat Neurosci* 16:580-586.
- Barres BA (2008) The mystery and magic of glia: a perspective on their roles in health and disease. *Neuron* 60:430-440.
- Begley DJ, Brightman MW (2003) Structural and functional aspects of the blood-brain barrier. *Prog Drug Res* 61:39-78.
- Ben-Ari Y, Khalilov I, Kahle KT, Cherubini E (2012) The GABA excitatory/inhibitory shift in brain maturation and neurological disorders. *The Neuroscientist : a review journal bringing neurobiology, neurology and psychiatry* 18:467-486.
- Beutner C, Lepperhof V, Dann A, Linnartz-Gerlach B, Litwak S, Napoli I, Prinz M, Neumann H (2013) Engineered stem cell-derived microglia as therapeutic vehicle for experimental autoimmune encephalomyelitis. *Gene Ther* 20:797-806.
- Bilican B, Serio A, Barmada SJ, Nishimura AL, Sullivan GJ, Carrasco M, Phatnani HP, Puddifoot CA, Story D, Fletcher J, Park IH, Friedman BA, Daley GQ, Wyllie DJ, Hardingham GE, Wilmot I, Finkbeiner S, Maniatis T, Shaw CE, Chandran S (2012) Mutant induced pluripotent stem cell lines recapitulate aspects of TDP-43 proteinopathies and reveal cell-specific vulnerability. *Proc Natl Acad Sci U S A*.
- Blackman MP, Djukic B, Nelson SB, Turrigiano GG (2012) A critical and cell-autonomous role for MeCP2 in synaptic scaling up. *J Neurosci* 32:13529-13536.
- Blaesse P, Airaksinen MS, Rivera C, Kaila K (2009) Cation-chloride cotransporters and neuronal function. *Neuron* 61:820-838.
- Bortone D, Polleux F (2009) KCC2 expression promotes the termination of cortical interneuron migration in a voltage-sensitive calcium-dependent manner. *Neuron* 62:53-71.
- Bos R, Sadlaoud K, Boulenguez P, Buttigieg D, Liabeuf S, Brocard C, Haase G, Bras H, Vinay L (2013) Activation of 5-HT_{2A} receptors upregulates the function of the neuronal K-Cl cotransporter KCC2. *Proc Natl Acad Sci U S A* 110:348-353.
- Bosch M, Hayashi Y (2011) Structural plasticity of dendritic spines. *Curr Opin Neurobiol* 22:383-388.
- Boulenguez P, Liabeuf S, Bos R, Bras H, Jean-Xavier C, Brocard C, Stil A, Darbon P, Cattaert D, Delpire E, Marsala M, Vinay L (2010) Down-regulation of the potassium-chloride cotransporter KCC2 contributes to spasticity after spinal cord injury. *Nat Med* 16:302-307.
- Brennand KJ, Simone A, Jou J, Gelboin-Burkhart C, Tran N, Sangar S, Li Y, Mu Y, Chen G, Yu D, McCarthy S, Sebat J, Gage FH (2011) Modelling schizophrenia using human induced pluripotent stem cells. *Nature* 473:221-225.
- Brenner M (2014) Role of GFAP in CNS injuries. *Neurosci Lett*.

- Buckingham SC, Campbell SL, Haas BR, Montana V, Robel S, Ogunrinu T, Sontheimer H (2011) Glutamate release by primary brain tumors induces epileptic activity. *Nat Med* 17:1269-1274.
- Burgalossi A, Jung S, Man KN, Nair R, Jockusch WJ, Wojcik SM, Brose N, Rhee JS (2012) Analysis of neurotransmitter release mechanisms by photolysis of caged Ca(2)(+) in an autaptic neuron culture system. *Nat Protoc* 7:1351-1365.
- Cahoy JD, Emery B, Kaushal A, Foo LC, Zamanian JL, Christopherson KS, Xing Y, Lubischer JL, Krieg PA, Krupenko SA, Thompson WJ, Barres BA (2008) A transcriptome database for astrocytes, neurons, and oligodendrocytes: a new resource for understanding brain development and function. *J Neurosci* 28:264-278.
- Campbell SL, Buckingham SC, Sontheimer H (2012) Human glioma cells induce hyperexcitability in cortical networks. *Epilepsia* 53:1360-1370.
- Cancedda L, Fiumelli H, Chen K, Poo MM (2007) Excitatory GABA action is essential for morphological maturation of cortical neurons in vivo. *J Neurosci* 27:5224-5235.
- Cassel S, Revel MO, Kelche C, Zwiller J (2004) Expression of the methyl-CpG-binding protein MeCP2 in rat brain. An ontogenetic study. *Neurobiol Dis* 15:206-211.
- Chahrour M, Zoghbi HY (2007) The story of Rett syndrome: from clinic to neurobiology. *Neuron* 56:422-437.
- Chahrour M, Jung SY, Shaw C, Zhou X, Wong ST, Qin J, Zoghbi HY (2008) MeCP2, a key contributor to neurological disease, activates and represses transcription. *Science* 320:1224-1229.
- Chambers SM, Fasano CA, Papapetrou EP, Tomishima M, Sadelain M, Studer L (2009) Highly efficient neural conversion of human ES and iPS cells by dual inhibition of SMAD signaling. *Nat Biotechnol* 27:275-280.
- Chang Q, Khare G, Dani V, Nelson S, Jaenisch R (2006) The disease progression of Mecp2 mutant mice is affected by the level of BDNF expression. *Neuron* 49:341-348.
- Chao HT, Zoghbi HY (2012) MeCP2: only 100% will do. *Nat Neurosci* 15:176-177.
- Chao HT, Zoghbi HY, Rosenmund C (2007) MeCP2 controls excitatory synaptic strength by regulating glutamatergic synapse number. *Neuron* 56:58-65.
- Chao HT, Chen H, Samaco RC, Xue M, Chahrour M, Yoo J, Neul JL, Gong S, Lu HC, Heintz N, Ekker M, Rubenstein JL, Noebels JL, Rosenmund C, Zoghbi HY (2012) Dysfunction in GABA signalling mediates autism-like stereotypies and Rett syndrome phenotypes. *Nature* 468:263-269.
- Chapleau CA, Calfa GD, Lane MC, Albertson AJ, Larimore JL, Kudo S, Armstrong DL, Percy AK, Pozzo-Miller L (2009) Dendritic spine pathologies in hippocampal pyramidal neurons from Rett syndrome brain and after expression of Rett-associated MECP2 mutations. *Neurobiol Dis* 35:219-233.
- Chell JM, Brand AH (2010) Nutrition-responsive glia control exit of neural stem cells from quiescence. *Cell* 143:1161-1173.
- Chen G, Trombley PQ, van den Pol AN (1995) GABA receptors precede glutamate receptors in hypothalamic development; differential regulation by astrocytes. *J Neurophysiol* 74:1473-1484.
- Chen G, Trombley PQ, van den Pol AN (1996) Excitatory actions of GABA in developing rat hypothalamic neurones. *J Physiol* 494 (Pt 2):451-464.
- Chen RZ, Akbarian S, Tudor M, Jaenisch R (2001) Deficiency of methyl-CpG binding protein-2 in CNS neurons results in a Rett-like phenotype in mice. *Nat Genet* 27:327-331.
- Chen WG, Chang Q, Lin Y, Meissner A, West AE, Griffith EC, Jaenisch R, Greenberg ME (2003) Derepression of BDNF transcription involves calcium-dependent phosphorylation of MeCP2. *Science* 302:885-889.

- Chen ZF, Paquette AJ, Anderson DJ (1998) NRSF/REST is required in vivo for repression of multiple neuronal target genes during embryogenesis. *Nat Genet* 20:136-142.
- Cheung AY, Horvath LM, Grafodatskaya D, Pasceri P, Weksberg R, Hotta A, Carrel L, Ellis J (2011) Isolation of MECP2-null Rett Syndrome patient hiPS cells and isogenic controls through X-chromosome inactivation. *Hum Mol Genet* 20:2103-2115.
- Cheval H, Guy J, Merusi C, De Sousa D, Selfridge J, Bird A (2012) Postnatal inactivation reveals enhanced requirement for MeCP2 at distinct age windows. *Hum Mol Genet* 21:3806-3814.
- Childress JF (2001) An ethical defense of federal funding for human embryonic stem cell research. *Yale J Health Policy Law Ethics* 2:109, 157-165.
- Chorin E, Vinograd O, Fleidervish I, Gilad D, Herrmann S, Sekler I, Aizenman E, Hershfinkel M (2011) Upregulation of KCC2 activity by zinc-mediated neurotransmission via the mZnR/GPR39 receptor. *J Neurosci* 31:12916-12926.
- Christodoulou J, Grimm A, Maher T, Bennetts B (2003) RettBASE: The IRSA MECP2 variation data-base - A new mutation database in evolution. *Human Mutation* 21:466-472.
- Christopherson KS, Ullian EM, Stokes CC, Mullowney CE, Hell JW, Agah A, Lawler J, Mosher DF, Bornstein P, Barres BA (2005) Thrombospondins are astrocyte-secreted proteins that promote CNS synaptogenesis. *Cell* 120:421-433.
- Clarkson J, Herbison AE (2006) Development of GABA and glutamate signaling at the GnRH neuron in relation to puberty. *Mol Cell Endocrinol* 254-255:32-38.
- Cobb BL, Fei Y, Jonsson R, Bolstad AI, Brun JG, Rischmueller M, Lester SE, Witte T, Illei G, Brennan M, Bowman S, Moser KL, Harley JB, Sawalha AH (2010) Genetic association between methyl-CpG binding protein 2 (MECP2) and primary Sjogren's syndrome. *Ann Rheum Dis* 69:1731-1732.
- Cohen DRS, Matarazzo V, Palmer AM, Tu Y, Jeon OH, Pevsner J, Ronnett GV (2003) Expression of MeCP2 in olfactory receptor neurons is developmentally regulated and occurs before synaptogenesis. *Molecular and Cellular Neuroscience* 22:417-429.
- Cohen I, Navarro V, Clemenceau S, Baulac M, Miles R (2002) On the origin of interictal activity in human temporal lobe epilepsy in vitro. *Science* 298:1418-1421.
- Cohen S, Greenberg ME (2008) Communication between the synapse and the nucleus in neuronal development, plasticity, and disease. *Annu Rev Cell Dev Biol* 24:183-209.
- Cohen S, Gabel HW, Hemberg M, Hutchinson AN, Sadacca LA, Ebert DH, Harmin DA, Greenberg RS, Verdine VK, Zhou Z, Wetsel WC, West AE, Greenberg ME (2011) Genome-wide activity-dependent MeCP2 phosphorylation regulates nervous system development and function. *Neuron* 72:72-85.
- Cong L, Ran FA, Cox D, Lin S, Barretto R, Habib N, Hsu PD, Wu X, Jiang W, Marraffini LA, Zhang F (2013) Multiplex genome engineering using CRISPR/Cas systems. *Science* 339:819-823.
- Consortium Hi (2012) Induced pluripotent stem cells from patients with Huntington's disease show CAG-repeat-expansion-associated phenotypes. *Cell Stem Cell* 11:264-278.
- Coull JA, Beggs S, Boudreau D, Boivin D, Tsuda M, Inoue K, Gravel C, Salter MW, De Koninck Y (2005) BDNF from microglia causes the shift in neuronal anion gradient underlying neuropathic pain. *Nature* 438:1017-1021.
- Dajani R, Koo SE, Sullivan GJ, Park IH (2013) Investigation of Rett syndrome using pluripotent stem cells. *J Cell Biochem* 114:2446-2453.
- Daley GQ et al. (2007) Ethics. The ISSCR guidelines for human embryonic stem cell research. *Science* 315:603-604.

- Dani VS, Nelson SB (2009) Intact long-term potentiation but reduced connectivity between neocortical layer 5 pyramidal neurons in a mouse model of Rett syndrome. *J Neurosci* 29:11263-11270.
- Dani VS, Chang Q, Maffei A, Turrigiano GG, Jaenisch R, Nelson SB (2005) Reduced cortical activity due to a shift in the balance between excitation and inhibition in a mouse model of Rett syndrome. *Proceedings of the National Academy of Sciences of the United States of America* 102:12560-12565.
- De Koninck Y (2007) Altered chloride homeostasis in neurological disorders: a new target. *Curr Opin Pharmacol* 7:93-99.
- de Wit J, O'Sullivan ML, Savas JN, Condomitti G, Caccese MC, Vennekens KM, Yates JR, 3rd, Ghosh A (2013) Unbiased discovery of glypican as a receptor for LRRTM4 in regulating excitatory synapse development. *Neuron* 79:696-711.
- del Gaudio D et al. (2006) Increased MECP2 gene copy number as the result of genomic duplication in neurodevelopmentally delayed males. *Genet Med* 8:784-792.
- Delpire E, Lu J, England R, Dull C, Thorne T (1999) Deafness and imbalance associated with inactivation of the secretory Na-K-2Cl co-transporter. *Nat Genet* 22:192-195.
- Deng L, Yao J, Fang C, Dong N, Luscher B, Chen G (2007) Sequential postsynaptic maturation governs the temporal order of GABAergic and glutamatergic synaptogenesis in rat embryonic cultures. *J Neurosci* 27:10860-10869.
- Derecki NC, Cronk JC, Lu Z, Xu E, Abbott SB, Guyenet PG, Kipnis J (2012) Wild-type microglia arrest pathology in a mouse model of Rett syndrome. *Nature* 484:105-109.
- Di Giorgio FP, Boulting GL, Bobrowicz S, Eggan KC (2008) Human embryonic stem cell-derived motor neurons are sensitive to the toxic effect of glial cells carrying an ALS-causing mutation. *Cell Stem Cell* 3:637-648.
- Di Giorgio FP, Carrasco MA, Siao MC, Maniatis T, Eggan K (2007) Non-cell autonomous effect of glia on motor neurons in an embryonic stem cell-based ALS model. *Nat Neurosci* 10:608-614.
- Doerflinger RM (1999) The ethics of funding embryonic stem cell research: a Catholic viewpoint. *Kennedy Inst Ethics J* 9:137-150.
- Dowell JA, Johnson JA, Li L (2009) Identification of astrocyte secreted proteins with a combination of shotgun proteomics and bioinformatics. *J Proteome Res* 8:4135-4143.
- Dzhala VI, Talos DM, Sdrulla DA, Brumback AC, Mathews GC, Benke TA, Delpire E, Jensen FE, Staley KJ (2005) NKCC1 transporter facilitates seizures in the developing brain. *Nat Med* 11:1205-1213.
- Ebert AD, Yu J, Rose FF, Jr., Mattis VB, Lorson CL, Thomson JA, Svendsen CN (2009) Induced pluripotent stem cells from a spinal muscular atrophy patient. *Nature* 457:277-280.
- Ebert DH, Gabel HW, Robinson ND, Kastan NR, Hu LS, Cohen S, Navarro AJ, Lyst MJ, Ekiert R, Bird AP, Greenberg ME (2013a) Activity-dependent phosphorylation of MeCP2 threonine 308 regulates interaction with NCoR. *Nature* 499:341-345.
- Ebert DH, Gabel HW, Robinson ND, Kastan NR, Hu LS, Cohen S, Navarro AJ, Lyst MJ, Ekiert R, Bird AP, Greenberg ME (2013b) Activity-dependent phosphorylation of MeCP2 threonine 308 regulates interaction with NCoR. *Nature* 499:341-U116.
- Egawa N et al. (2012) Drug screening for ALS using patient-specific induced pluripotent stem cells. *Sci Transl Med* 4:145ra104.
- Elmariah SB, Oh EJ, Hughes EG, Balice-Gordon RJ (2005) Astrocytes regulate inhibitory synapse formation via Trk-mediated modulation of postsynaptic GABAA receptors. *J Neurosci* 25:3638-3650.
- Erlandson A, Hagberg B (2005) MECP2 abnormality phenotypes: Clinicopathologic area with broad variability. *Journal of Child Neurology* 20:727-732.

- Eroglu C, Barres BA (2010) Regulation of synaptic connectivity by glia. *Nature* 468:223-231.
- Espuny-Camacho I, Michelsen KA, Gall D, Linaro D, Hasche A, Bonnefont J, Bali C, Orduz D, Bilheu A, Herpoel A, Lambert N, Gaspard N, Peron S, Schiffmann SN, Giugliano M, Gaillard A, Vanderhaeghen P (2013) Pyramidal neurons derived from human pluripotent stem cells integrate efficiently into mouse brain circuits in vivo. *Neuron* 77:440-456.
- Esteban MA et al. (2010) Vitamin C enhances the generation of mouse and human induced pluripotent stem cells. *Cell Stem Cell* 6:71-79.
- Ferrini F, Trang T, Mattioli TA, Laffray S, Del'Guidice T, Lorenzo LE, Castonguay A, Doyon N, Zhang W, Godin AG, Mohr D, Beggs S, Vandal K, Beaulieu JM, Cahill CM, Salter MW, De Koninck Y (2013) Morphine hyperalgesia gated through microglia-mediated disruption of neuronal Cl(-) homeostasis. *Nat Neurosci* 16:183-192.
- Fiumelli H, Briner A, Puskarjov M, Blaesse P, Belem BJ, Dayer AG, Kaila K, Martin JL, Vutsits L (2012) An ion transport-independent role for the cation-chloride cotransporter KCC2 in dendritic spinogenesis in vivo. *Cereb Cortex* 23:378-388.
- Flagella M, Clarke LL, Miller ML, Erway LC, Giannella RA, Andringa A, Gawenis LR, Kramer J, Duffy JJ, Doetschman T, Lorenz JN, Yamoah EN, Cardell EL, Shull GE (1999) Mice lacking the basolateral Na-K-2Cl cotransporter have impaired epithelial chloride secretion and are profoundly deaf. *J Biol Chem* 274:26946-26955.
- Fortin DA, Srivastava T, Soderling TR (2012) Structural modulation of dendritic spines during synaptic plasticity. *Neuroscientist* 18:326-341.
- Fu M, Yu X, Lu J, Zuo Y (2012) Repetitive motor learning induces coordinated formation of clustered dendritic spines in vivo. *Nature* 483:92-95.
- Funfschilling U, Supplie LM, Mahad D, Boretius S, Saab AS, Edgar J, Brinkmann BG, Kassmann CM, Tzvetanova ID, Mobius W, Diaz F, Meijer D, Suter U, Hamprecht B, Sereda MW, Moraes CT, Frahm J, Goebbels S, Nave KA (2012) Glycolytic oligodendrocytes maintain myelin and long-term axonal integrity. *Nature* 485:517-521.
- Fusaki N, Ban H, Nishiyama A, Saeki K, Hasegawa M (2009) Efficient induction of transgene-free human pluripotent stem cells using a vector based on Sendai virus, an RNA virus that does not integrate into the host genome. *Proc Jpn Acad Ser B Phys Biol Sci* 85:348-362.
- Fyffe SL, Neul JL, Samaco RC, Chao HT, Ben-Shachar S, Moretti P, McGill BE, Goulding EH, Sullivan E, Tecott LH, Zoghbi HY (2008) Deletion of *Mecp2* in *Sim1*-expressing neurons reveals a critical role for MeCP2 in feeding behavior, aggression, and the response to stress. *Neuron* 59:947-958.
- Gamba G (2005) Molecular physiology and pathophysiology of electroneutral cation-chloride cotransporters. *Physiol Rev* 85:423-493.
- Garg SK, Lioy DT, Cheval H, McGann JC, Bissonnette JM, Murtha MJ, Foust KD, Kaspar BK, Bird A, Mandel G (2013) Systemic delivery of MeCP2 rescues behavioral and cellular deficits in female mouse models of Rett syndrome. *J Neurosci* 33:13612-13620.
- Gauvain G, Chamma I, Chevy Q, Cabezas C, Irinopoulou T, Bodrug N, Carnaud M, Levi S, Poncer JC (2011) The neuronal K-Cl cotransporter KCC2 influences postsynaptic AMPA receptor content and lateral diffusion in dendritic spines. *Proc Natl Acad Sci U S A* 108:15474-15479.
- Ge S, Goh EL, Sailor KA, Kitabatake Y, Ming GL, Song H (2006) GABA regulates synaptic integration of newly generated neurons in the adult brain. *Nature* 439:589-593.
- Gemelli T, Berton O, Nelson ED, Perrotti LI, Jaenisch R, Monteggia LM (2006) Postnatal loss of methyl-CpG binding protein 2 in the forebrain is sufficient to mediate behavioral aspects of Rett syndrome in mice. *Biol Psychiatry* 59:468-476.

- Ghodsizadeh A, Taei A, Totonchi M, Seifinejad A, Gourabi H, Pournasr B, Aghdami N, Malekzadeh R, Almadani N, Salekdeh GH, Baharvand H (2010) Generation of liver disease-specific induced pluripotent stem cells along with efficient differentiation to functional hepatocyte-like cells. *Stem Cell Rev* 6:622-632.
- Giacometti E, Luikenhuis S, Beard C, Jaenisch R (2007) Partial rescue of MeCP2 deficiency by postnatal activation of MeCP2. *Proc Natl Acad Sci U S A* 104:1931-1936.
- Gill H, Cheadle JP, Maynard J, Fleming N, Whatley S, Cranston T, Thompson EM, Leonard H, Davis M, Christodoulou J, Skjeldal O, Hanefeld F, Kerr A, Tandy A, Ravine D, Clarke A (2003) Mutation analysis in the MECP2 gene and genetic counselling for Rett syndrome. *Journal of Medical Genetics* 40:380-384.
- Goffin D, Allen M, Zhang L, Amorim M, Wang IT, Reyes AR, Mercado-Berton A, Ong C, Cohen S, Hu L, Blendy JA, Carlson GC, Siegel SJ, Greenberg ME, Zhou Z (2011) Rett syndrome mutation MeCP2 T158A disrupts DNA binding, protein stability and ERP responses. *Nat Neurosci* 15:274-283.
- Gogolla N, Leblanc JJ, Quast KB, Sudhof TC, Fagiolini M, Hensch TK (2009) Common circuit defect of excitatory-inhibitory balance in mouse models of autism. *J Neurodev Disord* 1:172-181.
- Greco TM, Seeholzer SH, Mak A, Spruce L, Ischiropoulos H (2010) Quantitative mass spectrometry-based proteomics reveals the dynamic range of primary mouse astrocyte protein secretion. *J Proteome Res* 9:2764-2774.
- Grskovic M, Javaherian A, Strulovici B, Daley GQ (2011) Induced pluripotent stem cells--opportunities for disease modelling and drug discovery. *Nat Rev Drug Discov* 10:915-929.
- Gu J, Lee CW, Fan Y, Komlos D, Tang X, Sun C, Yu K, Hartzell HC, Chen G, Bamberg JR, Zheng JQ (2010) ADF/cofilin-mediated actin dynamics regulate AMPA receptor trafficking during synaptic plasticity. *Nat Neurosci* 13:1208-1215.
- Gulyas AI, Sik A, Payne JA, Kaila K, Freund TF (2001) The KCl cotransporter, KCC2, is highly expressed in the vicinity of excitatory synapses in the rat hippocampus. *Eur J Neurosci* 13:2205-2217.
- Guy J, Hendrich B, Holmes M, Martin JE, Bird A (2001) A mouse Mecp2-null mutation causes neurological symptoms that mimic Rett syndrome. *Nat Genet* 27:322-326.
- Hagerman R, Hoem G, Hagerman P (2010) Fragile X and autism: Intertwined at the molecular level leading to targeted treatments. *Mol Autism* 1:12.
- Hama H, Hara C, Yamaguchi K, Miyawaki A (2004) PKC signaling mediates global enhancement of excitatory synaptogenesis in neurons triggered by local contact with astrocytes. *Neuron* 41:405-415.
- Hamby ME, Sofroniew MV (2010) Reactive astrocytes as therapeutic targets for CNS disorders. *Neurotherapeutics* 7:494-506.
- Han X, Chen M, Wang F, Windrem M, Wang S, Shanz S, Xu Q, Oberheim NA, Bekar L, Betstadt S, Silva AJ, Takano T, Goldman SA, Nedergaard M (2013) Forebrain engraftment by human glial progenitor cells enhances synaptic plasticity and learning in adult mice. *Cell Stem Cell* 12:342-353.
- Hanna J, Wernig M, Markoulaki S, Sun CW, Meissner A, Cassady JP, Beard C, Brambrink T, Wu LC, Townes TM, Jaenisch R (2007) Treatment of sickle cell anemia mouse model with iPS cells generated from autologous skin. *Science* 318:1920-1923.
- Hansen DV, Rubenstein JL, Kriegstein AR (2011) Deriving excitatory neurons of the neocortex from pluripotent stem cells. *Neuron* 70:645-660.
- Hansen DV, Lui JH, Parker PR, Kriegstein AR (2010) Neurogenic radial glia in the outer subventricular zone of human neocortex. *Nature* 464:554-561.

- Hargus G, Cooper O, Deleidi M, Levy A, Lee K, Marlow E, Yow A, Soldner F, Hockemeyer D, Hallett PJ, Osborn T, Jaenisch R, Isacson O (2010) Differentiated Parkinson patient-derived induced pluripotent stem cells grow in the adult rodent brain and reduce motor asymmetry in Parkinsonian rats. *Proc Natl Acad Sci U S A* 107:15921-15926.
- Haydon PG (2001) GLIA: listening and talking to the synapse. *Nat Rev Neurosci* 2:185-193.
- He Q, Nomura T, Xu J, Contractor A (2014) The Developmental Switch in GABA Polarity Is Delayed in Fragile X Mice. *J Neurosci* 34:446-450.
- Hershinkel M, Kandler K, Knoch ME, Dagan-Rabin M, Aras MA, Abramovitch-Dahan C, Sekler I, Aizenman E (2009) Intracellular zinc inhibits KCC2 transporter activity. *Nat Neurosci* 12:725-727.
- Hertz L, Chen Y, Gibbs ME, Zang P, Peng L (2004) Astrocytic adrenoceptors: a major drug target in neurological and psychiatric disorders? *Curr Drug Targets CNS Neurol Disord* 3:239-267.
- Hester ME, Murtha MJ, Song S, Rao M, Miranda CJ, Meyer K, Tian J, Boulting G, Schaffer DV, Zhu MX, Pfaff SL, Gage FH, Kaspar BK (2011) Rapid and Efficient Generation of Functional Motor Neurons From Human Pluripotent Stem Cells Using Gene Delivered Transcription Factor Codes. *Mol Ther*.
- Hewitt SA, Wamsteeker JI, Kurz EU, Bains JS (2009) Altered chloride homeostasis removes synaptic inhibitory constraint of the stress axis. *Nat Neurosci* 12:438-443.
- Hockemeyer D, Wang H, Kiani S, Lai CS, Gao Q, Cassady JP, Cost GJ, Zhang L, Santiago Y, Miller JC, Zeitler B, Cherone JM, Meng X, Hinkley SJ, Rebar EJ, Gregory PD, Urnov FD, Jaenisch R (2011) Genetic engineering of human pluripotent cells using TALE nucleases. *Nat Biotechnol* 29:731-734.
- Horn Z, Ringstedt T, Blaesse P, Kaila K, Herlenius E (2010) Premature expression of KCC2 in embryonic mice perturbs neural development by an ion transport-independent mechanism. *Eur J Neurosci* 31:2142-2155.
- Hou P, Li Y, Zhang X, Liu C, Guan J, Li H, Zhao T, Ye J, Yang W, Liu K, Ge J, Xu J, Zhang Q, Zhao Y, Deng H (2013a) Pluripotent stem cells induced from mouse somatic cells by small-molecule compounds. *Science* 341:651-654.
- Hou Z, Zhang Y, Propson NE, Howden SE, Chu LF, Sontheimer EJ, Thomson JA (2013b) Efficient genome engineering in human pluripotent stem cells using Cas9 from *Neisseria meningitidis*. *Proc Natl Acad Sci U S A* 110:15644-15649.
- Hu BY, Zhang SC (2009) Differentiation of spinal motor neurons from pluripotent human stem cells. *Nat Protoc* 4:1295-1304.
- Hu BY, Weick JP, Yu J, Ma LX, Zhang XQ, Thomson JA, Zhang SC (2010) Neural differentiation of human induced pluripotent stem cells follows developmental principles but with variable potency. *Proc Natl Acad Sci U S A* 107:4335-4340.
- Hubner CA, Stein V, Hermans-Borgmeyer I, Meyer T, Ballanyi K, Jentsch TJ (2001) Disruption of KCC2 reveals an essential role of K-Cl cotransport already in early synaptic inhibition. *Neuron* 30:515-524.
- Hughes EG, Elmariah SB, Balice-Gordon RJ (2010) Astrocyte secreted proteins selectively increase hippocampal GABAergic axon length, branching, and synaptogenesis. *Mol Cell Neurosci* 43:136-145.
- Hyde TM, Lipska BK, Ali T, Mathew SV, Law AJ, Metitiri OE, Straub RE, Ye T, Colantuoni C, Herman MM, Bigelow LB, Weinberger DR, Kleinman JE (2011) Expression of GABA signaling molecules KCC2, NKCC1, and GAD1 in cortical development and schizophrenia. *J Neurosci* 31:11088-11095.

- Inoue K, Furukawa T, Kumada T, Yamada J, Wang T, Inoue R, Fukuda A (2012) Taurine inhibits K⁺-Cl⁻ cotransporter KCC2 to regulate embryonic Cl⁻ homeostasis via with-no-lysine (WNK) protein kinase signaling pathway. *J Biol Chem* 287:20839-20850.
- Israel MA, Yuan SH, Bardy C, Reyna SM, Mu Y, Herrera C, Hefferan MP, Van Gorp S, Nazor KL, Boscolo FS, Carson CT, Laurent LC, Marsala M, Gage FH, Remes AM, Koo EH, Goldstein LS (2012) Probing sporadic and familial Alzheimer's disease using induced pluripotent stem cells. *Nature* 482:216-220.
- Itzhaki I, Maizels L, Huber I, Zwi-Dantsis L, Caspi O, Winterstern A, Feldman O, Gepstein A, Arbel G, Hammerman H, Boulos M, Gepstein L (2011) Modelling the long QT syndrome with induced pluripotent stem cells. *Nature* 471:225-229.
- Jaenisch N, Witte OW, Frahm C (2010) Downregulation of potassium chloride cotransporter KCC2 after transient focal cerebral ischemia. *Stroke* 41:e151-159.
- Jaenisch R, Bird A (2003) Epigenetic regulation of gene expression: how the genome integrates intrinsic and environmental signals. *Nat Genet* 33 Suppl:245-254.
- Jeon H, Lee S, Lee WH, Suk K (2010) Analysis of glial secretome: the long pentraxin PTX3 modulates phagocytic activity of microglia. *J Neuroimmunol* 229:63-72.
- Jian L, Nagarajan L, De Klerk N, Ravine D, Bower C, Anderson A, Williamson S, Christodoulou J, Leonard H (2006) Predictors of seizure onset in Rett syndrome. *Journal of Pediatrics* 149:542-547.
- Jiang M, Chen G (2006) High Ca²⁺-phosphate transfection efficiency in low-density neuronal cultures. *Nat Protoc* 1:695-700.
- Jiang M, Chen G (2009) Ca²⁺ regulation of dynamin-independent endocytosis in cortical astrocytes. *J Neurosci* 29:8063-8074.
- Jin X, Huguenard JR, Prince DA (2005) Impaired Cl⁻ extrusion in layer V pyramidal neurons of chronically injured epileptogenic neocortex. *J Neurophysiol* 93:2117-2126.
- Johnson MA, Weick JP, Pearce RA, Zhang SC (2007) Functional neural development from human embryonic stem cells: accelerated synaptic activity via astrocyte coculture. *J Neurosci* 27:3069-3077.
- Jones PL, Veenstra GJ, Wade PA, Vermaak D, Kass SU, Landsberger N, Strouboulis J, Wolffe AP (1998) Methylated DNA and MeCP2 recruit histone deacetylase to repress transcription. *Nat Genet* 19:187-191.
- Juopperi TA, Kim WR, Chiang CH, Yu H, Margolis RL, Ross CA, Ming GL, Song H (2012) Astrocytes generated from patient induced pluripotent stem cells recapitulate features of Huntington's disease patient cells. *Mol Brain* 5:17.
- Kahle KT, Staley KJ, Nahed BV, Gamba G, Hebert SC, Lifton RP, Mount DB (2008) Roles of the cation-chloride cotransporters in neurological disease. *Nat Clin Pract Neurol* 4:490-503.
- Kang J, Jiang L, Goldman SA, Nedergaard M (1998) Astrocyte-mediated potentiation of inhibitory synaptic transmission. *Nat Neurosci* 1:683-692.
- Karow M, Chavez CL, Farruggio AP, Geisinger JM, Keravala A, Jung WE, Lan F, Wu JC, Chen-Tsai Y, Calos MP (2011) Site-specific recombinase strategy to create induced pluripotent stem cells efficiently with plasmid DNA. *Stem Cells* 29:1696-1704.
- Keene SD, Greco TM, Parastatidis I, Lee SH, Hughes EG, Balice-Gordon RJ, Speicher DW, Ischiropoulos H (2009) Mass spectrometric and computational analysis of cytokine-induced alterations in the astrocyte secretome. *Proteomics* 9:768-782.
- Kelsch W, Hormuzdi S, Straube E, Lewen A, Monyer H, Misgeld U (2001) Insulin-like growth factor 1 and a cytosolic tyrosine kinase activate chloride outward transport during maturation of hippocampal neurons. *J Neurosci* 21:8339-8347.

- Khazipov R, Tyzio R, Ben-Ari Y (2008) Effects of oxytocin on GABA signalling in the foetal brain during delivery. *Prog Brain Res* 170:243-257.
- Khirug S, Yamada J, Afzalov R, Voipio J, Khiroug L, Kaila K (2008) GABAergic depolarization of the axon initial segment in cortical principal neurons is caused by the Na-K-2Cl cotransporter NKCC1. *J Neurosci* 28:4635-4639.
- Kim JE, O'Sullivan ML, Sanchez CA, Hwang M, Israel MA, Brennand K, Deerinck TJ, Goldstein LS, Gage FH, Ellisman MH, Ghosh A (2011a) Investigating synapse formation and function using human pluripotent stem cell-derived neurons. *Proc Natl Acad Sci U S A* 108:3005-3010.
- Kim JY, Liu CY, Zhang F, Duan X, Wen Z, Song J, Feighery E, Lu B, Rujescu D, St Clair D, Christian K, Callicott JH, Weinberger DR, Song H, Ming GL (2012) Interplay between DISC1 and GABA signaling regulates neurogenesis in mice and risk for schizophrenia. *Cell* 148:1051-1064.
- Kim KY, Hysolli E, Park IH (2011b) Neuronal maturation defect in induced pluripotent stem cells from patients with Rett syndrome. *Proc Natl Acad Sci U S A* 108:14169-14174.
- Kishi N, Macklis JD (2004) MECP2 is progressively expressed in post-migratory neurons and is involved in neuronal maturation rather than cell fate decisions. *Molecular and Cellular Neuroscience* 27:306-321.
- Kline DD, Ogier M, Kunze DL, Katz DM (2010) Exogenous brain-derived neurotrophic factor rescues synaptic dysfunction in Mecp2-null mice. *J Neurosci* 30:5303-5310.
- Kobayashi M, Buckmaster PS (2003) Reduced inhibition of dentate granule cells in a model of temporal lobe epilepsy. *J Neurosci* 23:2440-2452.
- Koch P, Tamboli IY, Mertens J, Wunderlich P, Ladewig J, Stuber K, Esselmann H, Wiltfang J, Brustle O, Walter J (2012) Presenilin-1 L166P mutant human pluripotent stem cell-derived neurons exhibit partial loss of gamma-secretase activity in endogenous amyloid-beta generation. *Am J Pathol* 180:2404-2416.
- Kohara K, Yasuda H, Huang Y, Adachi N, Sohya K, Tsumoto T (2007) A local reduction in cortical GABAergic synapses after a loss of endogenous brain-derived neurotrophic factor, as revealed by single-cell gene knock-out method. *J Neurosci* 27:7234-7244.
- Krencik R, Zhang SC (2011) Directed differentiation of functional astroglial subtypes from human pluripotent stem cells. *Nat Protoc* 6:1710-1717.
- Krencik R, Weick JP, Liu Y, Zhang ZJ, Zhang SC (2011) Specification of transplantable astroglial subtypes from human pluripotent stem cells. *Nat Biotechnol* 29:528-534.
- Krey JF, Pasca SP, Shcheglovitov A, Yazawa M, Schwemberger R, Rasmusson R, Dolmetsch RE (2013) Timothy syndrome is associated with activity-dependent dendritic retraction in rodent and human neurons. *Nat Neurosci* 16:201-209.
- Kucukdereli H, Allen NJ, Lee AT, Feng A, Ozlu MI, Conatser LM, Chakraborty C, Workman G, Weaver M, Sage EH, Barres BA, Eroglu C (2011) Control of excitatory CNS synaptogenesis by astrocyte-secreted proteins Hevin and SPARC. *Proc Natl Acad Sci U S A* 108:E440-449.
- Lai CS, Franke TF, Gan WB (2012) Opposite effects of fear conditioning and extinction on dendritic spine remodelling. *Nature* 483:87-91.
- Landi S, Putignano E, Boggio EM, Giustetto M, Pizzorusso T, Ratto GM (2012) The short-time structural plasticity of dendritic spines is altered in a model of Rett syndrome. *Sci Rep* 1:45.
- Lee G, Papapetrou EP, Kim H, Chambers SM, Tomishima MJ, Fasano CA, Ganat YM, Menon J, Shimizu F, Viale A, Tabar V, Sadelain M, Studer L (2009) Modelling pathogenesis and treatment of familial dysautonomia using patient-specific iPSCs. *Nature* 461:402-406.

- Lee HH, Deeb TZ, Walker JA, Davies PA, Moss SJ (2011) NMDA receptor activity downregulates KCC2 resulting in depolarizing GABAA receptor-mediated currents. *Nat Neurosci* 14:736-743.
- Lemonnier E, Robin G, Degrez C, Tyzio R, Grandgeorge M, Ben-Ari Y (2013) Treating Fragile X syndrome with the diuretic bumetanide: a case report. *Acta Paediatr* 102:e288-290.
- Lemonnier E, Degrez C, Phelep M, Tyzio R, Josse F, Grandgeorge M, Hadjikhani N, Ben-Ari Y (2012) A randomised controlled trial of bumetanide in the treatment of autism in children. *Transl Psychiatry* 2:e202.
- Levy SE, Mandell DS, Schultz RT (2009) Autism. *Lancet* 374:1627-1638.
- Li H, Khirug S, Cai C, Ludwig A, Blaesse P, Kolikova J, Afzalov R, Coleman SK, Lauri S, Airaksinen MS, Keinänen K, Khiroug L, Saarma M, Kaila K, Rivera C (2007) KCC2 interacts with the dendritic cytoskeleton to promote spine development. *Neuron* 56:1019-1033.
- Li W, Pozzo-Miller L (2014) BDNF deregulation in Rett syndrome. *Neuropharmacology* 76 Pt C:737-746.
- Li Y, Wang H, Muffat J, Cheng AW, Orlando DA, Loven J, Kwok SM, Feldman DA, Bateup HS, Gao Q, Hockemeyer D, Mitalipova M, Lewis CA, Vander Heiden MG, Sur M, Young RA, Jaenisch R (2013) Global transcriptional and translational repression in human-embryonic-stem-cell-derived Rett syndrome neurons. *Cell Stem Cell* 13:446-458.
- Lie DC, Colamarino SA, Song HJ, Desire L, Mira H, Consiglio A, Lein ES, Jessberger S, Lansford H, Dearie AR, Gage FH (2005) Wnt signalling regulates adult hippocampal neurogenesis. *Nature* 437:1370-1375.
- Lieberman AP, Pitha PM, Shin HS, Shin ML (1989) Production of tumor necrosis factor and other cytokines by astrocytes stimulated with lipopolysaccharide or a neurotropic virus. *Proc Natl Acad Sci U S A* 86:6348-6352.
- Lioy DT, Garg SK, Monaghan CE, Raber J, Foust KD, Kaspar BK, Hirrlinger PG, Kirchhoff F, Bissonnette JM, Ballas N, Mandel G (2011) A role for glia in the progression of Rett's syndrome. *Nature* 475:497-500.
- Liu GH, Barkho BZ, Ruiz S, Diep D, Qu J, Yang SL, Panopoulos AD, Suzuki K, Kurian L, Walsh C, Thompson J, Boue S, Fung HL, Sancho-Martinez I, Zhang K, Yates J, 3rd, Izpisua Belmonte JC (2011) Recapitulation of premature ageing with iPSCs from Hutchinson-Gilford progeria syndrome. *Nature* 472:221-225.
- Liu J, Koscielska KA, Cao Z, Hulsizer S, Grace N, Mitchell G, Nacey C, Githinji J, McGee J, Garcia-Arocena D, Hagerman RJ, Nolte J, Pessah IN, Hagerman PJ (2012) Signaling defects in iPSC-derived fragile X premutation neurons. *Hum Mol Genet* 21:3795-3805.
- Liu X, Yao DL, Bondy CA, Brenner M, Hudson LD, Zhou J, Webster HD (1994) Astrocytes express insulin-like growth factor-I (IGF-I) and its binding protein, IGFBP-2, during demyelination induced by experimental autoimmune encephalomyelitis. *Mol Cell Neurosci* 5:418-430.
- Ludwig A, Uvarov P, Soni S, Thomas-Crusells J, Airaksinen MS, Rivera C (2011a) Early growth response 4 mediates BDNF induction of potassium chloride cotransporter 2 transcription. *J Neurosci* 31:644-649.
- Ludwig A, Uvarov P, Pellegrino C, Thomas-Crusells J, Schuchmann S, Saarma M, Airaksinen MS, Rivera C (2011b) Neurturin evokes MAPK-dependent upregulation of Egr4 and KCC2 in developing neurons. *Neural Plast* 2011:1-8.
- Lyst MJ, Ekiert R, Ebert DH, Merusi C, Nowak J, Selfridge J, Guy J, Kastan NR, Robinson ND, Alves FD, Rappaport J, Greenberg ME, Bird A (2013) Rett syndrome mutations abolish the interaction of MeCP2 with the NCoR/SMRT co-repressor. *Nature Neuroscience* 16:898-U268.

- Maezawa I, Jin LW (2010) Rett Syndrome Microglia Damage Dendrites and Synapses by the Elevated Release of Glutamate. *Journal of Neuroscience* 30:5346-5356.
- Maezawa I, Swanberg S, Harvey D, LaSalle JM, Jin LW (2009) Rett syndrome astrocytes are abnormal and spread MeCP2 deficiency through gap junctions. *J Neurosci* 29:5051-5061.
- Malhotra SK, Shnitka TK, Elbrink J (1990) Reactive astrocytes--a review. *Cytobios* 61:133-160.
- Marchetto MC, Winner B, Gage FH (2010a) Pluripotent stem cells in neurodegenerative and neurodevelopmental diseases. *Hum Mol Genet* 19:R71-76.
- Marchetto MC, Muotri AR, Mu Y, Smith AM, Cezar GG, Gage FH (2008) Non-cell-autonomous effect of human SOD1 G37R astrocytes on motor neurons derived from human embryonic stem cells. *Cell Stem Cell* 3:649-657.
- Marchetto MC, Carromeu C, Acab A, Yu D, Yeo GW, Mu Y, Chen G, Gage FH, Muotri AR (2010b) A model for neural development and treatment of Rett syndrome using human induced pluripotent stem cells. *Cell* 143:527-539.
- Maroof AM, Keros S, Tyson JA, Ying SW, Ganat YM, Merkle FT, Liu B, Goulburn A, Stanley EG, Elefanty AG, Widmer HR, Eggan K, Goldstein PA, Anderson SA, Studer L (2013) Directed differentiation and functional maturation of cortical interneurons from human embryonic stem cells. *Cell Stem Cell* 12:559-572.
- Marteyn A, Maury Y, Gauthier MM, Lecuyer C, Vernet R, Denis JA, Pietu G, Peschanski M, Martinat C (2011) Mutant human embryonic stem cells reveal neurite and synapse formation defects in type 1 myotonic dystrophy. *Cell Stem Cell* 8:434-444.
- Mauch DH, Nagler K, Schumacher S, Goritz C, Muller EC, Otto A, Pfrieder FW (2001) CNS synaptogenesis promoted by glia-derived cholesterol. *Science* 294:1354-1357.
- McCarthy KD, de Vellis J (1980) Preparation of separate astroglial and oligodendroglial cell cultures from rat cerebral tissue. *J Cell Biol* 85:890-902.
- McGraw CM, Samaco RC, Zoghbi HY (2011) Adult neural function requires MeCP2. *Science* 333:186.
- Medrihan L, Tantalaki E, Aramuni G, Sargsyan V, Dudanova I, Missler M, Zhang W (2008) Early defects of GABAergic synapses in the brain stem of a MeCP2 mouse model of Rett syndrome. *J Neurophysiol* 99:112-121.
- Meehan RR, Lewis JD, Bird AP (1992) Characterization of Mecp2, a Vertebrate DNA-Binding Protein with Affinity for Methylated DNA. *Nucleic Acids Research* 20:5085-5092.
- Mellen M, Ayata P, Dewell S, Kriaucionis S, Heintz N (2012) MeCP2 binds to 5hmC enriched within active genes and accessible chromatin in the nervous system. *Cell* 151:1417-1430.
- Mercado A, Mount DB, Gamba G (2004) Electroneutral cation-chloride cotransporters in the central nervous system. *Neurochem Res* 29:17-25.
- Miller JA, Horvath S, Geschwind DH (2010) Divergence of human and mouse brain transcriptome highlights Alzheimer disease pathways. *Proc Natl Acad Sci U S A* 107:12698-12703.
- Mitne-Neto M, Machado-Costa M, Marchetto MC, Bengtson MH, Joazeiro CA, Tsuda H, Bellen HJ, Silva HC, Oliveira AS, Lazar M, Muotri AR, Zatz M (2011) Downregulation of VAPB expression in motor neurons derived from induced pluripotent stem cells of ALS8 patients. *Hum Mol Genet* 20:3642-3652.
- Molofsky AV, Krencik R, Ullian EM, Tsai HH, Deneen B, Richardson WD, Barres BA, Rowitch DH (2012) Astrocytes and disease: a neurodevelopmental perspective. *Genes Dev* 26:891-907.
- Mou X, Wu Y, Cao H, Meng Q, Wang Q, Sun C, Hu S, Ma Y, Zhang H (2012) Generation of disease-specific induced pluripotent stem cells from patients with different karyotypes of Down syndrome. *Stem Cell Res Ther* 3:14.

- Myers VB, Haydon DA (1972) Ion transfer across lipid membranes in the presence of gramicidin A. II. The ion selectivity. *Biochim Biophys Acta* 274:313-322.
- Na ES, Nelson ED, Kavalali ET, Monteggia LM (2012a) The impact of MeCP2 loss- or gain-of-function on synaptic plasticity. *Neuropsychopharmacology* 38:212-219.
- Na ES, Nelson ED, Adachi M, Autry AE, Mahgoub MA, Kavalali ET, Monteggia LM (2012b) A mouse model for MeCP2 duplication syndrome: MeCP2 overexpression impairs learning and memory and synaptic transmission. *J Neurosci* 32:3109-3117.
- Nagai M, Re DB, Nagata T, Chalazonitis A, Jessell TM, Wichterle H, Przedborski S (2007) Astrocytes expressing ALS-linked mutated SOD1 release factors selectively toxic to motor neurons. *Nat Neurosci* 10:615-622.
- Nave KA (2010a) Myelination and support of axonal integrity by glia. *Nature* 468:244-252.
- Nave KA (2010b) Myelination and the trophic support of long axons. *Nat Rev Neurosci* 11:275-283.
- Nedergaard M, Ransom B, Goldman SA (2003) New roles for astrocytes: redefining the functional architecture of the brain. *Trends Neurosci* 26:523-530.
- Nelson ED, Kavalali ET, Monteggia LM (2006) MeCP2-dependent transcriptional repression regulates excitatory neurotransmission. *Curr Biol* 16:710-716.
- Nguyen MV, Felice CA, Du F, Covey MV, Robinson JK, Mandel G, Ballas N (2013) Oligodendrocyte lineage cells contribute unique features to Rett syndrome neuropathology. *J Neurosci* 33:18764-18774.
- Nicholas CR, Chen J, Tang Y, Southwell DG, Chalmers N, Vogt D, Arnold CM, Chen YJ, Stanley EG, Elefanty AG, Sasai Y, Alvarez-Buylla A, Rubenstein JL, Kriegstein AR (2013) Functional maturation of hPSC-derived forebrain interneurons requires an extended timeline and mimics human neural development. *Cell Stem Cell* 12:573-586.
- Oberheim NA, Takano T, Han X, He W, Lin JH, Wang F, Xu Q, Wyatt JD, Pilcher W, Ojemann JG, Ransom BR, Goldman SA, Nedergaard M (2009) Uniquely hominid features of adult human astrocytes. *J Neurosci* 29:3276-3287.
- Ogier M, Wang H, Hong E, Wang Q, Greenberg ME, Katz DM (2007) Brain-derived neurotrophic factor expression and respiratory function improve after amphetamine treatment in a mouse model of Rett syndrome. *J Neurosci* 27:10912-10917.
- Okabe Y, Takahashi T, Mitsumasu C, Kosai K, Tanaka E, Matsuishi T (2012) Alterations of gene expression and glutamate clearance in astrocytes derived from an MeCP2-null mouse model of Rett syndrome. *PLoS One* 7:e35354.
- Okita K, Nakagawa M, Hyenjong H, Ichisaka T, Yamanaka S (2008) Generation of mouse induced pluripotent stem cells without viral vectors. *Science* 322:949-953.
- Opitz T, De Lima AD, Voigt T (2002) Spontaneous development of synchronous oscillatory activity during maturation of cortical networks in vitro. *J Neurophysiol* 88:2196-2206.
- Palma E, Amici M, Sobrero F, Spinelli G, Di Angelantonio S, Ragozzino D, Mascia A, Scoppetta C, Esposito V, Miledi R, Eusebi F (2006) Anomalous levels of Cl⁻ transporters in the hippocampal subiculum from temporal lobe epilepsy patients make GABA excitatory. *Proc Natl Acad Sci U S A* 103:8465-8468.
- Pardridge WM (2003) Blood-brain barrier drug targeting: the future of brain drug development. *Mol Interv* 3:90-105, 151.
- Pasca SP, Portmann T, Voineagu I, Yazawa M, Shcheglovitov A, Pasca AM, Cord B, Palmer TD, Chikahisa S, Nishino S, Bernstein JA, Hallmayer J, Geschwind DH, Dolmetsch RE (2011) Using iPSC-derived neurons to uncover cellular phenotypes associated with Timothy syndrome. *Nat Med* 17:1657-1662.
- Payne JA, Rivera C, Voipio J, Kaila K (2003) Cation-chloride co-transporters in neuronal communication, development and trauma. *Trends Neurosci* 26:199-206.

- Pekny M, Nilsson M (2005) Astrocyte activation and reactive gliosis. *Glia* 50:427-434.
- Penzes P, Cahill ME, Jones KA, VanLeeuwen JE, Woolfrey KM (2011) Dendritic spine pathology in neuropsychiatric disorders. *Nat Neurosci* 14:285-293.
- Perrier AL, Tabar V, Barberi T, Rubio ME, Bruses J, Topf N, Harrison NL, Studer L (2004) Derivation of midbrain dopamine neurons from human embryonic stem cells. *Proc Natl Acad Sci U S A* 101:12543-12548.
- Rakic P (1978) Neuronal migration and contact guidance in the primate telencephalon. *Postgrad Med J* 54 Suppl 1:25-40.
- Rastegar M, Hotta A, Pasceri P, Makarem M, Cheung AY, Elliott S, Park KJ, Adachi M, Jones FS, Clarke ID, Dirks P, Ellis J (2009) MECP2 isoform-specific vectors with regulated expression for Rett syndrome gene therapy. *PLoS One* 4:e6810.
- Represa A, Ben-Ari Y (2005) Trophic actions of GABA on neuronal development. *Trends Neurosci* 28:278-283.
- Rett A (1966) [On a unusual brain atrophy syndrome in hyperammonemia in childhood]. *Wien Med Wochenschr* 116:723-726.
- Ricciardi S, Boggio EM, Grosso S, Lonetti G, Forlani G, Stefanelli G, Calcagno E, Morello N, Landsberger N, Biffo S, Pizzorusso T, Giustetto M, Broccoli V (2011) Reduced AKT/mTOR signaling and protein synthesis dysregulation in a Rett syndrome animal model. *Hum Mol Genet* 20:1182-1196.
- Ricciardi S, Ungaro F, Hambrock M, Rademacher N, Stefanelli G, Brambilla D, Sessa A, Magagnotti C, Bachi A, Giarda E, Verpelli C, Kilstrup-Nielsen C, Sala C, Kalscheuer VM, Broccoli V (2012) CDKL5 ensures excitatory synapse stability by reinforcing NGL-1-PSD95 interaction in the postsynaptic compartment and is impaired in patient iPSC-derived neurons. *Nat Cell Biol* 14:911-923.
- Riekkki R, Pavlov I, Tornberg J, Lauri SE, Airaksinen MS, Taira T (2008) Altered synaptic dynamics and hippocampal excitability but normal long-term plasticity in mice lacking hyperpolarizing GABA A receptor-mediated inhibition in CA1 pyramidal neurons. *J Neurophysiol* 99:3075-3089.
- Rinehart J, Vazquez N, Kahle KT, Hodson CA, Ring AM, Gulcicek EE, Louvi A, Bobadilla NA, Gamba G, Lifton RP (2011) WNK2 kinase is a novel regulator of essential neuronal cation-chloride cotransporters. *J Biol Chem* 286:30171-30180.
- Ristanovic D, Milosevic NT, Stulic V (2006) Application of modified Sholl analysis to neuronal dendritic arborization of the cat spinal cord. *J Neurosci Methods* 158:212-218.
- Rivera C, Voipio J, Payne JA, Ruusuvuori E, Lahtinen H, Lamsa K, Pirvola U, Saarma M, Kaila K (1999) The K⁺/Cl⁻ co-transporter KCC2 renders GABA hyperpolarizing during neuronal maturation. *Nature* 397:251-255.
- Rivera C, Voipio J, Thomas-Crusells J, Li H, Emri Z, Sipila S, Payne JA, Minichiello L, Saarma M, Kaila K (2004) Mechanism of activity-dependent downregulation of the neuron-specific K-Cl cotransporter KCC2. *J Neurosci* 24:4683-4691.
- Robinton DA, Daley GQ (2011) The promise of induced pluripotent stem cells in research and therapy. *Nature* 481:295-305.
- Saad B, Constam DB, Ortmann R, Moos M, Fontana A, Schachner M (1991) Astrocyte-derived TGF-beta 2 and NGF differentially regulate neural recognition molecule expression by cultured astrocytes. *J Cell Biol* 115:473-484.
- Samaco RC, Mandel-Brehm C, McGraw CM, Shaw CA, McGill BE, Zoghbi HY (2012) Crh and Oprm1 mediate anxiety-related behavior and social approach in a mouse model of MECP2 duplication syndrome. *Nat Genet* 44:206-211.
- Samaco RC, Mandel-Brehm C, Chao HT, Ward CS, Fyffe-Maricich SL, Ren J, Hyland K, Thaller C, Maricich SM, Humphreys P, Greer JJ, Percy A, Glaze DG, Zoghbi HY, Neul JL

- (2009) Loss of MeCP2 in aminergic neurons causes cell-autonomous defects in neurotransmitter synthesis and specific behavioral abnormalities. *Proc Natl Acad Sci U S A* 106:21966-21971.
- Scala E, Longo I, Ottimo F, Speciale C, Sampieri K, Katzaki E, Artuso R, Mencarelli MA, D'Ambrogio T, Vonella G, Zappella M, Hayek G, Battaglia A, Mari F, Renieri A, Ariani F (2007) MECP2 deletions and genotype-phenotype correlation in Rett syndrome. *Am J Med Genet A* 143A:2775-2784.
- Schousboe A, Bak LK, Waagepetersen HS (2013) Astrocytic Control of Biosynthesis and Turnover of the Neurotransmitters Glutamate and GABA. *Front Endocrinol (Lausanne)* 4:102.
- Sebastiano V, Maeder ML, Angstman JF, Haddad B, Khayter C, Yeo DT, Goodwin MJ, Hawkins JS, Ramirez CL, Batista LF, Artandi SE, Wernig M, Joung JK (2011) In situ genetic correction of the sickle cell anemia mutation in human induced pluripotent stem cells using engineered zinc finger nucleases. *Stem Cells* 29:1717-1726.
- Shahbazian MD, Antalffy B, Armstrong DL, Zoghbi HY (2002a) Insight into Rett syndrome: MeCP2 levels display tissue- and cell-specific differences and correlate with neuronal maturation. *Human Molecular Genetics* 11:115-124.
- Shahbazian MD, Young JI, Yuva-Paylor LA, Spencer CM, Antalffy BA, Noebels JL, Armstrong DL, Paylor R, Zoghbi HY (2002b) Mice with truncated MeCP2 recapitulate many Rett syndrome features and display hyperacetylation of histone H3. *Neuron* 35:243-254.
- Shi Y, Kirwan P, Smith J, Robinson HP, Livesey FJ (2012) Human cerebral cortex development from pluripotent stem cells to functional excitatory synapses. *Nat Neurosci* 15:477-486, S471.
- Shipman SL, Schnell E, Hirai T, Chen BS, Roche KW, Nicoll RA (2011) Functional dependence of neuroligin on a new non-PDZ intracellular domain. *Nat Neurosci* 14:718-726.
- Skene PJ, Illingworth RS, Webb S, Kerr ARW, James KD, Turner DJ, Andrews R, Bird AP (2010a) Neuronal MeCP2 Is Expressed at Near Histone-Octamer Levels and Globally Alters the Chromatin State. *Molecular Cell* 37:457-468.
- Skene PJ, Illingworth RS, Webb S, Kerr AR, James KD, Turner DJ, Andrews R, Bird AP (2010b) Neuronal MeCP2 is expressed at near histone-octamer levels and globally alters the chromatin state. *Mol Cell* 37:457-468.
- Soldner F, Laganieri J, Cheng AW, Hockemeyer D, Gao Q, Alagappan R, Khurana V, Golbe LI, Myers RH, Lindquist S, Zhang L, Guschin D, Fong LK, Vu BJ, Meng X, Urnov FD, Rebar EJ, Gregory PD, Zhang HS, Jaenisch R (2011) Generation of isogenic pluripotent stem cells differing exclusively at two early onset Parkinson point mutations. *Cell* 146:318-331.
- Song H, Stevens CF, Gage FH (2002a) Astroglia induce neurogenesis from adult neural stem cells. *Nature* 417:39-44.
- Song HJ, Stevens CF, Gage FH (2002b) Neural stem cells from adult hippocampus develop essential properties of functional CNS neurons. *Nat Neurosci* 5:438-445.
- Staerk J, Dawlaty MM, Gao Q, Maetzel D, Hanna J, Sommer CA, Mostoslavsky G, Jaenisch R (2010) Reprogramming of human peripheral blood cells to induced pluripotent stem cells. *Cell Stem Cell* 7:20-24.
- Sun C, Zhang L, Chen G (2013) An unexpected role of neuroligin-2 in regulating KCC2 and GABA functional switch. *Mol Brain* 6:23.
- Sun C, Cheng MC, Qin R, Liao DL, Chen TT, Koong FJ, Chen G, Chen CH (2011) Identification and functional characterization of rare mutations of the neuroligin-2 gene (NLGN2) associated with schizophrenia. *Hum Mol Genet* 20:3042-3051.

- Sun YG, Wu CS, Renger JJ, Uebele VN, Lu HC, Beierlein M (2012) GABAergic synaptic transmission triggers action potentials in thalamic reticular nucleus neurons. *J Neurosci* 32:7782-7790.
- Takahashi K, Yamanaka S (2006) Induction of pluripotent stem cells from mouse embryonic and adult fibroblast cultures by defined factors. *Cell* 126:663-676.
- Takahashi K, Okita K, Nakagawa M, Yamanaka S (2007) Induction of pluripotent stem cells from fibroblast cultures. *Nat Protoc* 2:3081-3089.
- Tang X, Zhou L, Wagner AM, Marchetto MC, Muotri AR, Gage FH, Chen G (2013) Astroglial cells regulate the developmental timeline of human neurons differentiated from induced pluripotent stem cells. *Stem Cell Res* 11:743-757.
- Tao R, Li C, Newburn EN, Ye T, Lipska BK, Herman MM, Weinberger DR, Kleinman JE, Hyde TM (2012) Transcript-specific associations of SLC12A5 (KCC2) in human prefrontal cortex with development, schizophrenia, and affective disorders. *J Neurosci* 32:5216-5222.
- Tornberg J, Voikar V, Savilahti H, Rauvala H, Airaksinen MS (2005) Behavioural phenotypes of hypomorphic KCC2-deficient mice. *Eur J Neurosci* 21:1327-1337.
- Trappe R, Laccone F, Cobilanschi J, Meins M, Huppke P, Hanefeld F, Engel W (2001) MECP2 mutations in sporadic cases of Rett syndrome are almost exclusively of paternal origin. *American Journal of Human Genetics* 68:1093-1101.
- Tropea D, Giacometti E, Wilson NR, Beard C, McCurry C, Fu DD, Flannery R, Jaenisch R, Sur M (2009) Partial reversal of Rett Syndrome-like symptoms in MeCP2 mutant mice. *Proceedings of the National Academy of Sciences of the United States of America* 106:2029-2034.
- Tudor M, Akbarian S, Chen RZ, Jaenisch R (2002) Transcriptional profiling of a mouse model for Rett syndrome reveals subtle transcriptional changes in the brain. *Proceedings of the National Academy of Sciences of the United States of America* 99:15536-15541.
- Tyzio R, Nardou R, Ferrari DC, Tsintsadze T, Shahrokhi A, Eftekhari S, Khalilov I, Tsintsadze V, Bouchoud C, Chazal G, Lemonnier E, Lozovaya N, Burnashev N, Ben-Ari Y (2014) Oxytocin-mediated GABA inhibition during delivery attenuates autism pathogenesis in rodent offspring. *Science* 343:675-679.
- Uvarov P, Ludwig A, Markkanen M, Rivera C, Airaksinen MS (2006) Upregulation of the neuron-specific K⁺/Cl⁻ cotransporter expression by transcription factor early growth response 4. *J Neurosci* 26:13463-13473.
- van den Pol AN, Obrietan K, Chen G (1996) Excitatory actions of GABA after neuronal trauma. *J Neurosci* 16:4283-4292.
- Van Esch H, Bauters M, Ignatius J, Jansen M, Raynaud M, Hollanders K, Lugtenberg D, Bienvenu T, Jensen LR, Gecz J, Moraine C, Marynen P, Fryns JP, Froyen G (2005) Duplication of the MECP2 region is a frequent cause of severe mental retardation and progressive neurological symptoms in males. *Am J Hum Genet* 77:442-453.
- Vanhatalo S, Palva JM, Andersson S, Rivera C, Voipio J, Kaila K (2005) Slow endogenous activity transients and developmental expression of K⁺-Cl⁻ cotransporter 2 in the immature human cortex. *Eur J Neurosci* 22:2799-2804.
- Wan MM, Lee SSJ, Zhang XY, Houwink-Manville I, Song HR, Amir RE, Budden S, Naidu S, Pereira JLP, Lo IFM, Zoghbi HY, Schanen NC, Francke U (1999) Rett syndrome and beyond: Recurrent spontaneous and familial MECP2 mutations at CpG hotspots. *American Journal of Human Genetics* 65:1520-1529.
- Wearne SL, Rodriguez A, Ehlenberger DB, Rocher AB, Henderson SC, Hof PR (2005) New techniques for imaging, digitization and analysis of three-dimensional neural morphology on multiple scales. *Neuroscience* 136:661-680.

- Weaving LS, Ellaway CJ, Gecz J, Christodoulou J (2005) Rett syndrome: clinical review and genetic update. *Journal of medical genetics* 42:1-7.
- Weaving LS, Williamson SL, Bennetts B, Davis M, Ellaway CJ, Leonard H, Thong MK, Delatycki M, Thompson EM, Laing N, Christodoulou J (2003) Effects of MECP2 mutation type, location and X-inactivation in modulating Rett syndrome phenotype. *American Journal of Medical Genetics Part A* 118A:103-114.
- Wernig M, Lengner CJ, Hanna J, Lodato MA, Steine E, Foreman R, Staerk J, Markoulaki S, Jaenisch R (2008) A drug-inducible transgenic system for direct reprogramming of multiple somatic cell types. *Nat Biotechnol* 26:916-924.
- Yagi T, Ito D, Okada Y, Akamatsu W, Nihei Y, Yoshizaki T, Yamanaka S, Okano H, Suzuki N (2011) Modeling familial Alzheimer's disease with induced pluripotent stem cells. *Hum Mol Genet* 20:4530-4539.
- Yang Y, Ge W, Chen Y, Zhang Z, Shen W, Wu C, Poo M, Duan S (2003) Contribution of astrocytes to hippocampal long-term potentiation through release of D-serine. *Proc Natl Acad Sci U S A* 100:15194-15199.
- Yao J, Qi J, Chen G (2006) Actin-dependent activation of presynaptic silent synapses contributes to long-term synaptic plasticity in developing hippocampal neurons. *J Neurosci* 26:8137-8147.
- Yasui DH, Xu H, Dunaway KW, Lasalle JM, Jin LW, Maezawa I (2013) MeCP2 modulates gene expression pathways in astrocytes. *Mol Autism* 4:3.
- Yazawa M, Hsueh B, Jia X, Pasca AM, Bernstein JA, Hallmayer J, Dolmetsch RE (2011) Using induced pluripotent stem cells to investigate cardiac phenotypes in Timothy syndrome. *Nature* 471:230-234.
- Yeo M, Berglund K, Augustine G, Liedtke W (2009) Novel repression of *Kcc2* transcription by REST-RE-1 controls developmental switch in neuronal chloride. *J Neurosci* 29:14652-14662.
- Yeo M, Berglund K, Hanna M, Guo JU, Kittur J, Torres MD, Abramowitz J, Busciglio J, Gao Y, Birnbaumer L, Liedtke WB (2013) Bisphenol A delays the perinatal chloride shift in cortical neurons by epigenetic effects on the *Kcc2* promoter. *Proc Natl Acad Sci U S A* 110:4315-4320.
- Yizhar O, Fenno LE, Prigge M, Schneider F, Davidson TJ, O'Shea DJ, Sohal VS, Goshen I, Finkelstein J, Paz JT, Stehfest K, Fudim R, Ramakrishnan C, Huguenard JR, Hegemann P, Deisseroth K (2011) Neocortical excitation/inhibition balance in information processing and social dysfunction. *Nature* 477:171-178.
- Yu J, Vodyanik MA, Smuga-Otto K, Antosiewicz-Bourget J, Frane JL, Tian S, Nie J, Jonsdottir GA, Ruotti V, Stewart R, Slukvin, II, Thomson JA (2007) Induced pluripotent stem cell lines derived from human somatic cells. *Science* 318:1917-1920.
- Yu W, Lu B (2012) Synapses and dendritic spines as pathogenic targets in Alzheimer's disease. *Neural Plast* 2012:247150.
- Yu W, Polepalli J, Wagh D, Rajadas J, Malenka R, Lu B (2012) A critical role for the PAR-1/MARK-tau axis in mediating the toxic effects of Abeta on synapses and dendritic spines. *Hum Mol Genet* 21:1384-1390.
- Zamanian JL, Xu L, Foo LC, Nouri N, Zhou L, Giffard RG, Barres BA (2012) Genomic analysis of reactive astrogliosis. *J Neurosci* 32:6391-6410.
- Zeng H, Guo M, Martins-Taylor K, Wang X, Zhang Z, Park JW, Zhan S, Kronenberg MS, Lichtler A, Liu HX, Chen FP, Yue L, Li XJ, Xu RH (2010) Specification of region-specific neurons including forebrain glutamatergic neurons from human induced pluripotent stem cells. *PLoS One* 5:e11853.

- Zhang SC, Wernig M, Duncan ID, Brustle O, Thomson JA (2001) In vitro differentiation of transplantable neural precursors from human embryonic stem cells. *Nat Biotechnol* 19:1129-1133.
- Zhang Y, Barres BA (2010) Astrocyte heterogeneity: an underappreciated topic in neurobiology. *Curr Opin Neurobiol* 20:588-594.
- Zhang Y, Barres BA (2013) A smarter mouse with human astrocytes. *Bioessays* 35:876-880.
- Zhou H, Wu S, Joo JY, Zhu S, Han DW, Lin T, Trauger S, Bien G, Yao S, Zhu Y, Siuzdak G, Scholer HR, Duan L, Ding S (2009) Generation of induced pluripotent stem cells using recombinant proteins. *Cell Stem Cell* 4:381-384.
- Zhou Z, Hong EJ, Cohen S, Zhao WN, Ho HY, Schmidt L, Chen WG, Lin Y, Savner E, Griffith EC, Hu L, Steen JA, Weitz CJ, Greenberg ME (2006) Brain-specific phosphorylation of MeCP2 regulates activity-dependent Bdnf transcription, dendritic growth, and spine maturation. *Neuron* 52:255-269.
- Zoghbi HY, Bear MF (2012) Synaptic dysfunction in neurodevelopmental disorders associated with autism and intellectual disabilities. *Cold Spring Harb Perspect Biol* 4.

VITA

Xin Tang

Educational Background

- The Pennsylvania State University 2009 – Present, expect to graduate on May, 2014
- Ph. D. candidate, Biology Department, Dr. Gong Chen's lab
 - Dissertation title 'Use of human induced-Pluripotent Stem Cells to understand molecular mechanisms of autism'
- Yale University 2007 - 2009
- M.Sc., Combined program in the Biomedical and Biological Sciences
- Huazhong University of Science and Technology, China 2003 - 2007
- B. Sc., Biomedical Engineering (*Cum Laude*)

Awards and Honors

- First prize, Penn State University neuroscience research retreat poster presentation award 2014
- First prize, the first Penn State University Gong Chen lab annual scientific image contest 2013
- J. Ben and Helen D. Hill memorial fund award, The Pennsylvania State University 2012
- Chinese Scholarship Council – Yale world scholars program fellowship 2007
- HUST first-class scholarship 2003-07

Manuscripts published

Tang X., Zhou L., Wagner A. M., Marchetto M. C., Muotri A., Gage F., and Chen G. (2013) Astroglial cells regulate the developmental timeline of human neurons differentiated from induced pluripotent stem cells. *Stem Cell Research*, 2013, Vol. 11, issue 2. 743-757. (Cover article). News press: <http://medicalxpress.com/news/2013-06-alzheimer-schizophrenia-autism-mature-brain.html> <http://world.people.com.cn/n/2013/0726/c1002-22332207.html> (Chinese)

Fan Y., **Tang X.**, Vitriol E., Chen G., and Zheng J. Q. (2011). Actin capping protein is required for dendritic spine development and synapse formation. *Journal of Neuroscience*, 31(28): 10228-33.

Gu J., Lee C. W., Fan Y., Komlos D., **Tang X.**, Sun C., Yu K., Hartzell H. C., Chen G., Bamberg J. R., and Zheng J. Q. (2010). ADF/Cofilin-mediated actin dynamics regulate AMPA Receptor trafficking during synaptic plasticity. *Nature Neuroscience*, 13: 1208–1215.

Harel N., Song K., **Tang X.**, Strittmatter S. (2010). Nogo receptor deletion and multimodal exercise improve distinct aspects of recovery in cervical spinal cord injury. *Journal of Neurotrauma*, 27: 2055-2066.

Wang R., McGrath B. C., Kopp R. F., Roe M. W., **Tang X.**, Chen G., Cavener D. R. (2013) Insulin secretion and Ca²⁺ dynamics in β -cells are regulated by PERK eIF2 α kinase in concert with calcineurin. *Journal of Biological Chemistry*, 2013 Oct 10. (Epub ahead of print)

Manuscripts submitted and in preparation:

Tang X., Kim J., Zhou L., Zhang L., Carromeu C., Muotri A., Gage F., Chen G., *Membrane transporter KCC2 mediates the functional output of MeCP2 through direct regulation of GABA functional switch and glutamatergic transmission*. Submitted.

Zhou L., **Tang X.**, Li X., Bai Y., Buxbaum J., Chen G., *Identification of transthyretin as a novel interacting partner for extrasynaptic delta subunit-containing GABAA receptors*. Submitted.

Tang X., and Chen G., *Cofilin regulates neuronal Calcium homeostasis under pathological conditions through voltage-gated Calcium channel and NMDA receptors*. Manuscript in preparation

Tang X., Cao C., Ma H., Chen G., *Gene expression and functional comparisons between human and mouse astrocytes reveal major differences in stem cell and synapse supporting pathways*. Manuscript in preparation.